SECURITY MARKING

The classified or limited status of this report applies to each page, unless otherwise marked.
Separate page printouts MUST be marked accordingly.

CONFIDENTIAL

2

AFRPL-TR-68-159-Vol I

TCO-56-9-8

Copy [redacted]

AD 500267

FINAL REPORT
DEMONSTRATION OF 156 INCH MOTOR WITH
SEGMENTED FIBERGLASS CASE AND ABLATIVE NOZZLE

VOLUME I--MOTOR DESIGN AND FABRICATION (U)

CONTRACT AF 04(611)-11603

December 1968

Prepared for

AIR FORCE
ROCKET PROPULSION LABORATORY
DIRECTORATE OF LABORATORIES
AIR FORCE SYSTEMS COMMAND
UNITED STATES AIR FORCE
Edwards AFB, California

THIOKOL CHEMICAL CORPORATION
WASATCH DIVISION
Brigham City, Utah

IN ADDITION TO SECURITY REQUIREMENTS WHICH MUST BE MET, THIS DOCUMENT IS SUBJECT TO SPECIAL EXPORT CONTROLS AND EACH TRANSMITTAL TO FOREIGN NATIONALS MAY BE MADE ONLY WITH PRIOR APPROVAL OF AFRPL (RPPR/STINFO), EDWARDS, CALIFORNIA 93523.

CONFIDENTIAL

SPECIAL NOTICES

Qualified users may obtain copies of this report from the Defense Documentation Center.

Do not return this copy. When not needed, destroy in accordance with pertinent security regulations.

When U. S. Government drawings, specifications, or other data are used for any purpose other than a definitely related Government procurement operation, the Government thereby incurs no responsibility nor any obligations whatsoever, and the fact that the Government may have formulated, furnished, or in any way supplied the said drawings, specifications, or other data, is not to be regarded by implication or otherwise, or in any manner licensing the holder or any other person or corporation, or conveying any rights or permission to manufacture, use, or sell any patented invention that may in any way be related theretc.

1-73

CONFIDENTIAL

(18) (19)

AFRPL-TR-68-159-Vol-1

~~TC0-56-9-8~~

(9) FINAL REPORT. 1 Apr 68 - 8 Aug 68

(6) DEMONSTRATION OF 156 INCH MOTOR WITH SEGMENTED FIBERGLASS CASE AND ABLATIVE NOZZLE.

VOLUME I--MOTOR DESIGN AND FABRICATION (U).

(15) ~~CONTRACT~~ AF 04(611)-11603

(11) Dec 68

Prepared by

THIOKOL CHEMICAL CORPORATION
WASATCH DIVISION
Brigham City, Utah

(10) Thomas/Walker
Program Manager

Robert F./Zeigler

~~Robert Zeigler~~
Project Engineer

Publications No. 0968-20171

CONFIDENTIAL

(401 221)

FOREWORD

This final technical engineering report documents all effort and results relative to Contract AF 04(611)-11603, "Demonstration of 156 Inch Motor with Segmented Fiberglass Case and Ablative Nozzle." The program motor, designated by the Air Force as the 156-8 rocket motor, was identified as the TU-312L.02 motor for internal processing at Thiokol.

The contract with Thiokol Chemical Corporation, Wasatch Division, was funded by SAMSO and performed under the overall direction of Captain Richard Neely (RPMMS), Solid Rocket Division of the Air Force Rocket Propulsion Laboratory, Directorate of Laboratories (DOL), Air Force Systems Command, Edwards AFB, California.

The report is organized into two volumes. Volume I describes the motor design and fabrication, and Volume II covers the motor static test and hydroburst. This document contains no classified information extracted from other documents.

This document has been reviewed and approved.

Charles R. Cooke
Chief Solid Rocket Division
AFRPL, Edwards, California

(U)

ABSTRACT

(U) The 156-8 motor program, Demonstration of 156 Inch Motor with Segmented Fiberglass Case and Fixed Ablative Nozzle, was conducted by Wasatch Division, Thiokol Chemical Corporation for the Air Force Space and Missile Systems organization. The program was under the technical direction of the Air Force Rocket Propulsion Laboratory. The primary objectives of the program were to successfully static test fire the rocket motor followed by a hydroburst test of the fiberglass case. These objectives were attained. The 156-8 motor was static test fired 25 Jun 1968 and all systems performed satisfactorily. This test successfully demonstrated the segmented fiberglass case design and the joint seal design. All motor and nozzle components were intact and in good condition at the completion of the test. The motor operated at very close to the predicted ballistic values. Post-test inspection of the motor and components disclosed that the internal insulation, nozzle design, and joint seal design were satisfactory and the nozzle performed as predicted. Inadequacies in the CO_2 quench system permitted some charring through of the insulation in the forward dome which necessitated repair prior to the hydroburst test on 8 Aug 1968. Burst occurred at 1,095 psi, initiating in a heat affected area of the forward segment.

PRECEDING PAGE BLANK-NOT FILMED

TABLE OF CONTENTS

PRECEDING PAGE BLANK-NOT FILMED

TABLE OF CONTENTS (Cont)

TABLE OF CONTENTS (Cont)

PRECEDING PAGE BLANK-NOT FILMED

LIST OF ILLUSTRATIONS

LIST OF ILLUSTRATIONS (Cont)

LIST OF ILLUSTRATIONS (Cont)

LIST OF ILLUSTRATIONS (Cont)

LIST OF ILLUSTRATIONS (Cont)

PRECEDING PAGE BLANK-NOT FILMED

LIST OF ILLUSTRATIONS (Cont)

LIST OF ILLUSTRATIONS (Cont)

LIST OF ILLUSTRATIONS (Cont)

LIST OF ILLUSTRATIONS (Cont)

LIST OF TABLES

LIST OF TABLES (Cont)

LIST OF TABLES (Cont)

SECTION I

(U) INTRODUCTION AND SUMMARY

(U) A. INTRODUCTION

(U) On 12 Apr 1966, Thiokol Chemical Corporation received notification from the Air Force Space Systems Division of the award of contract AF 04(611)-11603 for the Demonstration of a 156 Inch Diameter Motor with Segmented Fiberglass Case and Fixed Ablative Nozzle. As detailed in the Statement of Work, Exhibit "A" to the contract, the program objective was to successfully static test fire a one million pound thrust class, 156 in. diameter, segmented fiberglass reinforced plastic case, solid propellant rocket motor followed by the hydroburst test of the fiberglass case.

(U) The program was accomplished through use of a Government furnished case and nozzle which were fabricated under Air Force Materials Laboratory (AFML) contracts AF 33(657)-11303 and AF 33(657)-11301, respectively.

(U) These two contracts were part of the 623A program which was initiated by AFML in early 1963 to develop the technology required for fabricating large (156 in. diameter) segmented fiberglass reinforced plastic rocket motor cases and large ablative nozzles.

(U) These programs were established to develop the technology required to fabricate large rocket motor components and thus allow the attainment of cost reduction and performance improvements projected with these components.

(U) The program for developing manufacturing methods, controls, and processes for large segmented fiberglass cases was awarded to Thiokol Chemical Corporation, Wasatch Division. Thompson Ramo Wooldridge, Inc (TRW) was awarded the program to develop fabrication techniques and processes for large ablative nozzles that would eliminate the need for using large, complex hydroclaving equipment for manufacturing.

(U) Extensive development work under both of these programs has resulted in the three-segment, 156 in. diameter, fiberglass rocket motor case (weighing 45 percent less than a comparable 18 percent nickel maraging steel case) and a large ablative nozzle that was fabricated without the use of hydroclave facilities. The manufacturing technology required to fabricate large rocket motor components has been demonstrated through (1) the hydrostatic proof testing of the segmented 156 in. diameter case, and (2) subscale testing of nozzles fabricated with the same manufacturing techniques utilized in fabricating the large ablative nozzle.

(U) A necessary prime step in this component technology program was the integration of these components in an actual motor static test demonstration. To accomplish the objective of this program Thiokol used demonstrated state-of-the-art technology in preparing the Government furnished case and nozzle for static test firing. The scope of work required to accomplish the program objective is described in the following task breakdown:

- Task I -- Subscale Joint Seal Development
  - 1.1 Subscale Joint Seal Analysis and Design
  - 1.2 Subscale Joint Seal Fabrication and Test
- Task II -- Motor Demonstration
  - 2.1 Motor Design and Analysis
  - 2.2 Motor Propellant Processing and Test
  - 2.3 Motor Insulation and Liner Fabrication and Test
  - 2.4 Motor Ignition System Fabrication and Test
  - 2.5 Motor Static Test Firing
- Task III -- Motor Case Hydroburst Test
- Task IV -- Special Tooling and Facilities
- Task V -- Systems Support
- Task VI -- Program Management
- Task VII -- Reports and Documentation

(U) The contractual period of performance for technical effort was from 12 Apr 1966 thru 23 Dec 1966. During this period the basic contract was modified by Contract Change Notice. This modification affected the propellant repair in the forward segment and directed additional propellant cutout effort, thereby increasing the target cost by $10, 000. The scheduled completion of technical effort was subsequently changed to read "on or before 1 Apr 1968." Unforeseen problems encountered during assembly of the motor segments made it impossible to comply with the 1 April date. The contract was modified a second time to reflect a static test date of 25 Jun 1968, which was met. The 31 Jul 1969 date for the hydroburst was delayed slightly due to the motor case requiring repairs to prevent leakage and allow pressurization. The case was successfully burst on 8 Aug 1968.

(U) The final report is contained in two volumes. Volume I contains (1) a program summary; (2) detailed discussions on the design and fabrication of the motor components including the segmented fiberglass reinforced plastic case, the propellant and grain, insulation and liner, ignition system and the nonhydroclaved nozzle; and (3) subscale joint seal development. Volume II contains (1) the static test report including test results and detailed postfire analysis of components; (2) hydroburst test results; and (3) conclusions and recommendations.

(U) B. SUMMARY

(U) The 156-8 motor demonstration program performed under this contract encompassed the design, manufacture, static testing and hydroburst test of a 156 in. diameter, segmented fiberglass reinforced plastic case, solid propellant rocket motor utilizing a fixed external nonhydroclaved nozzle. The motor design and fabrication was conservative and limited to state-of-the-art technology in order that the primary objective of demonstrating the case segment joints and the joint seal and insulation concept for large motors would not be compromised.

(U) 1. DESIGN CRITERIA

(U) Design criteria specified in the contract Statement of Work included the following:

1. The motor design shall incorporate existing, available, case and nozzle components from contracts AF 33(657)-11303 and AF 33(657)-11301.

2. The motor will be capable of successful operation after being subjected to either horizontal or vertical storage at any thermal environment between 60 and 100° F for any period of time sufficient to produce a maximum temperature gradient through the grain.
3. The grain design for the motor will be of a segmented configuration.
4. The propellant shall be one of the polybutadiene/AP/AL family of propellants. Use of staples is specifically prohibited.
5. The segment joint seals will be located in the joint insulation and will be designed for: (1) high reliability, (2) assembly with a minimum of tooling, (3) disassembly without damage to the segment insulation, and (4) minimum possibility of incorrect assembly.
6. Insulation and liner designs for the motor shall include, but not be limited to, proven materials compatible with the propellant. The materials shall meet motor performance requirements. The insulation material shall be V-44 or equivalent and standard insulation techniques shall be used. Propellant shrinkage flaps will be provided at each of the six propellant termination surfaces.
7. A headend Pyrogen igniter shall be used and will consist of three main components: the safety and arming device; initiating Pyrogen igniter; and a booster Pyrogen igniter.
8. The motor will have a mass fraction goal of 0.91.
9. The motor shall have a burn time of 115 to 120 seconds.
10. The motor should produce a burning time average thrust of 900,000 pounds.

(U) 2. MOTOR DESIGN AND PROCESSING

(U) The 156-8 motor design is shown in Figure 1 and a detailed discussion is contained in the following sections.

(U) The motor case used in this program was the segmented fiberglass reinforced plastic case made by the B. F. Goodrich Co on contract AF 33(657)-11303. Upon completion of the hydrotest requirement of that contract, it was discovered that the case bladder was unbonded. The bladder was subsequently removed from all three segments and replaced as a part of this contract. The new bladder material was V-45 silica-filled NBR rubber.

(U) The joint seal and insulation material was V-44 asbestos filled NBR rubber. After installation of the case bladder and joint seal insulation, the case segments were transported to the test area and assembled in the hydrostatic test stand where the case was hydroproof tested at the MEOP of 880 psi per Exhibit A of the work statement.

(U) UF-2121 liner was applied to the case interior, by the sling lining technique, to provide good bonding between the propellant and the bladder and insulation material. Details of the insulation and liner design effort are contained in Sections IV and VI, respectively.

(U) The propellant for this motor, designated TP-H1011, was a polybutadiene acrylonitrile/AP/AL type and was identical to the Stage I Minuteman propellant. The motor had a segmented cylindrical perforate (CP) grain design in order to maintain a relatively neutral pressure trace. The bayonet casting technique was employed during motor loading. Due to the large size and excessive time required for casting, this technique resulted in a propellant void problem in the area opposite the casting bayonets. A detailed discussion of the propellant casting problem and the subsequent propellant removal and recasting are presented in Section VIII.

(U) A conventional headend Pyrogen ignition system was utilized for motor ignition. This system employed a Minuteman type safety and arming device, an initiating Pyrogen igniter, and the booster Pyrogen igniter. The booster Pyrogen

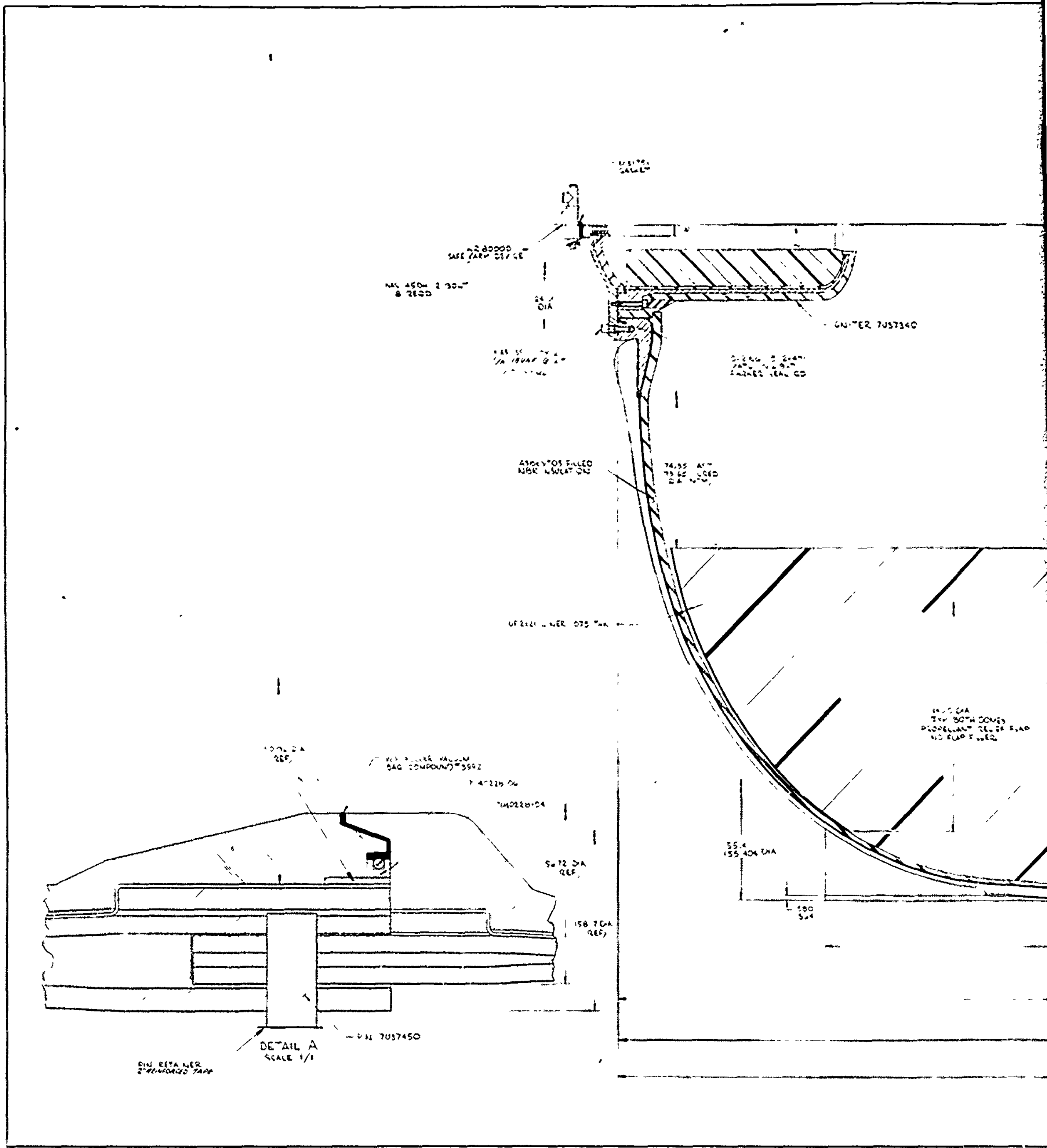
DETAIL A
SCALE 1/1

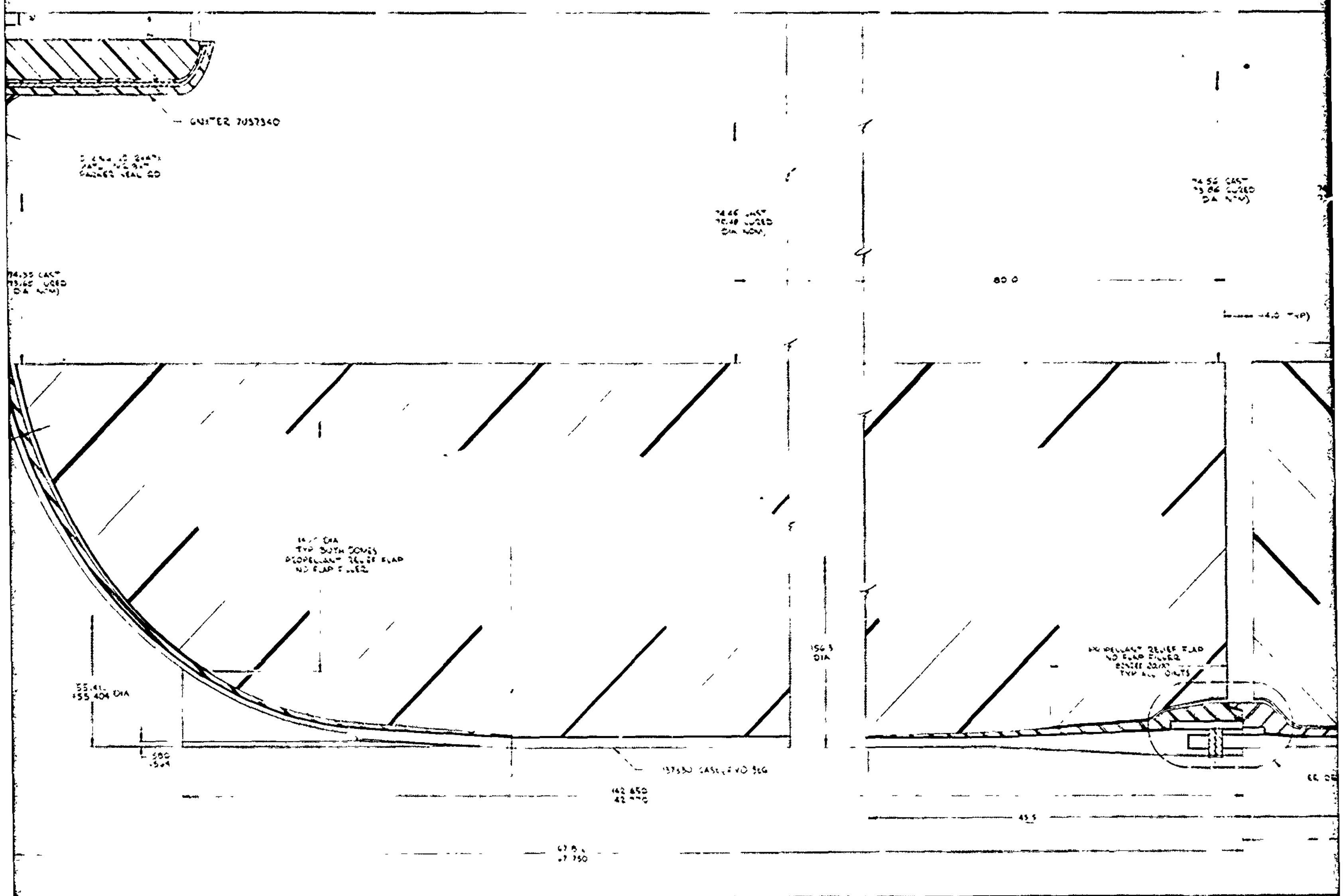

2

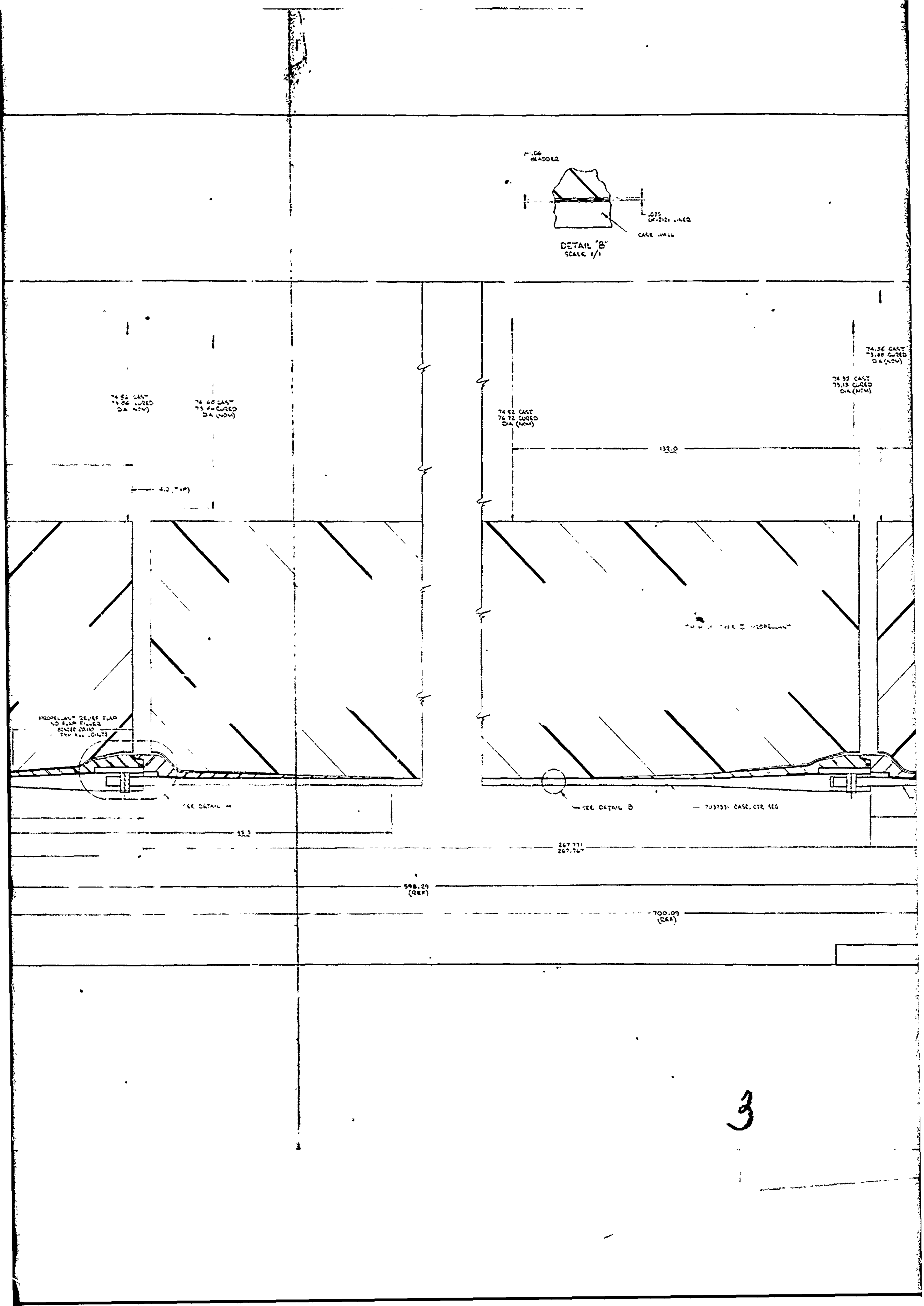
DETAIL "B"
SCALE 1/1
CASE WALL
74.52 CAST
76.72 CURED
DIA (NOM)
132.0
SEE DETAIL B
CASE, CTR SEG
598.29
(REF)
700.09
(REF)

3

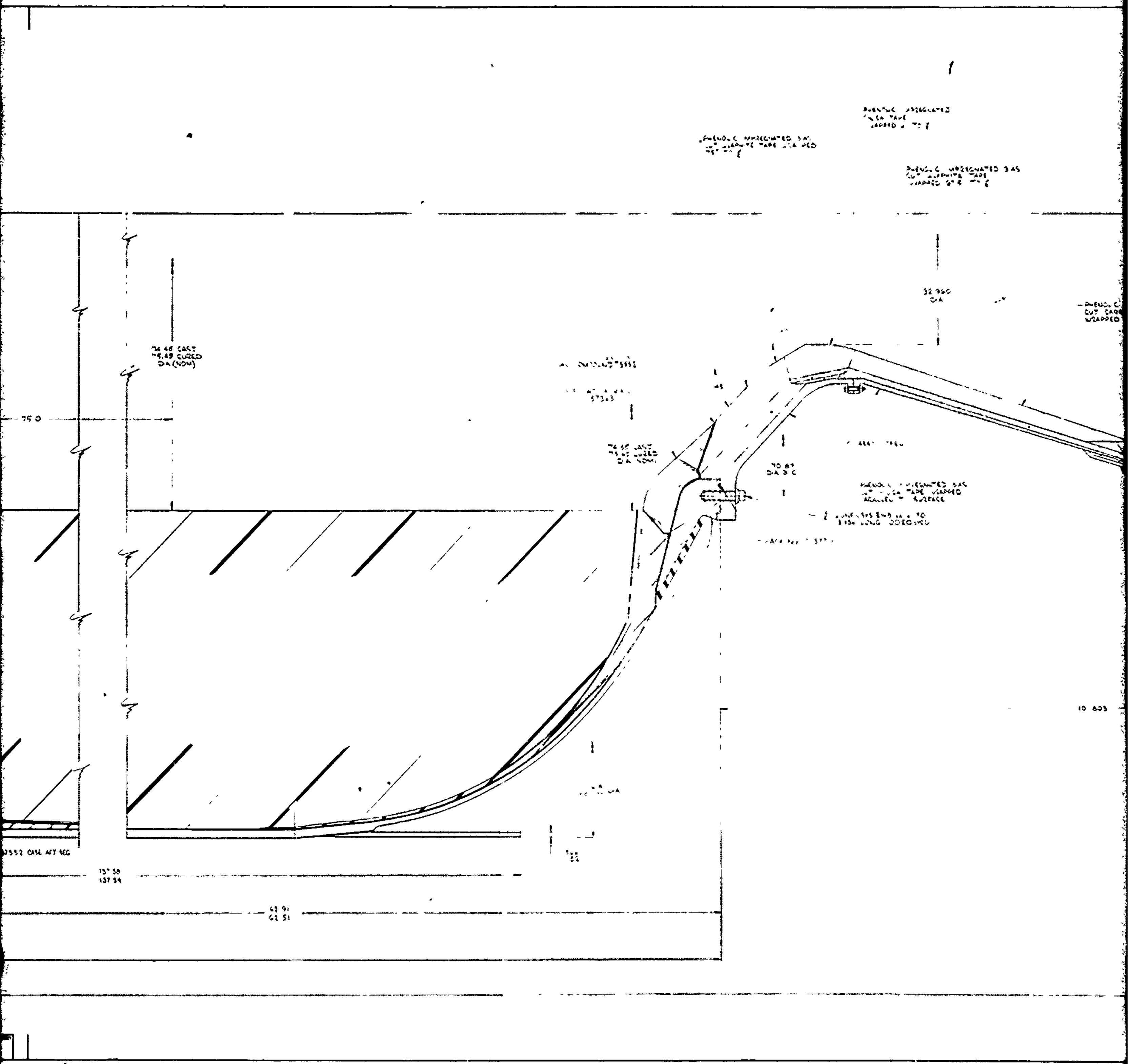

(U) F

4

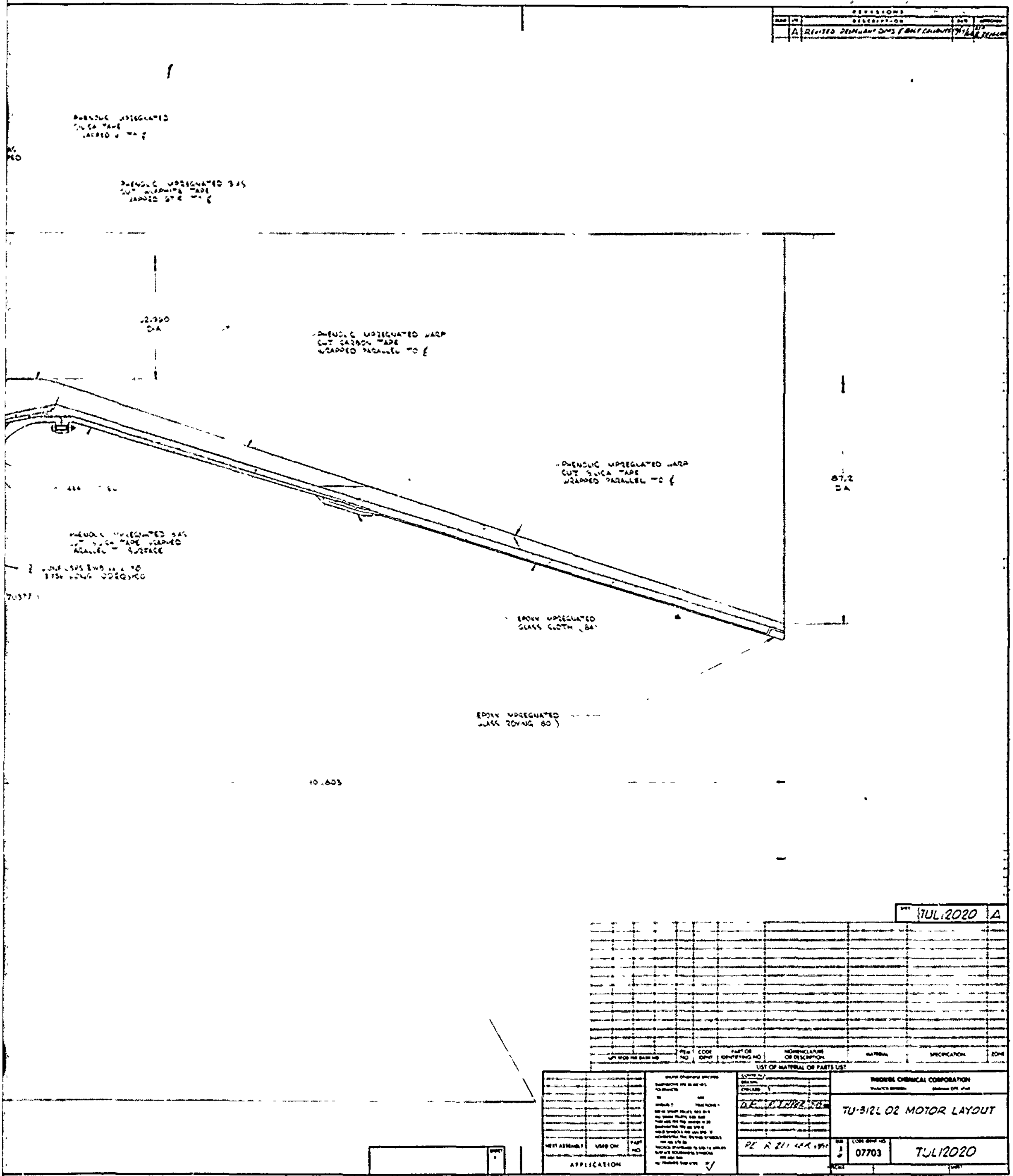

(U) Figure 1. 156-8 Motor Layout Drawing

4

5

metal case was externally insulated with V-45 rubber. The igniter cap was designed with ports for injection of CO_2 gas for motor quench after static testing. Ignition system design and fabrication details are presented in Section IX.

(U) As previously stated, the fixed ablative nozzle for the 156-8 motor was provided as a GFP component. Section X presents a discussion of the nozzle design review and analysis that was conducted to ensure the nozzle's compatibility with the motor and proposed handling procedures, and to predict the performance of the nozzle.

(U) 3. STATIC TEST

(U) The loaded motor segments were transported to the test area and assembled horizontally in the bay. During assembly the segments were supported with jacks at each skirt and each segment joint. After assembly was complete the jacks supporting the motor at the segment joints were lowered, placing all the motor weight on the skirts. As the load increased, the aft skirt began to separate from the case. The jacks at the aft joint were then raised to remove the motor weight from the aft skirt. A structural analysis of the skirt separation condition determined that if the skirt could be made to support the static weight of the motor, it would survive the static test condition. The skirt was repaired by the addition of a rubber shear ply over the separated area and overwrapping the shear ply with fiberglass cloth. This resulted in an 18 in. wide band of fiberglass and shear ply bonded to the skirt and to the motor case. The weight of the motor was again put on the skirt and the repair was found to have been successful.

(U) Prior to installation of the nozzle, the motor was subjected to a 50 $\pm$ 10 psi leak check. This was accomplished by the installation of a flat plate over the aft polar opening. After the case was pressurized, it was checked for leaks with Leak-Tec. No leaks were apparent and processing continued with the installation of the nozzle.

(U) The motor was static fired on 25 Jun 1968. Motor ignition occurred normally and no abnormality in motor or component performance was observed during the firing. A review and analysis of the test data confirmed the successful operation. The motor operated longer and at a slightly lower pressure than predicted with no adverse effects on the test objectives. All motor and component parts were in excellent condition at completion of the firing. Charring of the insulation and degradation of the nozzle plastic parts were prevented to a great degree by the CO_2 quench system. Due to the angle of the holes in the Pyrogen cap through which the CO_2 was injected, there was some charring through of the insulation in the forward dome.

(U) The case was removed from the static test bay after removal of the nozzle and transported to the manufacturing area where the damaged areas of the bladder were repaired and a 50 psi leak check was again performed. No leakage was apparent and the case was transported to the hydrotest facility. During transportation to the test area, the case was pressurized to about 5 psi in order to prevent loosening of the bladder repairs. It became apparent during installation of the case in the hydrotest stand that the case was leaking. The case was filled with water and pressurized with line pressure of approximately 40 psi. The joint seals performed as expected and the air leak was sealed. The case was subsequently pressurized to burst which occurred at 1, 095 psi. The motor static test operations, test results, postfire analysis and hydroburst test results are presented in Sections IV and V of Volume II.

SECTION II

(U) CASE DESIGN, FABRICATION, AND REPAIR

(U) A. CASE DESIGN SUMMARY

(U) The 156-8 rocket motor case consisted of three filament wound segments designed to be assembled at the test site. The segments were connected with steel pins through steel-glass composite tongue and clevis joints. The basic cylinder was wound from S994 glass, wet wrapped with an Epon 826/NMA/DMP-30 resin system. The maximum diameter of the pressure vessel was 158 inches. The forward and aft segments were fitted with skirts. The forward skirt was designed to accept the thrust loads and the aft skirt to accept missile weight loads.

(U) The basic pressure vessel was sealed internally with a Buna-N bladder 0.060 in. thick.

(U) The polar opening was fitted with 2014-T652 aluminum pole pieces to accept the igniter on the forward end and the nozzle on the aft end.

(U) 1. DESIGN CRITERIA

(U) The case was designed in 1963 under Contract AF 33(657)-11303, at which time it was not planned for a static test demonstration. The 156-8 motor was in effect designed around the existing mating case and nozzle.

(U) The case was originally designed to burst at 1,440 psi. The design called for an internal pressure of 1,200 psi with a minimum safety factor of 1.2. After the case was transferred to the 156-8 program, the maximum expected operating pressure (MEOP) was established at 860 psig and the minimum safety factor was changed to 1.25 because of design changes and repairs. The final design refined the MEOP to 854 psig. However, all previous stress calculations were made using the 860 psig value, and it was not considered economically feasible to rework all the design calculations. Therefore, all calculations in this report reflect the 860 psig.

(U) The material properties used for the design are shown in Table I. The case was designed for glass tensile stress and the forward skirt for buckling. The polar bosses were stress or deflection limited. Joints were designed for pin bearing and the transfer of the shear load from the steel to glass composite.

(U) 2. STRUCTURAL ANALYSIS

(U) a. Static Test--The case glass-resin structure was S-994 HTS glass fibers and Epon 826/NMA/DMP-30 hardener.

(U) The forward segment (Figure 2) was designed with a 9 deg wrap angle, which was the minimum to prevent dome slippage. There were 34 polar wound layers and 47.5 hoop layers to withstand internal pressure and discontinuities. The maximum reduction of 1 hoop layer and 2.5 polar layers due to dry glass condition resulted in 46.5 hoop layers and 31.5 polar layers before static test. There was further reduction to 44.5 hoop layers and 29.5 polar layers prior to hydroburst due to charring in static test. The original composite thickness in the cylinder was 1.05 inches.

(U) The center segment (Figure 3) was designed with a 5 deg polar wrap angle, which was chosen because of geometric restrictions imposed by the segment and the mandrel. Twenty eight polar wound layers and 48 hoop wound layers were used to withstand internal pressure. These layers were reduced to 27 and 47.5, respectively, prior to static test due to dry glass removal with the original bladder. The original composite thickness in the cylinder was 0.965 inch.

(U) The aft segment (Figure 4) was of a helical (geodesic) design with a cylinder winding angle of 30 deg and 25 minutes. The helical wrapping pattern was used because of the relatively large opening in the dome for nozzle attachment. Forty helical wound layers and 38 hoop layers were used to withstand internal pressure and discontinuities. Both these layers were reduced to 37.5 each prior to static test

TABLE I

(U) MATERIAL PROPERTIES

Glass - S-994 HTS Finish	
Density, ρ_G (lb/cu in.)	0.090
Modulus of Elasticity, E_G (psi x 10^6)	12.3
Bearing Strength Composite, F_{br} (psi)	50,000
Hoop Glass Strength, $F_{G\theta}$ (psi)	335,000
Helical, Polar Glass Strength, $F_{G\alpha}$ (psi)	301,500
Epon 826/NMA/DMP-30 Resin System	
Density (lb/cu in.)	0.043
Modulus of Elasticity (psi x 10^6)	0.5
Tensile Strength (psi)	6,000
Shear Strength (psi)	7,000
Compressive Strength (psi)	25,000
2014-T652 Aluminum Alloy Forging	
Density, ρ_{Al} (lb/cu in.)	0.100
Modulus of Elasticity, E_{Al} (psi x 10^6)	10.5
Tensile Strength, F_{tu} (psi)	60,000
Shear Strength, F_{su} (psi)	36,000
Tensile Strength at 0.2% Offset, F_{ty} (psi)	55,000
Buna-N Rubber (B. F. Goodrich 39322)	
Shear Strength, F_{su} (psi)	750
Modulus of Rigidity (psi)	350
Density, ρ_r (lb/cu in.)	0.044
AM-355 Stainless Steel	
Density, ρ_s (lb/cu in.)	0.282
Modulus of Elasticity, E_s (psi x 10^6)	30
Tensile Strength, F_{tu}, Min (psi)	250,000

TABLE I (Cont)

(U) MATERIAL PROPERTIES

Shear Strength, F_{su}, Min (psi)	150,000
Tensile Strength at 0.2% Offset, F_{ty}, Min (psi)	212,000
<u>18% Nickel Steel</u>	
Density, ρ (lb/cu in.)	0.289
Modulus of Elasticity (psi x 10^6)	27
Tensile Strength, F_{tu}, Min (psi)	281,800
Shear Strength, F_{su}, Min (psi)	169,080
Tensile Strength at 0.2% Offset, F_{ty}, Min (psi)	270,000
<u>USP E717 Epoxy Resin</u>	
Density (lb/cu in.)	0.043
Modulus of Elasticity (psi x 10^6)	0.5
Shear Strength (psi)	10,000

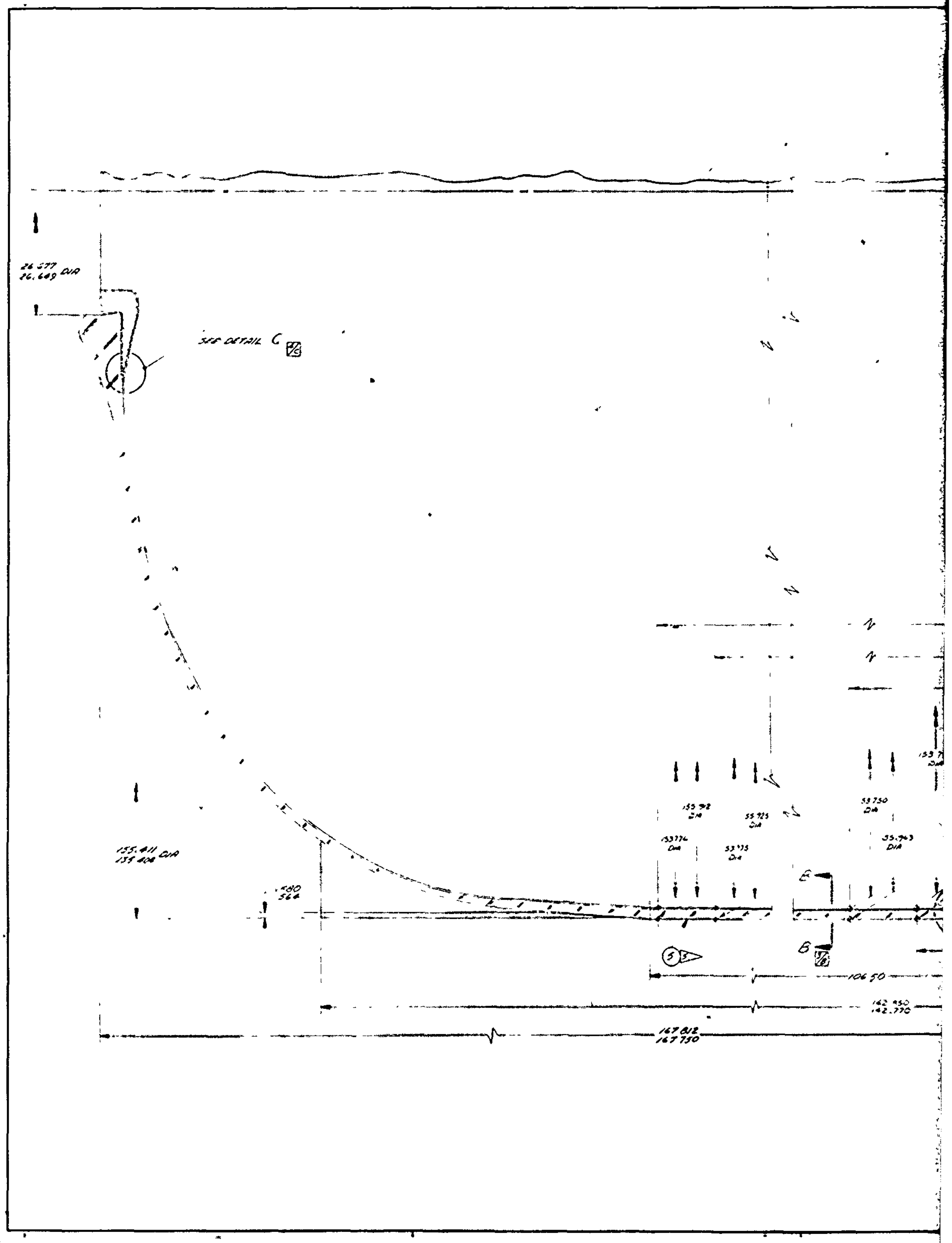

26.577
26.649 DIA
SEE DETAIL C
167.812
167.750
106.50
142.950
142.770
B
B

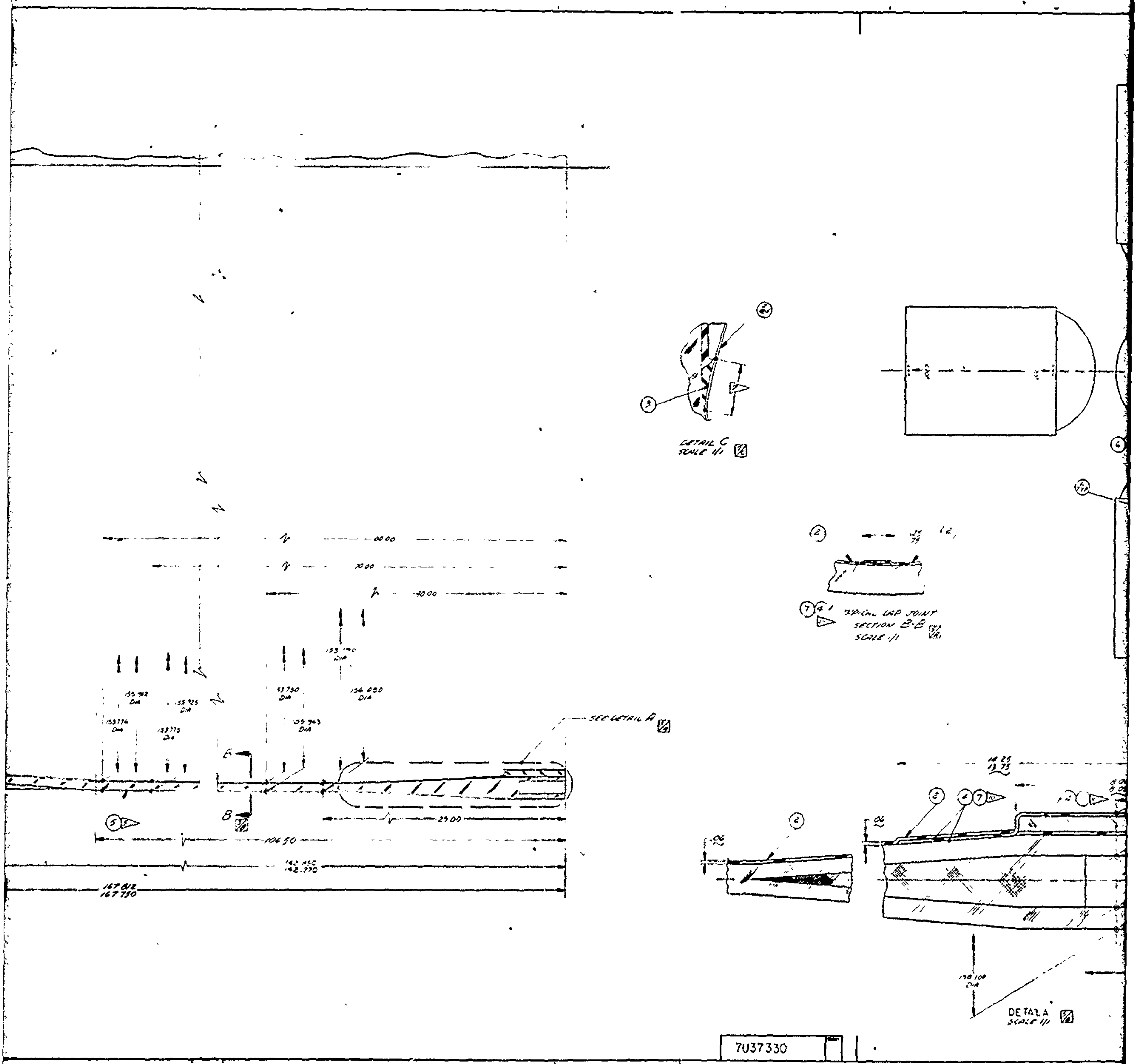
DETAIL C
SCALE 1/1
TYPICAL LAP JOINT
SECTION B-B
SCALE 1/1
SEE DETAIL A
106.50
29.00
DETAIL A
SCALE 1/1
7U37330

2

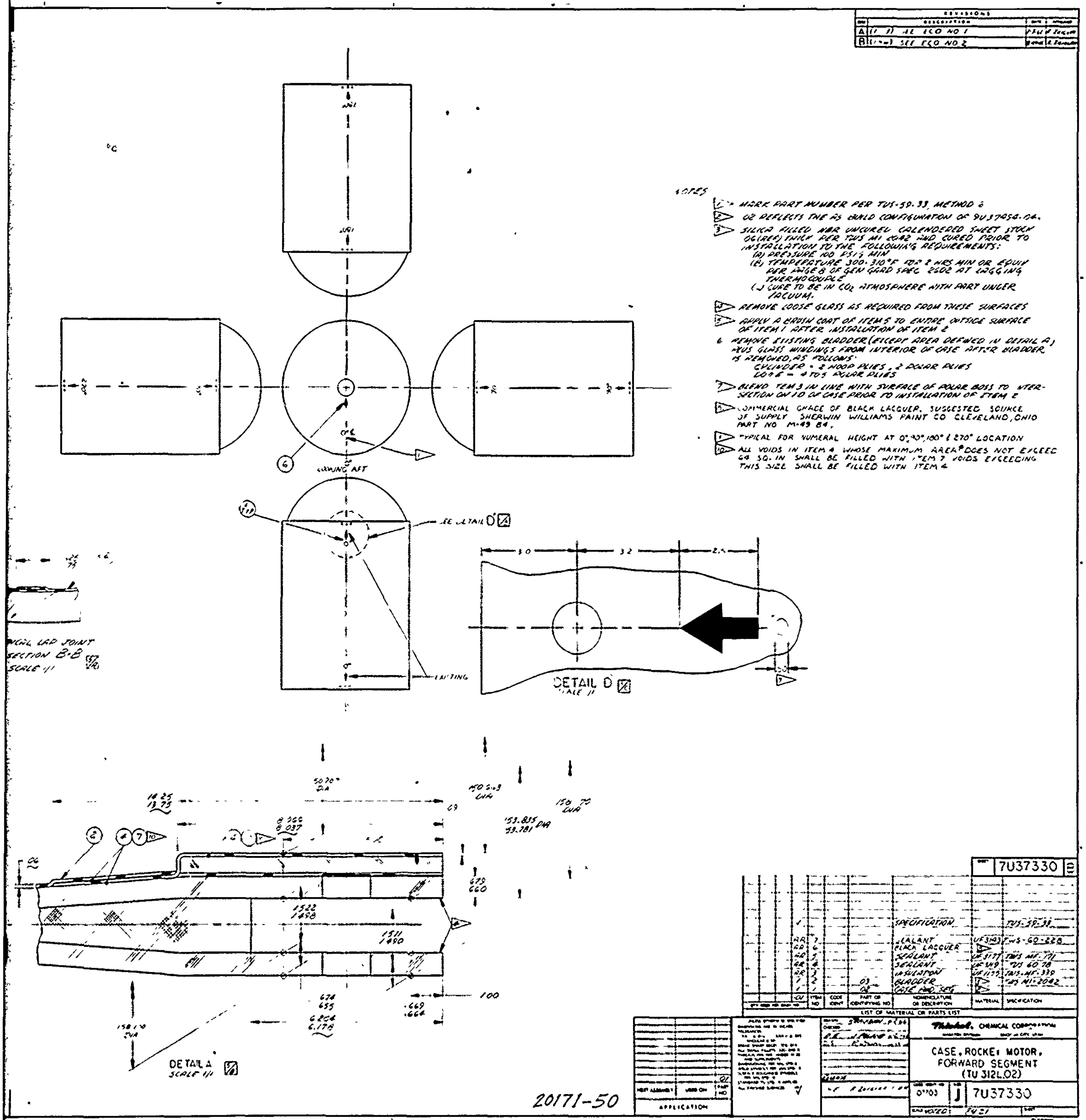

(U) Figure 2. 156-8 Forward Segment

3

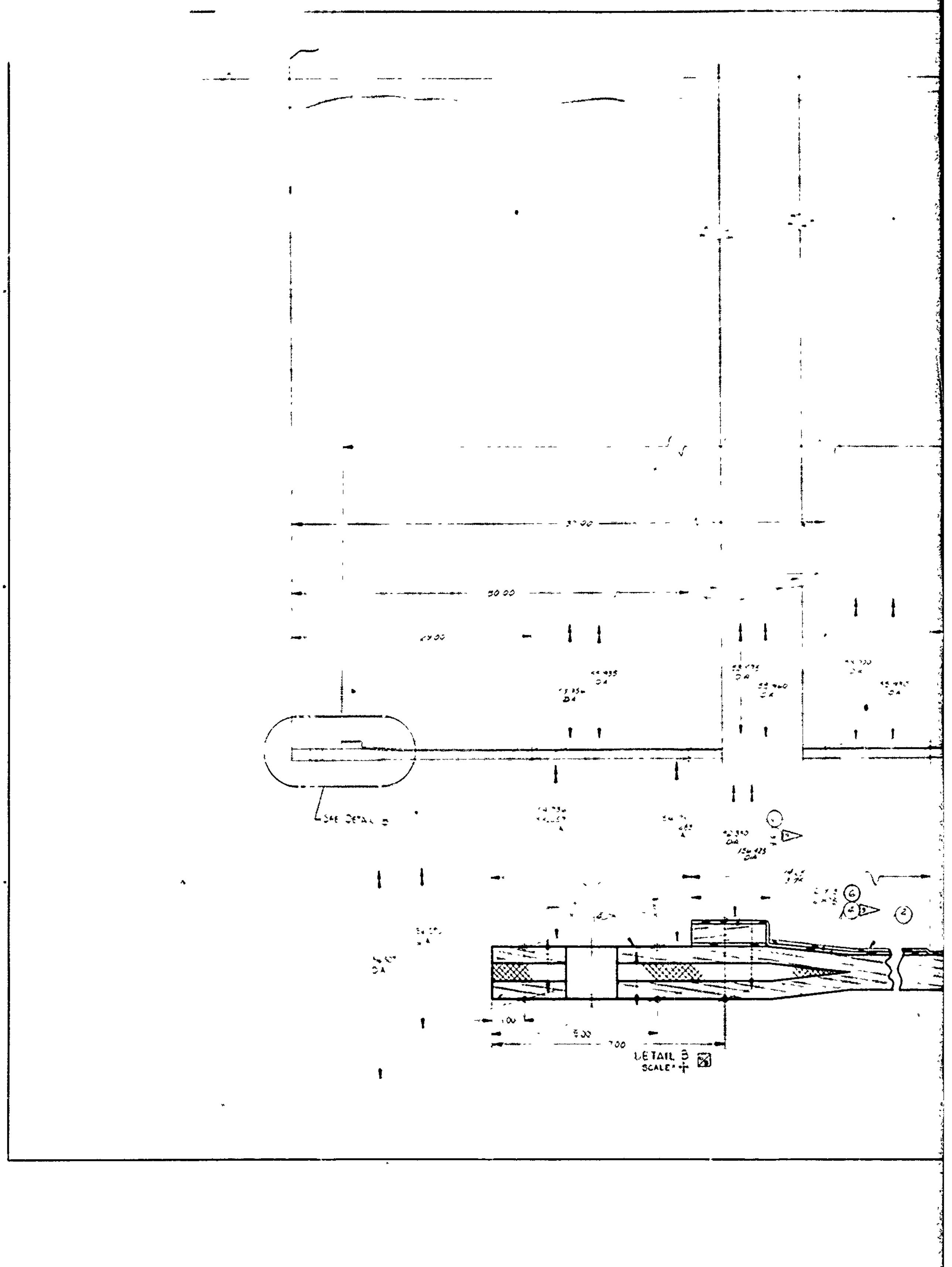
DETAIL B

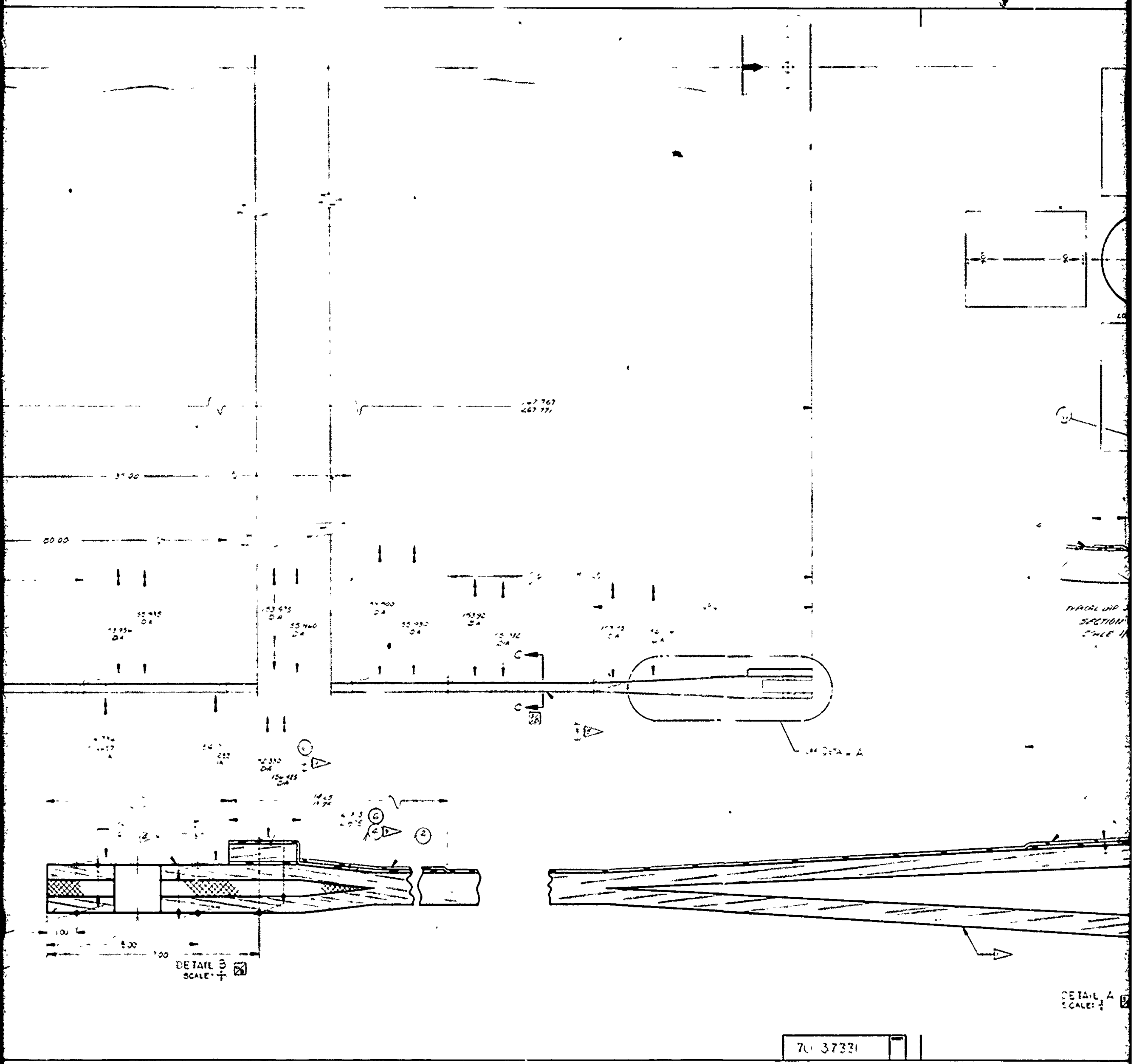

2

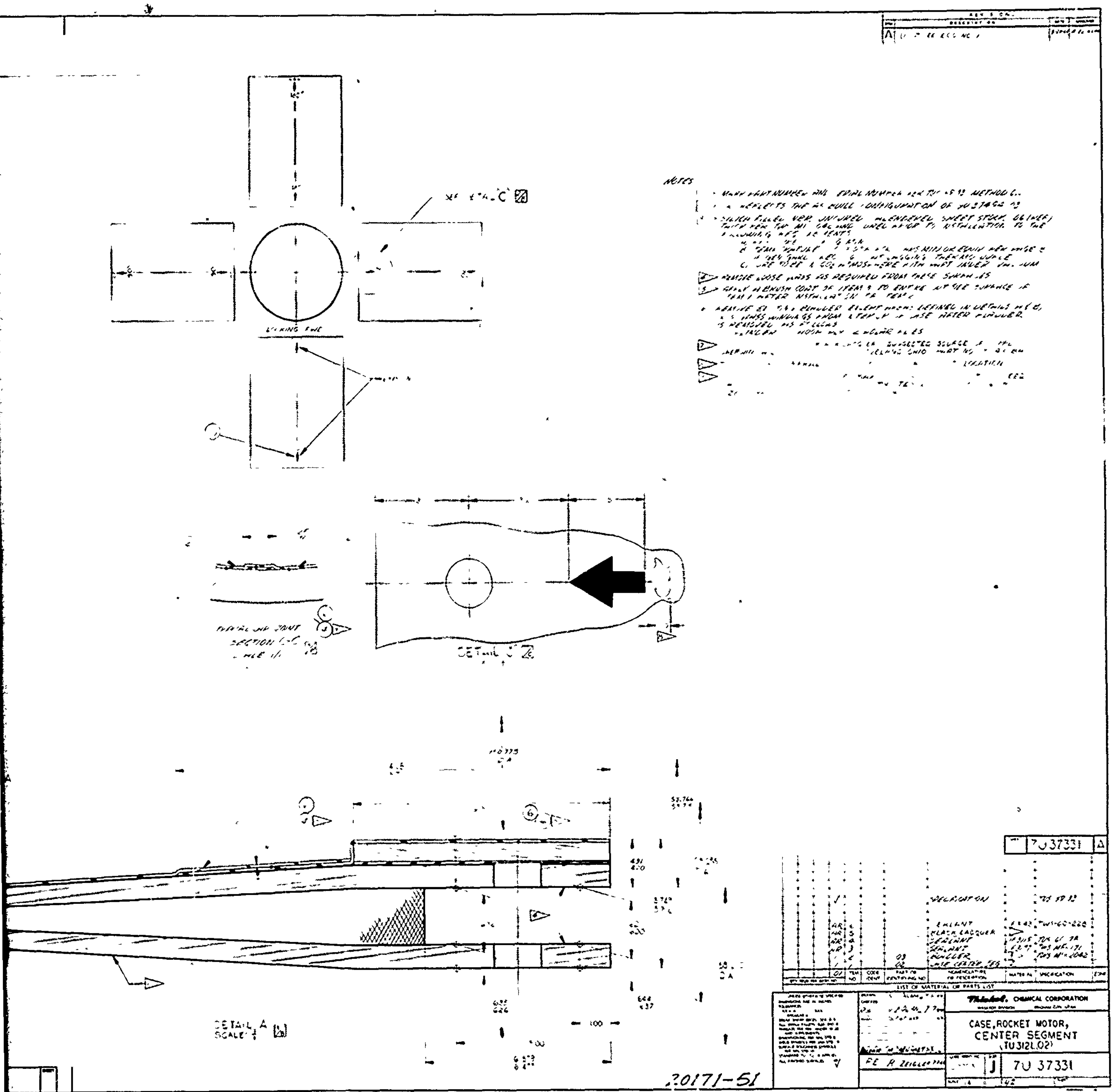

(C) Figure 3. 156-S Center Segment

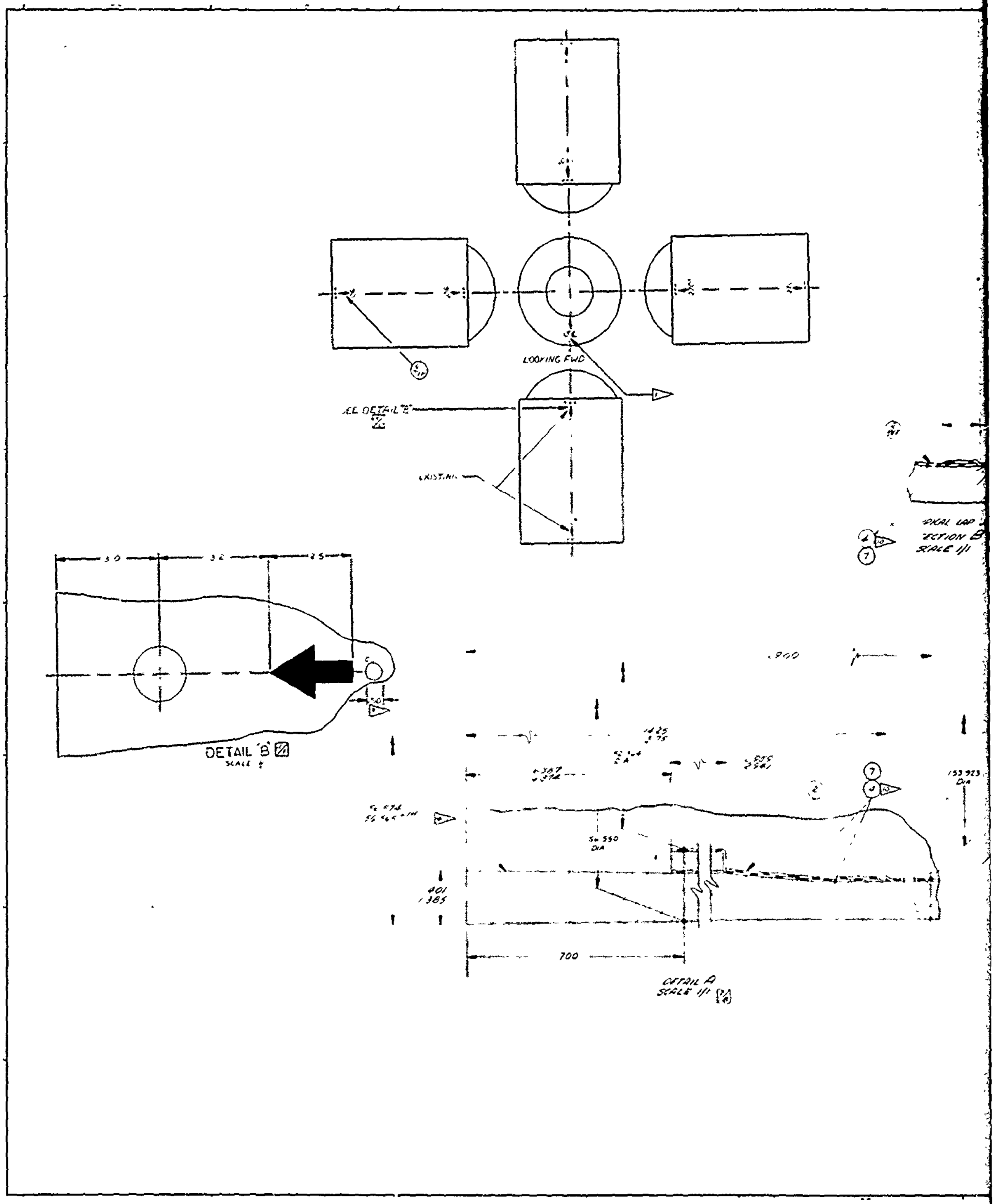
LOOKING FWD
SEE DETAIL "B"
EXISTING
DETAIL 'B'
SCALE
.900
700
DETAIL A
SCALE 1/1
TYPICAL LAP
SECTION B
SCALE 1/1

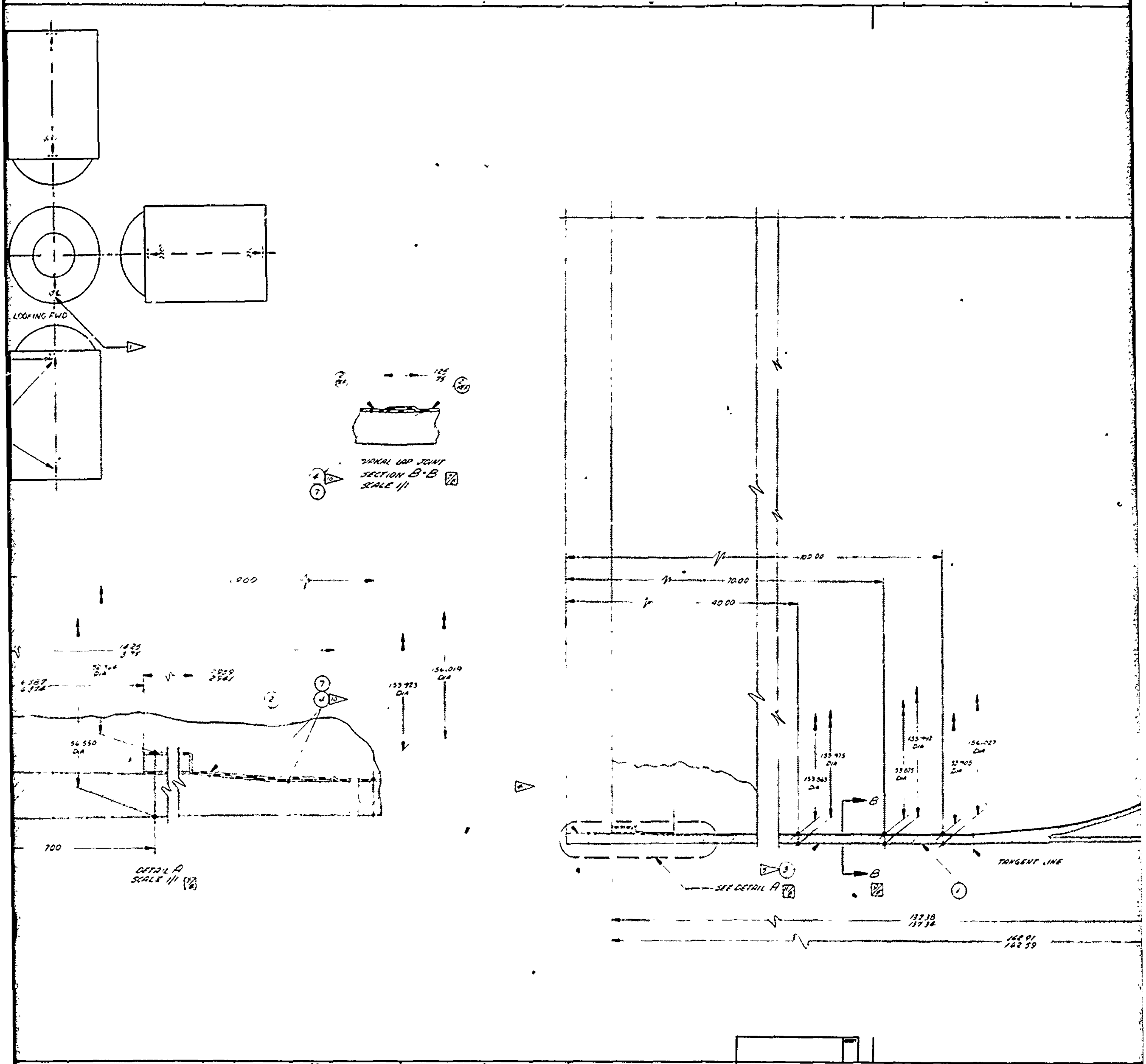
LOOKING FWD
SECTION B-B
SCALE 1/1
DETAIL A
SCALE 1/1
SEE DETAIL A
TANGENT LINE

2

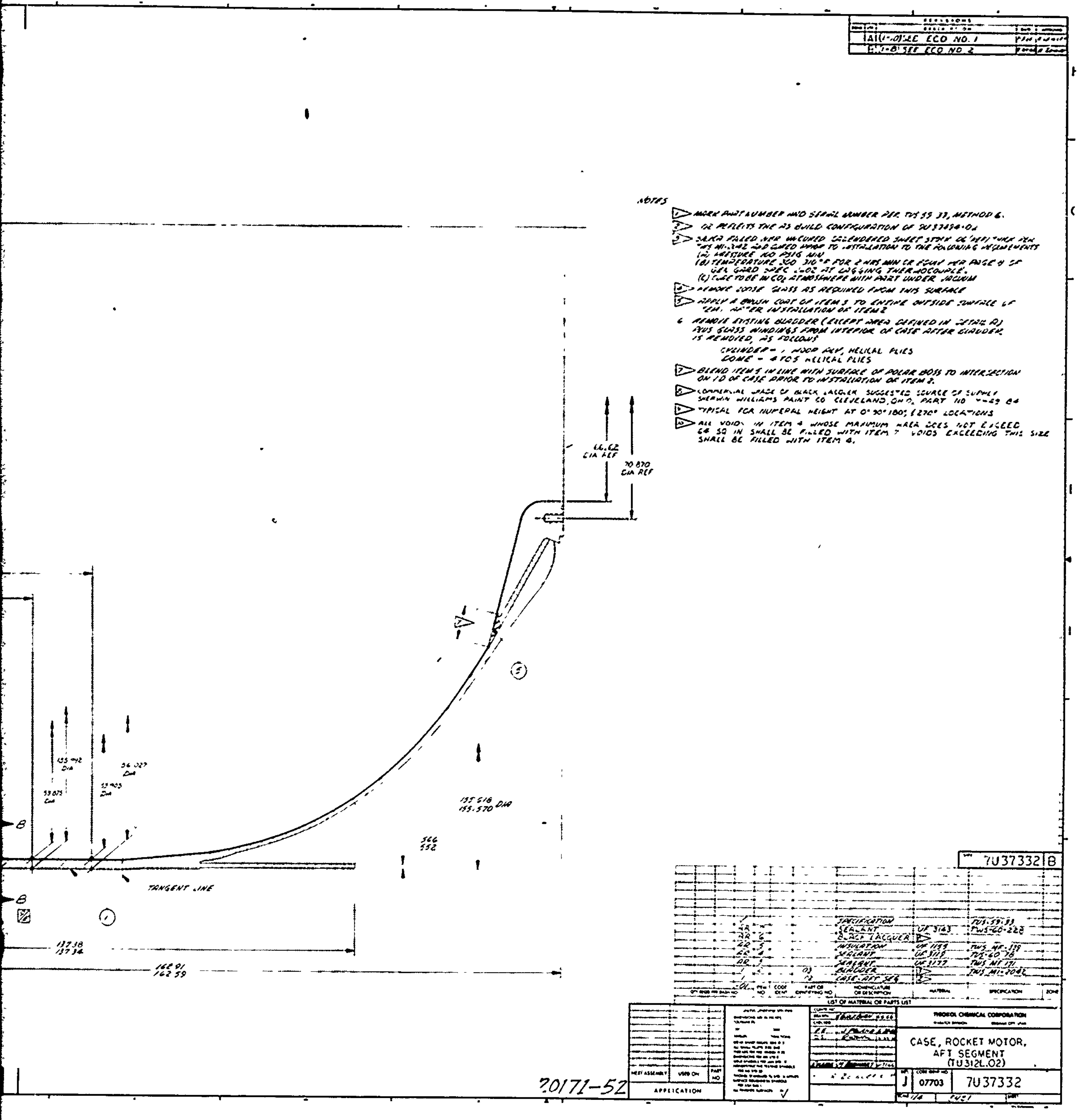

( )Figure 4. 156-8 Aft Segment

3

due to dry glass removal. An additional hoop layer was lost in a localized area of the aft segment prior to hydroburst. The original composite thickness was 1.03 inches in the cylinder.

(U) The segments were assembled by means of mating clevis joints designed to be critical in bearing (Figure 1). The tongue and clevis structures were composed of 0.020 in. AM-355 steel shims laminated between (polar or helical) fiberglass layers of the basic case. The longitudinal load carried by the fiberglass was transferred to the shims in interlaminar shear. The shims transferred this longitudinal load to the joint pin and thus to the stainless steel shims of the adjoining segment. In forward and aft segments where there was a large wrap angle, glass mat had to be added to transfer the shear load. Rubber replaced the hoop windings for 1.5 in. adjacent to the shim stacks, and longitudinal slits were made between the shim stacks to reduce hoop discontinuity. The clevis pin was fabricated from 18 percent nickel steel designed for shear and bending.

(U) The polar openings in the forward and aft domes were reinforced with forged 2014-T652 aluminum alloy rings.

(U) The B. F. Goodrich Buna-N rubber shear ply was placed between the case and polar bosses to reduce stress due to case distortion. It was also used as a shear ply between the skirts and the case.

(U) The skirts on the forward and aft segments were wound simultaneously with identical thickness and composition because of a manufacturing economy. The composite thickness of 0.602 in. was determined from load induced in the forward skirt by a simulated thrust load and weight of water incurred during hydrotest. Due to failure in hydrotest, the original forward skirt was replaced with one of the same configuration using S-994 glass preimpregnated with U.S. Polymeric's E717 epoxy resin. Gen Gard V-45 Buna-N rubber was bonded between the replacement skirt and dome to provide a shear load transfer and to accept longitudinal case expansion.

(U) Table II lists all pertinent margins-of-safety for the original design based on a MEOP of 860 psig. Table III lists the revised margins prior to static test due to joint damage, glass removal, and aft skirt repair. Table IV lists the revised margins prior to hydroburst test due to glass removal.

(U) b. Hydrotest--There were three hydrotests of the 156-8 segmented fiberglass case. The first hydrotest was conducted to verify the design and fabrication of the segmented fiberglass case, the second was to verify the structural integrity of the case following the replacement of the forward skirt, and the third was to verify that the replacement bladder and seal design were pressure tight. Hydrotests were conducted in test stand T-17 (Figure 5). The first two were conducted under Contract AF 33(657)-11303.

(U) The first test was conducted on 1 Oct 1965. The case was pressurized to a hydroproof pressure of 998 psig. After the pressure had been held at the hydroproof level of 998 psig for 48 sec, the forward skirt crumpled just below the attachment shear ply. Since the failed skirt continued to transmit the 1,700,000 lb thrust and weight loading, the hydroproof pressure was held for the remainder of the scheduled 2 min cycle. Pressure was then reduced at the rate of 7 psig/second.

(U) Except for the skirt failure, the case performed as expected during the hydrostatic test. The joints showed no delamination or bearing deformation in the shim composite. The forward dome was crazed in the meridional direction; however, it has been shown in other fiberglass programs that the meridional dome crazing has no detrimental effects on the glass fibers.

(U) Inspection of the skirt showed that the inner 29 percent of the skirt had a low resin content and was delaminated. The failed skirt was therefore removed, and an identical replacement was fabricated out of prepreg roving and bonded to the case.

(U) Following the skirt rework, the case was hydrotested the second time on 29 Mar 1966. A manifold pressure of 200 psig at 1,200 gpm was needed to maintain a pressurization rate of 5.93 psig/second. The case was held at an average proof pressure of 990 psig of 123 sec, the maximum pressure being 1,003 psig.

TABLE II

(U) MOTOR CASE DESIGN SUMMARY

Item	Design Strength	Stress or Load at MEOP 860	Safety Factor
Joint Bearing			
Tongue (lb/pin)*	269, 300	159, 000	1.70
Clevis (lb/pin)*	152, 400	88, 000	1.73
Pin			
Bending (psi)*	270, 000 (yield)	193, 000	1.40
Shear (psi)*	168, 000	66, 200	2.52
Case Wall Hoop Glass			
Forward Segment (psi)**	335, 000	202, 000	1.66
Center Segment (psi)	335, 000	202, 000	1.66
Aft Segment (psi)**	335, 000	202, 000	1.66
Skirt			
Compression (lb/in.)	8, 250	3, 080	2.68
Forward Attachment, Shear (psi)	750	348	2.15
Aft Attachment, Shear (psi)	750	254	2.96
Polar Boss (Forward)			
Bending (psi)	63, 000	23, 900	2.64
Tension (psi)	220, 000	98, 200	2.20
Polar Boss (Aft)			
Bending (psi)	63, 000	36, 900	1.70
Tension (psi)	100, 000	37, 700	2.65

*These margins were reduced for static test due to joint damage (see Table III).

**These margins were reduced for static test and further reduced for hydroburst (see Table IV).

TABLE III

(U) REVISION OF MARGINS FOR STATIC TEST

Item	Design Strength	Stress or Load at MEOP of 860 psig	Safety Factor
Joint Bearing			
Tongue (lb/pin)	237, 000	159, 000	1.50
Clevis (lb/pin)	126, 500	88, 000	1.42
Pin			
Bending (psi)	270, 000	239, 000	1.13
Shear (psi)	168, 000	83, 000	2.02
Joint Composite			
Longitudinal Stress (psi)	84, 000	67, 000	2.25
Case Wall Hoop Glass			
Forward Segment (psi)	335, 000	218, 000	1.54
Center Segment (psi)	335, 000	204, 000	1.64
Aft Segment (psi)	335, 000	204, 000	1.64
Skirt			
Aft Attachment, Shear Skirt Overwrap (psi)	400	150	2.67

TABLE IV

(U) REVISION OF MARGINS FOR HYDROBURST

Item	Design Strength	Stress or Load at MEOP of 860 psig	Safety Factor
Case Wall Hoop Glass			
Forward Segment (psi)	335,000	228,000	1.47
Aft Segment (psi)	335,000	206,000	1.62

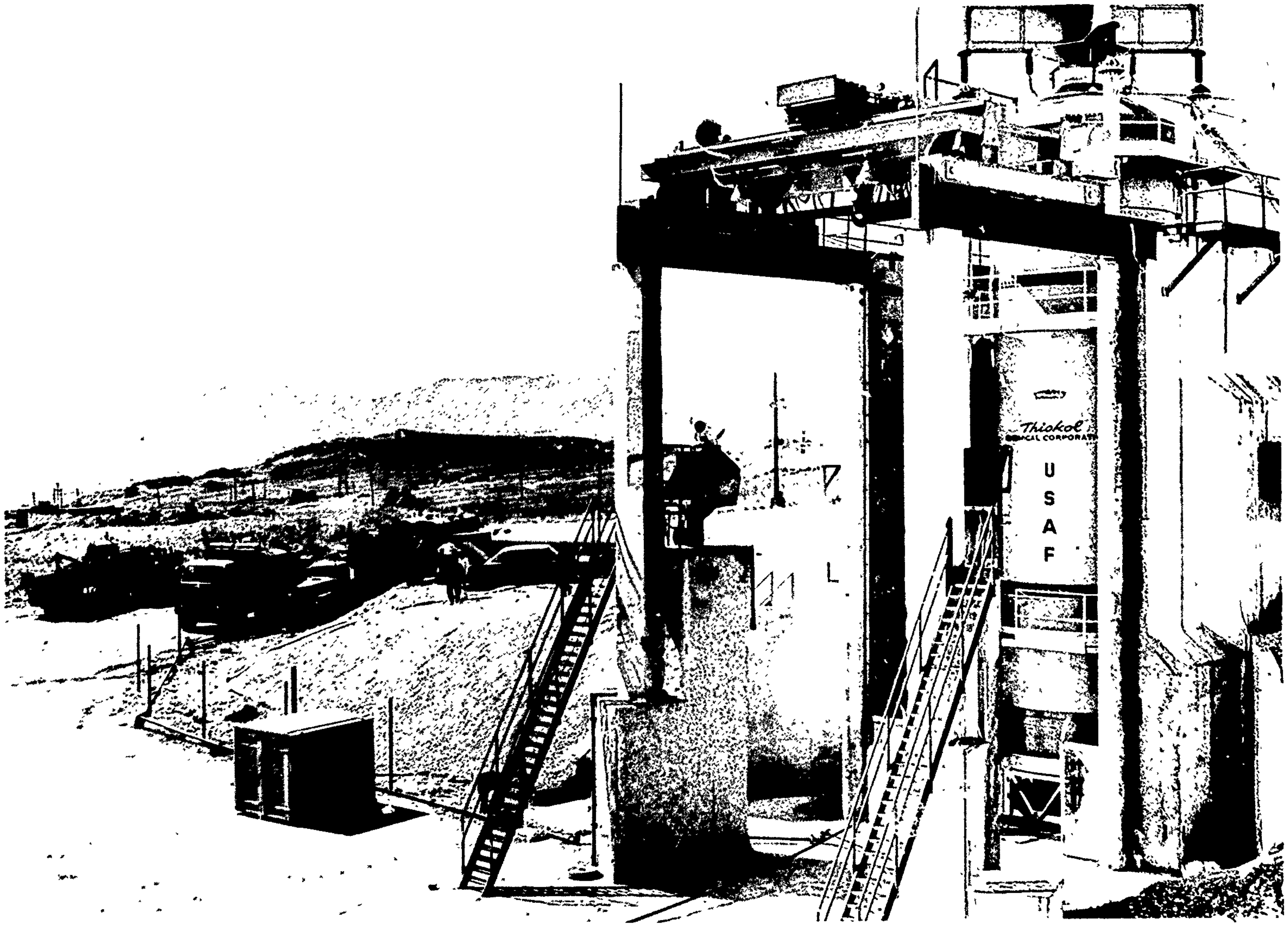

(U) Figure 5. 156-8 Case in Hydrotest Stand, Pressure Pump Trucks in Background

(U) The case performed as expected during the hydrostatic proof test. The replacement skirt transmitted a simulated thrust load of 1.73×10^6 pounds. The only evidence of damage from the test was loss of a glass cloth patch on the forward segment for retention of previously broken strands and failure of two strands in the aft segment. Both of these discrepancies could be repaired prior to subsequent use of the case.

(U) Following this second hydrotest, the case was transferred to the 156-8 motor demonstration program. Post-test inspection of the case revealed inadequate adhesion within the inner plies of the glass resin composite. The existing bladder and inner four to five plies of glass were removed until a sound structure was found. Following removal and cleanup, a new bladder of 0.06 in. thick cured V-45 rubber was bonded to the case with UF-3119.

(U) Segment insulation was fabricated and installed. After installation, seal and joint interfaces were machined in the segment insulation. Seals were fabricated with neoprene rubber in a channel shape and fitted with a compression spring to hold the legs of the channel against the sealing surfaces at low pressures.

(U) The case was assembled and then hydrotested on 30 Sep 1966. The case pressure was increased at 2.3 psig/sec to a maximum of 897, held for 123 sec and depressurized at 6.3 psig/second.

(U) The case withstood the hydrotest with no structural failure and no leakage in the joint areas. There was a small amount of leakage in the forward segment 42 in. from the joint. Post inspection revealed a small cut in the bladder. The cut was repaired by patching with Buna-N prior to loading the segments for static test.

(U) c. Breakover and Handling--Several conditions had to be checked to insure that process handling would not induce excessive loads on the case. Prior to segment loading, the segments were handled by brackets attached to the tongues, clevises, or skirts. Handling empty segments did not impose any significant loads. Loaded segments were handled with potted lifting rings or handling harness as shown on page 293. The segments were lifted from the loading pit in the vertical position. The segment was then broken over to a horizontal position, and remained horizontal during assembly for static test. The weight and center-of-gravity locations of the loaded segments relative to the harness are shown in Figure 6. Following static test, the case was transported in the assembled condition, rather than disassembling the segments. The aft part of the case was lifted by the aft polar boss because of the aft skirt overwrap failure during static test. The case was broken over at the hydroburst test stand and lowered into the testing position.

(U) When handling the individual segments, the worst load occurs during loaded segment breakover. A summary of the loaded case capability and safety factors appears in Table V. Note that the minimum safety factor for 1g loading is 4.2. The limiting condition on the forward and aft segments is bearing stress by the skirt bushings. The limiting condition on the center segment is case wall buckling.

(U) The case was removed from static test stand T-24 and loaded on the transporter. The case was then transported to manufacturing to have a new bladder installed for hydroburst. The case was handled by lifting from a plate attached to the aft polar boss and two brackets which attached to the forward skirt. After bladder repair the case was taken to T-23, broken over to the vertical position, and lowered into the hydrotest pit by the aft boss. Table VI gives a summary of the loads and safety factors. The minimum safety factor is in the forward skirt and is equal to 4.7.

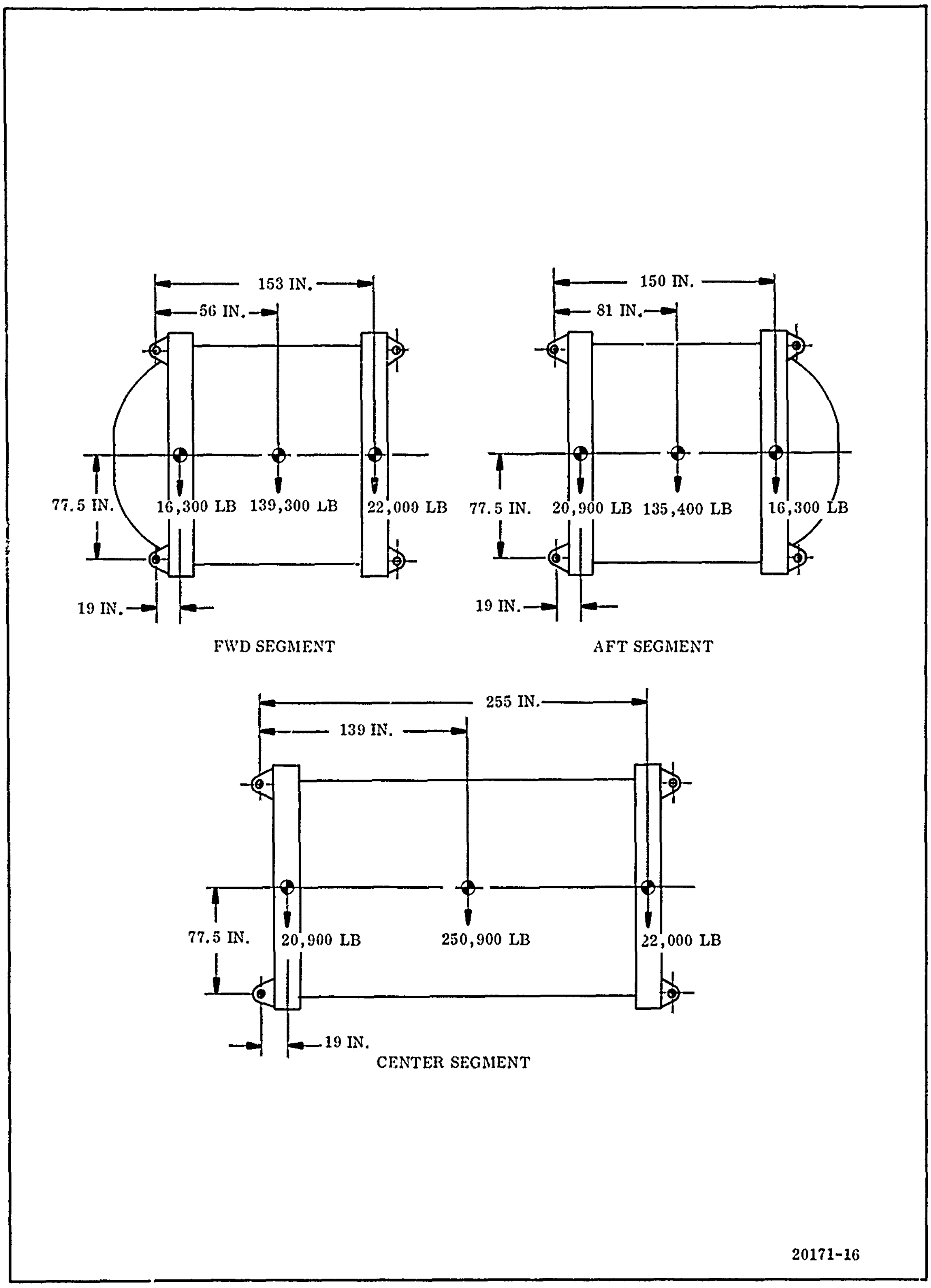

(U) Figure 6. C G Locations for Loaded Segments

TABLE V

(U) LOADED SEGMENT LOADS AND SAFETY FACTORS

Segment	Maximum Lug Load (lb)	Maximum Axial Load (lb/in.)	Maximum Shear Load (lb/in.)
Forward	88, 900	1, 620	450
Center	146, 900	3, 430	580
Aft	86, 300	1, 470	490

CASE CAPABILITY

Description	Type of Load	Load (lb/in.)
Skirt Buckling	Axial	8, 250
Skirt Shear Ply	Axial	7, 200
Skirt Bearing from Bushing	Shear	3, 940
Shear Tearout Skirt	Shear	4, 970
Bolt Shear	Shear	3, 620
Center Segment Buckling	Axial	14, 320

CASE SAFETY FACTORS, 1g LOADING

Segment	Minimum Safety Factor Axial	Minimum Safety Factor Shear
Forward	4.4	8.7
Center	4.2	N/A
Aft	4.9	8.0

TABLE VI

(U) EMPTY CASE LOADS AND SAFETY FACTORS

Location	Horizontal Maximum Lug Load (lb)	Vertical Maximum Lug Load (lb)
Aft Attachment	14,500	29,000
Forward Attachment	7,250	N/A

ATTACHMENT CAPABILITY

	Type of Load	Load (lb)
Boss to Case Interface	Vertical, Compression	7.05×10^6
Boss to Case Interface	Horizontal, Tension	0.682×10^6
Boss to Case Interface	Horizontal, Shear	1.63×10^6
Skirt Bearing	Horizontal, Bearing	33,700
Bolt Shear	Horizontal, Shear	30,200

MINIMUM CASE SAFETY FACTORS

Location	Safety Factor
Aft Boss	>10
Forward Skirt	4.7

(U) B. CASE FABRICATION

(U) The case was fabricated as four separate components: (1) forward and aft skirt, (2) forward segment, (3) center segment, and (4) aft segment. The case was fabricated at B. F. Goodrich's Aerospace and Defense Products Division under Contract AF 33(657)-11303. After fabrication the case was hydrotested at the Thiokol Wasatch Division. During hydrotest the forward skirt failed. The old skirt was removed and replaced with a skirt fabricated at Thiokol's Pocatello facility.

(U) 1. CASE FABRICATION AT VENDOR

(U) The segments and skirts were wet wound with S-994 HTS glass roving with a resin content of 25 percent by weight. The resin system used was Epon 826/NMA/DMP-30.

(U) The case segments were fabricated on collapsible aluminum mandrels. The mandrels consisted of radial extrusions and stiffener rings. A layer of plaster was screeded over steel reinforcement wire to define the case contour.

(U) The forward and aft skirts were fabricated simultaneously (Figures 7 and 8) by winding over a cylindrical section with false domes. The mandrel was covered with B. F. Goodrich Buna-N uncured rubber for the shear plies and then 46 intermittent layers of polar and hoop glass were wound over the uncured rubber. The skirts were cured and machined to final dimensions.

(U) The forward segment mandrel had a polar boss and dome at one end and a false dome at the clevis end. There were a total of 96 building sequences during fabrication. These sequences consisted of intermittent layers of polar, reinforcement mats, shims, buffer and hoop layers (Figures 9 and 10). After winding and cure, the forward skirt was mated to the forward segment (Figure 11), and the assembly was then cured. The false dome was cut from the segment and the mandrel removed.

(U) Figure 7. Skirt Mandrel at Start of Polar Winding Sequence

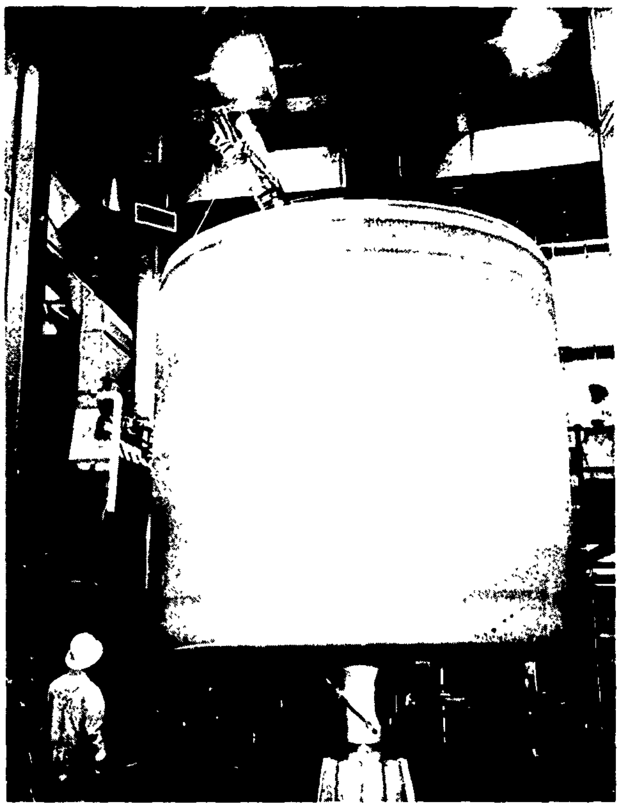

(U) Figure 8. Application of Third Polar Winding

(U) Figure 9. Application of Fiberglass Mat

(U) Figure 10. Shim Placement

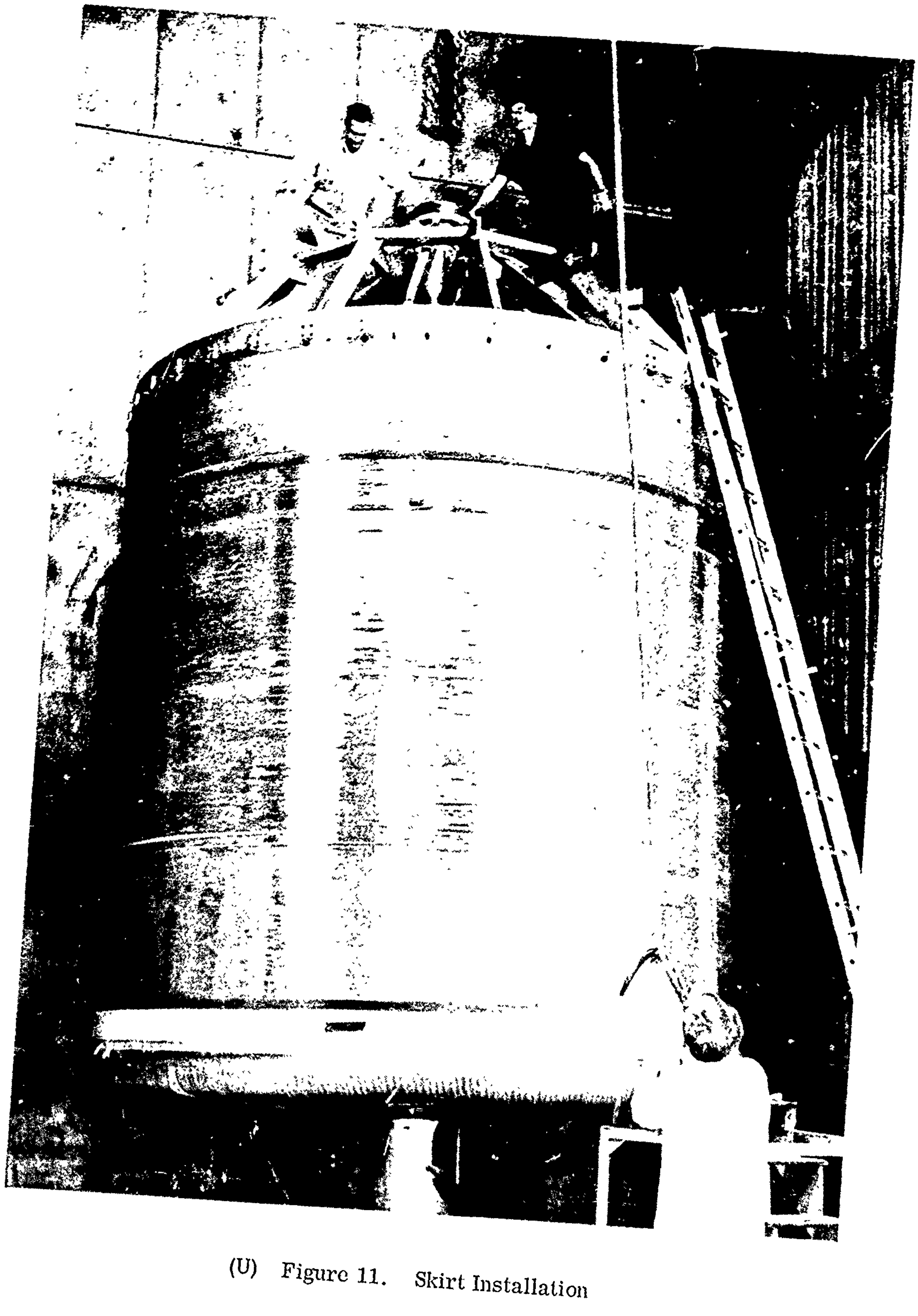

(U) Figure 11. Skirt Installation

(U) The center segment mandrel had false domes on both the clevis and tongue ends. There was a total of 112 building sequences during fabrication. The sequences consisted of intermittent layers of polar, reinforcement mat shims, buffer, and hoop layers. The segment was cured, the ends machined, and the mandrel removed.

(U) The aft segment mandrel had a polar boss and dome on one end and a false dome on the tongue end. There was a total of 105 building sequences consisting of intermittent layers of helical, reinforcement mats, shims, buffer, and hoop layers. After winding, the cured aft skirt was mated to the aft segment and the assembly cured. The false dome was cut from the segment and the mandrel removed.

(U) The segments were then assembled and the clevis and tongue match bored. The boring operation consisted of a three step operation: (1) Trepan laminated to prepunched hole diameter, (2) hole enlarged to 0.010 in. of final diameter with Wohlhaupter head, and (3) final diameter bored with conventional boring bar. Slits were sawed between the tongue and clevis shim stacks to allow for circumferential expansion.

(U) 2. FORWARD SKIRT REPLACEMENT

(U) During hydrotest the forward skirt buckled at 998 psig. Visual examination showed that 29 percent of the skirt was resin starved and delaminated. Analysis showed that if the skirt had been sound, it would have withstood the load. Therefore, the decision was made to fabricate a new skirt of the same strength to replace the old one.

(U) The original skirt was removed by making longitudinal cuts down to the shear ply. The shear ply was removed with a coarse sanding disc. Visual inspection showed no damage to the forward dome.

(U) The replacement skirt was wrapped on a steel mandrel which was swept with plaster. S-994 HTS glass roving, preimpregnated with USP-E-717 epoxy resin, was used to fabricate the skirt. Uncured strips of Gen Gard V-45 NBR rubber were applied over the mandrel. The 44 layers of interspersed hoop and polar glass were wrapped over the mandrel and uncured rubber. The polar wrap angle was 10 degrees. The skirt was oven cured and machined to final size.

(U) Several tests were conducted to select a room cure adhesive which had a shear strength of 750 psi. The following adhesive was chosen to bond the replacement skirt to the forward dome.

Ingredient	Percent by Weight
Liquid Epoxy Resin	38.4
Versamid 140	38.4
Asbestos Floats	23.2

The skirt was placed in correct alignment with the case and pressed into position with a hydraulic piston (Figure 12). The bond was cured at 90°F for 18 hours. The skirt was cut off with an abrasive wheel, and the holes were drilled for the aluminum bushings. The aluminum bushings were installed and bonded in place with epoxy resin.

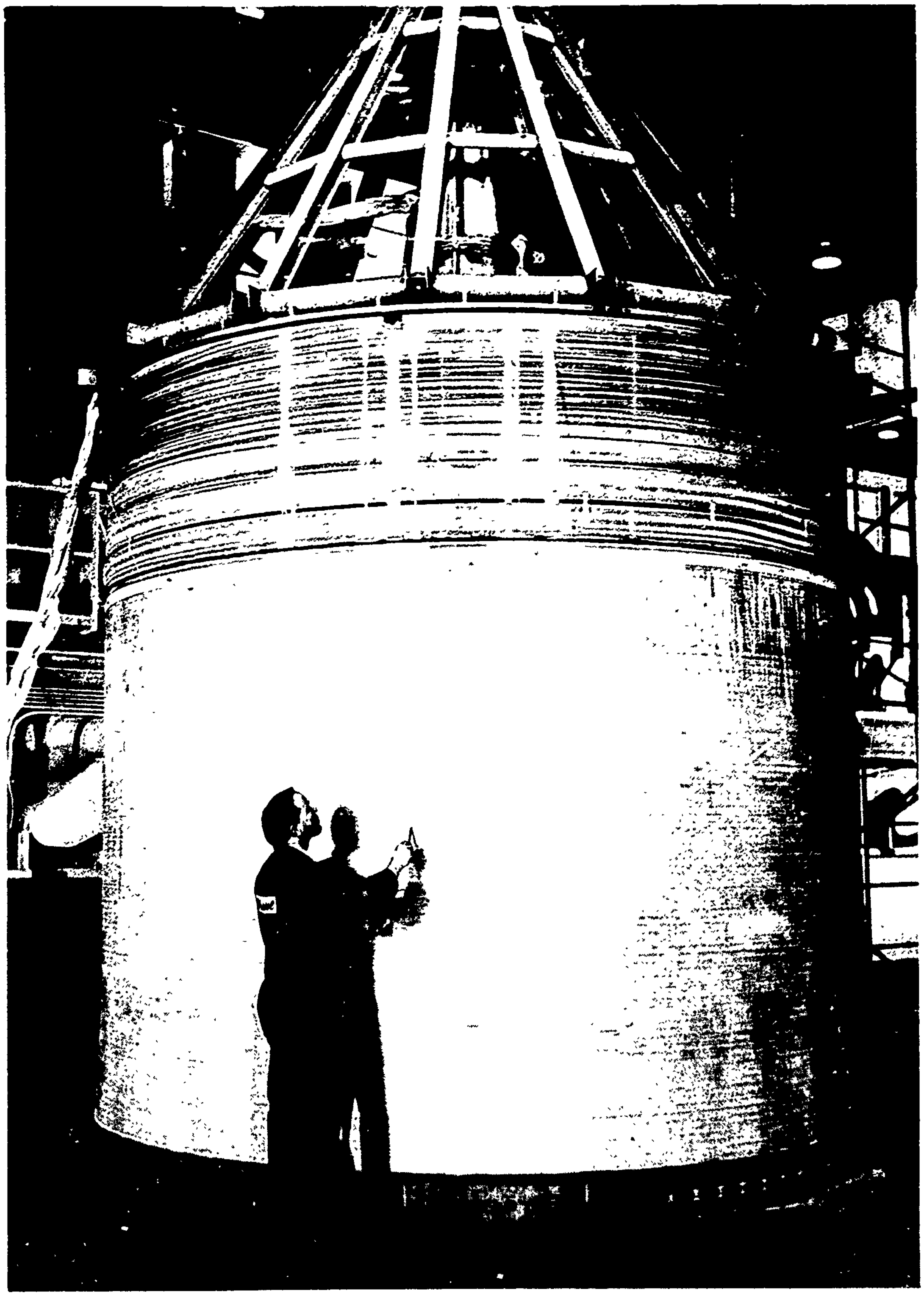

(U) Figure 12. Skirt Placement on Segment

(U) C. CASE REPAIR

(U) 1. BLADDER REPLACEMENT

(U) a. Repair Considerations--The original bladder (0.090 in. thick B. F. Goodrich Buna-N rubber) was inadequately bonded to the basic wall structure of the segments. This condition was attributed to a lack of resin in the initial fiberglass layers at the segment inside diameters. A good bond must be maintained between the segment walls and bladder to support the propellant, which will adhere to the bladder when cast and cured. Therefore a plan was initiated to replace the original bladder with a 0.060 in. thick bladder of Gen Gard V-45.

(U) A series of peel tests and visual inspections were made of each segment to determine the number of dry glass layers and the surfaces necessary for structural bond requirements. Removal of fiberglass material from segment walls results in lower factors of safety than indicated in the 156-8 case design report; however, as previously stated, the case was designed for an ultimate pressure of 1,200 psig with a minimum safety factor of 1.2. Therefore, at a MEOP of 860 psig, the safety factor and strength level of the segments after case repair, although reduced, was considered adequate and within design requirements.

(U) b. Case Repair--The bladder was completely removed from the cylinder and domes of each segment except for a 14 in. strip at the joint ends (Figure 13). The original bladder was not removed in the joint areas to avoid disturbing the internal hoop rings in the segments. These rings provide the required hoop strength in the joint areas and are also the mating surfaces of the segments. Therefore, it was essential that the hoop rings not be disturbed. Also Buna-N strips bonded over the joints for hydrotest seal were removed (Figure 14).

(U) The 14 in. strip of original bladder was bonded back to the case wall by injecting UF-3119 between the bladder and case wall. The UF-3119 was then cured under vacuum at ambient temperature.

(U) Figure 13. Bladder and Loose Glass Removal

(U) Figure 14. Removal of Buna-N Strips from Joint Areas

(U) After bladder material was removed, the loose (unbonded) fiberglass in each segment was removed until a sound laminate was evident. The amount of glass requiring removal was different in each segment. In the forward segment, one layer of circumferential (hoop) windings and one layer of polar windings were removed from the cylinder. Two and one-half layers of polar windings were removed from the forward segment dome, extending from the edge of the forward boss to the beginning of the cylinder.

(U) One half layer of hoop windings and one layer of polar windings were removed from the center segment. In the helically wound aft segment, one half layer of hoop windings and two helical layers were removed from the cylinder. Two and one-half layers of helical windings were removed from the aft dome, extending from the edge of the polar boss to the beginning of the cylinder.

(U) To determine the bond strength to the fiberglass laminate following dry glass removal, four test plates (2 by 4 in.) were bonded in the cylindrical areas of each segment using UF-3119 and UF-3177 for tensile adhesion tests. Both formulations were cured under vacuum at ambient temperature. One sample plate from each formulation in each segment was step pulled as shown below.

Step	Time (min)	Tensile Load (psi)
1	1.0	10
2	1.0	20
3	1.0	30
4	1.0	40
5	1.0	50
6	1.0	60
7	1.0	70

(U) The other test plate of each formulation was pulled for 1 min at 70 psi. The test arrangement is shown in Figure 15. All test plates passed the tensile adhesion test except the UF-3177 full load test plate in the center segment which failed after 57 sec at 70 psi. Inspection of the failed plate showed an actual bond area of approximately 4 sq in., indicating that failure had actually occurred above bond strength.

(U) Figure 15. Adhesion Test Arrangement

The tensile adhesion tests demonstrated that either UF-3119 or UF-3177 were adequate for bonding the replacement bladder into the segments. UF-3119 was selected because of superior working qualities.

(U) Upon the successful demonstration of a sound fiberglass laminate to which a new bladder could be bonded with assurance of sufficient bond strength to support the propellant grain, bladder installation was initiated. The new bladder material (General Tire and Rubber Co silica filled NBR (V-45) procured in 36 in. wide rolls) was wound onto a large (44 in. diameter) drum with Trevarno film between layers and autoclave cured.

(U) The material was then cut into strips that extended the full length of the segments (Figure 16) and bonded into the segments with UF-3119) They were cured by installing vacuum bags on both the inside of the segment over the bladder strip and on the outside of the segment behind the strip of bladder being installed (Figure 17), then applying vacuum and curing for minimum of 12 hours. The configuration of the repaired case segments was shown in Figures 2 thru 4.

(U) To verify that the required bond strength was obtained between the new case bladder and fiberglass laminate, two 2 by 4 in. test plates were bonded into the cylindrical section of each case segment after the bladder was installed. All test plates passed the tensile adhesion test of 70 psi for 1.0 minute.

(U) c. Effects of Repair on Case Design Strength--In addition to the case strength reduction resulting from the glass removal, other deviations occurred in handling and testing the case segments. The factors that caused degradation in the case strength are explained as follows.

1. Glass removal because of bladder unbondedness.
2. Loss of 4 of the 3,200 center segment clevis joint shims during assembly of the case for the second hydrotest under Contract AF 33(657)-11303.
3. The local cutting of 1 1/2 helical layers adjacent to the aft polar boss after bladder removal.

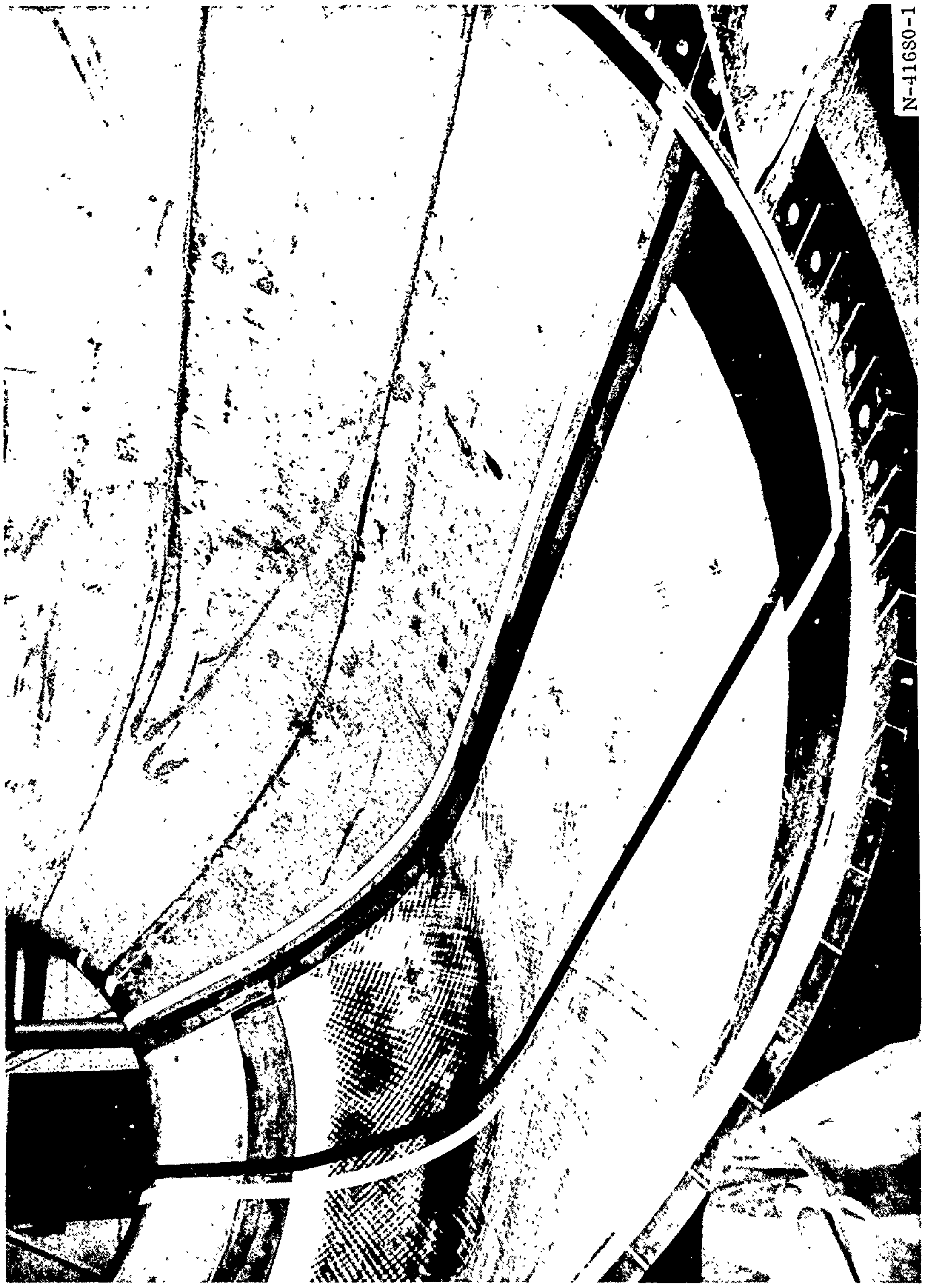

(U) Figure 16. Replacement Bladder Partially Installed

(U) Figure 17. Vacuum Bag Installation Over Bladder

4. Scratches on the forward segment, occurring during skirt repair under Contract AF 33(657)-11303, which locally cut 2.5 layers of hoop windings.

(U) The combined effect of the above discrepancies was a reduction of the predicted burst strength of the case from above 1,500 psig to 1,440 psig. The analysis of the effects of each of the above discrepancies is presented in the following sections.

(U) (1) Glass Removal--The number of polar or helical and hoop layer of fiberglass required by the original design and the number remaining after bladder and glass removal are shown below.

	Original		Rework	
	Polar/Helical Layers	Hoop Layers	Polar/Helical Layers	Hoop Layers
Forward Segment	34	47.5	31.5	46.5
Center Segment	28	48	27	47.5
Aft Segment	40	38	37.5	37.5

(U) Stresses and safety for the above conditions were shown in Tables II thru IV.

(U) In the analysis of case strength after glass removal, Thiokol assumed that the maximum amount of glass removed from any one segment was removed from the entire segment; that is, in the forward segment where 2.5 layers of polar windings were removed from the dome area and only one polar layer was removed from the cylinder; 2.5 layers were assumed to be removed from the entire segment.

(U) (2) Shim Damage--During the assembly of the case for the second hydrotest under Contract AF 33(657)-11303, interference between the center and aft segments resulted in the loss of four shims from the outside diameter of the inner clevis leg of the center segment. The four damaged shim stacks, which were reduced in total number of shims from 16 to 15, were randomly spaced around the segment (i.e., no two shim stacks incurring damage were adjacent to one another). For the purpose of analysis, it was assumed that the 16th shim (the outer shim of the inner leg) from all 100 shim stacks was damaged. Since there will be some distribution of load from the damaged shim stacks to the adjacent undamaged stacks, the analysis of the effect of the damage is conservative.

(U) The clevis joint was originally designed for an ultimate strength of 152,400 lb per clevis leg per pin. The shims next to the clevis gap (the No. 16 and 17 shims) were the most highly loaded shims in each stack, thus the loss of the No. 16 shims shifted the loading coefficient curve (Figure 18) and reduced the ultimate strength to 146,900 lb per leg per pin. Additional shims were removed during case assembly for static test. The minimum margins-of-safety were shown in Table III.

(U) (3) Local Cutting on Aft Dome--During the removal of the helical glass in the aft segment, 1.5 helical layers, over and above the 2.5 layers removed, were cut in a local area next to the aft polar boss. The cut was 1.5 layers deep by 3/16 in. wide by 2 in. long. Assuming the cut rendered the complete 1.5 layers ineffective, the effective glass thickness was reduced four percent. The cut reduced the factor of safety to 1.68 at MEOP of 860.

(U) (4) Local Scratches on Forward Segment--During the installation of the replacement skirt on the forward segment under Contract AF 33(657)-11303, the locking knob on a drill clamping fixture loosened from the attaching bolt, allowing the fixture to drop. When the fixture dropped, it hit the segment in four places and caused local abrasion of the outer 2.5 layers of hoop fibers. Based upon the assumption that the 2.5 locally damaged hoop layers were ineffective in carrying hoop loading, the resultant safety factor at a MEOP of 860 psig was shown in Table III.

(U) 2. DAMAGED JOINT

(U) There were three clevis legs on the forward segment that were damaged in the process of handling the case. The worst clevis leg was displaced 0.20 in. radially outward (Figure 19). Cracks progressed axially about 1.5 in. from the hole at the end of the saw cut between shims. The immediate area around the cracks

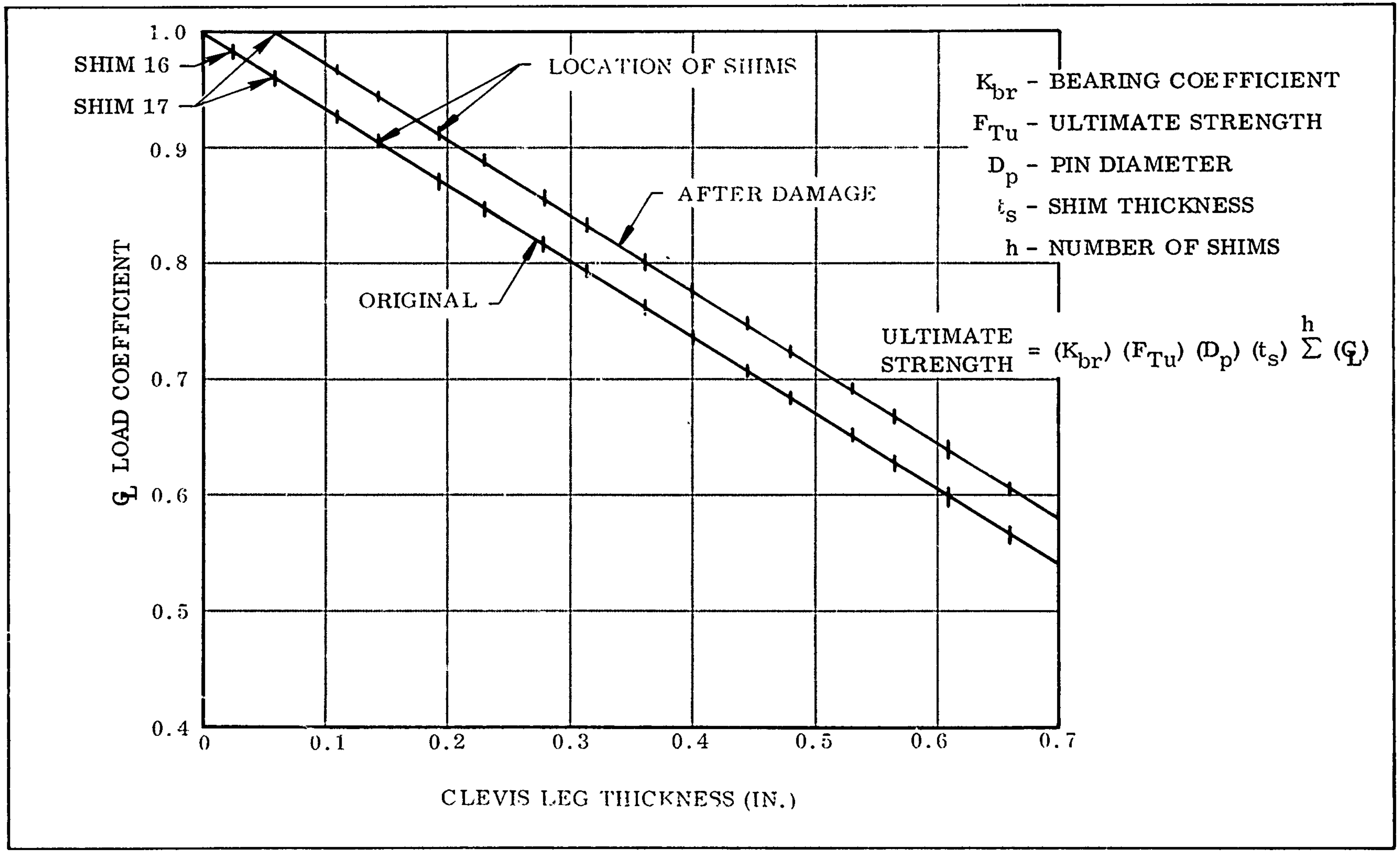

(U) Figure 18. Relative Deflections for Clevis Leg Shims

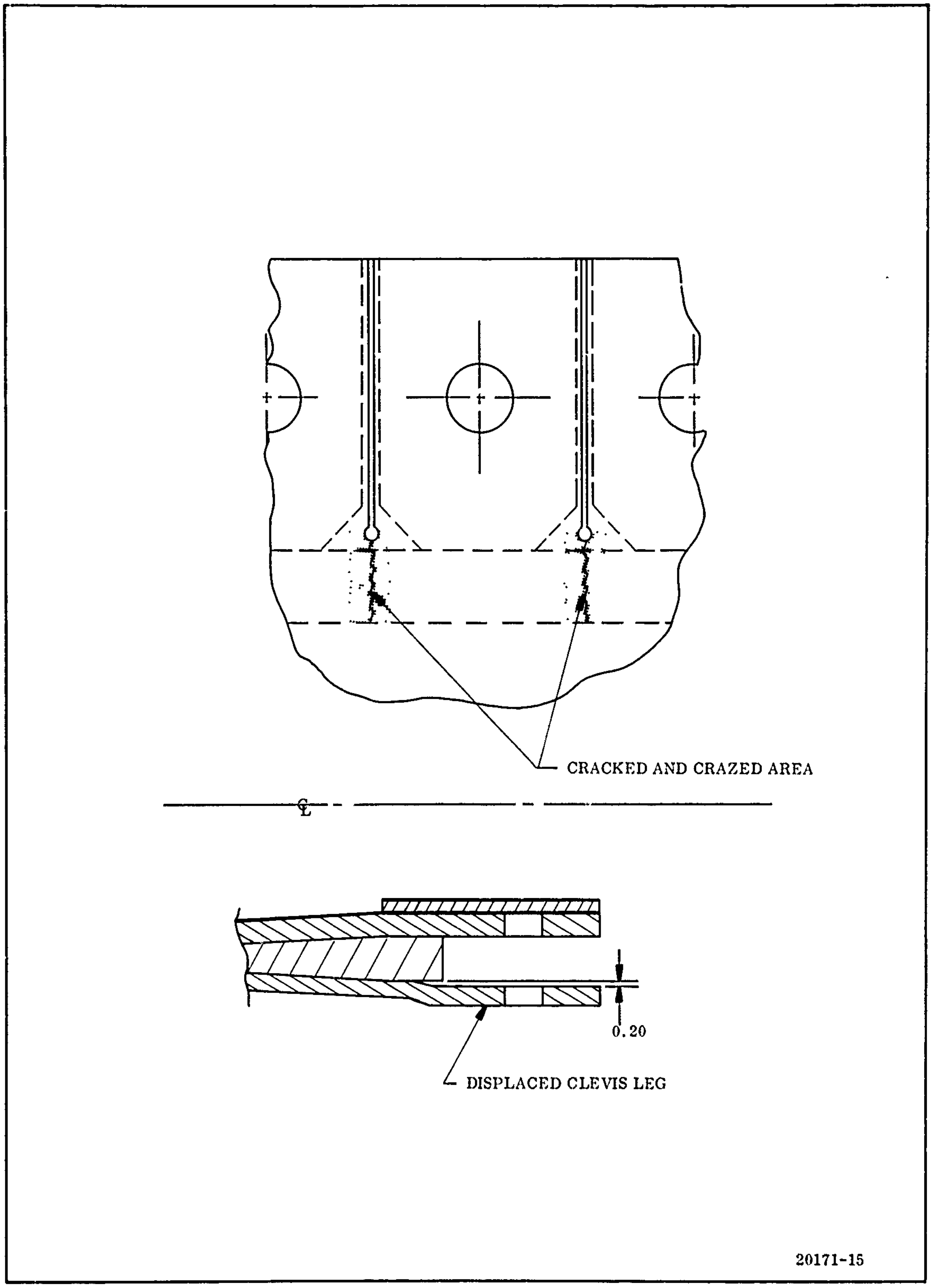

(U) Figure 19. 156-8 Damaged Clevis Legs was crazed. The cause of the damage could not be traced, but it is felt that the problem was due to improper installation of the rounding rings. The rounding screws left indentations in the glass behind the shim where the rubber replaced the hoop windings. The rounding ring screws had very small contact pads and were apparently overtorqued to round the loaded segment. This condition in combination with an axial force from a rounding ring probably caused the damage.

(U) It was felt that the pin should be removed from the damaged clevises because the extent of the fiber damage was not known. An orthotropic finite element analysis was used to analyze the pin removed condition (Figure 20). The input contained material properties in three directions for the glass steel composite, glass rubber composite, and the glass composite. Boundary conditions were the following: side one, free in the Y direction and fixed in X direction; side two in the area of the pins, fixed in the Y direction with a deflection in the X direction equal to the hoop deflection; side three, free in the Y direction with hoop deflection input in the X direction; side four, free in the X direction with a case load of 25, 000 psi in the Y direction.

(U) It can be seen from the graph in Figure 20 that a high stress exists at the end of the cracked area. Stresses of that magnitude are unacceptable and, therefore, a pin must be added to the damaged clevis leg. If an undersized pin were inserted, the pin load would be reduced to a level that the damaged clevis could accept.

(U) Several computer runs were made using different pin boundary conditions. After examining the information, it was felt that the optimum combination would be a 0.080 in. undersized pin in the damaged shim and a 0.010 in. undersized pin in the two adjacent clevises. This would result in 36 percent of the nominal load in the damaged clevis. From Figure 20 it can be seen that the effects of the undersized pins cannot be detected on the fourth clevis on either side of the damaged area. The clevis legs adjacent to the damaged clevis accept 122 percent of the nominal load. This condition did not affect the joint strength as static test pressure was considerably below the design pressure.

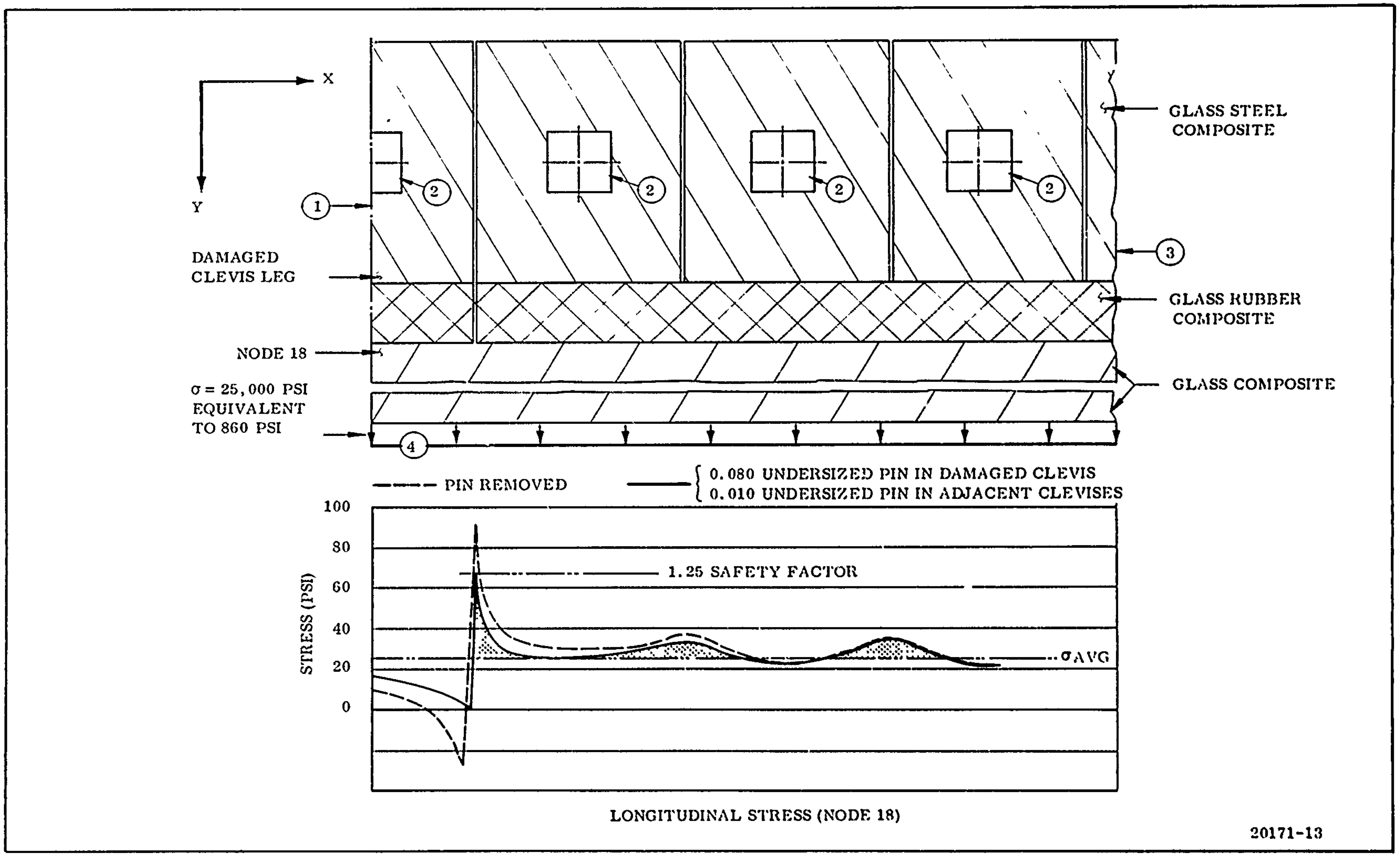

(U) Figure 20. Results of Finite Element Analysis

(U) A finite element analysis was conducted reducing the material properties in the area of the cracks to account for resin crazing. This analysis indicated that it may be possible to accept the load induced by pin removal. Since the amount of damage in the clevis leg was not known, the possibility remained that the damaged clevis might fail during firing. If the clevis did fail, there was a good chance that the joint would accept the static firing load.

(U) It was felt that using undersized pins minimized the risk. A summary of the loads and safety factors is shown in Figure 21.

(U) 3. AFT SKIRT REPAIR

(U) The aft skirt failed during motor assembly in the test stand. Prior to skirt failure the motor was supported by jacks and fore and aft trunnion supports shown in Figure 22. As the load was removed from the jack supports, the skirt case junction separated as shown in Figure 23. The total load was not removed from the jacks until the amount and cause of the damage could be assessed. After investigating the cause and type of damage, it was apparent that the motor could not be fired without repairing the skirt or supporting the motor in a different manner.

(U) The failure occurred in the skirt laminate and not between the laminate and rubber shear ply. Fore and aft movement of the skirt relative to the case was detected on the outer surface of the case. The 2.5 layers of hoop at the forward end of the skirt were buckled and had separated from the skirt in many areas.

(U) The failure of the skirt was caused by a combination of compressive loads and interlaminar tension. Figure 24 shows the static reaction loads on the case. The shear load from the case tends to be transferred through the rubber shear ply into the skirt. The shear deformation in the rubber changes the load distribution in the skirt from a pure cosine shear distribution to a cosine normal load distribution supported by shear as shown in Figure 25(A). Taking a section of the skirt as a ring it can be seen that the top 90 deg of the ring is in compression, and has the

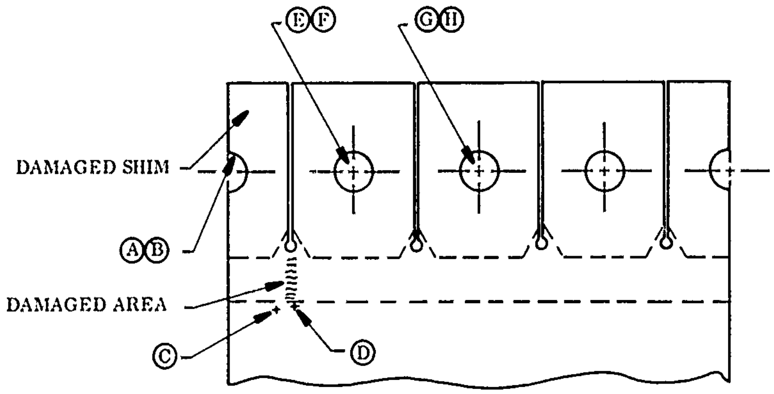

MEOP = 860 PSI

BOUNDARY CONDITIONS

A & B Δ AX = 0.080

E & F Δ AX = 0.010

LOCATION	TYPE OF STRESS	σ ACT (PSI)	σ ULT (PSI)	S.F.	NOTES
A - PIN	BENDING	123,000	270,000	2.20*	36% OF AVG PIN LOAD
B - SHIM	BEARING	89,400	317,000	3.54	36% OF AVG PIN LOAD
C - GLASS	SHEAR	28,000	50,000	1.78	COMPOSITE STRESS
D - GLASS	TENSION	67,000	84,000	1.25	COMPOSITE STRESS
E - SHIM	BEARING	289,000	408,000	1.42	122% OF AVG PIN LOAD
F - PIN	BENDING	239,000	270.000	1.13*	122% OF AVG PIN LOAD
G - SHIM	BEARING	254,000	412,000	1.60	108% OF AVG PIN LOAD
H - PIN	BENDING	208,000	270,000	1.30*	108% OF AVG PIN LOAD

*STRESSES BASED ON YIELD

20171-18

(U) **Figure 21. Stress Summary**

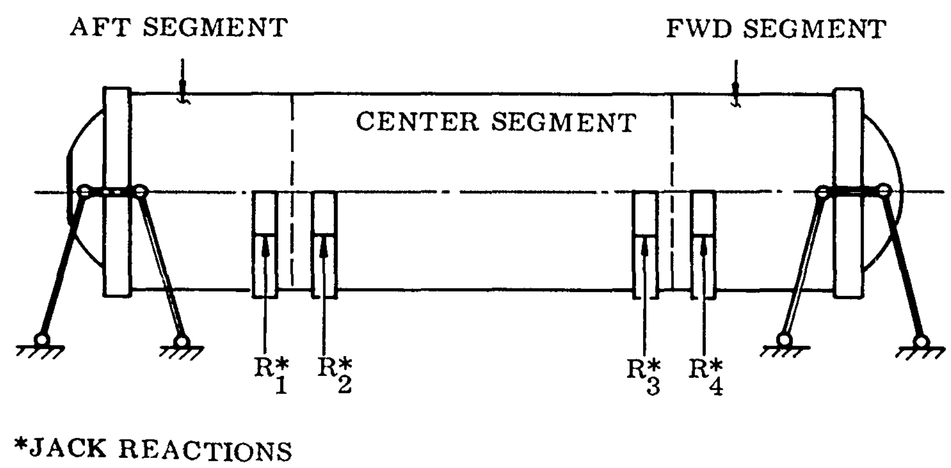

20171-500

(U) Figure 22. Motor Support Schematic

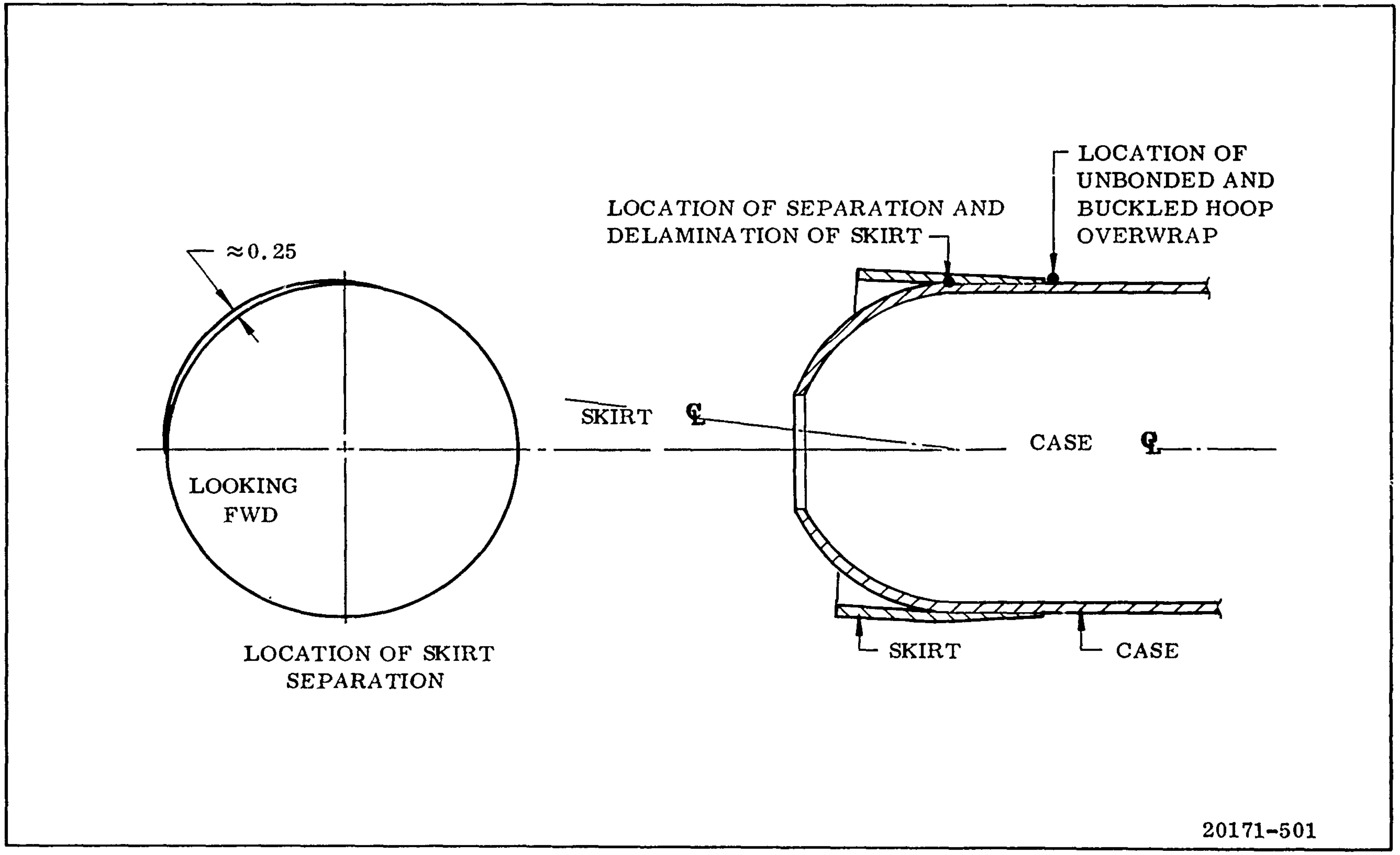

(U) Figure 23. Skirt Unbond Location

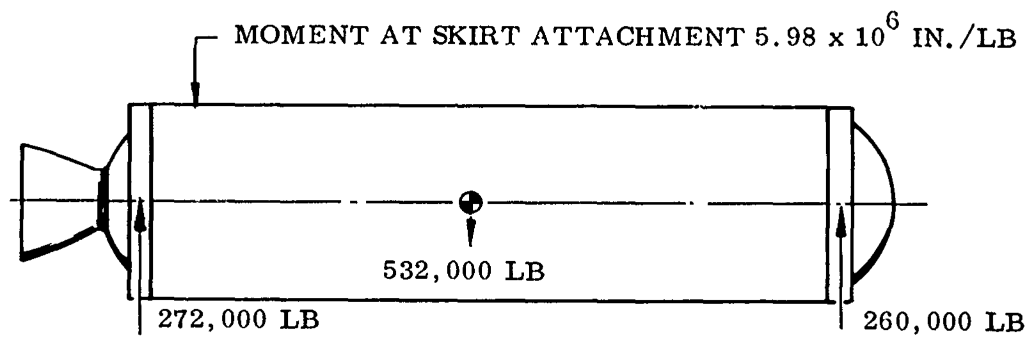

(U) Figure 24. Static Reaction Loads

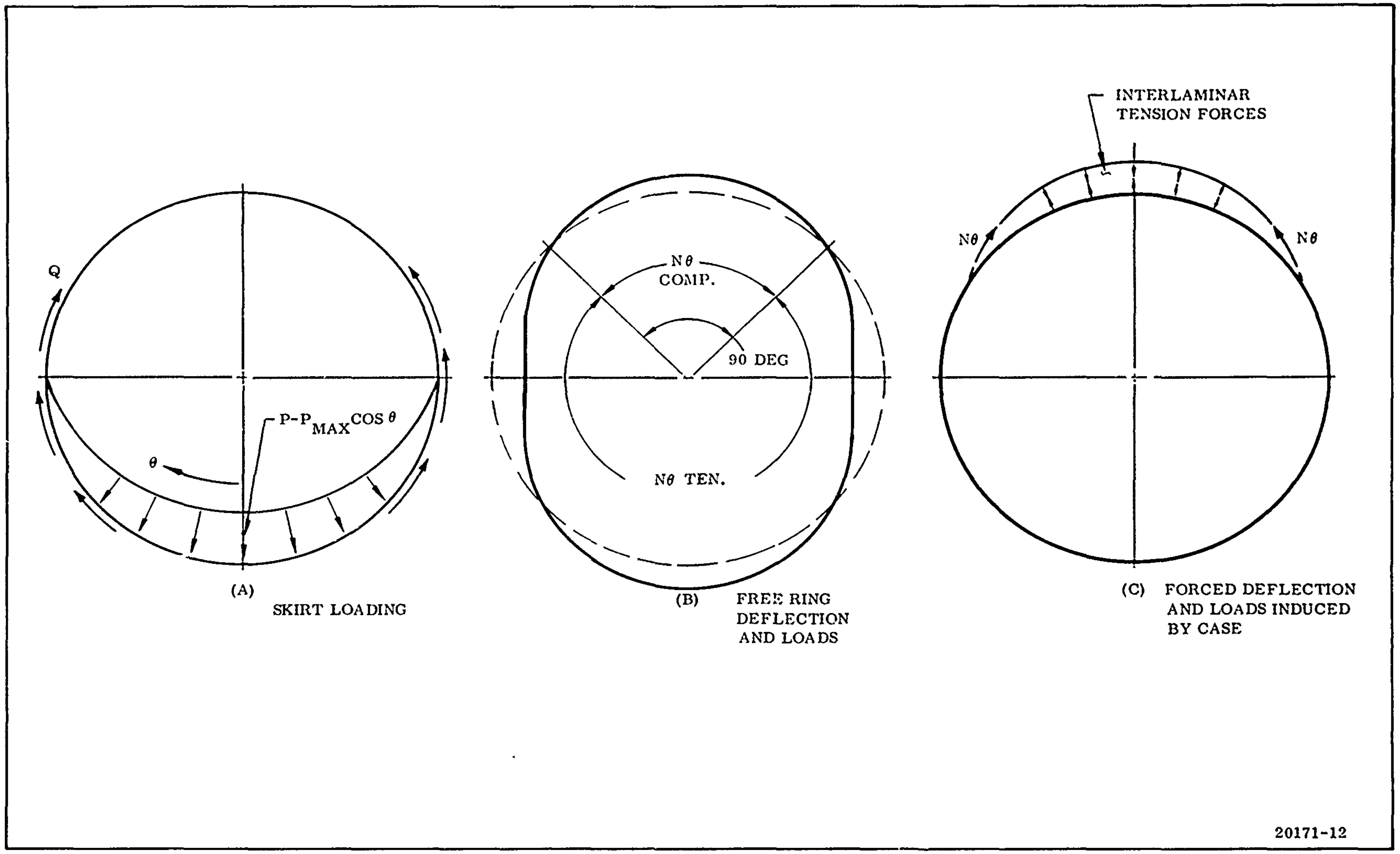

(U) Figure 25. Deflections and Loads

free deflection shape shown in Figure 25(B). The case forces the lower half of the ring to remain round with the deflection shape shown in Figure 25(C). The case also tends to force the top of the ring to conform to the case shape, thus inducing tension forces in that area.

(U) During hydrotest resulting in failure of the forward skirt, the inner 29 percent of the skirt was observed to have been delaminated during fabrication. The forward skirt was replaced but the aft skirt remained unchanged. This existing delamination of the skirt in combination with compressive and interlaminar tension caused the aft skirt failure.

(U) The motor could not be fired without repairing the skirt or supporting the case in a different manner. The top of the skirt was unbonded to the case thus reducing its moment carrying capability. If the delamination progressed as further load was added to the skirt, the moment would tear the skirt from the case.

(U) Several schemes of additional motor support were investigated. Additional support would have to accommodate the case axial and radial growth and support both vertical and transverse loads. A support system of this type would be costly and time consuming.

(U) The other method investigated was repair of the aft skirt to case attachment. A glass cloth overwrap was determined to be the best method of repair. Several resin systems were investigated and several panel specimens were fabricated and tested to determine process parameters and bond strength. Results of these tests are shown in Table VII.

(U) First the case was raised so the skirt could be returned to its original position. The surface was disc and belt sanded and cleaned with MEK (Figure 26). In some places the 2.5 layers of hoop wrap were removed in order to get good bond strength.

(U) A 0.030 in. V-45 rubber shear ply was bonded to the case with UF-1149 and vacuum bag cured. A gel coat of UF-1149 was then applied to the rubber and allowed to cure for six hours. Eleven layers of 15 in. No. 181 E glass were handwrapped

TABLE VII

(U) SKIRT REPAIR DATA

	ERL-2795/ DMP 30-6/PHR	ERL-2795 TETA/12PHR	31A/ 9425/15PHR
Resin Content (percent)	50	50	50
Tensile Strength (psi)	36, 350	41, 150	36, 900
	35, 900	42, 600	33, 300
	37, 900	38, 430	36, 000
Flexural Strength (psi)	54, 500	50, 100	45, 800
	51, 020	53, 720	46, 600
	51, 220	50, 440	47, 800
Interlaminar Shear,	13, 700	15, 900	13, 500
Short Beam (psi)	14, 500	15, 200	13, 000
	13, 500	15, 300	12, 500
Interlaminar Shear,	713	988	906
Notched (psi)	971	1, 110	996
Time to Resin Gel, 1 gal., 80° F (hr)	2	0.5	0.5
Time to Resin Cure, Shore A-70 (hr)	23	22	14.5
Exotherm Temperature, 1 gal. (°C)	150	170	700

SPECIMEN 1

Description	Layup
1. Single Lap Shear	1. Skirt section
2. Shear Area, 1 by 0.75 in.	2. UF-1149
	3. V-45 rubber, 0.030
	4. UF-1149
	5. Cured panel

	Shear Stress (psi)	Comments
1.	613	
2.	655	
3.	485	
4.	--	Not bonded due to skirt section curvature.

SPECIMEN 2

Description	Layup
1. Single Lap Shear	1. Cured glass panel
2. Shear Area, 1 by 1 in.	2. UF-1149
	3. V-45 rubber, 0.030
	4. UF-1149 gel coat, 6 or 24 hr cure
	5. 20 layer layup of cloth and resin

	Gel Coat Cure (hr)	Shear Stress (psi)	Comments
1.	6	508	Failure of UF-1149
2.	6	430	
3.	6	467	Failure at bondline
4.	6	468	
5.	24	258	
6.	24	228	No bond between fully
7.	24	213	cured UF-1149 and layup
8.	24	295	

TABLE VII (Cont)

(U) SKIRT REPAIR DATA

SPECIMEN 3

Description	Layup
1. Single Lap Shear	1. Cured glass panel
2. Shear Area, 1 by 1 in.	2. Surface sanded and cleaned with MEK, or a 6 hr gel coat of UF-1140
	3. 20 layer layup of cloth and resin

	Step No. 2	Shear Stress (psi)	Comments
1.	MEK	1,310	Gel coat not required between layers of glass
2.	MEK	1,530	
3.	MEK	1,710	
4.	MEK	1,365	
5.	6 Hr Gel Coat	456	Results similar to Specimen 2
6.	6 Hr Gel Coat	554	
7.	6 Hr Gel Coat	595	
8.	6 Hr Gel Coat	467	

SPECIMEN 4

Description	Layup
1. Single Lap Shear	1. Cured glass panel
2. Shear Area, 1 by 8 in.	2. UF-1149
	3. V-45 rubber, 0.030
	4. UF-1149 gel coat, 6 hr cure
	5. 20 layer layup of cloth and resin

	Axial Load (lb)	Comments
1.	1,570	About 10-20 percent voids due to air pockets
2.	1,640	
3.	1,580	
4.	1,725	

SPECIMEN 5

Description	Layup
1. Double Lap Shear	1. Steel bonded to V-45
2. Shear Area, 1 by 1 in.	2. UF-1149
	3. Cured glass panel
	4. UF-1149
	5. Steel bonded to V-45

	UF-1149 Thickness (in.)	Stress (psi)	Failure Location Glass or Metal Side
1.	0.005	535	Glass
2.	0.005	527	50 Percent Glass
3.	0.005	420	Glass
4.	0.005	414	50 Percent Glass
5.	0.005	435	50 Percent Glass
6.	0.032	600	Metal
7.	0.032	780	Metal
8.	0.032	488	Glass
9.	0.032	572	Glass
10.	0.032	492	50 Percent Glass
11.	0.060	[illegible]	Metal
12.	0.060	820	Metal
13.	0.060	790	Metal
14.	0.060	862	Metal
15.	0.060	810	Metal

(U) Figure 26. Sanding of Case

over the gel coat and vacuum bag cured (Figure 27). The resin system used was ERL-2795/DMP-30/6 PHR. The glass was sanded and 11 more layers wrapped and vacuum bag cured. This process was repeated to obtain four layups of 11 layers or a total of 44 layers of glass.

(U) In analyzing the repaired skirt it was assumed the original bond transfers no load. This assumption yields a degree of conservatism to the analysis. The following glass (181 E) moduli and strengths were used in the analysis and strengths were verified by tests.

(U)

Angle of Loading (deg)	Modulus (psi)	Tensile Strength (psi)	Compressive Strength (psi)	Shear Strength (psi)
0	3,320,000	35,000	--	--
90	3,210,000	33,000	--	--
0	3,280,000	--	35,000	--
90	3,140,000	--	29,600	--
0 and 90	570,000	--	--	9,180

The Gen Gard V-45 rubber has a shear modulus of 350 psi and a shear strength of 500 psi; UF-1149 shear strength is 400 psi.

(U) The most severe loading condition was considered to occur before firing, and the compressive bias on the rubber was expected to strengthen the case during firing. However, the case to skirt overwrap developed five longitudinal cracks during firing. The aft skirt continued to support the load and did not fail. Analysis of the overwrap failure is included in Volume II under the static test section.

(U) Figure 27. Wrapping of Glass Cloth

(U) Shown below is a summary of the repair ring calculated stresses and safety factors.

Material	Direction of Stress	Loading	Type of Stress	Stress (psi)	Safety Factor
181 Glass	Axial	Moment	Tension or Compression	510	Large
181 Glass	--	Vertical Shear	Shear	1,780	5.16
181 Glass	Hoop	Vertical Shear	Tension	21,000	1.67
181 Glass	Hoop	Case Expansion	Tension	16,000	2.20
Rubber	--	Moment Case Expansion	Shear	150	3.34
Rubber	--	Vertical Shear	Shear	140	3.57
UF-1149	--	Moment Case Expansion	Shear	150	2.67
UF-1149	--	Vertical Shear	Shear	140	2.86

(U) NOTE: $\text{Safety Factor} = \dfrac{\text{Allowable Load}}{\text{Actual Load}}$

SECTION III

(U) JOINT SEAL DESIGN AND FABRICATION AND TESTING

(U) A. DESIGN CRITERIA

(U) The case segment seal was designed to seal the case at the maximum MEOP of 880 psig specified in the contract technical requirements. The design was planned for seal manufacture by conventional methods.

(U) The seal had to be embedded in the insulation since the fiberglass case surfaces are porous. The seal design was required to withstand 1.4 in. case deflection and the 0.015 in. longitudinal movement in the joint areas as demonstrated in two hydrotests under Contract AF 33(657)-11303.

(U) B. DESIGN

(U) The joint seal had a "U" configuration as shown in Figure 28. It was designed to be pressure actuated; however, to insure sealing at initial low pressures and to compensate for necessary wide tolerance in the seal and insulation, the seal was designed to be in compression. A wire spring was placed within the seal ring to insure that, in the nonpressurized state, the seal leg surfaces would be in contact with the insulation surfaces. The seal ring and spring when assembled had an axial width between 0.0674 and 0.770 inch. The cavity in the insulation had an axial depth between 0.592 and 0.637 inch. Therefore, the seal-spring combination was between 0.037 and 0.178 in. larger than the cavity.

(U) The design provided a 0.125 in. thick nylon backup ring which impressed 0.030 to 0.070 in. into the insulation in the tongue side upon segment assembly. The nylon backup ring restricted the seal from extruding between the softer NBR joint insulation material.

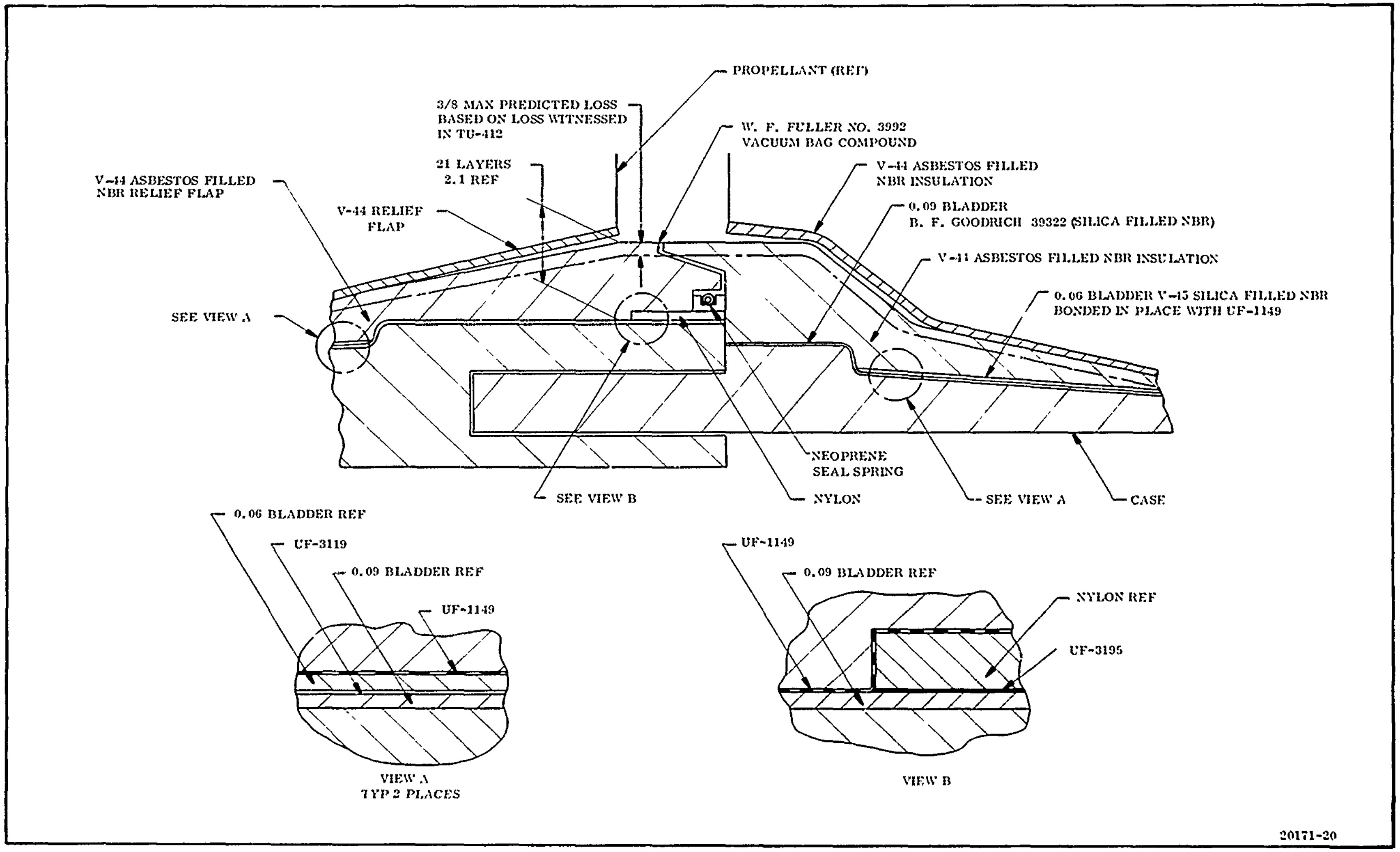

(U) Figure 28. Joint Detail

(U) Because a smaller silicone rubber seal of approximately the same configuration is used successfully in the Minuteman motor adjacent to case-closure threads, much confidence was placed on the seal and general design.

(U) 1. MATERIAL SELECTION

(U) The material selected for fabrication of the seal was neoprene rubber per MIL-R-417. The seal had a vulcanized splice joining the end to form a ring (Figure 28). Nylon was selected for the backup ring because its elongation is compatible with the circumferential growth of the case. The properties of nylon are given in Table VIII. Selection of bonding materials was based on experience and test results given in Section VI-A.

(U) 2. STRUCTURAL ANALYSIS

(U) An analysis of the seal rings in both the 156 in. motor and the subscale motor has been completed using a finite element computer program. This program is capable of calculating the stresses, strains, and displacements in any three dimensional axisymmetric body of revolution. The input was generated by dividing the generating surface of the body of revolution into a finite number of quadrilateral elements which intersect at node points. Arbitrary values of pressure and shear may be applied on any surface of each quadrilateral; boundary displacements may be input at each node point; and arbitrary temperature and body forces may be input for each quadrilateral.

(U) For this analysis, the seal ring and insulation in the area of a joint were analyzed. The minimum expected burst pressure (1, 100 psi at that particular time) was input along the internal surface of the insulation, within the slot leading to the seal ring and on the internal surface of the seal ring. Since the slot was filled with an extruded vacuum compound which has a high viscosity, the pressure was assumed to be transmitted along the slot with no pressure loss.

TABLE VIII

(U) PROPERTIES OF NYLON

Physical Properties*	
Density (lb/cu ft)	71.1
Tensile Strength (psi)	1,050
Compressive Strength (psi)	9,600
Flexural Strength (psi)	13,200
Elongation (%)	--
Hardness (Rockwell B)	--
Thermal Properties*	
Thermal Conductivity (Cal/sec/cm^2-° C/cm)	5.85
Specific Heat (Cal/gm-° C)	0.4
Thermal Expansion (in. x 10^{-5}/° C)	8
Method of Installation	
Bonded in place with UF-3195.	

*Nominal values.

(U) The legs of the seal ring were initially held in contact with the insulation by a steel spring. It was therefore assumed that no pressure entered the interface between the insulation and seal ring.

(U) Radial deflections obtained from extensometer and strain gage readings during hydrostatic test of a 156 in. case were extrapolated for a pressure of 1,100 psi giving a radial increase of 1.4 inches. This deflection was input at the insulation nodes adjacent to the case in the 156 in. motor.

(U) Since steel shims were embedded in the clevis and tongue of each segment joint, the axial growth in the case near the joints was considered negligible. However, the segments could separate during case pressurization due to the tolerance of the connecting pins. Therefore, an analysis was conducted to determine the effect of a 0.015 in. separation of two segments. It was found that the insulation is nearly in a hydrostatic compression stress field. Since the pressure in the void between insulation segments resulting from case segment separation was negligible as compared to the 1,100 psi compressive stress field in the insulation, the insulation filled the void a short distance from the case. Thus the effect of case axial movement was dissipated before reaching the insulation in the area of the seal ring.

(U) The insulation was an asbestos filled NBR (V-44) which had a Shore A hardness of approximately 80 and a minimum elongation of 200 percent. This indicated a modulus of approximately 750 psi. Since the insulation was nearly incompressible, a Poisson's ratio of 0.5 was used. The seal ring was made of a neoprene rubber which had a modulus and Poisson's ratio approximately the same as the insulation (Shore A hardness of 80).

(U) Figure 29 indicated the change in shape of the seal ring and surrounding insulation. The solid line represents the original geometry and the broken line represents the superimposed geometry after pressurization with the case used as a zero displacement reference point. The apparent decrease in volume of the insulation after pressurization was not experienced since the radii of the case and insulation increase with pressure. The upper portion of the seal ring (point 1) is displaced 0.022 in. in a direction parallel to the motor centerline while the lower

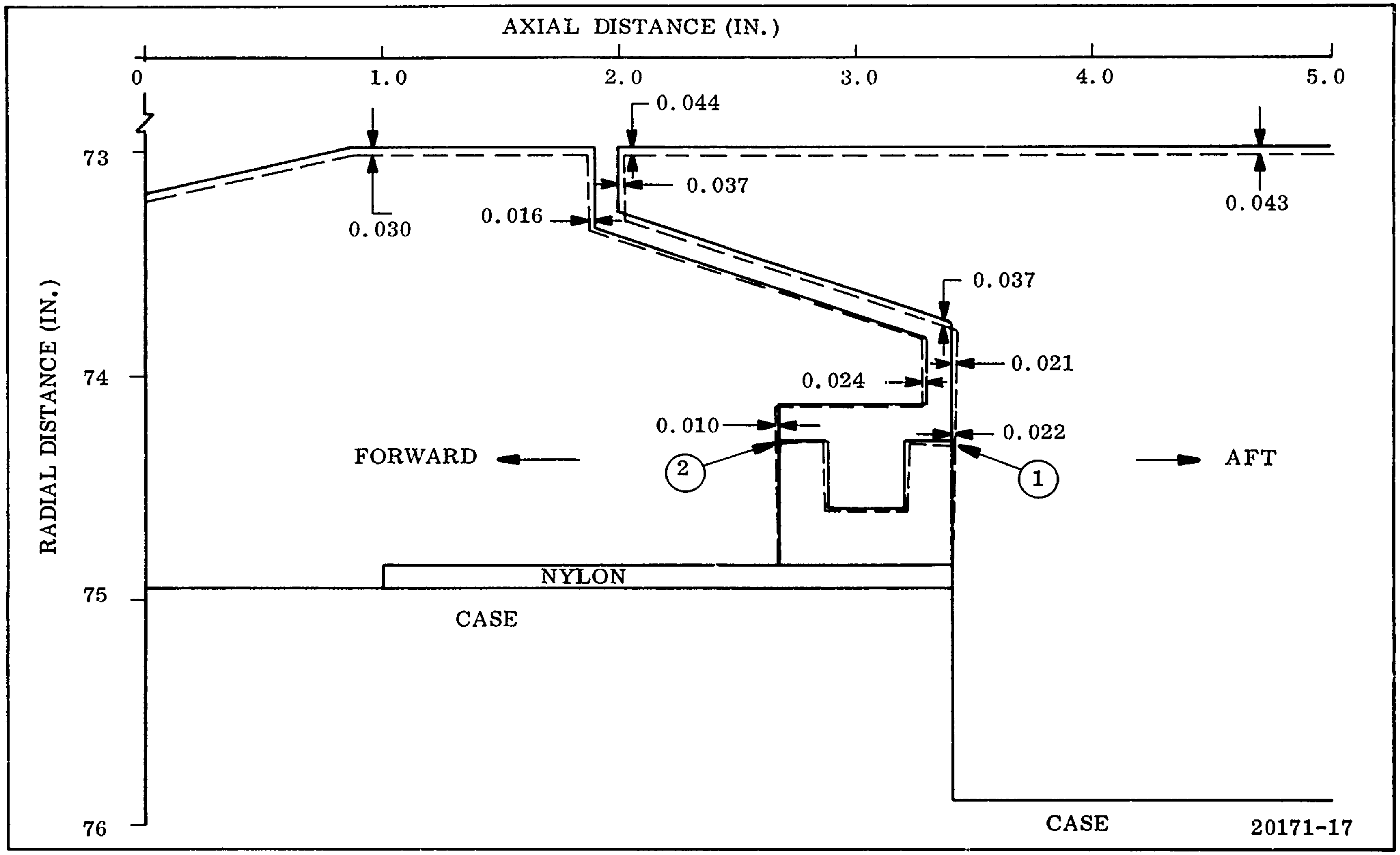

(U) Figure 29. Displacements for the 156-8 Motor Seal portion (point 2) is displaced 0.010 in. in the opposite direction. Thus the maximum axial expansion of the seal ring was 0.032 inch.

(U) The maximum strains within the seal ring were as follows: radial strain, -6 percent (compressive); hoop strain, +2 percent (tensile); axial strain, +4 percent (tensile). These were well within the capability limits of the seal. The minimum compressive stress appearing within the seal is 1,056 psi. This is a 44 psi (4 percent) decrease in axial stress and appears near the nylon ring. This loss was attributed to the fact that the insulation is bonded to the case which prevents axial movement of the insulation.

(U) 3. THERMAL ANALYSIS

(U) The joint insulation was designed for no temperature rise at the seal during static test. The bulk of material in the area of the joint was to provide for the seal seating. The material loss was predicted to be 3.2 mil/sec resulting in a maximum expected loss of 0.375 in. of material. This material loss is shown in Figure 28. It resulted in erosion back to the first step of the double step joint. This left 0.95 in. of insulative material protecting the seal at end of firing.

(U) C. SUBSCALE JOINT DEVELOPMENT

(U) 1. SUBSCALE SEAL DESIGN

(U) The design of the subscale test vessel was such that the circumferential strain in the seal would duplicate as closely as possible that of the full scale case, and other displacements would be insignificant. Therefore, the subscale test assembly (Figure 30) consisted of two segments of a fiberglass cylinder joined near the center with an insulation joint of the same general cross sectional configuration and size as the 156 in. diameter motor. This assembly included the same cross sectional nylon backup ring and an Epocast filler section which simulated the hoop

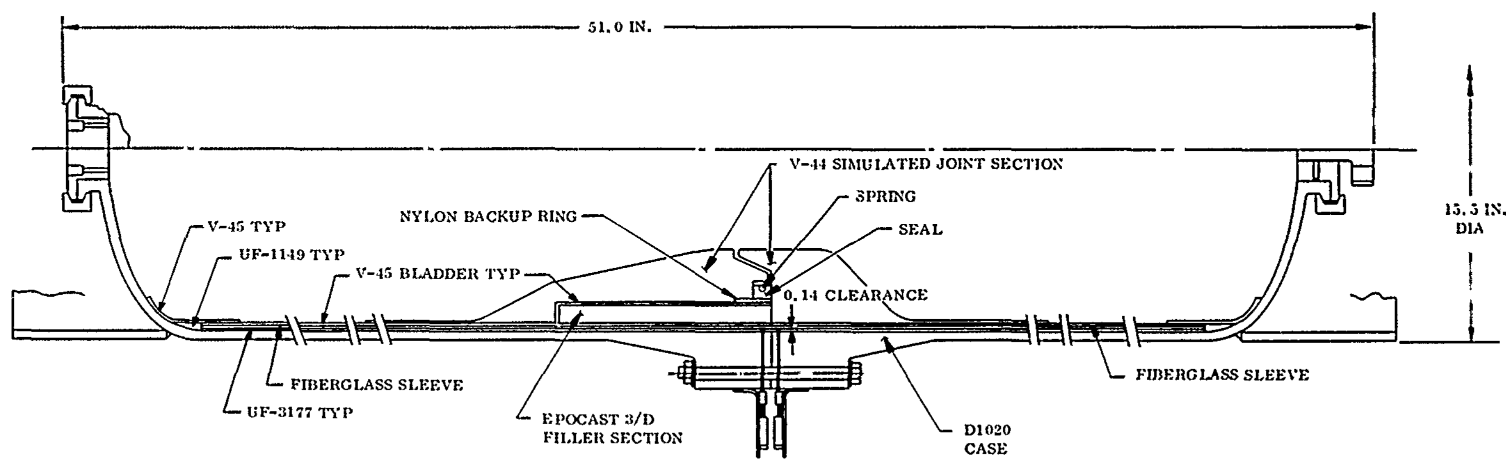

(U) Figure 30. Subscale Test Assembly Design windings next to the clevis joint of the full scale motor case. The test installation was enclosed in the DU 1020-01 case and the two sections bolted together at the center. The DU 1020-01 case was purposely not sealed so that sealing of the subscale joint only would be tested. The fiberglass cylinder was supported and sealed at each end only, leaving the test joint free to move radially 0.14 in. before being restrained by the relatively rigid steel DU 1020-01 case, thus insuring that the maximum hoop strain in the joint seal area would be that of full scale joint. Extensometers were installed to indicate the radial movement of the joint.

(U) Figure 31 shows the insulation and seal ring deflections for the subscale motor. During hydrotests this motor was placed inside a steel case which had a radius 0.140 in. larger than the radius of the subscale motor. This increase was used as a radial deflection of the case in the analysis and was subtracted from the deflections before plotting the displaced configuration in Figure 31.

(U) Of particular importance in this analysis was the effect of radial growth on the deflections within the insulation. Because this test vessel had a smaller radius but the same insulation cross sectional dimensions as the 156-8 motor, the effect of radial expansion was greatly magnified. The total longitudinal expansion between points 1 and 2 was 0.059 inch. Therefore, it was concluded that after a successful demonstration of the seal in the subscale motor, no difficulty would be experienced in the full scale motor.

(U) The maximum strains in the subscale seal ring were as follows: radial strain, -8.8 percent (compressive); hoop strain, 3 percent (tensile); axial strain, 6.1 percent (tensile). The minimum compressive stress appearing within the seal was 1,056 psi.

(U) The above analyses assumed that no pressure was initially introduced into the interface between the seal ring and the surrounding insulation. A wire spring was placed within the seal ring to assure that in the nonpressurized state the surfaces are adjacent. The seal ring and spring, when assembled, had an axial length between 0.674 and 0.770 inch. The cavity in the insulation had an axial length between 0.652 and 0.622 inch. Therefore, the ring-spring combination was between 0.022 and 0.148 in.

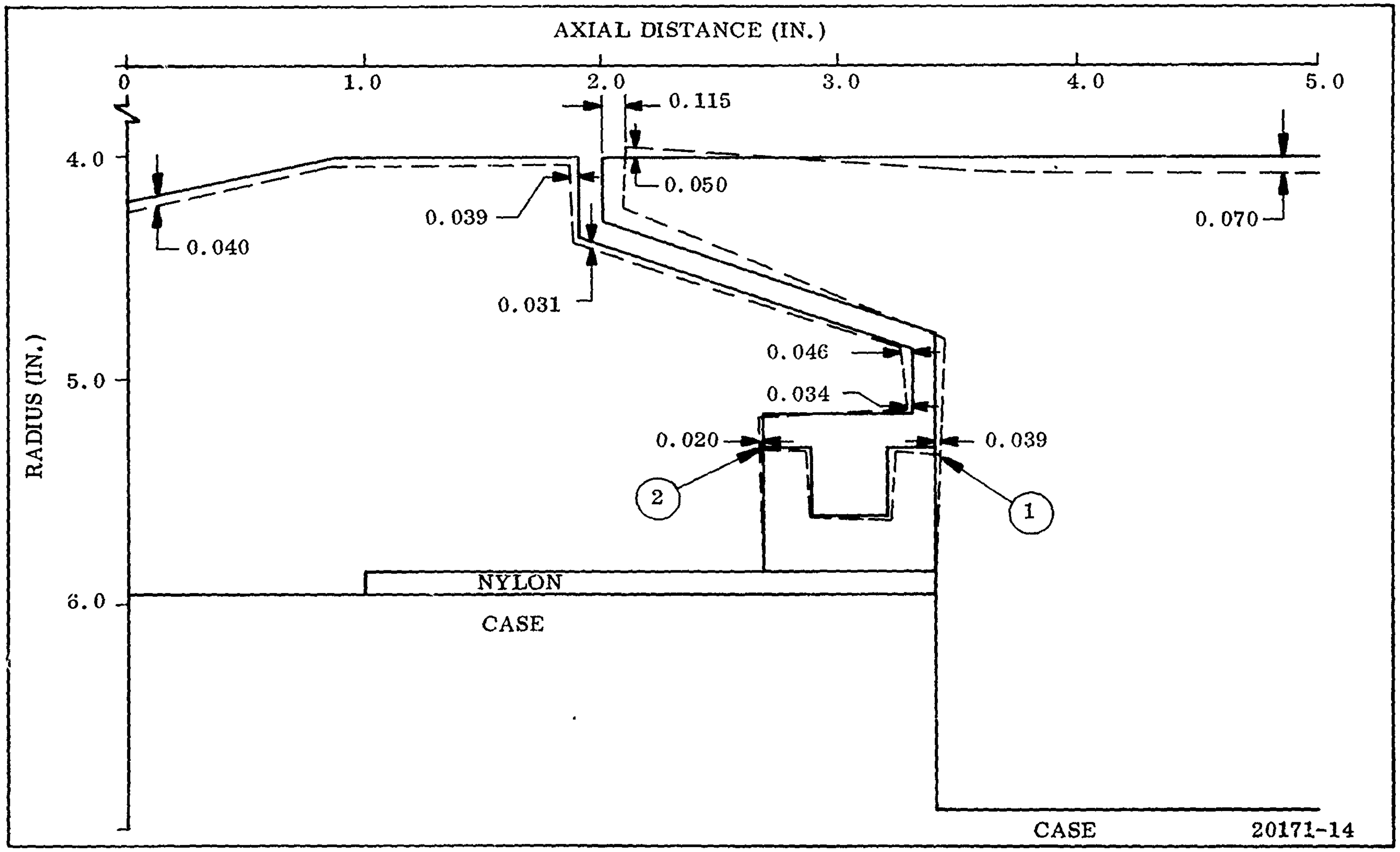

(U) Figure 31. Displacements for Subscale Seal larger than the cavity and was therefore in a state of compression before motor pressurization similar to that of the full scale joint.

(U) 2. SUBSCALE FABRICATION

(U) The basic joint insulation and fiberglass sleeves were fabricated on a mandrel. The mandrel consisted of a wood and mesh core which could be removed by destruction. Over this core, plaster was screeded to the proper contour. After oven drying, the plaster was covered with Teflon tape as a release material. The Teflon tape was then coated with a mixture of 30 percent MEK and 70 percent Caram 216 to provide precure tackiness. The insulation consisted of asbestos filled NBR (same as full scale motor insulation) sheet stock on the prepared mandrel using standard layup procedures after which it was hydroclave cured.

(U) The OD of the cured insulation was then machined to the desired configuration to accept the nylon ring and Epocast filler section.

(U) A 0.090 in. wide slit was made longitudinally in the insulation joint section to simulate the insulation joints in the full scale motor. This slit was cleaned and filled with UF-3195 and cured at ambient temperature.

(U) The nylon backup ring was grit blasted and bonded in place with UF-3195. The cavity of the filler section was then lined with uncured Buna-N. The filler section of Epocast 31D was cast and cured. The Teflon expansion slit formers were removed and the voids filled with UF-3194. An uncured layer of Buna-N rubber was then bonded to the OD of the mandrel to simulate the bladder and to provide a surface to accept the glass wrapping.

(U) The assembly was then wrapped with a sequence of hand wrapped fiberglass cloth (style 143 wet wrapped) with USP E717 resin and machine winding of preimpregnated rovings. Upon completion of the winding, the part was B staged and then oven cured. Following the cure the sleeves on the mandrel were parted by machining and sawing. The mandrel was then removed.

(U) The sleeve assemblies were installed in the steel cases and centered in the aft end of the case with a centering tool. A strip of V-45 was bonded over the inside forward end of the cylinder and to the case with UF-1149. The UF-1149 was cured for 16 hr at 80 ± 20° F. With the cases in the vertical position, UF-3177 was poured between the OD of the cylinder and the case wall to the required level to bond the forward end of the fiberglass cylinder to the case wall and ambient cured.

(U) The joint seal configuration was machined to blueprint configuration with cutting heads which would be used on the full scale motor.

(U) The neoprene channel seal was fabricated at the vendors facility in the same manner as the full scale motor seal. It was extruded from a die in a long strip and cured, then cut to the proper length, and the ends vulcanized together to form a ring. The spring was fabricated from off-the-shelf steel wire tension spring. The ends were brazed together to form a ring.

(U) 3. SUBSCALE TESTING AND DATA ANALYSIS

(U) The objective of the subscale tests was to verify the design, fabrication, and assembly techniques for the full scale motor segment joint seals. The testing was performed in accordance with Test Plan TWR-1425. The test assembly was shown in Figure 30.

(U) Instrumentation consisted of a pressure measurement and two extensometers measuring radial displacement of the joint section relative to the steel case. Instrumentation was recorded continuously throughout each pressure cycle.

(U) The assembly was submitted to three tests. Each test consisted of the following steps.

1. Assembling the vessel.
2. Pressurization to 100 psig.
3. Checking for leaks.
4. Pressurization to 1,100 psig and holding for 120 seconds.

5. Depressurization.
6. Pressurization to 1,100 psig and holding for 120 seconds.
7. Depressurization.
8. Disassembling.
9. Inspecting.

(U) In the assembly for the first test (Figures 32 and 33), the seal was lubricated with PBAA. In assembly for the second two tests, the PBAA lubricant was used in the same manner; however, the joint gap was also potted with W. P. Fuller vacuum bag compound No. 3992 in the same manner which the 156-8 joint was potted for static test.

(U) The test was an unqualified success No leakage occurred during the hydrotest. As can be seen in Figures 34 and 35, the extensometers measured a radial displacement of up to 0.14 in., representing a circumferential strain of 0.14/7.3 = 0.0192 in./in. These data were typical of all three tests. An earlier test of the full size case measured a maximum radial deflection in the joint of 1.34 in., representing a circumferential strain of (1.34/78) (1,100/1,000) = 0.0188 in./in., thus the subscale test was considered as successfully and closely duplicating the actual full scale case strains. A difference existed in the indicated growth at D001 (female joing) and D002 (male joint). This difference was actually due to the gap between the fiberglass sleeve and the DU-1020 case variation. Calling attention to the compressive marks near the outside perimeter of the insulation (Figure 36), the pattern qualitatively substantiates the results of the stress analysis.

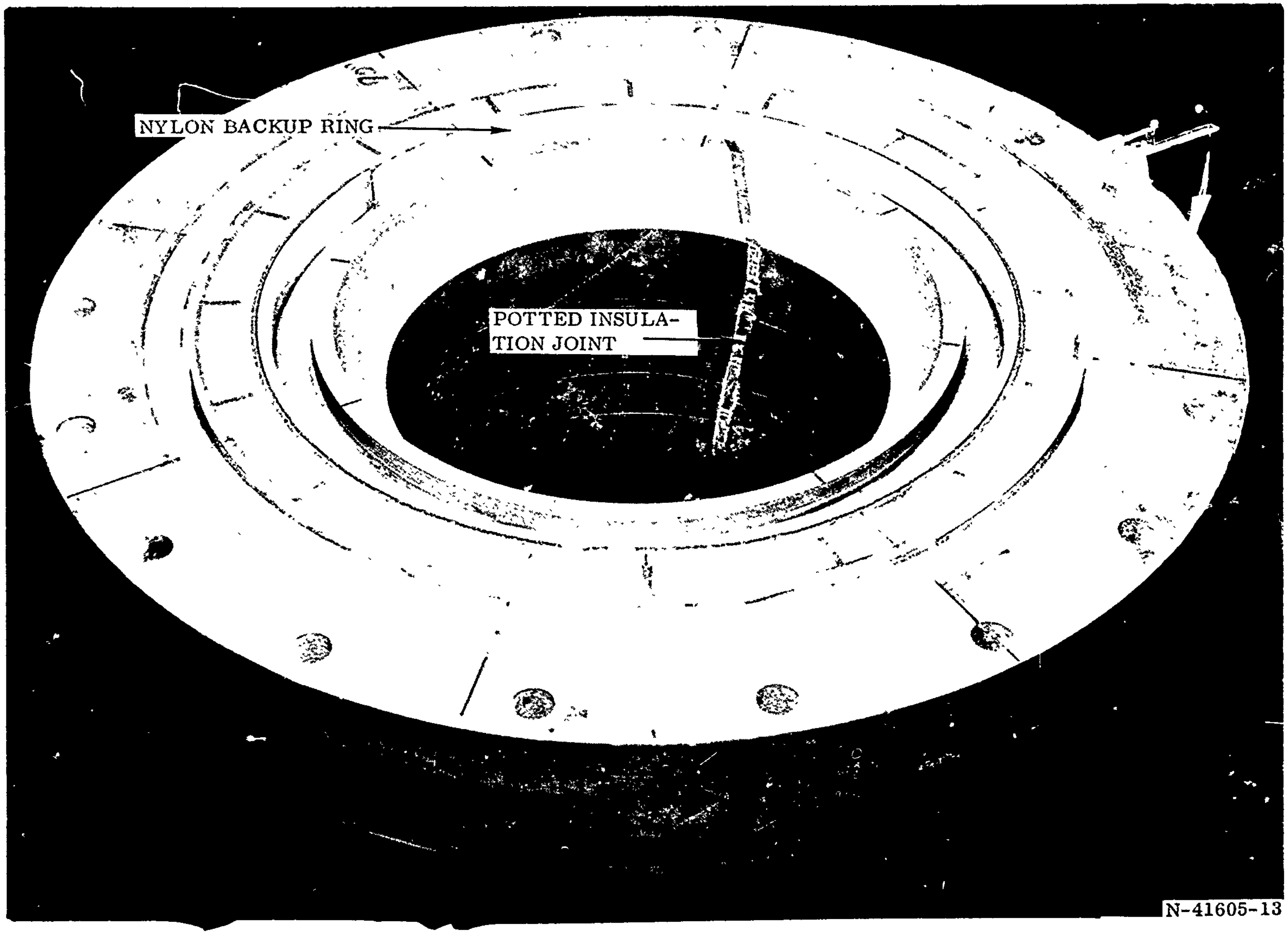

(U) Figure 32. Female Joint Insulation

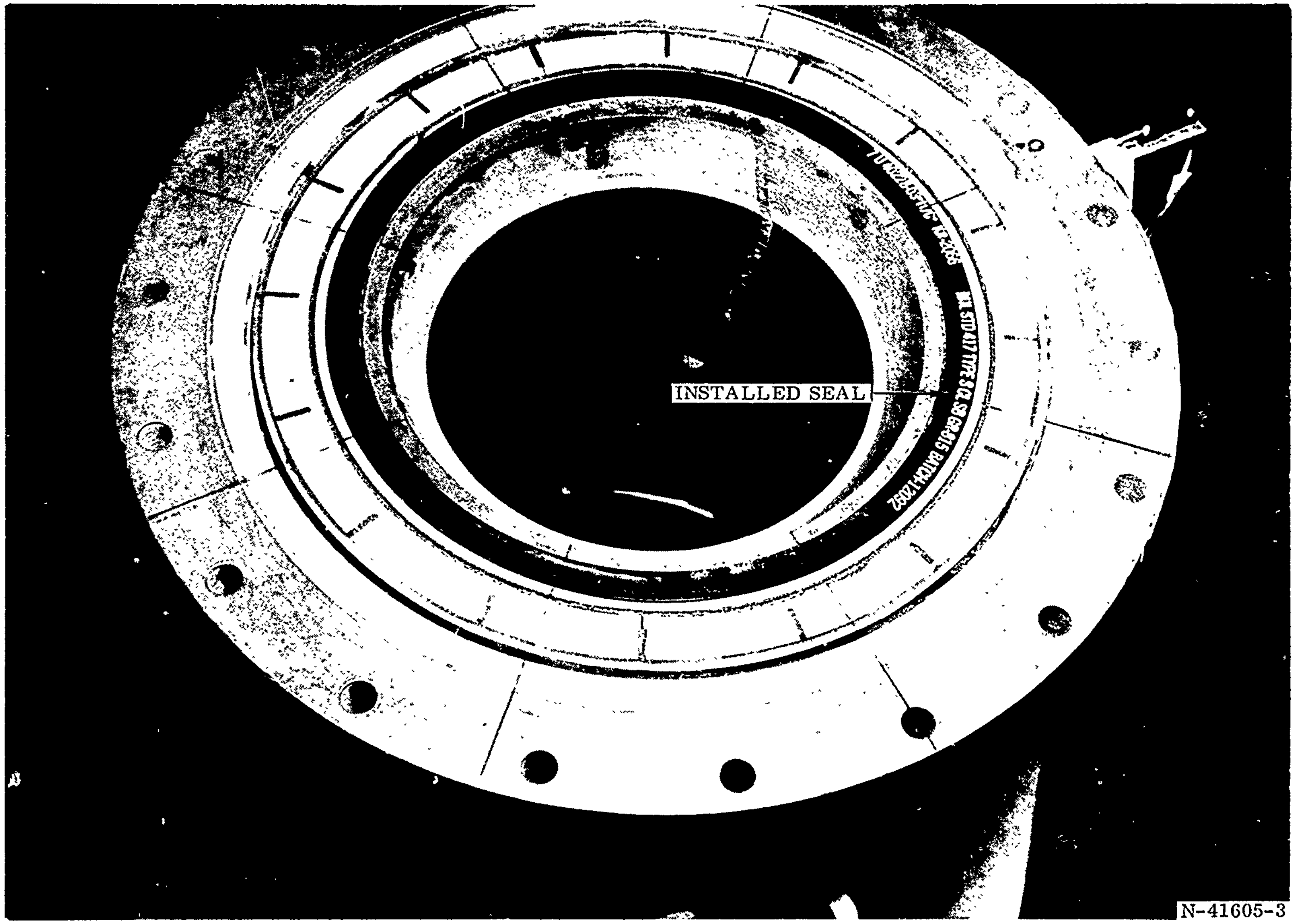

(U) Figure 33. Female Joint with Seal Installed

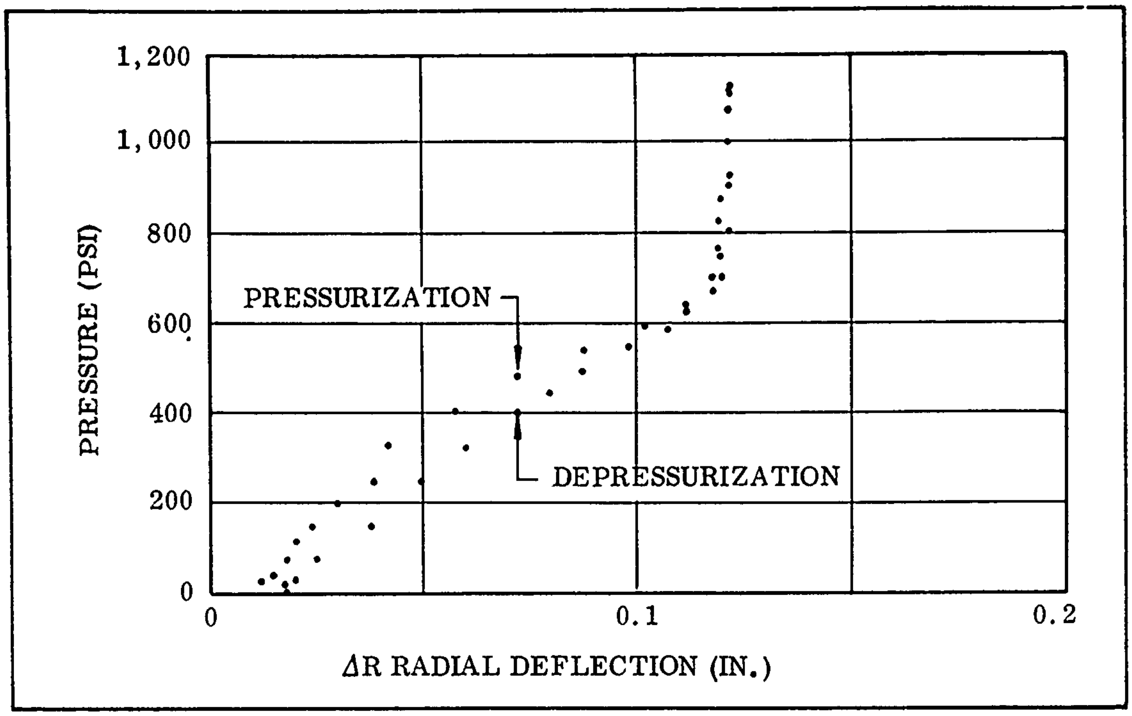

(U) Figure 34. D001 Extensometer Trace, Test No. 1, First Pressurization

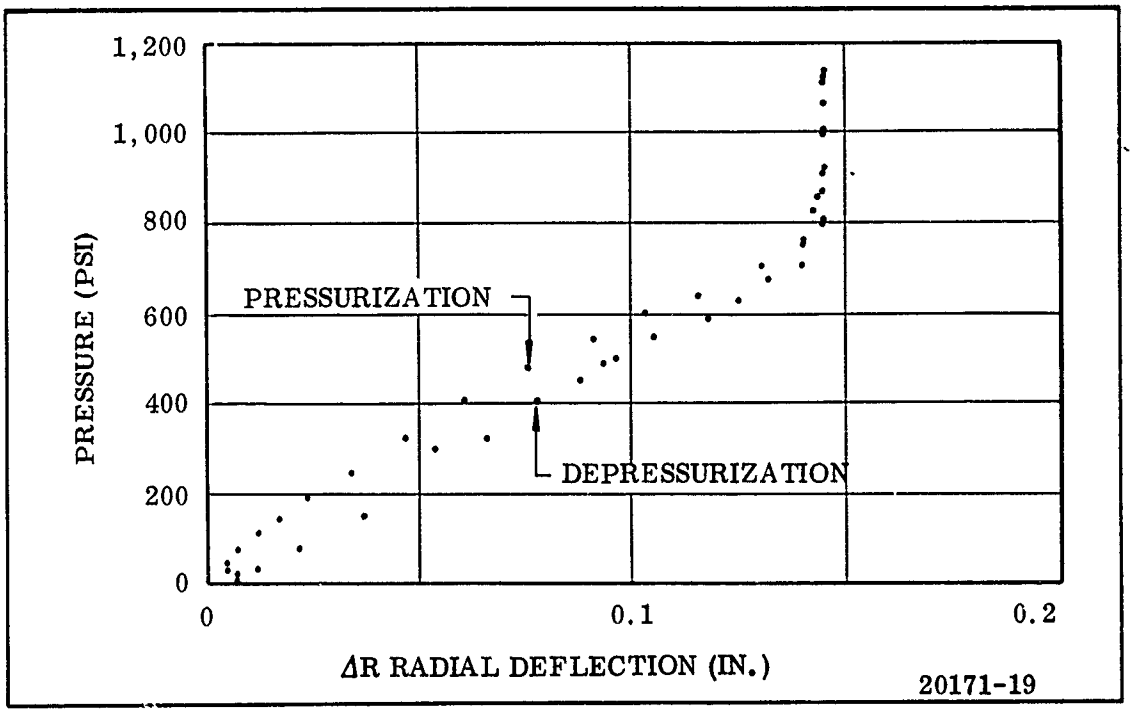

(U) Figure 35. D002 Extensometer Trace, Test No. 1, First Pressurization

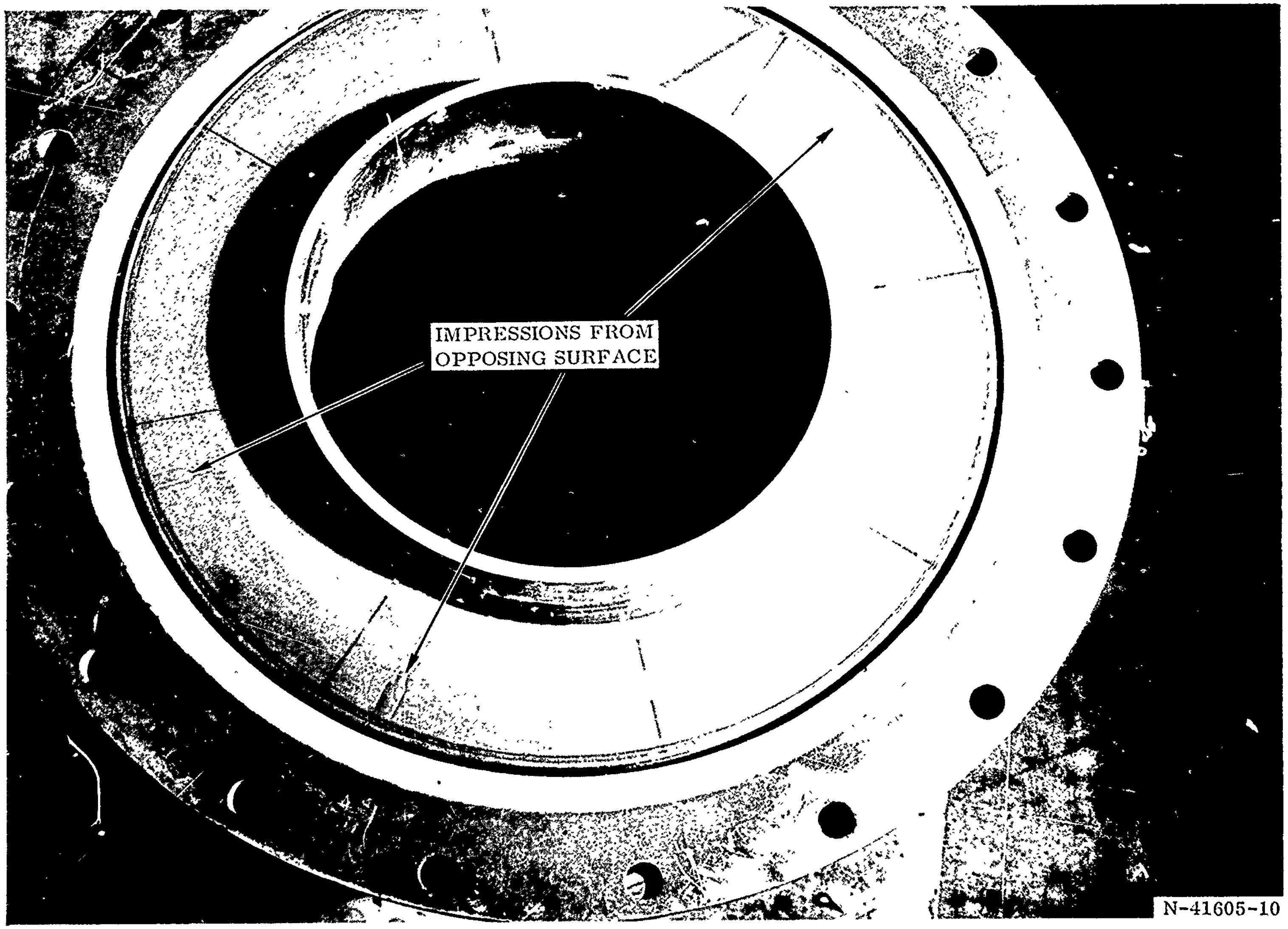

(U) Figure 36. Male Joint

SECTION IV

(U) INSULATION

(U) A. DESIGN

(U) 1. DESIGN CRITERIA

(U) The internal case insulation was designed to assure that the structural integrity of the case would not be degraded by the thermal effects of the chamber environment throughout motor operation.

(U) 2. MATERIAL SELECTION

(U) The insulation materials selected for use in the 156-8 motor are as follows.

(U) Silica cloth phenolic (MX2600) was selected for use in the aft segment where the gas velocity is above Mach 0.12. In other areas of the aft segment dome the insulation material was asbestos-filled NBR (V-44).

(U) The insulation material used for the segment joint areas on all segments and as the headend insulator was asbestos-filled NBR. The case bladder material was silica-filled NBR (V-45).

(U) The selection of these materials was based on the following considerations.

1. Proven performance in solid propellant rocket motors.
2. Proven fabrication techniques.
3. Proven installation techniques.
4. Compatibility with the joint seal design.

(U) The V-45 material was selected as the bladder material because its consistency insured a positive seal to prevent leakage through the fiberglass case wall. It also served as an insulation for a short period of time (approximately 5 sec) during tailoff.

(U) 3. INSULATION DETAILS

(U) The silica-filled NBR bladder covered the entire inner surface of each case segment and was used to insure pressure-tight case segments. Relief flaps were included at the propellant grain ends of each case segment to relieve any stresses imposed on the propellant grain during cure, cooldown, storage, transportation and test. The gaps between relief flaps and primary insulation were unfilled.

(U) Asbestos and silica-filled NBR insulation covered the flame exposed areas of the bladder lined case and protected the case from degradation due to heat. The thickness of the insulation was contoured so that it is proportional to flame exposure time. Insulation details are shown on Drawings 7U37320, 7U37321, 7U37322, and 7U37323.

(U) The design nominals of compositions and physical and thermal properties of insulation materials are given in Tables IX thru XII.

(U) 4. FORWARD DOME INSULATION

(U) The asbestos-filled NBR insulation in the forward dome of the forward segment varied in thickness from 0.80 in. at the igniter port to 0.10 in. at the cylinder-dome tangent point. The insulation extended 4 in. onto the cyclindrical section. The forward relief flap extended from the propellant grain internal diameter to a diameter of 140 in. which was 2/3 of the web thickness measured along the dome contour. This flap relieved stresses in the dome area. The flap thickness was 0.2 inch.

TABLE IX

(U) CASE BLADDER

(Generic Name: Silica-filled NBR, Gen Gard V-45)

Physical Properties*	
Density (lb/cu ft)	75
Tensile Strength (psi)	2,000
Elongation (%)	400
Hardness (Shore A)	70
Thermal Properties**	
Thermal Conductivity (Btu/sq ft-hr-° F/ft)	0.13
Specific Heat (Btu/lb° F)	0.34
Assumed Ablation Temperature (° F)	800

Method of Fabrication

Autoclave cured as 0.060 sheet stock

Method of Installation

Bonded in place with UF-3119

*Values represent minimum value used for design purposes.
**Nominal values.

TABLE X

(U) CASE INSULATION

(Generic Name: Asbestos-filled NBR, Gen Gard V-44)

Physical Properties*	
Density (lb/cu ft)	80
Tensile Strength (psi)	1,600
Elongation (%)	200
Hardness (Shore A)	80
Thermal Properties**	
Thermal Conductivity (Btu/sq ft-° F-hr/ft)	0.10
Specific Heat (Btu/lb° F)	0.42
Assumed Ablation Temperature (° F)	800

Method of Fabrication

0.100 sheet stock, hand laid up in mold and autoclave cured.

Method of Installation

Bonded in place with UF-1149

*Values represent the minimum values used for design purposes.
**Nominal values.

TABLE XI

(U) INSULATION RING

(Generic Name: Silica Cloth Phenolic, Fiberite MX2600)

Physical Properties*	
Density (lb/cu ft)	109
Tensile Strength (psi)	14,000
Compressive Strength (psi)	18,000
Flexural Strength (psi)	20,000
Hardness (Barcol)	60
Thermal Properties**	
Thermal Conductivity (Btu/sq ft-hr-° F/ft)	0.225
Specific Heat (Btu/lb-° F)	0.24
Assumed Ablation Temperature (° F)	800

Method of Fabrication

Tape wrapped and hydroclave cured.

Method of Installation

Bond in place with UF-3195.

*Values represent minimum design values.
**Nominal values.

TABLE XII

(U) INSULATION EROSION RATES

Motor Location	Material	Predicted Erosion Rates (mil/sec)	Test Data Source*
Head End and Segment Joints Igniter Cap	Silica filled NBR, Asbestos filled NBR, and Mastic (TI-H704B)	2 to 4	1, 2, 3, 4, 5
Aft End	Asbestos filled NBR	10 to 30	1, 2, 3, 4, 5
	Mastic	12 to 35	1, 2
	Silica phenolic	9 to 13	2, 4
	Carbon fiber NBR phenolic	3 to 6	2
	Graphite phenolic	3 to 6	2

*Test Data Source:

1. Thiokol Chemical Corporation (Space Booster Division), Contract AF 04(695)-351.

2. Thiokol Chemical Corporation (Wasatch Division), Contract AF 04(695)-363.

3. Lockheed Propulsion Corporation, Contract AF 04(695)-364.

4. United Technology Corporation, Contract AF 04(695)-156.

5. Aerojet-General Corporation, Contract AF 04(695)-350.

(U) 5. AFT DOME INSULATION

(U) The aft dome insulation consisted of a tape wrapped, silica cloth, phenolic ring adjacent to the aft dome-nozzle joint and asbestos-filled NBR in the remainder of the dome area. The premolded silica cloth phenolic was used in the aft dome area to withstand the high gas velocity (above Mach 0.12) in the area during motor firing.

(U) The asbestos-filled NBR insulation in the aft dome extended from the premolded insulation forward and 4 in. onto the cylindrical section. Thickness of the insulation varied from 4.00 in. at the interface with the premolded insulation down to 0.10 inch. The dome relief flap was 0.20 in. thick and extended from the propellant grain internal diameter to a diameter of 140 in. which was 2/3 of the web thickness measured down the dome contour.

(U) 6. JOINT INSULATION

(U) a. Aft End (Clevis Portion)--The clevis portion of each of the two joints at the aft ends of both the forward segment and the center segment was insulated with asbestos-filled NBR from the center of the joint forward to a position 4.0 in. forward of web burnout. The insulation tapered from 2.10 in. thickness over the joint to 0.10 in. at the forward end. The split flap insulation at the aft end of the forward segment and at the aft end of the center section extended forward from the propellant surface for 20 in. (1/2 of the web thickness) and was 0.20 in. in thickness.

(U) b. Forward End (Tongue Portion)--The tongue portion of each of the two joints at the forward ends of both the center segment and the aft segment was insulated with asbestos-filled NBR from the center of the joint aft to 4.0 in. beyond the web burnout area. The insulation was 2.80 in. in thickness over this portion of the joint and tapered to 0.10 in. in thickness at the aft end. The relief flap at the forward end of the center segment and at the forward end of the aft segment was 0.20 in. in thickness and extended aft from the propellant face for 20 inches.

(U) 7. DESIGN DETAILS

(U) a. Insulation Erosion Rates--A compilation of data from previous programs both at Thiokol and other companies has yielded correlations between material loss rates and various other parameters. For asbestos-filled NBR, it was shown that the material loss rate correlates closely with gas velocities (Mach number). Figure 37 shows the relationship between the erosion rate of NBR insulation and Mach number. The erosion rate of silica phenolic correlates closely with the enthalpy convective heat transfer coefficient (Figure 38). General erosion rates for various areas of rocket motors were given in Table XII.

(U) b. Insulation Thickness Requirements--The thickness requirements were determined by multiplying the predicted material loss rate by the time of exposure and multiplying by a safety factor of 1.5 to allow for variations in materials, propellant gas properties, and insulation thickness tolerances. Additional material was added to provide thermal insulation to the case walls after web time. This additional material thickness, 0.2 in. for areas of maximum exposure to combustion gases and 0.1 in. in other areas, gave an additional margin-of-safety. Based on previous data, a material loss rate of 3.2 mils/sec was selected as an erosion rate for the forward dome and joint areas.

(U) The designed material loss rates in the aft dome were obtained from a combination of heat transfer and flow analyses in conjunction with the correlations presented in Figures 37 and 38. Figure 39 shows the relationship between motor location and parameters necessary to determine the material loss rate shown on Figure 40.

(U) c. Structural Requirements--The thermal stress analysis of the silica cloth phenolic ring insures that it will withstand stresses induced during the motor test. The ring is considered to be acted on by two sets of loads, internal case pressure of 1,200 psi and a temperature gradient of from 5,400 to 870°F between the initial surface and 0.3 in. from the surface. The internal case pressure resulted in a maximum stress

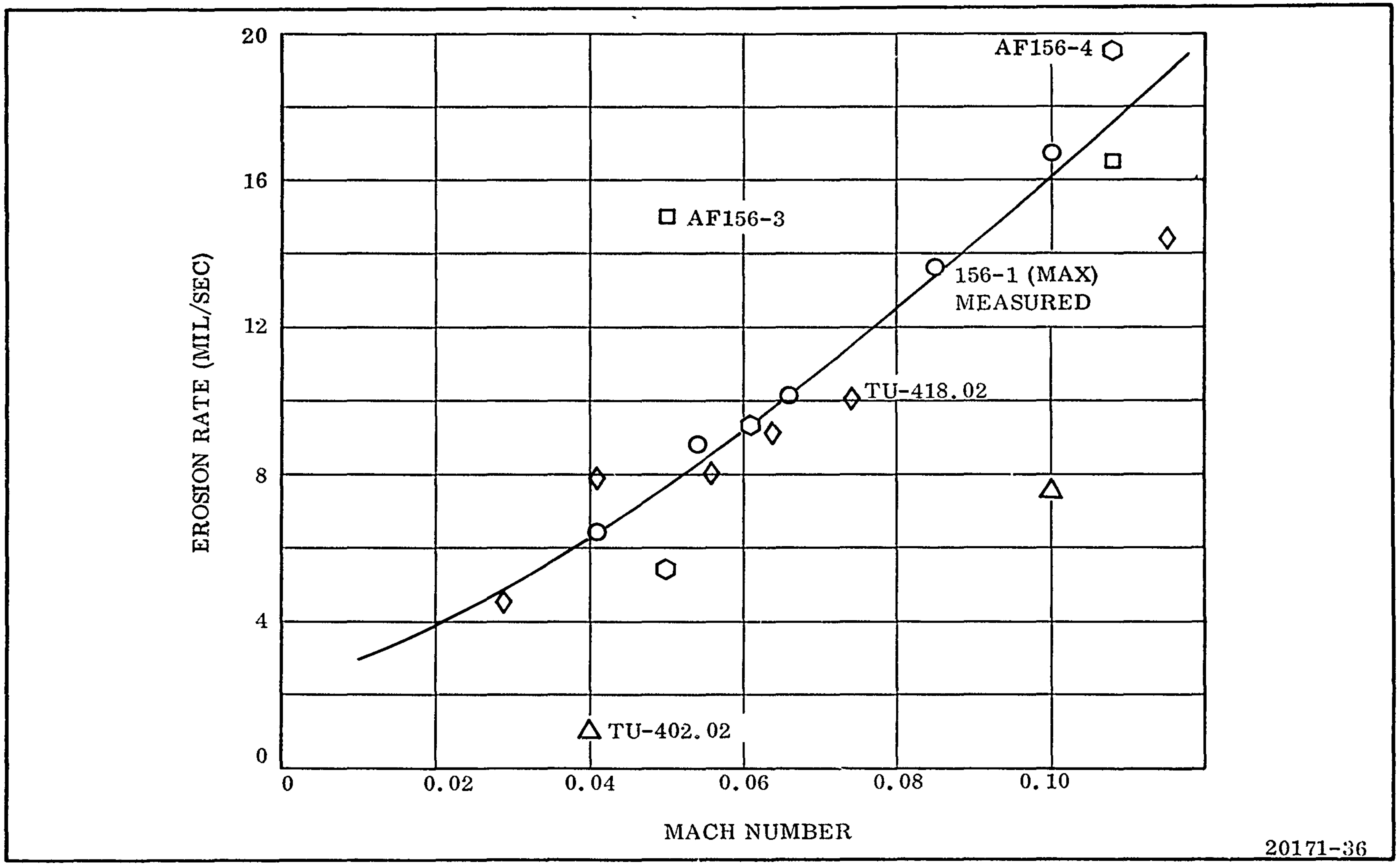

(U) Figure 37 . Predicted Erosion Rate vs Mach Number in 156-8 Motor Compared with Measured Erosion of V-44 Insulation in Other Large Motors

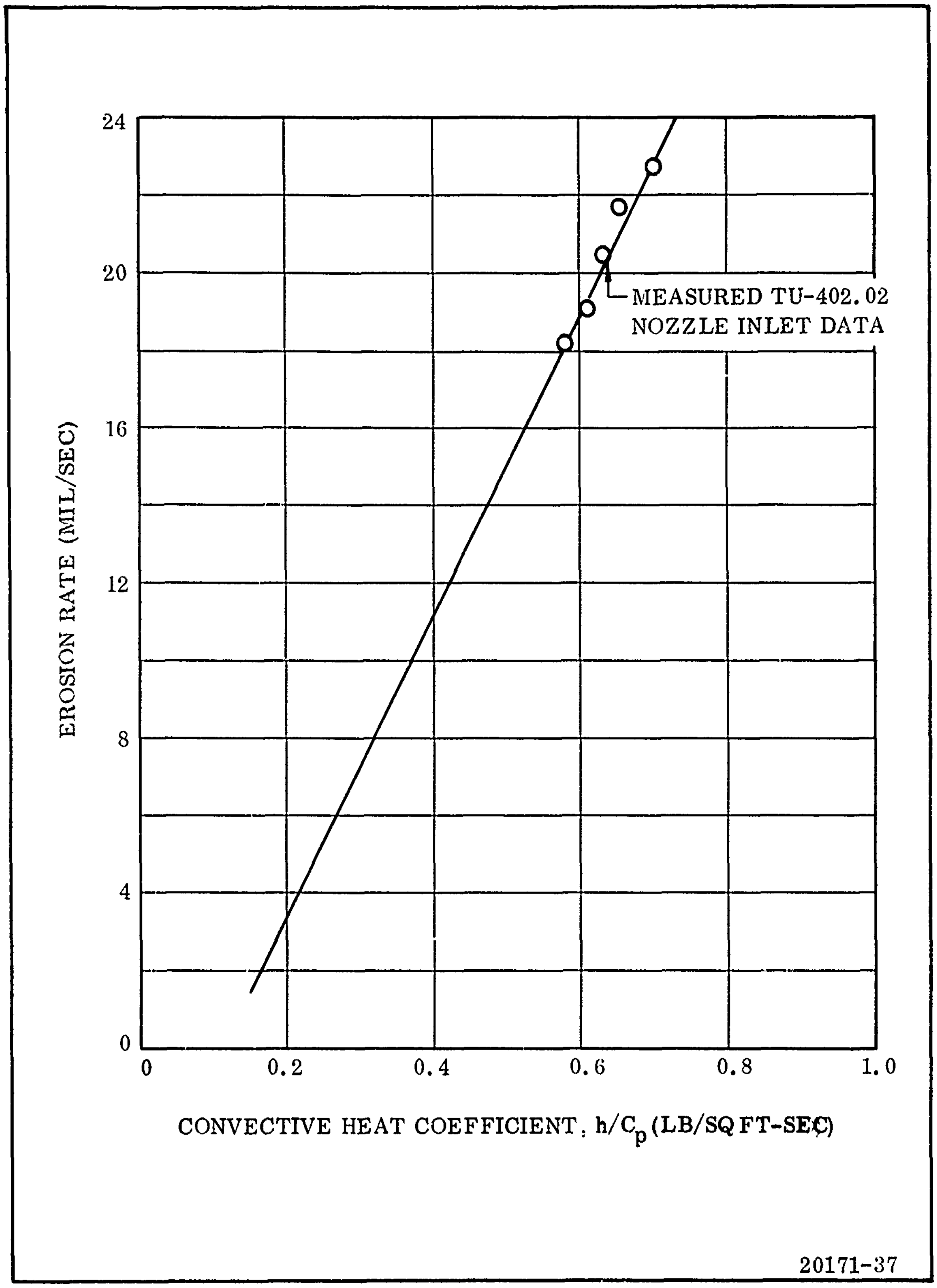

(U) Figure 38 . Predicted Erosion Rate of Silica Cloth Phenolic as a Function of Heat Transfer Coefficient

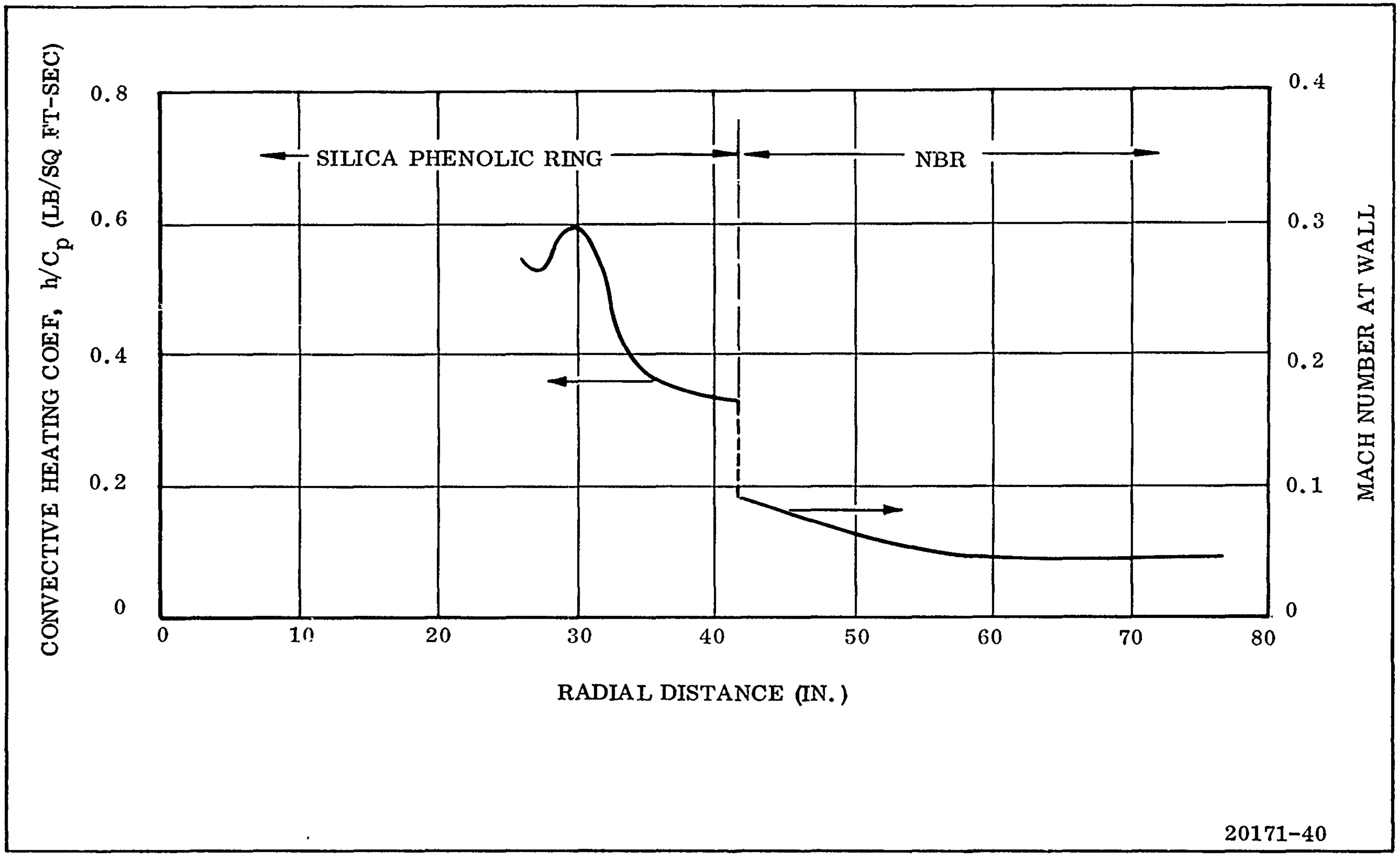

(U) Figure 39. Predicted Mach Flow and Heat Coefficient Through Aft Dome

SECTION	INSULATION MATERIAL	LOCATION, IN.	EXPOSURE TIME WEB BURN SEC	EXPOSURE TIME EFFECTIVE SEC	PREDICTED MAT'L LOSS RATE MIL/SEC	PRE MAT
A-A	V-44	13.0 RAD.	120		3.2	
B-B	V-44	41.48 RAD.	110	120	3.2	
C-C	V-44	Fwd dome line	Tailoff		3.2	
D-D	V-44	39.22 fwd of prop. face	Tailoff		3.2	
E-E	V-44	19.61 fwd of prop. face	60		3.2	
F-F	V-44	3.27 fwd of prop. face	110	120	3.2	
G-G	V-44	Center of slot	120		3.2	
H-H	V-44	3.27 aft of prop. face	110	120	3.2	
J-J	V-44	19.61 aft of prop. face	60		3.2	
K-K	V-45	Cyl. area liner & bladder only	Tailoff		3.2	
L-L	V-44	7.5 aft of aft dome datum	4.0		3.2	
M-M	V-44	50.93 RAD.	80	98.4	9.3	
N-N	V-44	40.00 RAD.	113	120	17.7	2
P-P	Silica Phenolic	37.00 RAD.	120	120	9.3	1
R-R	Silica Phenolic	31.5 RAD.	120	120	17.4	2

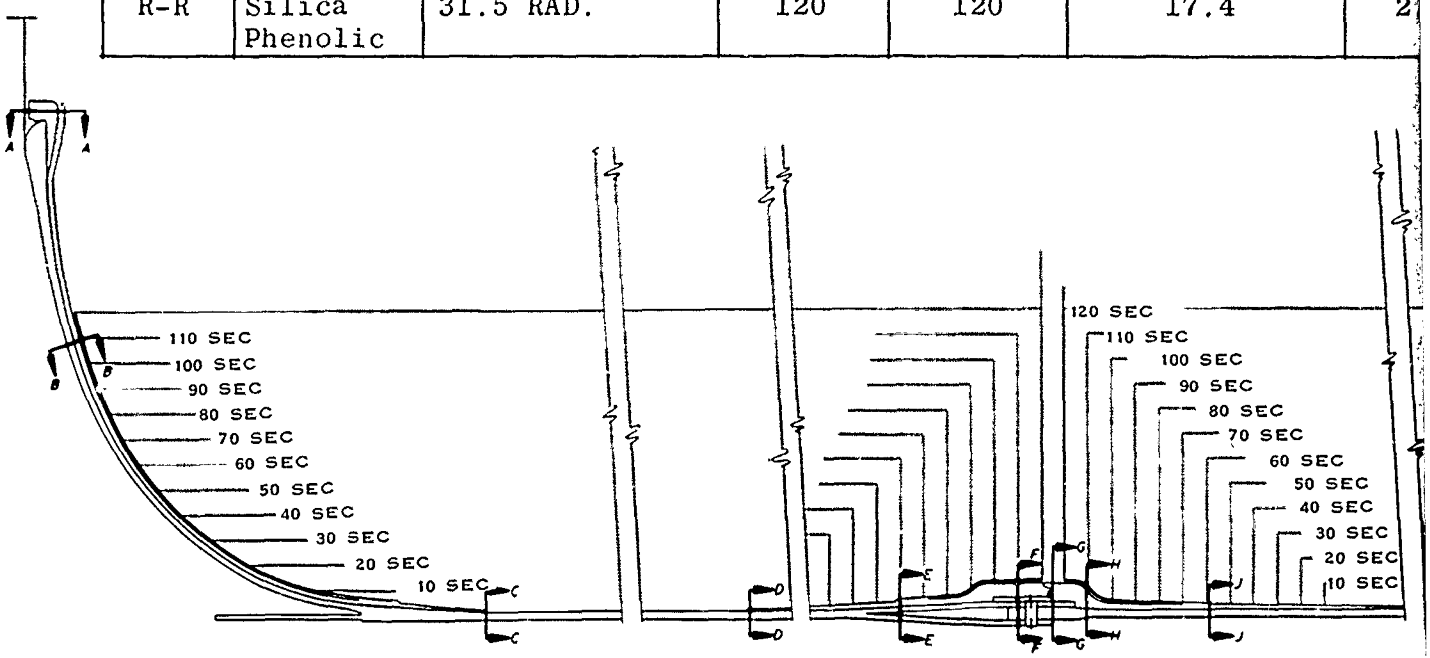

* Total thickness arrived at to meet desired contour and use of

** .06" thick bladder and .085" thick liner provide thermal prote
all other areas these items not considered.

MAT'L TE C	PREDICTED MAT'L LOSS INCHES	ADDED FOR 1.5 SAFETY FACTOR INCHES	ADDED FOR THERM PROTECT INCHES	INSUL DESIGN THICKNESS INCHES	TOTAL INSUL DESIGN THK. * INCHES	COMBINED SAFETY FACTOR
	.384	.192	.20	.776	.80	2.08
	.384	.192	.20	.776	.80	2.08
			.10	.100	.10	
			.10	.100	.10	
	.192	.096	.145	.433	.50	2.60
	.384	.192	.20	.776	1.50	3.91
	.384	.192	.20	.776	2.10	5.47
	.384	.192	.20	.776	1.30	3.39
	.192	.096	.145	.433	.50	2.60
			.09	.090	** -	-
	.013	.007	.10	.120	.30	23.44
	.915	.458	.184	1.557	1.60	3.25
	2.124	1.062	.20	3.386	3.50	2.47
	1.120	.560	.365	2.045	4.00	3.66
	2.090	1.045	.365	3.500	3.55	2.57

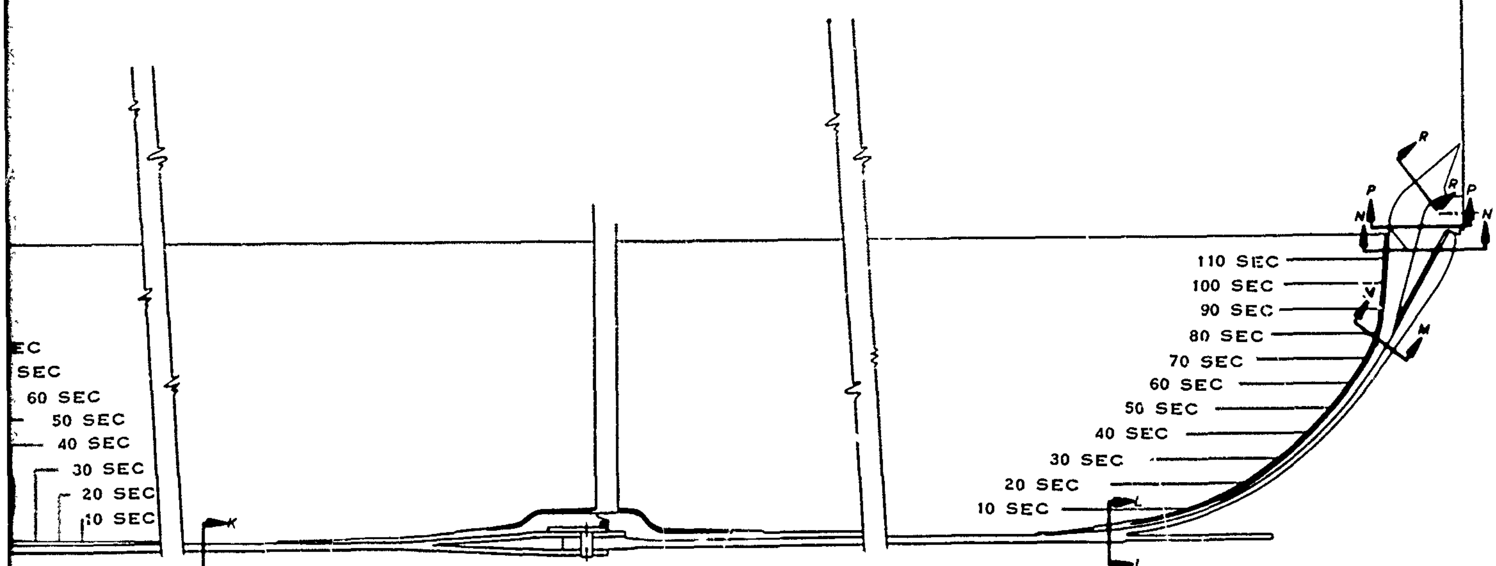

d use of .1" stock.

rmal protection--

(U) Figure 40. 156-8 Insulation Design Thickness of 5,408 psi in compression at Point A, Figure 41. The thermal stress analysis indicated a maximum stress of 7,540 psi at a point 0.3 in. from the initial surface. Adding these two stresses directly, a maximum combined stress of 12,948 psi compression occurred. As the ring surface eroded, the stresses due to internal case pressure decreased and conditions improved. A conservative value for the compressive strength of silica cloth phenolic at 870°F is 15,000 psi.

(U) d. Predicted Material Loss--More recent data and consequent design analysis refinements resulted in better methods for predicting material loss in aft dome areas than were available at the time the 156-8 was designed. Recent data showed good correlation between heat flux (q_t) and material loss rate for silica cloth phenolic and between enthalpy heat transfer coefficient (h/C_p) and material loss rate for asbestos-filled NBR. These correlations are shown on Figures 42 and 43. From flow and heat transfer analysis, the relationship between q_t and h/C_p and motor location was determined (Figures 44 and 45). From these relationships, the predicted material loss was determined and the resulting safety factor was calculated. The safety factor column in Figure 40 is based on predicted material loss using the more recent design analysis techniques. A profile showing the predicted erosion in the aft dome is shown on Figure 46.

(U) During installation of the insulation pieces in the forward dome and joint sections, considerable voids occurred in the bond behind the large insulation pieces. The design was changed in the aft dome insulation to reduce the voids. The change consisted of providing 0.125 in. bleeder holes drilled through the insulation on 12 in. centers. The holes were drilled 45 deg to the chamber gas flow to minimize erosion into the UF-1149 which would fill the holes during bleedout.

(U) e. Insulation Weight Loss vs Time--The predicted insulation weight loss vs time for the 156-8 motor is shown on Figure 47.

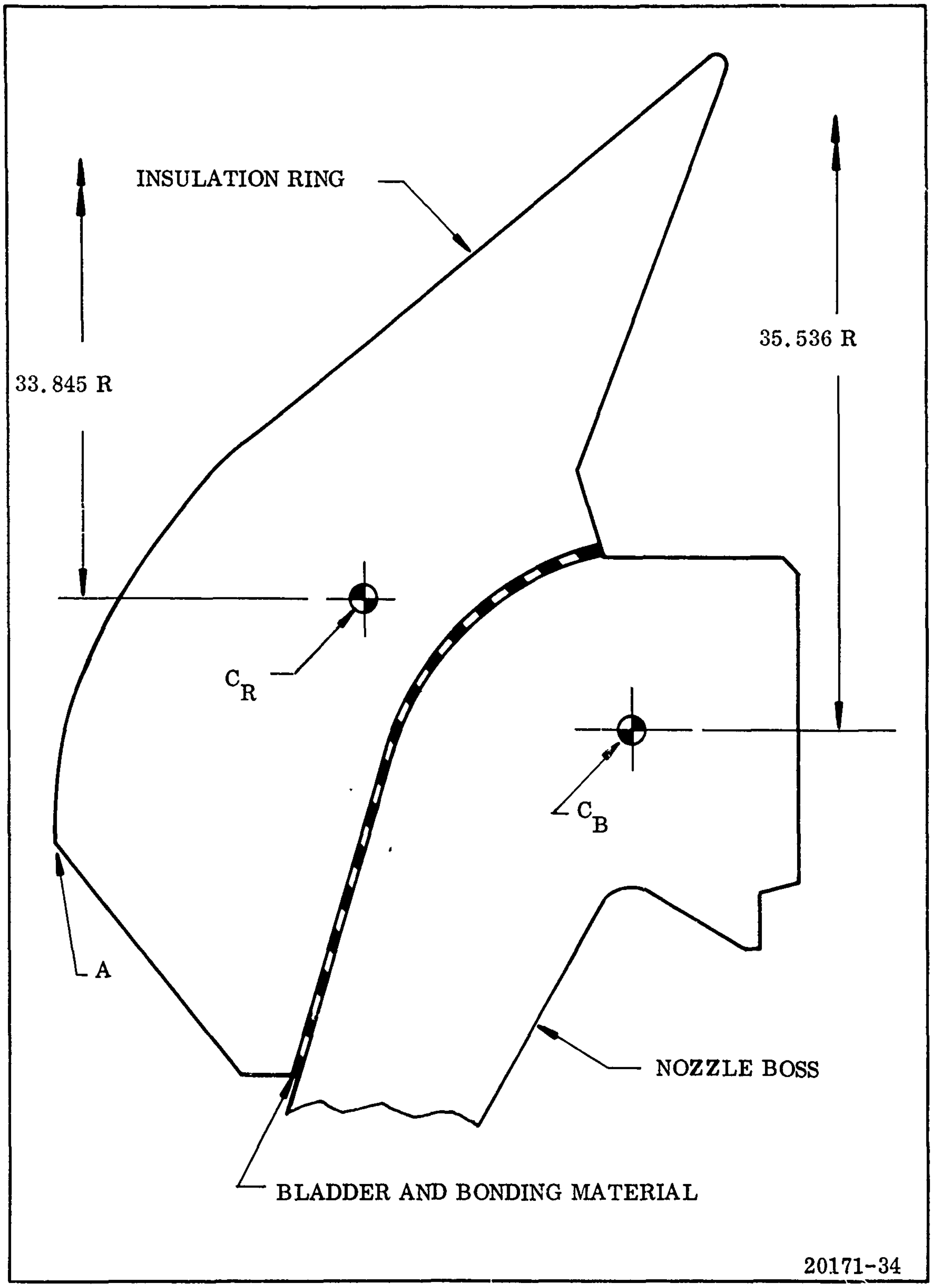

(U) Figure 41 . 156-8 Rocket Motor Polar Boss and Insulation Ring Assembly

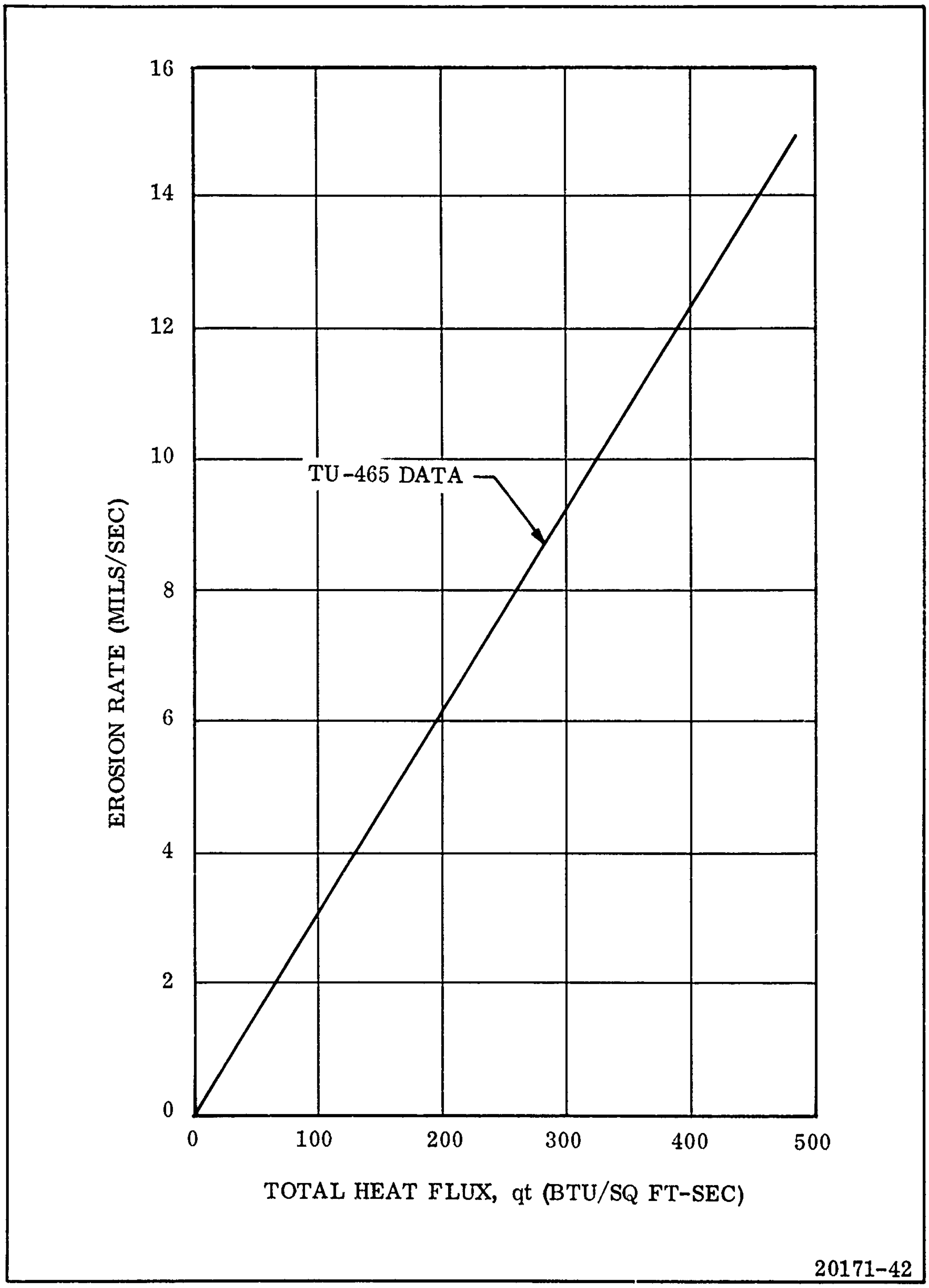

(U) Figure 42 . Silica Cloth Erosion Rate vs Total Heat Flux

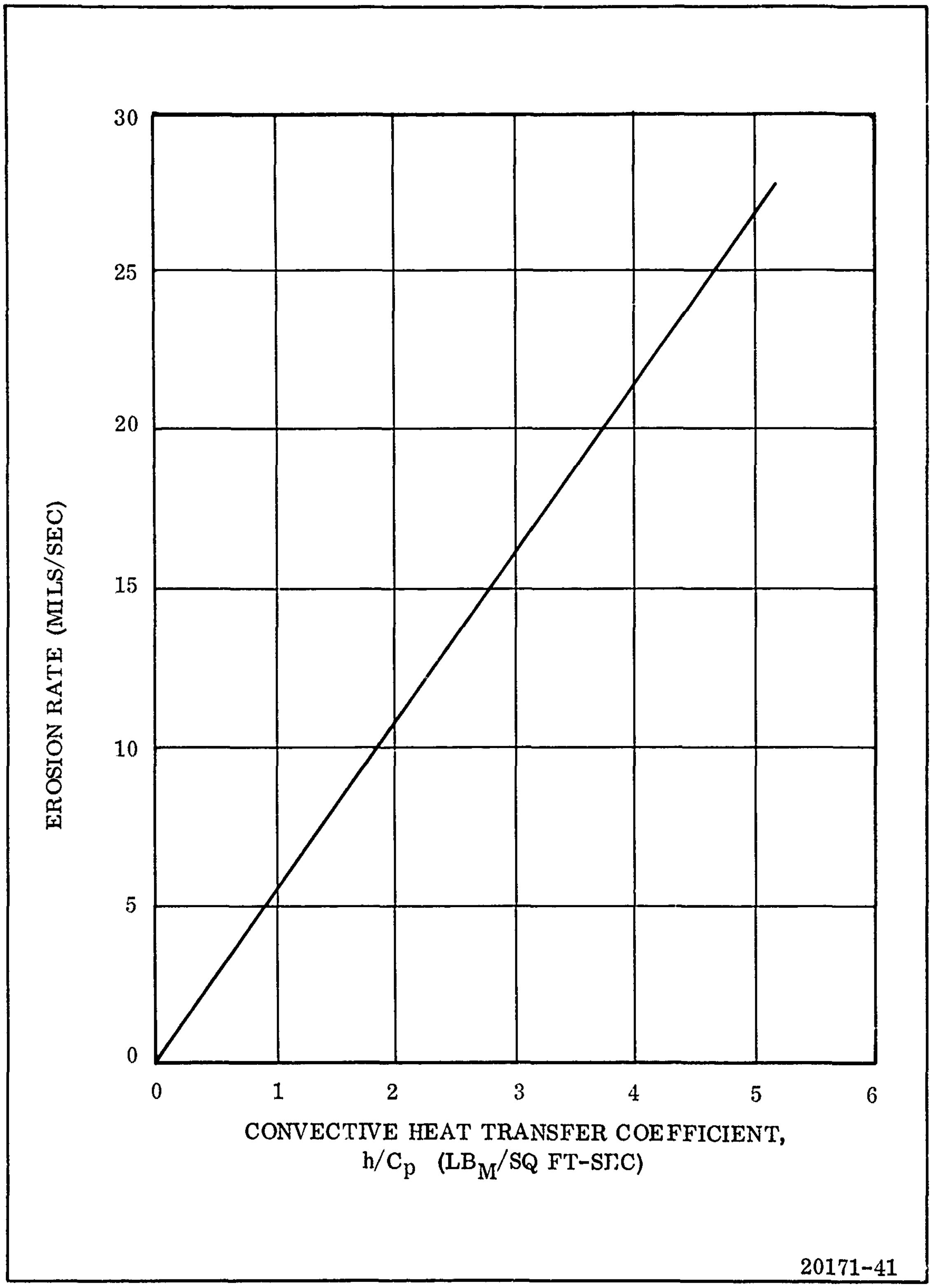

(U) Figure 43 . V-44 Erosion Rate vs Convective Heat Transfer Coefficient

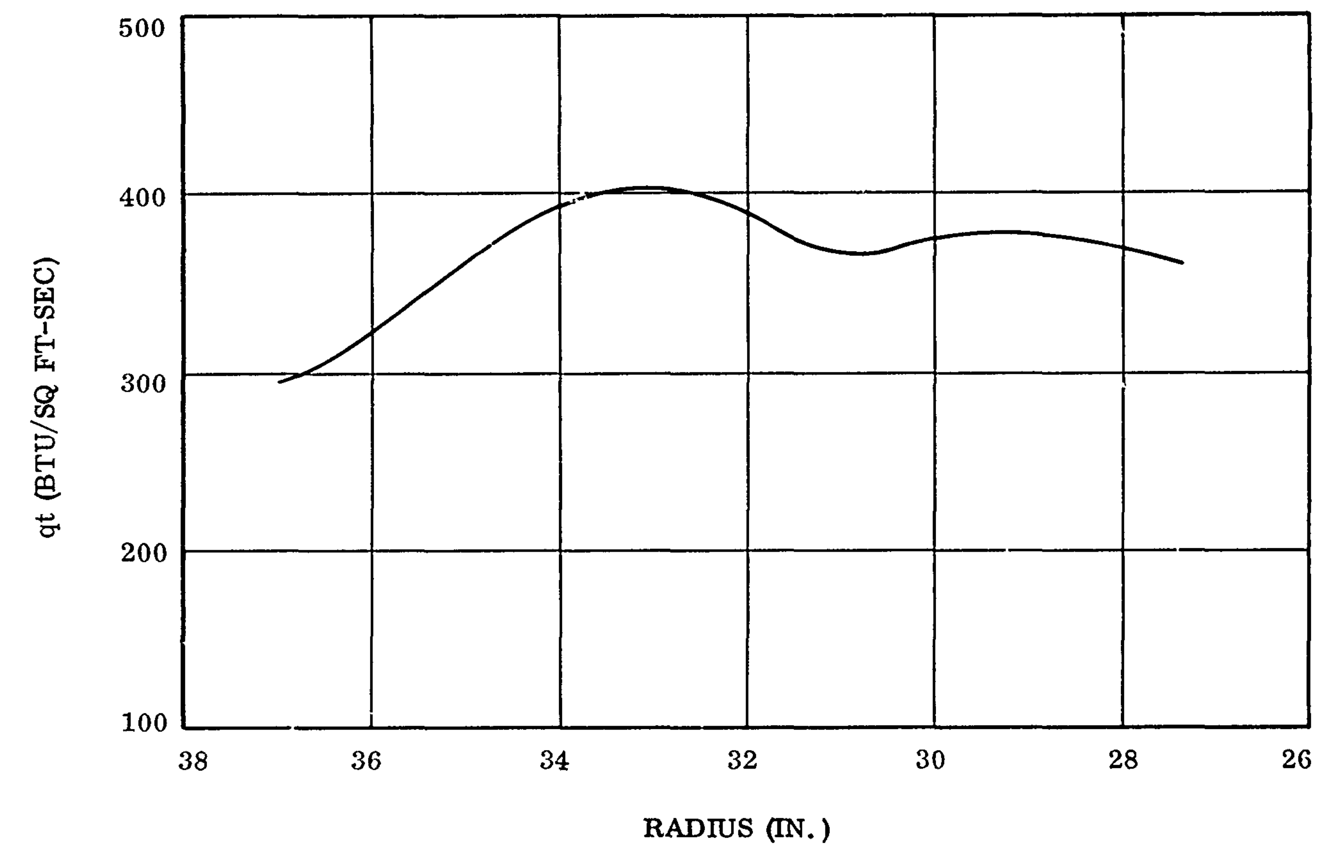

(U) Figure 44 . 156-8 Rocket Motor Aft Dome Total Heat Flux Variation on Silica Cloth

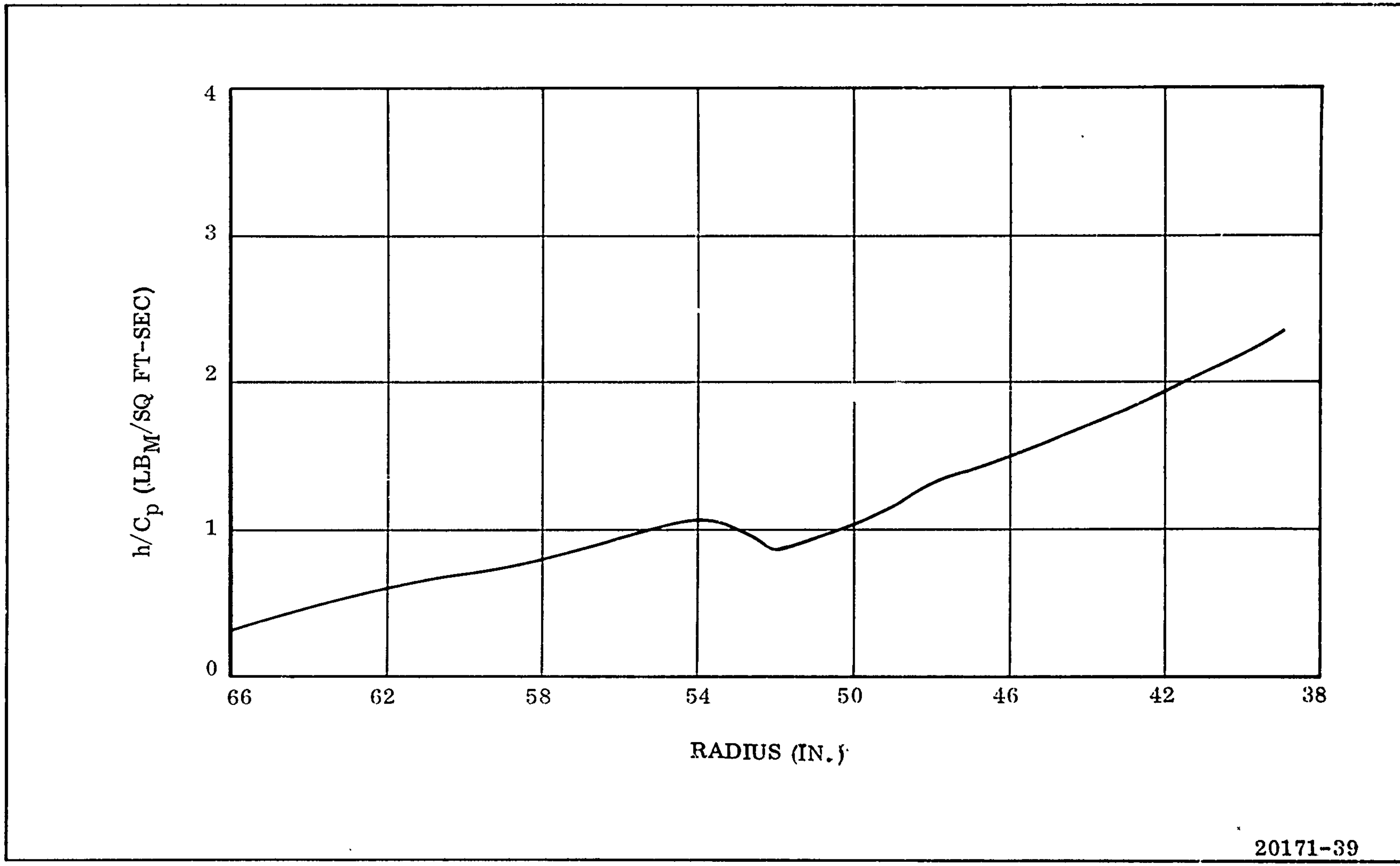

(U) Figure 45 . 156-8 Rocket Motor Aft Dome Heat Transfer Coefficient Variation on Asbestos Filled NBR

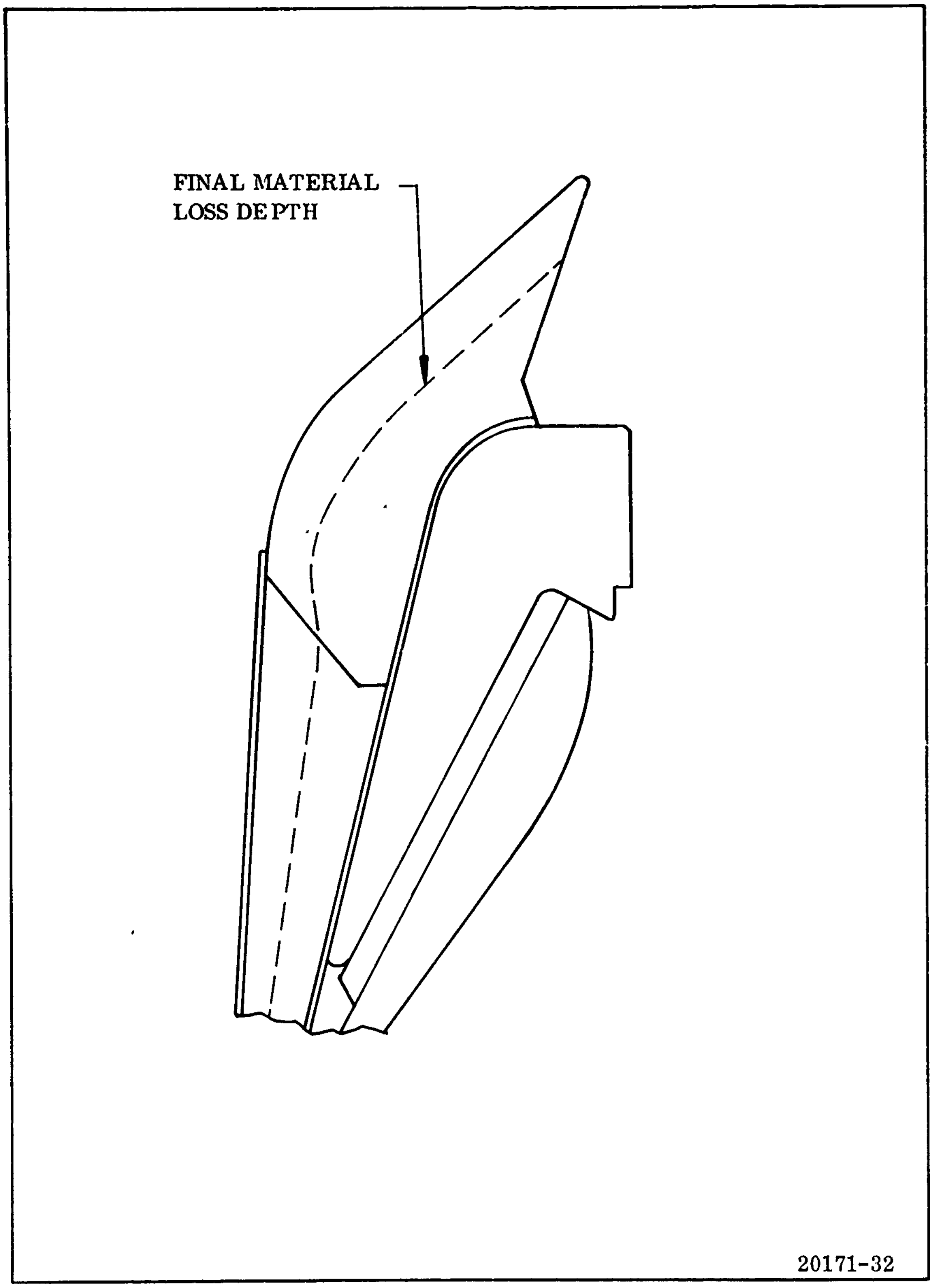

(U) Figure 46 . Predicted Material Loss Profile in Insulation Ring

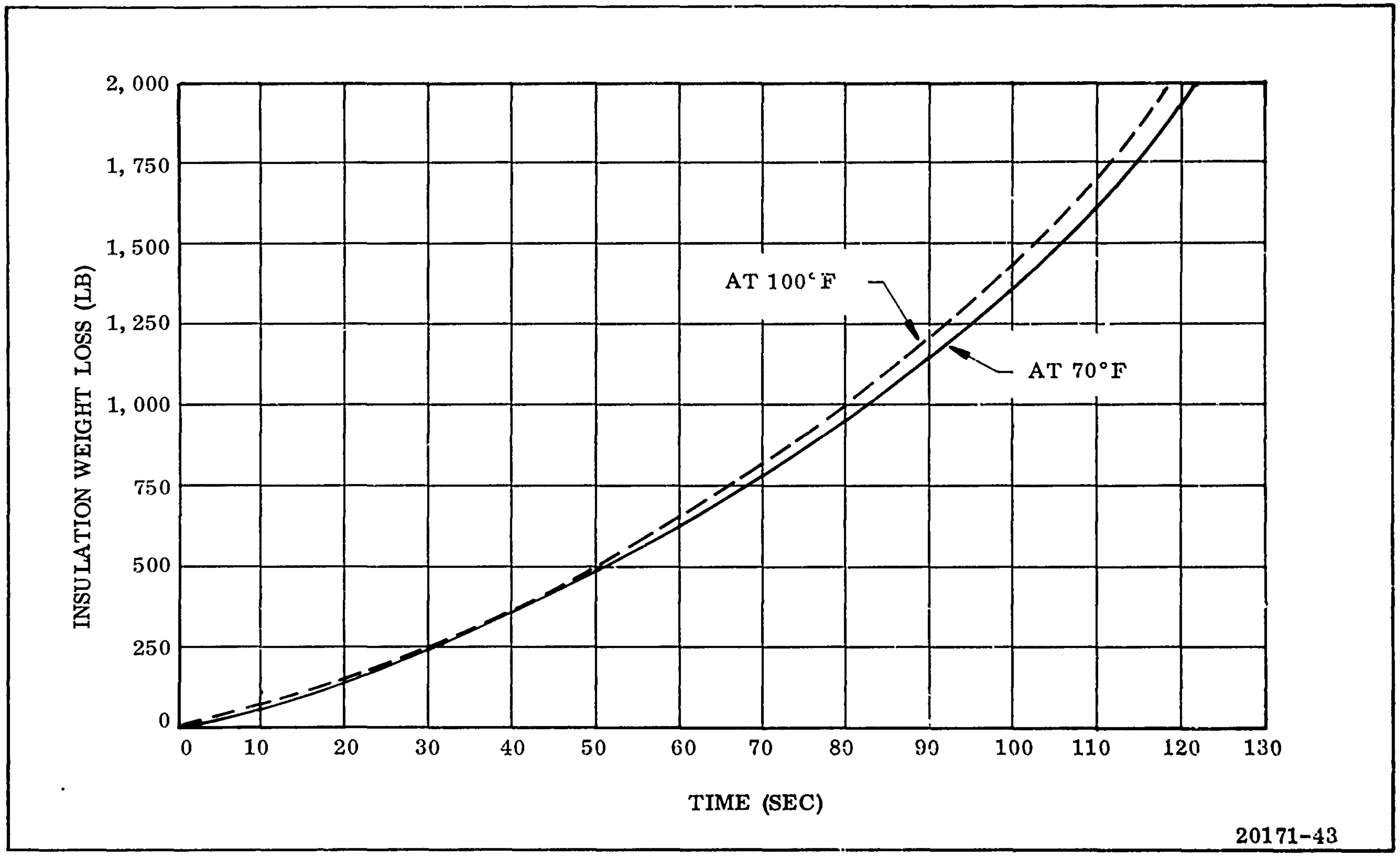

(U) Figure 47 . 156-8 Rocket Motor Predicted Insulation Weight Loss vs Time

(U) B. FABRICATION

(U) 1. JOINT INSULATION

(U) a. Mold Preparation--The molds for fabricating the case segment joint insulation were constructed in a 156 in. diameter autoclave. The autoclave was the center segment of the TU-412 (AF 156-1) motor with end closures and heating element. The segment was positioned horizontally in the modular pallet and fitted with a cable-winch assembly to provide 360 deg rotation.

A sweep template was fabricated which contained two configurations:

1. Contour of the ID of the clevis (female) joint area of the 156-8 case where insulation would be installed.
2. Contour of the ID of the tongue (male) joint of the 156-8 case where insulation would be installed.

The sweep template, mounted from the modular pallet, was positioned in the TU-412 center segment so the template was spring loaded against the end of the segment (Figure 48). Due to an out-of-round condition in the TU-412 segment, the template had to be moved radially inward to provide clearance between the segment wall and the sweep template. This reduced the circumferential length of the joint mold and therefore necessitated addition of a makeup section mold in the middle of the TU-412 segment.

(U) Plaster saturated hemp was applied to the segment wall at each of the two sweep template contours. Plaster was applied on top of the hemp over a 45 deg arc of the circumference. The plaster was swept to configuration and allowed to dry slightly before proceeding to the next 45 deg arc. A 3 to 4 in. gap was left between adjacent 45 deg mold sections to allow plaster runout and to provide an index point for the template prior to sweeping. After completing the first two ring molds, the template was set up at the opposite end of the TU-412 segment and a second set of mold rings were fabricated. The gaps between each 45 deg section of the mold rings were filled with plaster and hand blended to the mold configuration. Voids in the plaster mold surface were filled and hand finished.

(U) Since the sweep template had not been designed for sweeping molds onto the center of the TU-412 center segment for the makeup sections, an alternate procedure was required for fabricating the short plaster molds that had to be added. A 3 ft section of each mold ring, at the segment ends, was covered with Teflon tape and a hemp reinforced plaster model was cast on each section. After hand finishing, the models were covered with Teflon tape. Plaster was then cast onto the Teflon covered models to duplicate the ring mold configurations. The short plaster molds were installed on the TU-412 segment wall on top of wet plaster. Three plaster cubes were cast and bonded on the segment wall opposite the short mold sections to counterbalance the segment (Figure 49).

(U) The plaster was dried for 12 hr at 135°F and then spray coated with three coats of clear lacquer sealer. Each sealer coat was dried tack free before application of the subsequent coat.

(U) b. Insulation Layup and Vulcanization--Uncured asbestos-filled NBR (V-44) was laid up in 90 deg sections on each plaster mold ring; thus, each ring (joint) insulator was fabricated in four sections for ease of handling, both during layup and during installation operations. Each short mold section was laid up separately.

(U) Prior to the layup of each section, Teflon tape was applied to the surface of the plaster mold. The Teflon was coated with UF-3196 to provide a low strength bond between the Teflon and the first layer of NBR insulation. The strength of this bond was sufficient to support the weight of the 90 deg insulation section when it was at the 12 o'clock position during insulation layup, and when the TU-412 segment was in a vertical position.

(U) The 0.100 in. thick uncured asbestos filled NBR insulation (V-44) sheet stock was unrolled from the 200 lb, 36 in. wide roll, and cut to the required configuration. The edges were skived at 45 deg, the surface activated with MEK, and then allowed

N41681-3

Figure 48. Joint Insulation Contour Sweep Template

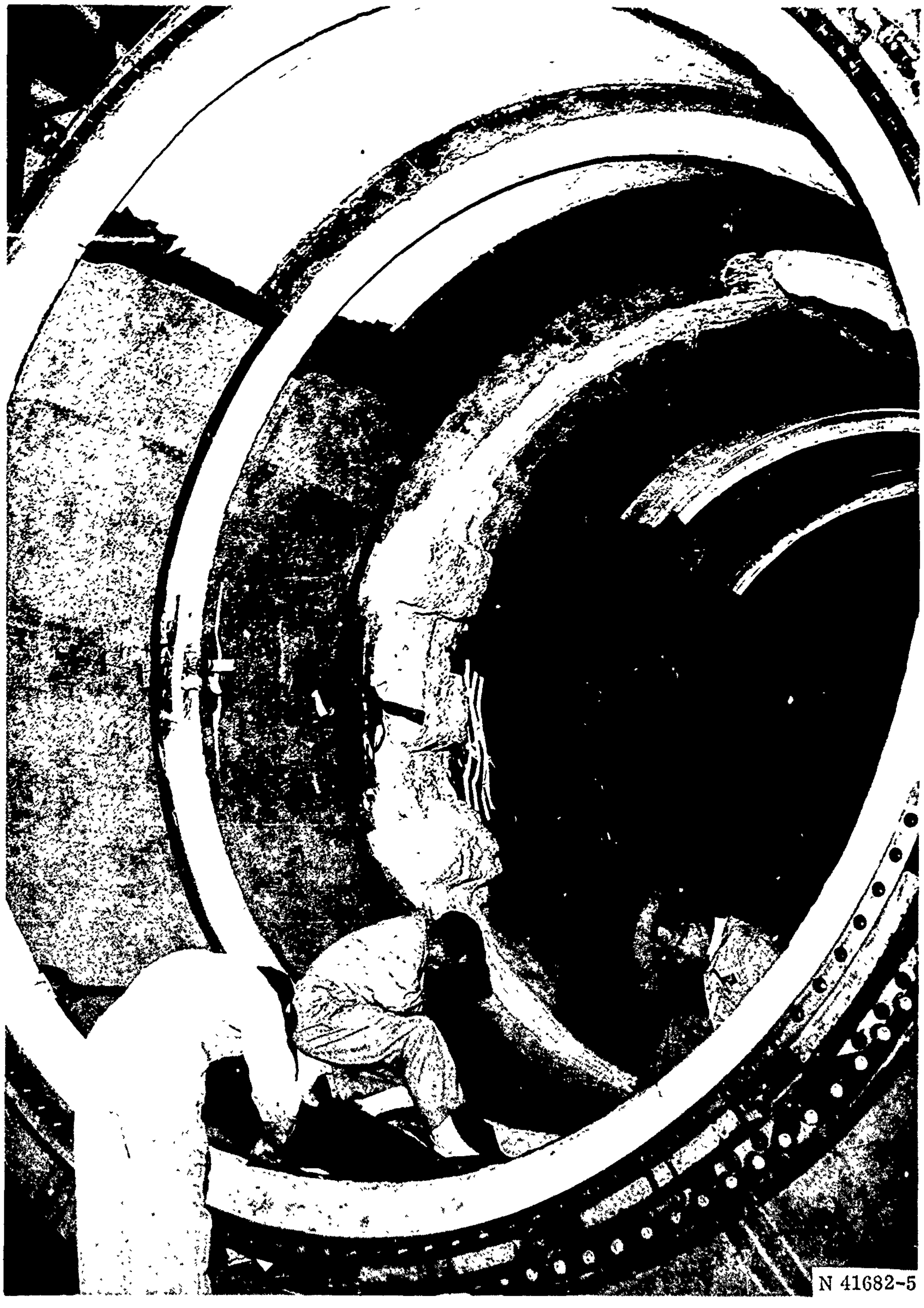

Figure 49. Layup of Joint Insulation

to dry for 3 to 5 minutes. After being placed in position, each layer was rolled and stitched to eliminate air pockets beneath the insulation layer (Figure 50). Thermocouples, for use in insulation cure, were embedded in the insulation during layup (Figure 51) and bonded in place with UF-3196.

(U) Propellant relief flaps were fabricated integrally with each 90 deg insulation section and each short section. Teflon tape was applied over the insulation layup where the flap was to be separated from the insulation. The Teflon was coated with UF-3196 and the V-44 sheet was applied to the layup. Only that area of the sheet that was to be vulcanized to the insulation was activated with MEK prior to layup.

(U) Joints between each 90 deg section were formed by skiving the joint insulation longitudinally at a 45 deg angle and then covering the skived edge with two layers of Teflon tape to prevent vulcanization of the 90 deg sections. Each V-44 layer of the adjacent 90 deg section was skived and butted against the Teflon coated edge to form the mating joint.

(U) Following insulation layup, the rings and short sections were covered with a vacuum bag consisting of Trevarno release cloth, rubber coated horsehair, and two mil, high temperature, nylon vacuum bag material. Joints and edges of the nylon were sealed with high temperature vacuum tape.

(U) The bottom dome was installed on the segment, the segment placed vertically in the cure pit, and the upper dome installed. After minor repairs to the vacuum bag, the electric heater was installed in the upper dome. The autoclave was pressure checked and any leaks corrected. Instrumentation was connected to recorders. The segment was then pressured with CO_2 to 100 psig. The pit temperature and the interior of the segment were raised to approximately 200°F and held at that temperature until the lowest thermocouple reached 205°F. The 205°F temperature was maintained for one hour, the period defined as the soak period.

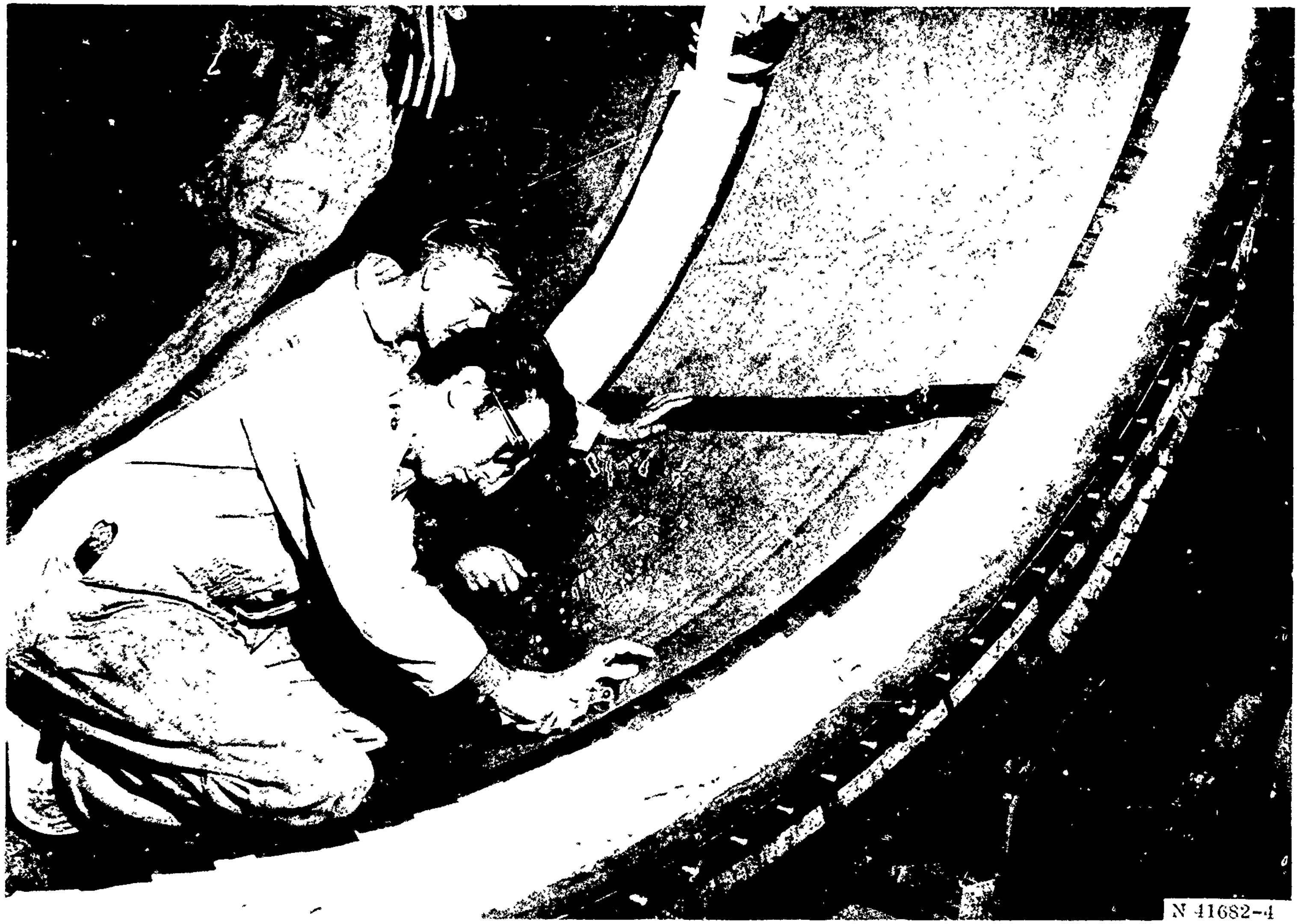

Figure 50. Rolling and Stitching V-44 Sheets for Laminate

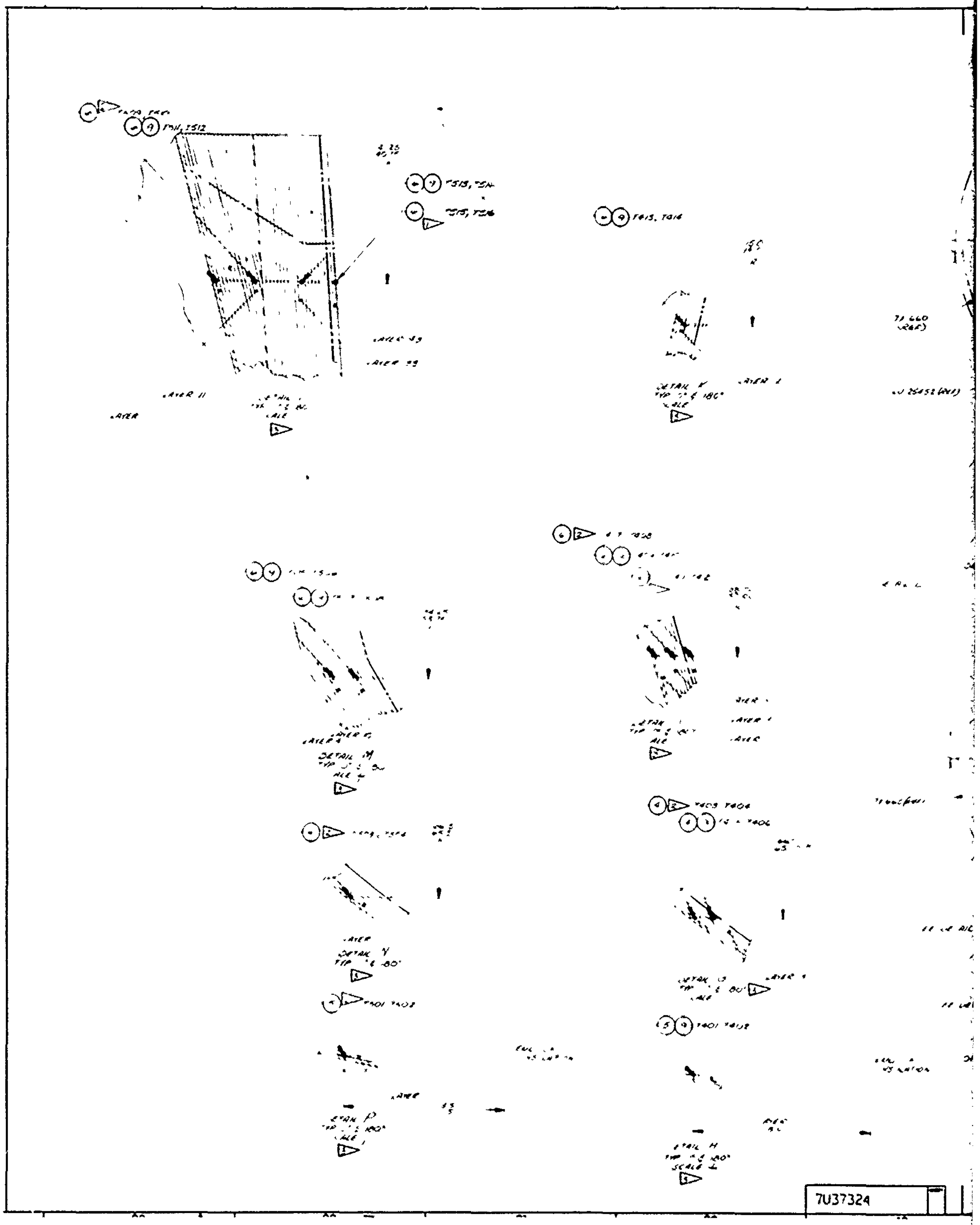
7U37324

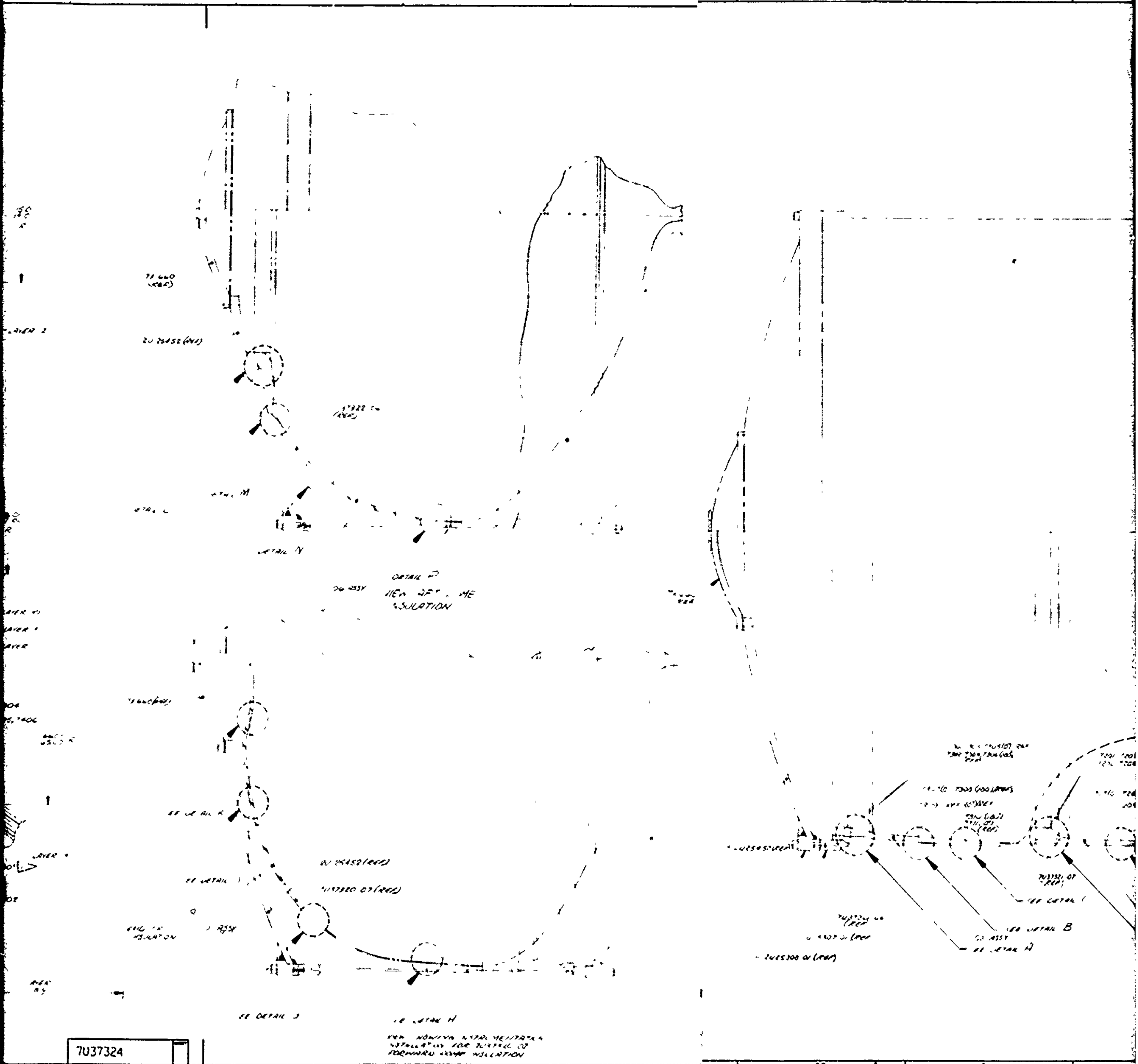

2

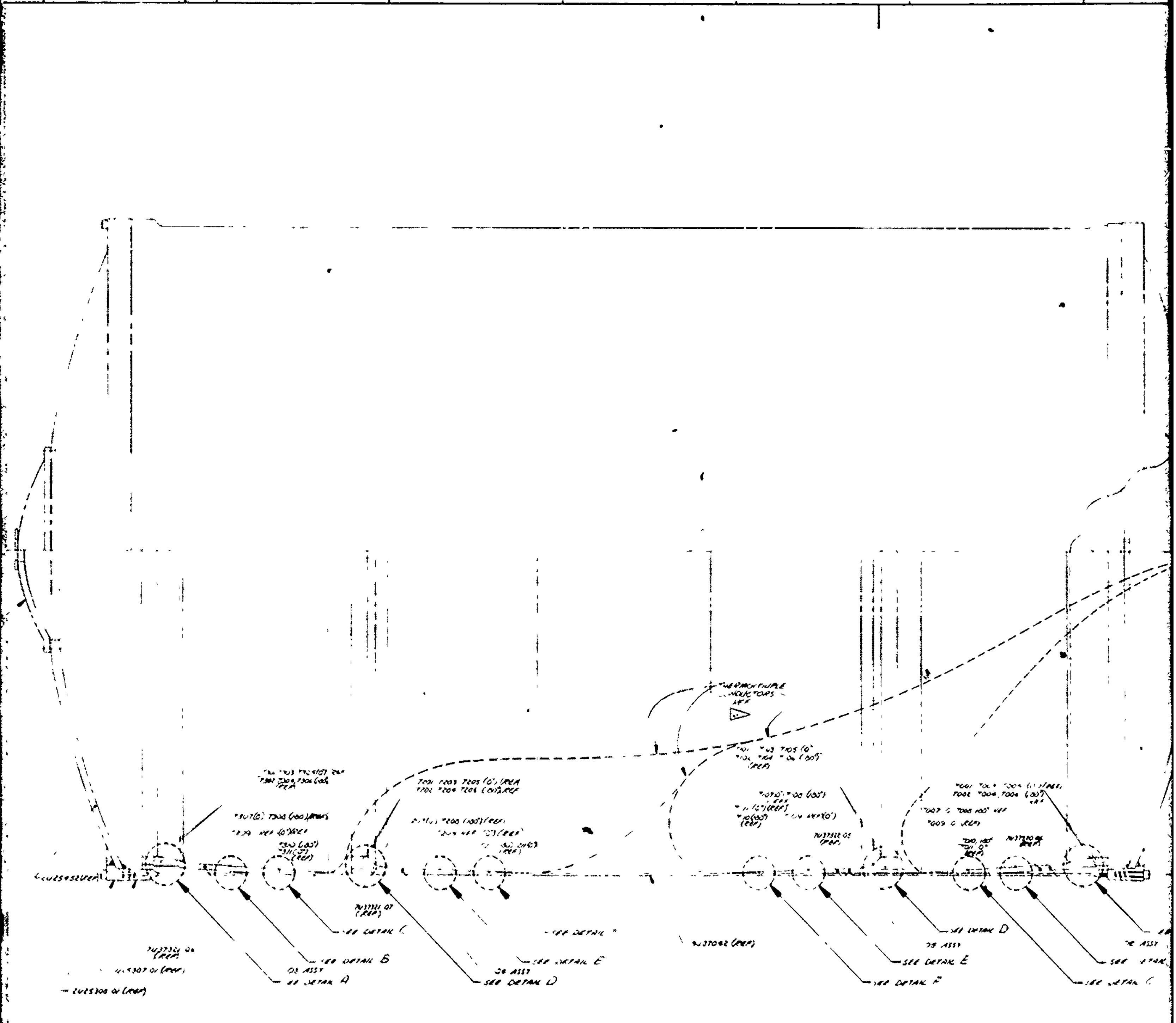
THERMOCOUPLE CONDUCTORS REF
SEE DETAIL A
SEE DETAIL B
SEE DETAIL C
SEE DETAIL D
SEE DETAIL E
SEE DETAIL F
7U37324

3

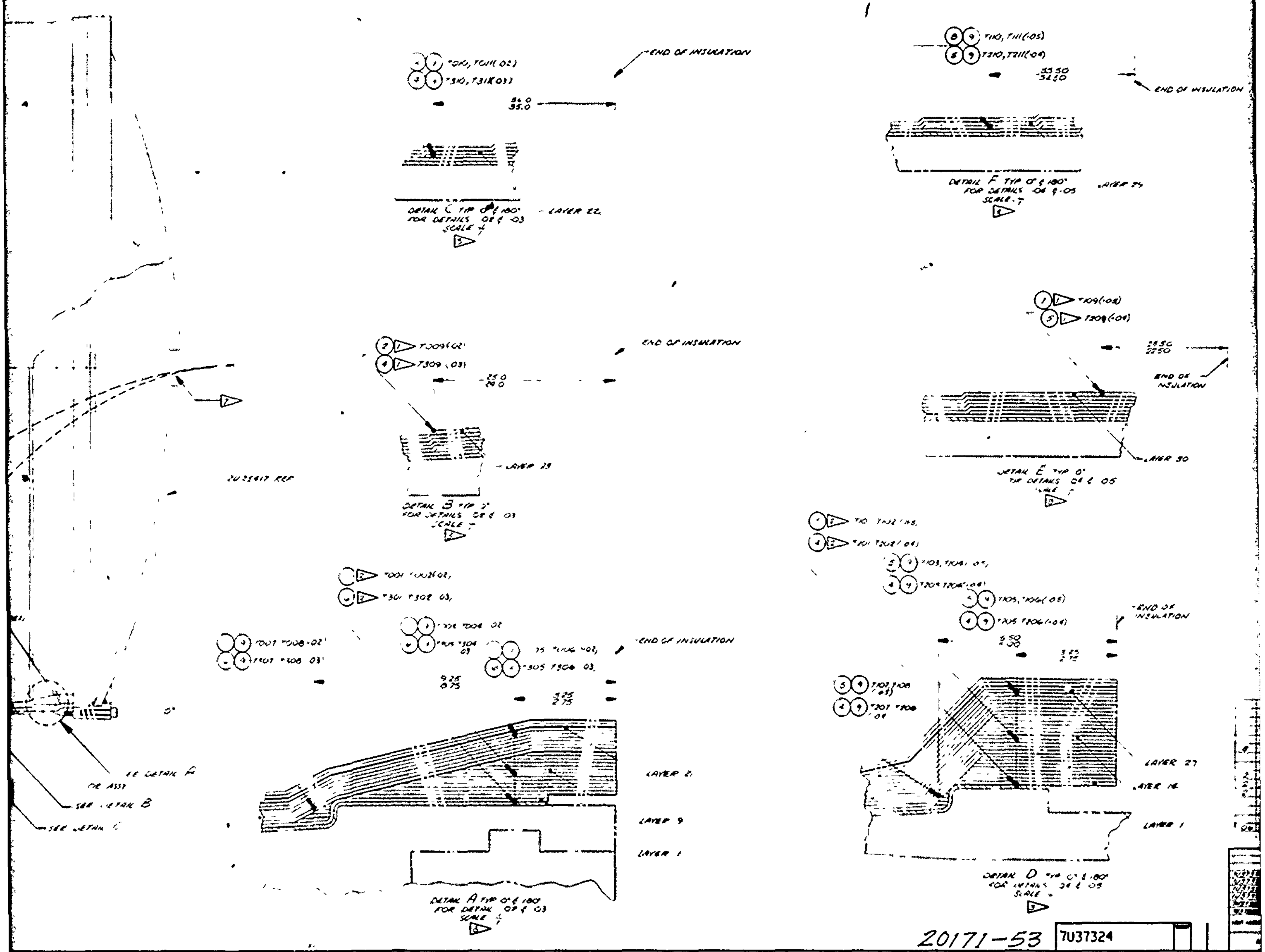

END OF INSULATION
DETAIL C TYP 0° & 180° FOR DETAILS 02 & 03
LAYER 22
DETAIL F TYP 0° & 180° FOR DETAILS 04 & 05
END OF INSULATION
DETAIL B TYP 0° FOR DETAILS 02 & 03
LAYER 23
DETAIL E TYP 0° FOR DETAILS 04 & 05
LAYER 30
END OF INSULATION
SEE DETAIL A
SEE DETAIL B
SEE DETAIL C
LAYER 21
LAYER 9
LAYER 1
DETAIL A TYP 0° & 180° FOR DETAIL 02 & 03
LAYER 27
LAYER 14
LAYER 1
DETAIL D TYP 0° & 180° FOR DETAILS 04 & 05
20171-53
7U37324

4

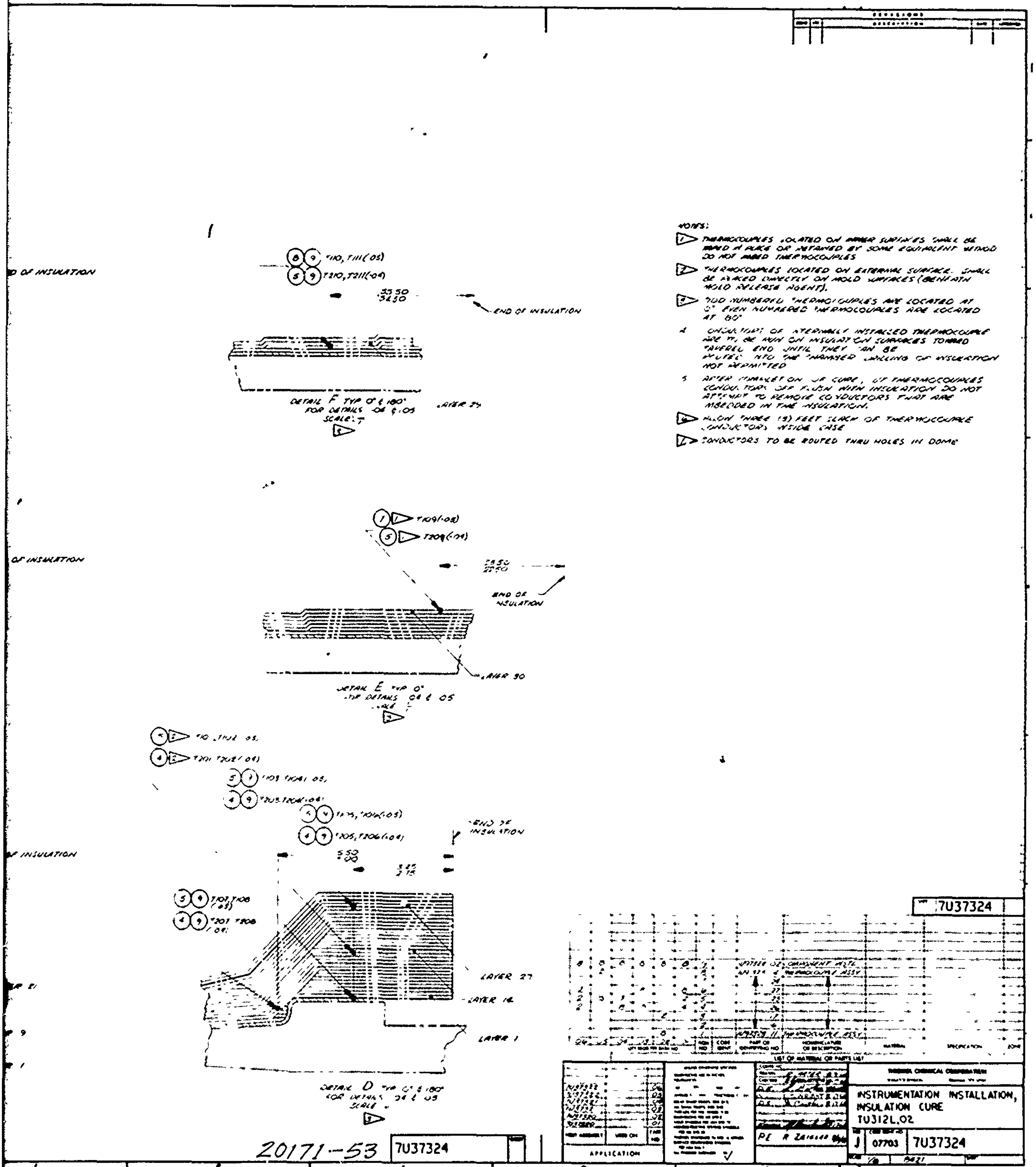

(U) Figure 51. Insulation Thermocouple Location

(U) Following soak, the pit and interior segment temperatures were raised to 315°F and held at that temperature until the required state of cure was reached. After cure, the insulation was cooled, under pressure, to a temperature of 150°F. Figure 52 shows the thermal history of the cure cycle. The elapsed time during soak, cure, and cooldown was 93.5 hr, and the cure equivalents on the insulation ranged from 1.87 minimum to 15.68 maximum. A cure equivalent is the minimum time required at a given temperature (i.e., 8 hr at 270°F, 2.5 hr at 300°F, or 1.25 hr at 320°F) to cure asbestos-filled NBR (V-44) insulation. The excessive elapsed time for the cure cycle resulted from equipment troubles and poor heat transfer through the thick plaster molds to the insulation layers adjacent to the mold surfaces.

(U) After reaching 150°F on cooldown, the segment was depressurized and the insulation sections removed. Each section was inspected and buffed preparatory to installation in the 156-8 case segments.

(U) c. Joint Insulation Installation--Prior to installing the joining NBR insulation sections in the individual segments, the nylon backup rings for the joint seals were bonded into the clevis (female) joints of the forward and center segments. The 1/8 in. thick by 2.25 in. wide nylon backup material was grit blasted and cut to the required length.

(U) The area of the segments where the nylon would be bonded was cleaned with MEK while the nylon was cleaned with trichloroethylene. Both were coated with UF-3195, and the nylon was installed in the segments and held in place with nylon reinforced tape. Where the nylon did not locally conform to the segment contour, C-clamps were added to secure the nylon rings in place. The UF-3195 was cured for 24 hr at 80 ($\pm$ 20)°F. An error in butt joining the end of the nylon ring necessitated removal of a 10 in. section (5 in. on each side of the butt joint) of the ring. The ends were beveled and a splice section was fitted into place with the beveled ends of the splice section mating with the beveled ends of the ring to form a skived joint. The splice sections were bonded in place with UF-3195 and held with C-clamps during the 24 hr cure.

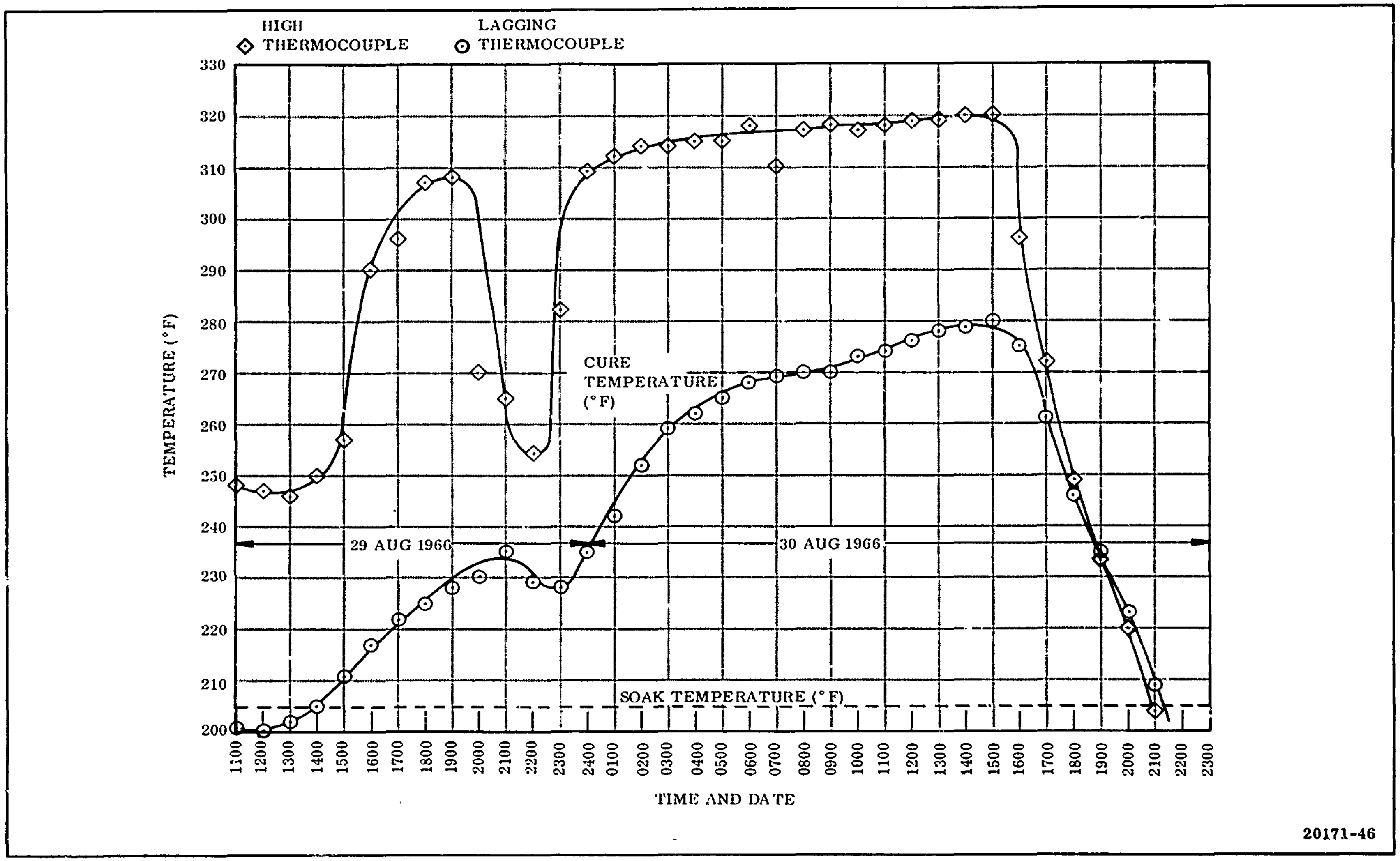

(U) Figure 52. Insulation Cure Cycle

(U) Installation of the NBR insulation sections into each case segment followed the same procedure. Both the buffed insulation section and the case segment were coated with UF-1149 adhesive (Figure 53) and the insulation section was placed into position in the segment. A vacuum bag of Trevarno release cloth, rubberized horsehair, and 2 mil thick nylon vacuum bag material was installed over the insulation section and sealed with vacuum tape (Figure 54). The UF-1149 adhesive was cured for 12 hr at 80 ($\pm$ 20)°F under vacuum. After removal of the vacuum bag, the Teflon tape around the installed section was removed, which also removed excess adhesive that had flowed out from under the insulation. The next insulation section was then installed.

(U) When the last insulation section was installed in the forward segment, the UF-1149 did not cure during the 12 hr cure period due to an error in the weighup of the UF-1149 materials. This section was peeled out and the UF-1149 removed from the bladder and insulation section by softening with MEK and scraping with spatulas. The insulation and bladder were buffed lightly to remove any remaining adhesive. After removal of the section, small voids were detected under the bladder, apparently caused by removal of the insulation section. These voids were filled with UF-3143 using hypodermic needles, and the insulation section subsequently was reinstalled.

(U) The propellant relief flaps vulcanized to each insulation section were connected by bonding three inch wide strips of 0.100 in. thick precured V-44 to each side of the flap, over the gaps. The strips were bonded over the joints with UF-1149 under vacuum.

(U) A considerable number of voids detected under the thin areas of the joint insulation sections were filled with UF-3143 with hypodermic needles. The UF-3143 was cured for 4 hr at 80 ($\pm$ 20)°F.

(U) d. Insulation Machining--Each unharnessed, unrounded segment was positioned vertically in a casting pit for joint insulation machining. A three legged spider type frame was attached to the joint end and secured to the segment utilizing the joint pin holes. The center of the routing machine frame (Thiokol Dwg 2U25245-03) was attached to a pivot post in the center of the spider frame. The routing machine frame

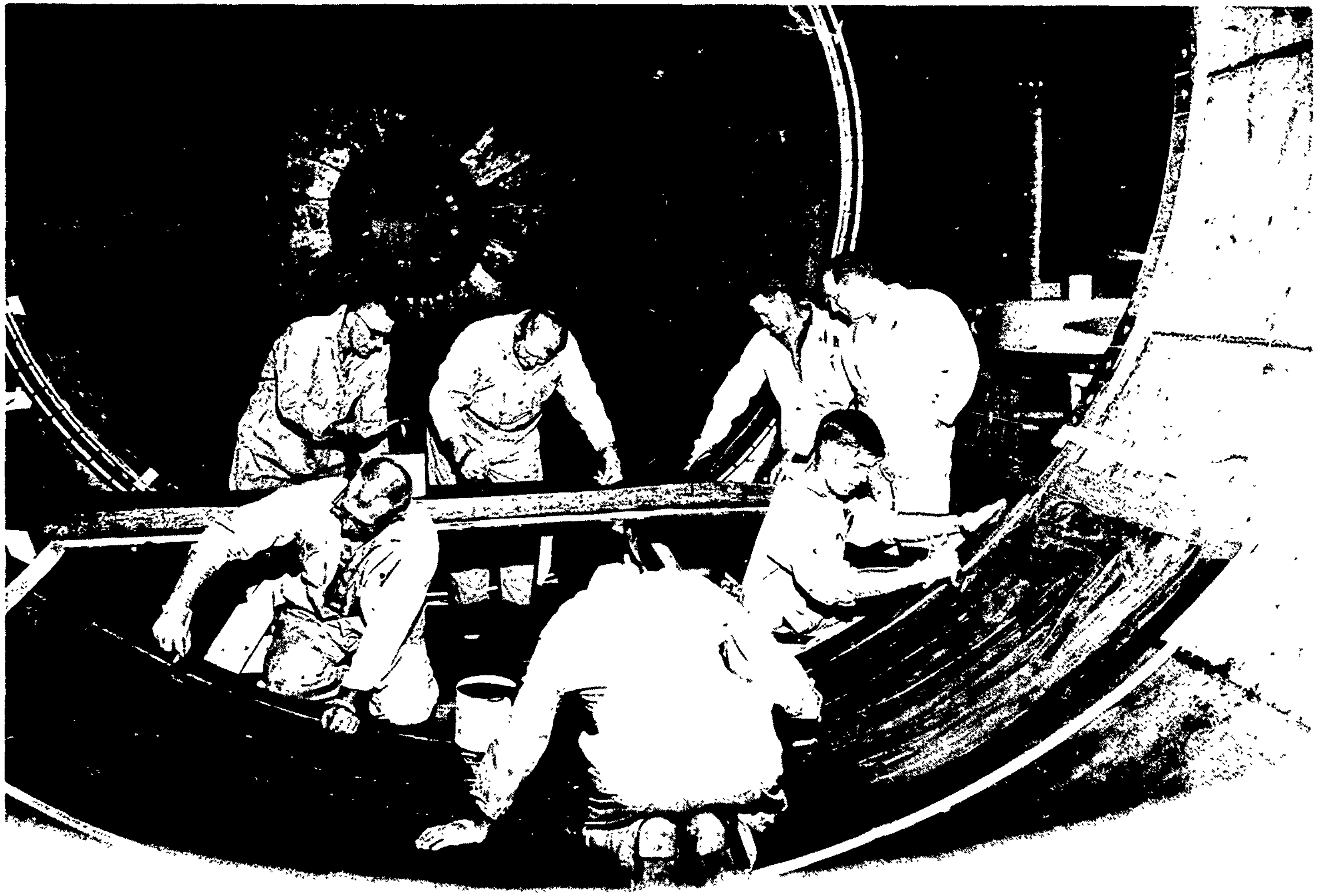

N 41786-5

(U) Figure 53. Application of UF-1149 to Insulation and Case

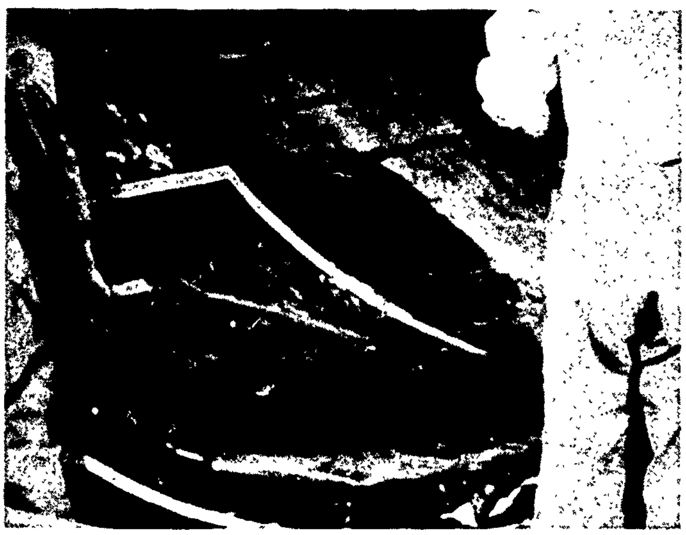

(U) Figure 54. Installation of Vacuum Bag consisted of three legs 120 deg apart with one leg carrying the router and router motor and the other legs providing support. Each supporting leg had a roller that rolled on the joint end while the leg carrying the router motor had a spring loaded roller arrangement that tracked the inside and end of the joint. This design allowed the router and router motor to duplicate the shape of the case segment as they tracked around the end of the segment. The router motor was powered by compressed air and the machine was pushed by hand around the segment end during machining operation (Figure 55).

(U) Depth of the cut was controlled by adjusting the router motor up and down. The groove in the insulation for the joint seal was rough machined with a carbide burr cutter and finished with a diamond grit router operated at 8,000 rpm. The diamond grit routers for the angled and flat surfaces (Figure 56) were designed to provide the required contours. These same routers had been used previously in machining the subscale case insulation.

(U) Several problems were encountered during the joint machining operation. Pushing the machine was very difficult during rough cutting because the spring was exerting too much force against the router motor slide and causing too much friction between the inside joint roller and the inside surface of the joint. The spring was removed and the rollers were held against the joint by hand at the same time the machine was being pushed. The excess roller force on the inside of the joints caused some shims to loosen at the extreme edge of the joint. This problem was solved by covering the inside of the shims with a thin piece of sheet metal and allowing the rollers that tracked the inside surface of the joint to roll against the sheet metal. All loose shims were post bonded prior to hydrotest.

(U) Several discrepancies were found during inspection of the machined insulation. Irregular surfaces, which exceeded maximum tolerances, were covered with UF-3119 and smoothed by hand to bring the surfaces into required tolerance. The insulation on the female joint of the center segment had been gouged by the router cutter when the operator released the machine while the motor was running. The gouge was filled with UF-3119 and hand worked to the required configuration.

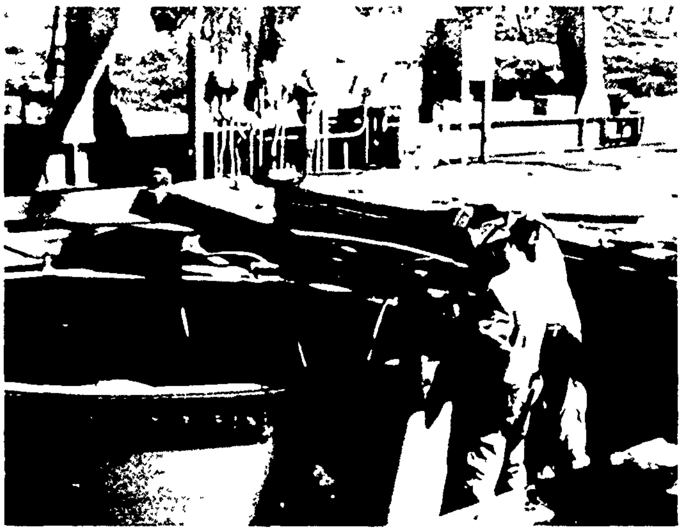

(U) Figure 55. Machining Insulation Joint

(U) Figure 56. Routing Insulation Joint

(U) 2. DOME INSULATION

(U) a. Phenolic Insulation Ring Fabrication--The silica cloth phenolic insulation ring (Thiokol Dwg 7U37323), which was used in the aft segment nozzle entrance area, was fabricated by Rohr Corporation, Space Products Division, Riverside, California.

(U) The ring was fabricated of Fiberite MX2600 material in a bias tape form. It was wrapped on a conical mandrel using a Betz boring mill adapted for wrapping with a side mounted wrapping head. The material was hydroclave cured with the progressive cure reaching the maximum temperature of 330 (± 10)°F and a pressure of 1,000 (± 25) psi. The vacuum in the bag was maintained throughout cure.

(U) The cured part was again machined to dimension using the Betz boring mill (Figures 57 and 58). Figure 57 shows the cut to remove the quality control (QC) ring. The complete OD was machined with the part on the mandrel. The part was then turned over for machining of the ID (Figure 58). Figure 59 shows hand finishing of the completed part.

(U) The two most significant problems involved were:

1. To obtain raw material which would meet Thiokol Specification TWR-941, and
2. To obtain processible material.

Several lots of Fiberite material were tested and found to be out of specification. Two lots of material were received at Rohr. The first was found to be unprocessible because the tack was insufficient to cause the wraps to adhere in winding.

(U) The lot of raw material which was accepted had a high volatile content of 4.59 percent average as opposed to the specification requirement of 4.0 percent maximum, and a breaking strength in the wrap direction of 137 lb/in. as opposed to specification minimum of 150 lb/in. Since the Rohr Corporation advised that the part could be fabricated and meet cured part specification utilizing this material, it was released for fabrication.

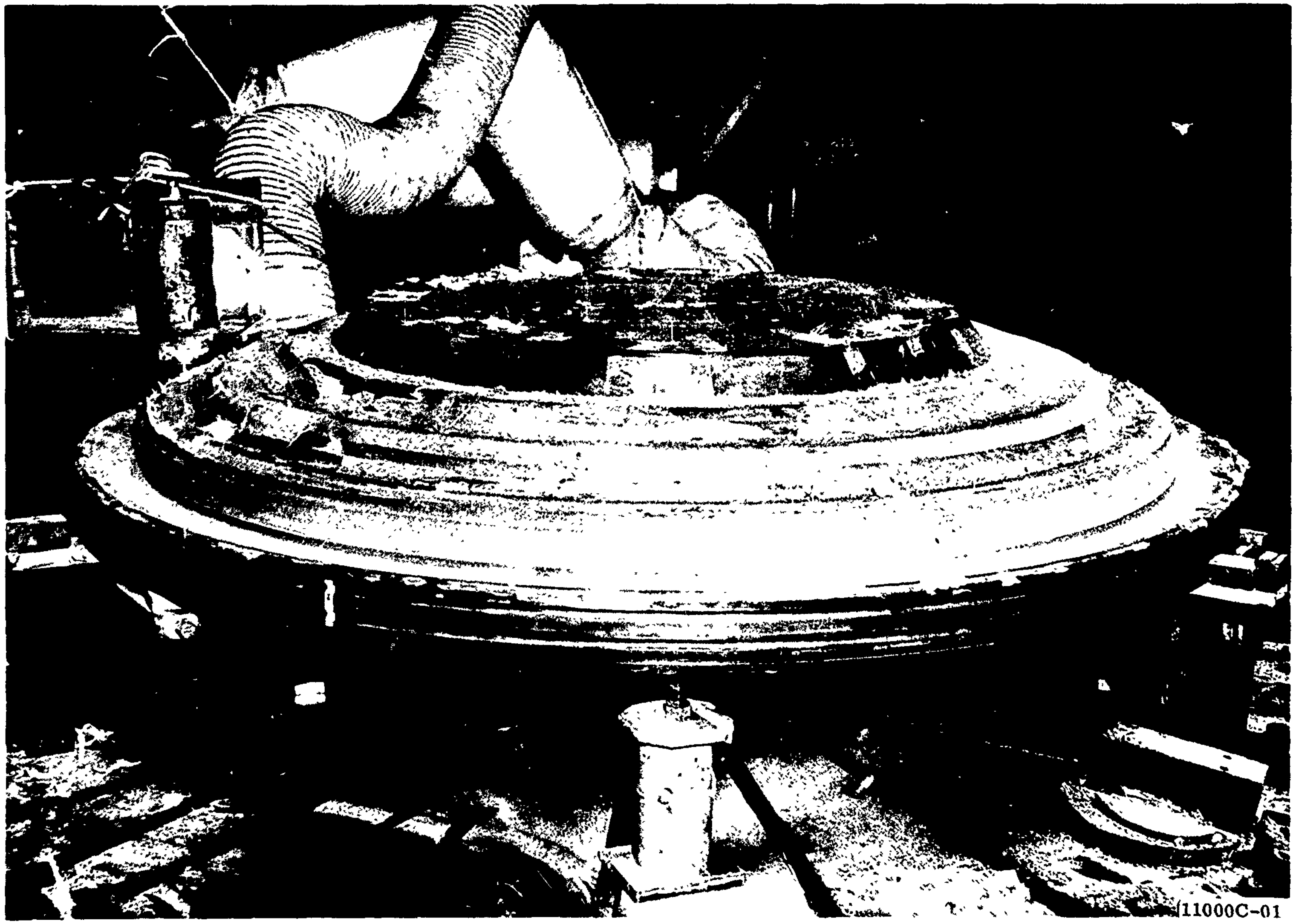

(U) Figure 57. Machining OD of Silica Cloth Phenolic Insulation Ring

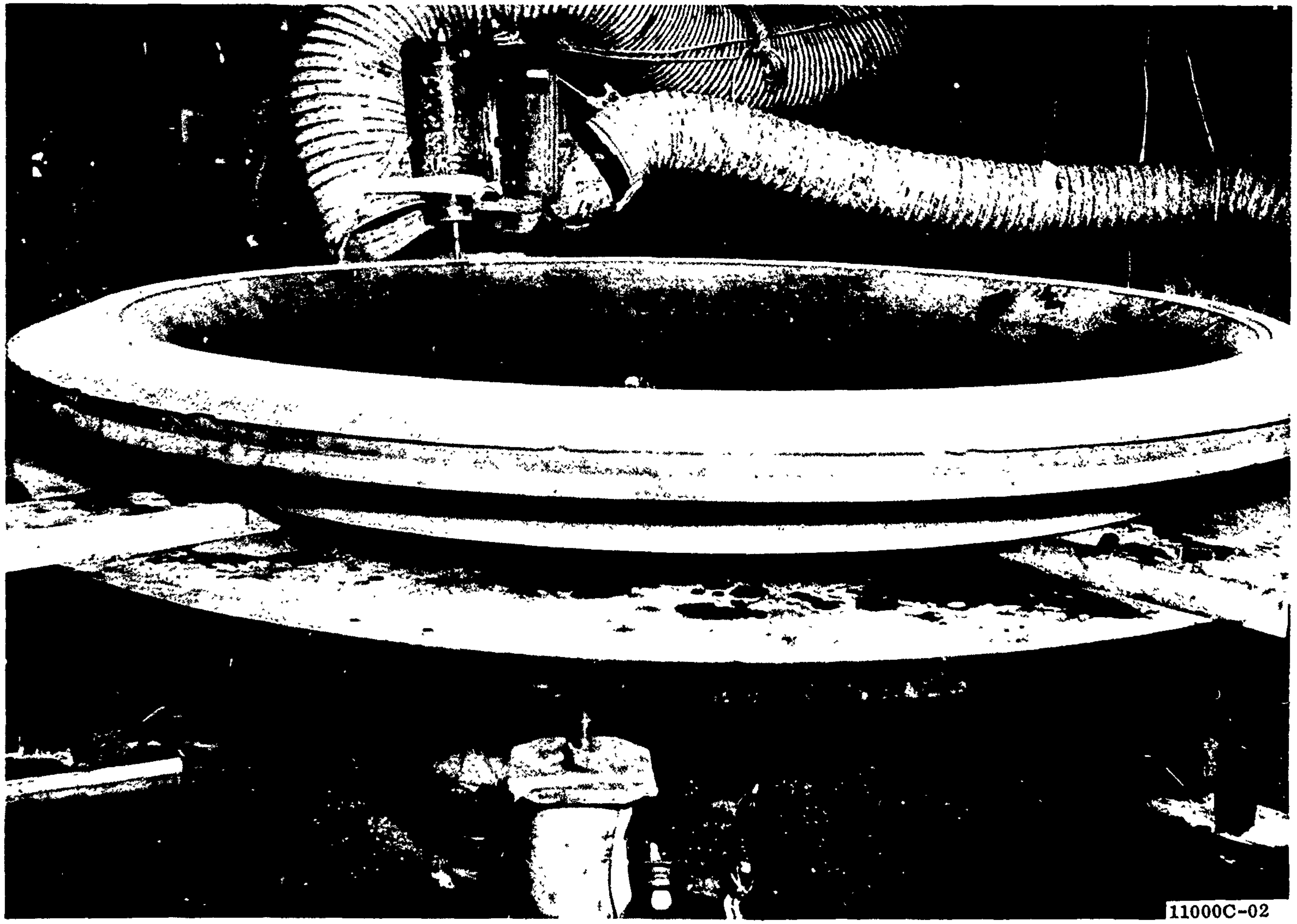

(U) Figure 58. Machining ID of Silica Cloth Phenolic Insulation Ring

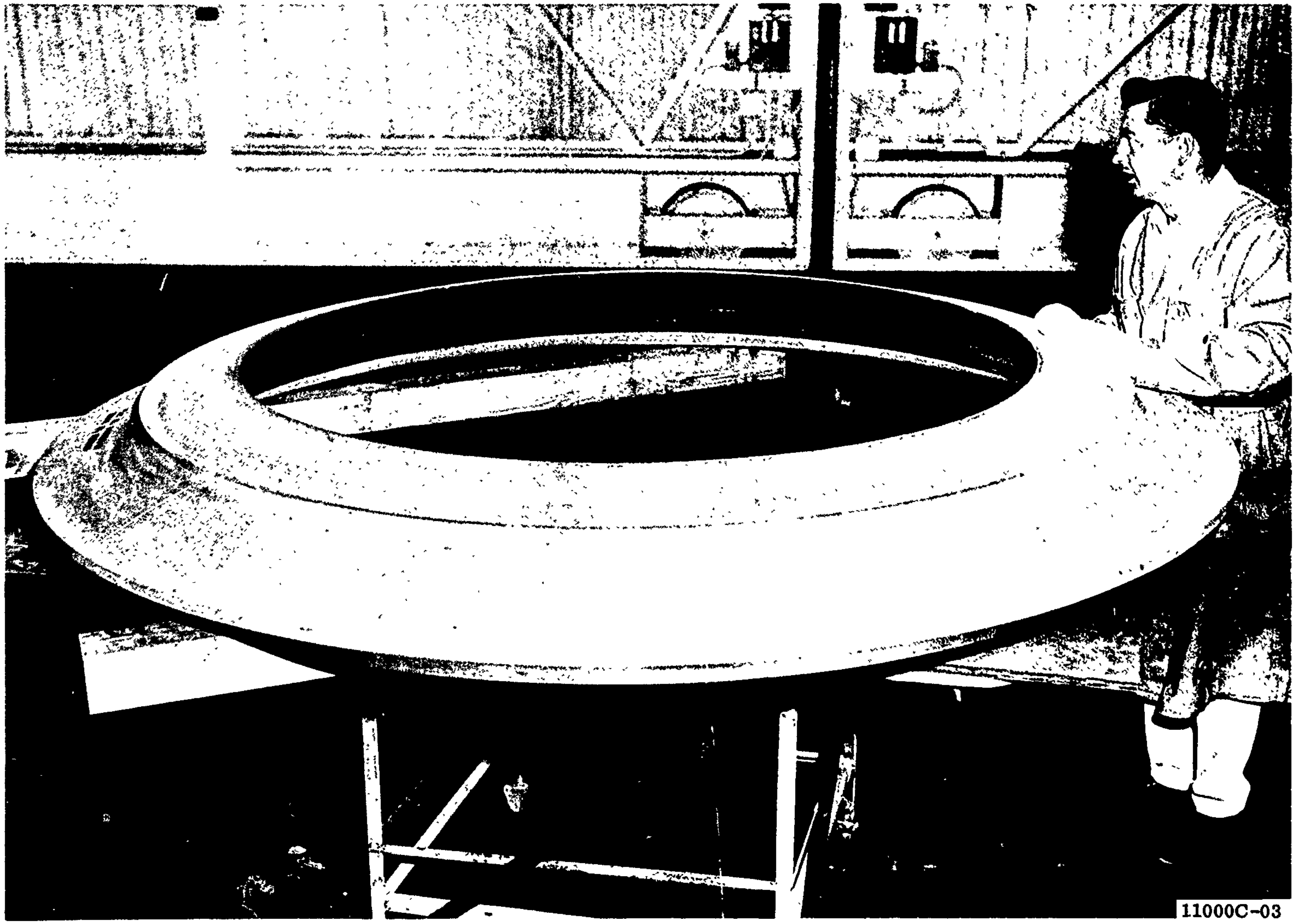

(U) Figure 59. Completed Silica Cloth Phenolic Insulation Ring

(U) The tests conducted on the cured Quality Control test ring and the flat laminate test slabs cured with the part and radiographic and dimensional inspection revealed an acceptable part.

(U) Results of tests performed on the Quality Control test ring and flat laminates cured with the part are listed in Table XIII and compared with specification limits.

(U) b. Dome Insulation Mold Preparation, and NBR Insulation Layup and Cure--The asbestos-filled NBR (V-44) dome insulation was laid up on molds prepared in the TU-412 motor center segment, vulcanized in a CO_2 atmosphere, and then removed. Since difficulty has been encountered with heat input in curing the joint insulation in the TU-412 center segment, Thiokol concluded that additional heating capacity would be required for curing the thick aft dome insulator. Therefore, a steam coil embedded in the plaster mold was planned to provide the additional heating capacity.

(U) The forward dome mold was swept in the TU-412 center segment in the vertical position. The sweep template configuration was developed by taking a plaster splash from the case segment dome and transferring the splash configuration to the template blade. The template was secured to a pivot post (Figure 60) attached to the bolt circle of the TU-412 segment curing dome. Sand was poured on top of the curing dome to within three to four inches of the template. Plaster saturated hemp was placed on top of the sand and covered with plaster to within 1.0 to 1.5 in. of the template. The copper tubing steam coil was installed, held in place with metal clips secured into the plaster, and covered with a final layer of plaster. After plaster cure, the steam coil was pressurized to 100 psi to check for leaks and plaster cracking. No leaks were detected, and plaster cracking was minimal. The plaster mold was then swept to final configuration (Figure 61) and cured 12 hr at 135°F.

(U) The mold surface was sealed with three coats of clear lacquer, and Teflon tape was applied. The V-44 headend dome insulation was laid up in four sections with one radial joint and four longitudinal joints (Figure 62). During layup, the inlet side of the steam coil was damaged. Since the steam coil was not needed for

TABLE XIII

(U) INSULATION RING PHYSICAL PROPERTIES

Property	Specification Min	Specification Max	QC Ring	Flat Laminate
Density (lb/cu in.)	1.7	--	1.73	--
Volatile Content (%)	--	2.0	0.233	--
Resin Content (%)	--	36.0	34.29	--
Tensile Strength (psi)				
Parallel to Weave	12,000	--	13,144	13,075
Tensile Modulus (psi x 10^6)				
Parallel to Weave	2.0	--	2.33	3.47
Compressive Strength (psi)				
Parallel to Weave	20,000	--	49,440	40,452
Compressive Modulus				
Parallel to Weave	2.0	--	2.08	3.04
Interlaminar Shear (psi)	3,000	--	--	9,329
Hardness (Shore D Units)	90	--	93	--
Flexural Strength (psi)				
Parallel to Weave	20,000	--	23,224	--
Flexural Modulus (psi x 10^6)				
Parallel to Weave	2.25	--	--	3.37

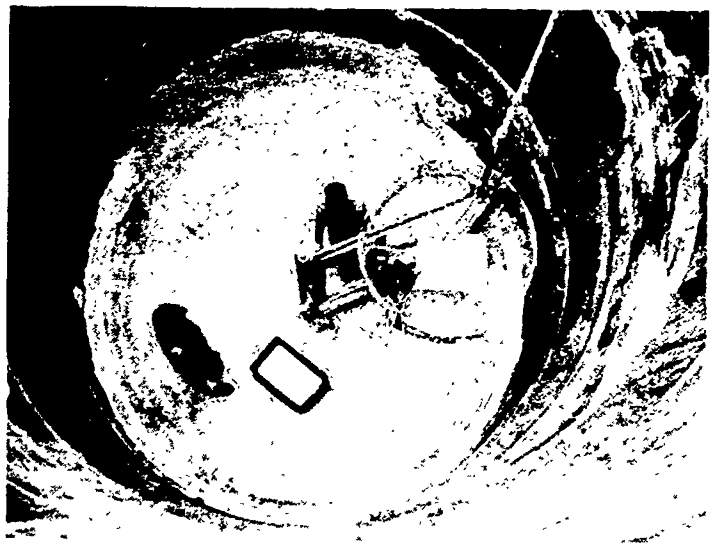

(U) Figure 60. Sweep Template for Forward Dome Contour

(U) Figure 61. Sweep of Plaster Mold for Forward Dome Insulation

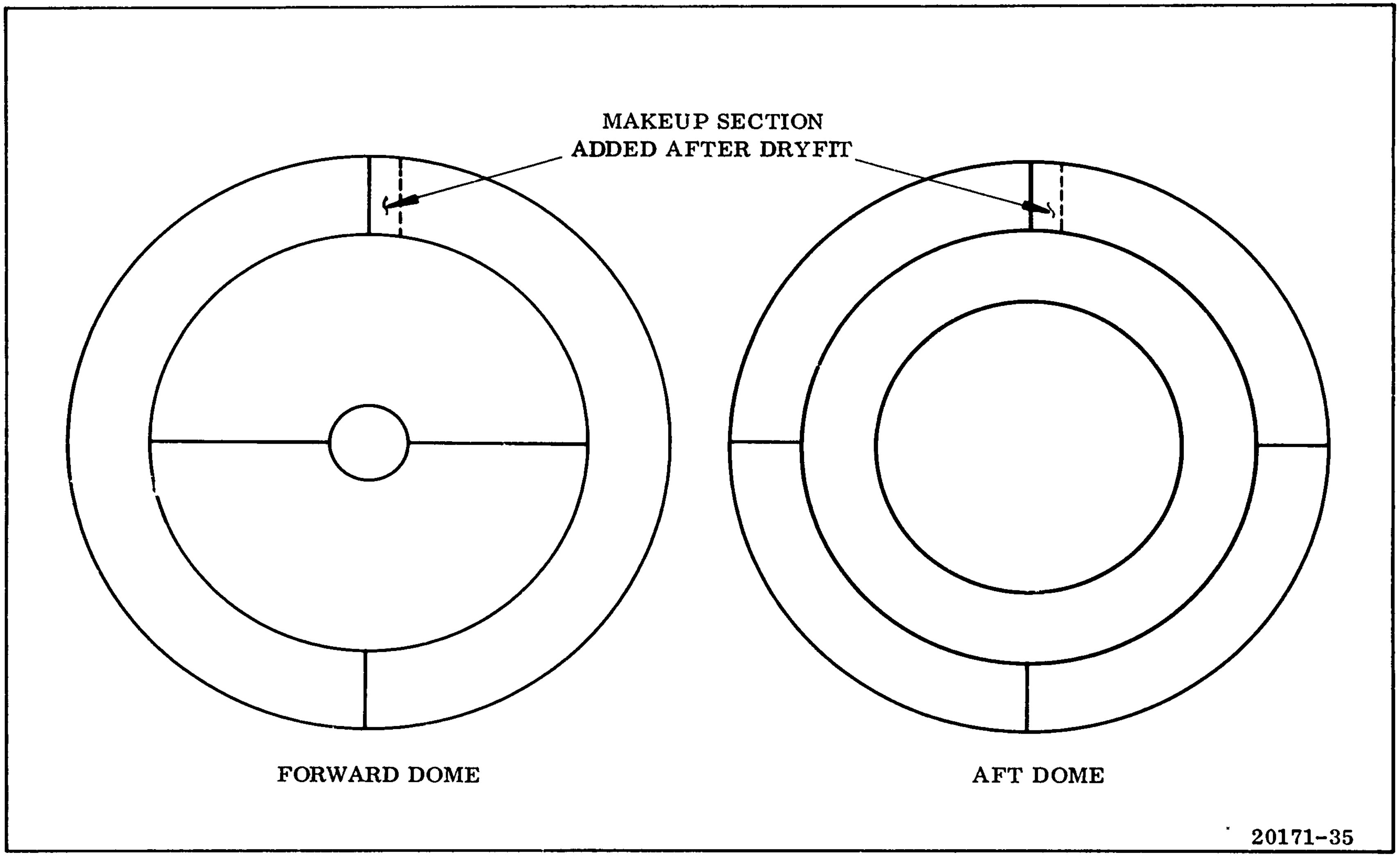

(U) Figure 62 . Dome Sectioning Patterns the thin headend insulation, the damage was not repaired. Insulation layup techniques were the same for the dome insulation as those used for the joint insulation layup. After completion of dome layup, Teflon tape was applied to the area on the insulation surface that would be covered by the propellant relief flap. The Teflon tape was covered with UF-3196, and the flap then was laid up using standard layup methods. A preformed, two mil nylon, vacuum bag was attempted on the headend dome insulation; however, due to installation difficulty, the preformed bag was replaced with the conventional sectioned vacuum bag. When the TU-412 segment was pressurized to 100 psig with CO_2, the vacuum decreased to 13 in. Hg. The soak temperature was reached without difficulty; however, trouble developed with the internal heater circulating fan during temperature rise. After repairing the fan, the curing cycle continued; however, the temperature rise rate was slower than anticipated due to a high CO_2 loss rate. When the lowest thermocouple reached 236°F (after soak), the vacuum was turned off and the cure was completed without vacuum. Figure 63 shows the thermal history of the headend dome insulation cure. Cooldown was accomplished with the same techniques used for the joint insulation. The propellant relief flap and insulation sections were removed from the mold (Figure 64) and buffed.

(U) The aft dome plaster mold was swept into the 156-1-C segment, on top of the forward dome mold, after chipping out a minimum amount of plaster in areas of interference with the aft dome sweep template. As with the forward dome template, the aft dome sweep template was developed from a plastic splash of the segment dome. The steam coil was repaired, the final plaster sweep was made, and insulation was laid up in the same manner as used for the headend insulation. The aft dome insulation consisted of five sections with one radial and four longitudinal joints (Figure 62). The insulation section around the silica-phenolic ring was a continuous ring, and four sections were out toward the case wall. No problems were encountered during the cure cycle, and vacuum was maintained at 15 in. Hg during soak and 16.25 to 17 in. Hg during cure. The steam coil significantly reduced the cure cycle time. Figure 65 shows the thermal history of the aft dome insulation cure.

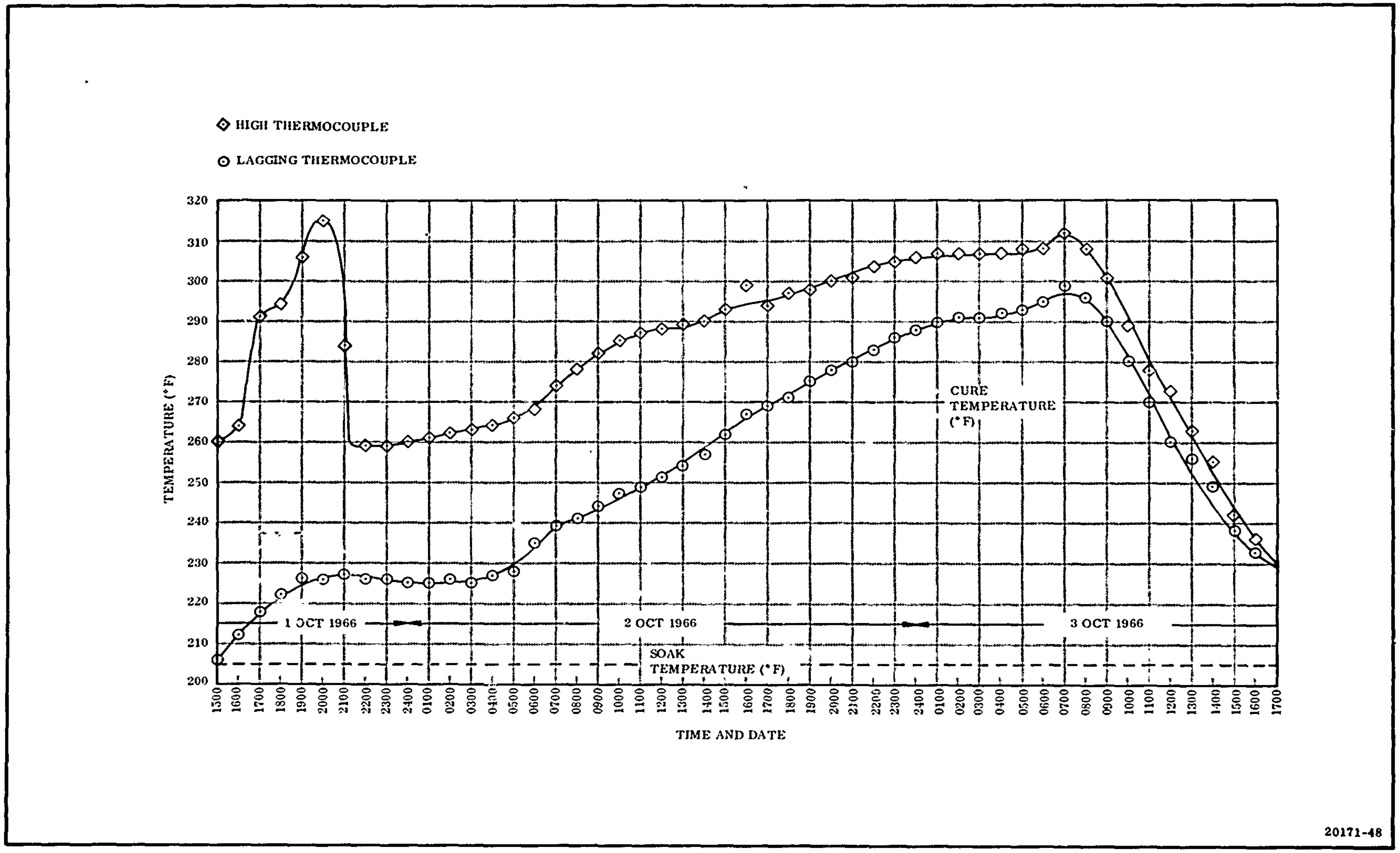

(U) Figure 63. Headend Insulation Cure Cycle

(U) Figure 64. Removal of Insulation from Mold

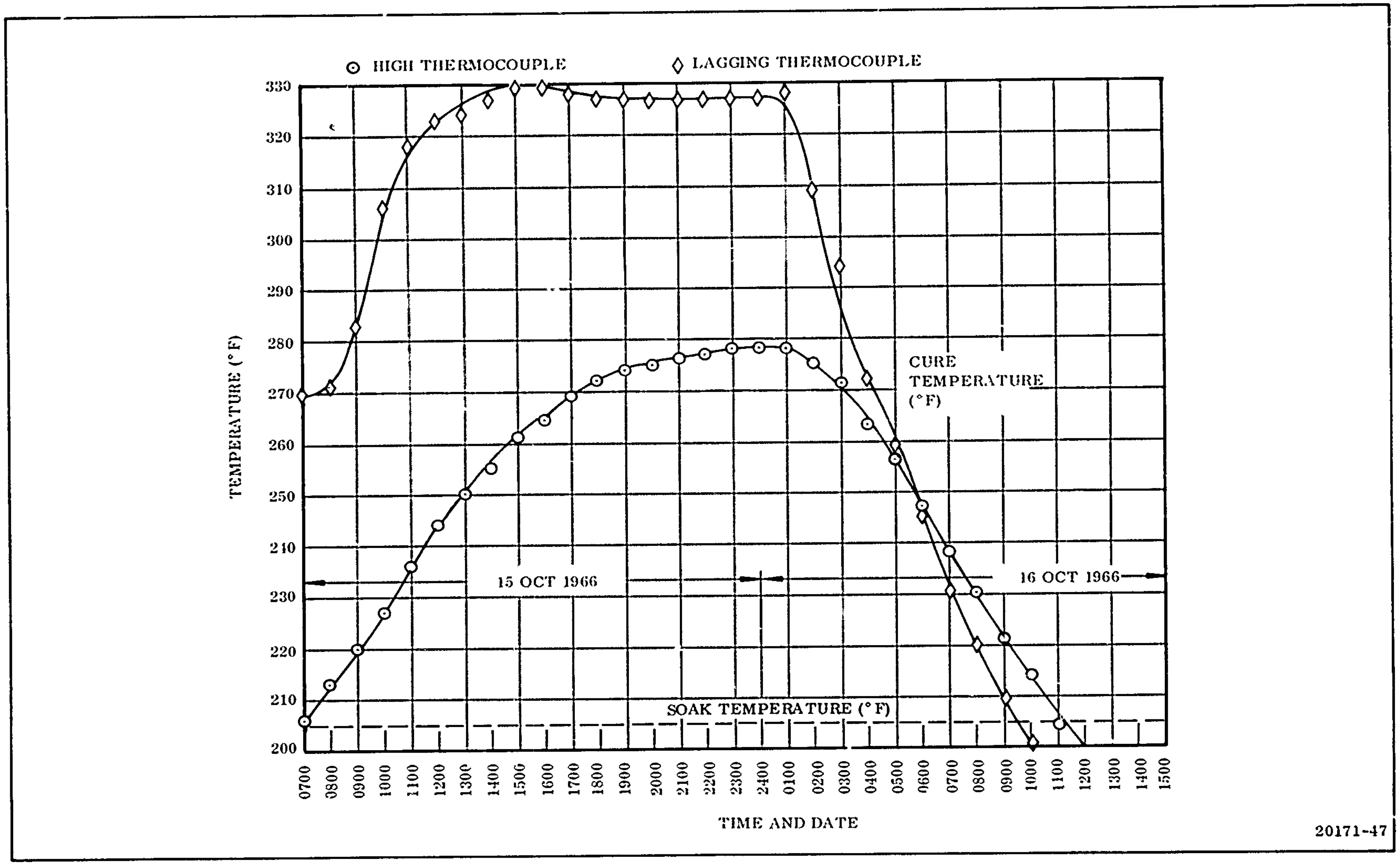

(U) Figure 65. Aft Dome Cure Cycle

(U) The elapsed time for the headend dome insulation cure was 83.75 hr with 2.28 to 13.29 equivalent cures on the insulation. The elapsed time for the aft dome insulation was 49.25 hr with 1.46 to 17.22 equivalent cures.

(U) c. Dome Insulation Installation--The forward segment dome insulation was installed with the segment in the vertical position and the dome end down. The insulation was first buffed to remove any contamination and abrade the surface for better adhesion. Dryfit of the insulation revealed that due to shrinkage, a keystone (or makeup piece) approximately 8 in. in circumferential length was required. This was laid up, to the required thickness, of uncured V-44 on a small mold. It then was cured in an autoclave using standard methods.

(U) The buffed insulation was cleaned with MEK and bonded in place one piece at a time with UF-1149 bonding material. The bonding material was cured at ambient temperature under vacuum.

(U) Post bonding inspection revealed very large voids behind the insulation pieces in the area of maximum curvature of the ovaloid shaped dome.

(U) These areas were repaired, with the segment remaining in the vertical position, by drilling 0.125 in. holes through the insulation at both the lower extremity and the upper extremity of each void. UF-3119 sealant then was injected into the lower hole while vacuum was applied to the upper hole. Minor voids under thin sections of insulation were repaired by a standard method of injecting UF-3119 into one side of the voids with a hypodermic needle while entrapped air was drawn out on the opposite side with another hypodermic needle. All repairs were successful and resulted in sound bonds after ambient cure of the sealant vacuum.

(U) The aft segment insulation was installed with the dome end down, the same position as that used for the forward insulation installation. The phenolic insulation ring was dry fitted to the inside surface of the segment polar boss. NBR shims were used to maintain the required bonding gap and dimension to the aft face of the polar boss. Teflon tape was applied to the periphery of the bond areas to facilitate cleanup of sealant squeezeout. The insulation ring and the bond area in the segment were cleaned with MEK. UF-3195 was applied to the insulation ring and the bond area in the segment. The insulation ring was installed and clamped in place. The UF-3195 was cured for 24 hr at 80 (± 20)°F.

(U) After cleanup of excess sealant around the insulation ring, the first section of the dome NBR insulation was dry fitted to the segment and insulation ring. The dome insulation section would not fit around the phenolic insulation ring because the dome insulation section ID had shrunk 2.1 percent after removal from the plaster mold after cure; therefore, the ID was machined to the required dimensions on a 120 in. vertical turret lathe. The surfaces of the insulation were buffed to remove mold release contaminants and to abrade the surfaces for better adhesion. The insulation and bond areas in the segment were cleaned with MEK and UF-1149 was applied to the insulation and segment bond areas. The insulation was installed and bonded using standard vacuum bagging techniques. Again, a makeup section was required (Figure 62) and fabricated in the same manner as that used for the forward dome. To minimize voids under the thicker insulation, as experienced on the forward segment sections, three circumferential rows of 1/8 in. diameter holes on 12 in. centers were drilled through the insulation. The holes were drilled 45 deg to the motor gas flow so the gas would not erode the UF-1149 excessively from the holes. The remaining insulation sections and the splice piece were installed using the same methods and techniques.

(U) The use of small air bleed holes minimized the voids. Only minor voids occurred behind these insulation pieces in which bleeder holes were drilled. The voids were repaired using hypodermic needles.

(U) The propellant relief flaps for the head and aft ends were installed in one piece. The flaps were dry fitted and Teflon tape was applied around the outside and inside of the bond areas. The bond areas of the flaps were abraded and cleaned with MEK, and the bond areas on the insulation were cleaned with MEK. UF-1149 was applied to the flap bond areas and the insulation bond areas. The flaps were installed using standard vacuum bagging methods and techniques. The flaps were cured in place for 12 hr at 80 (± 20)°F.

SECTION V

(U) JOINT SEAL AND BLADDER HYDROTEST

(U) A. TEST OBJECTIVES

(U) The 156-8 case with segment joint insulation and seal installed was hydro-proof tested to 880 psig for 123 seconds. This pressure was chosen as a conservative pressure over the contract maximum MEOP of 880 psia. The objectives of the test were to:

1. Verify the design and fabrication processes of the segmented case seal,
2. Verify the structural integrity of the case after removal of the four to five plies of glass during bladder repair,
3. Verify that the replacement bladder was pressure tight, and
4. Verify the design and fabrication of the igniter cap.

(U) B. TEST CONFIGURATION

(U) The 156-8 case segments, as hydrotested, were per configuration 7U37320-09, 7U37321-01, and 7U37322-08. These configurations included the installed V-45 bladder and the installed and finish machined joint insulation. The head and aft end dome insulation was not installed (Figure 66).

(U) The assembly included (1) the joint seals (Thiokol Dwg 7U40228-02) installed exactly as it would be during motor static test and (2) the headend cap (Thiokol

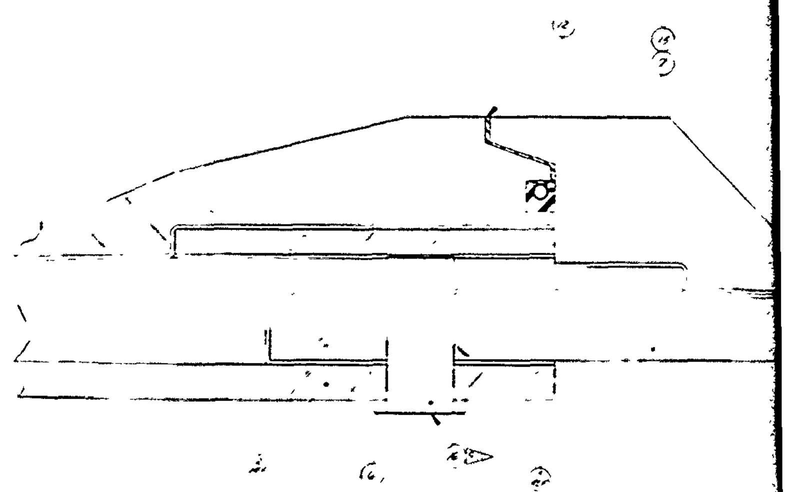

DETAIL
ROTATED 90° CLOCKWISE

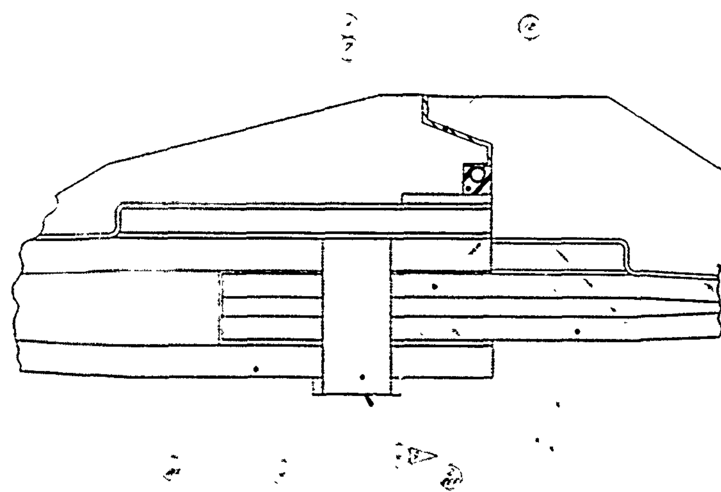

DETAIL B
ROTATED 90° CLOCKWISE

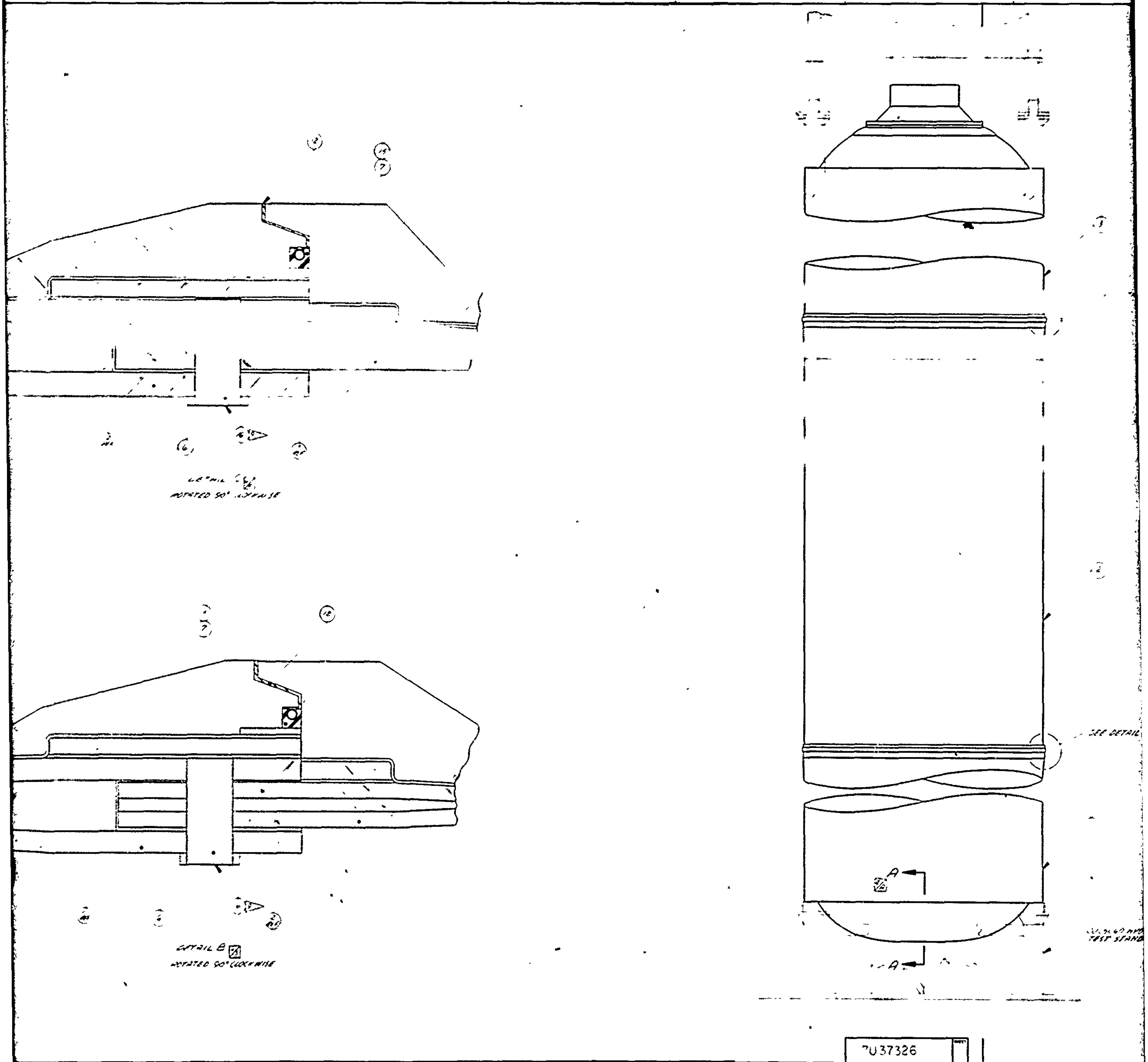

2

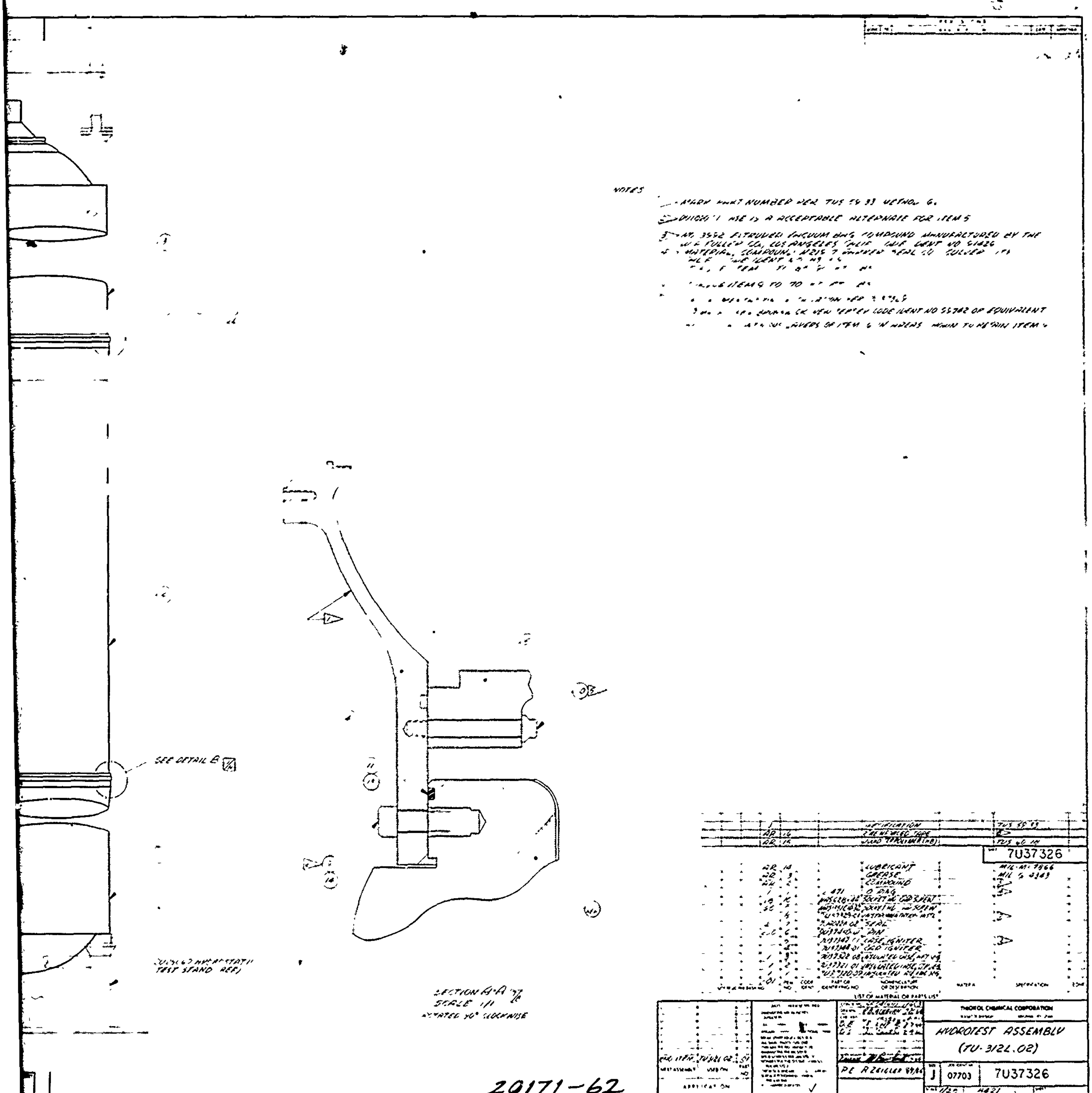

(U) Figure 66. 156-8 Hydrotest Assembly

3

Dwg 7U37344-01) and attached igniter case (Thiokol Dwg 7U37342-01) to assess their structural integrity during motor pressurization.

(U) The motor case was instrumented as shown in Figure 67 to obtain data on the case structure.

(U) The case was tested in a reactive hydrostatic test stand (Figure 68). The lower portion of this test stand serves as a base and a thrust adapter to which the forward skirt of the case fits. The middle section of the test stand consists of four large tubular columns which are sectioned for convenience of assembly. The upper section consists of a thrust piston and cross members attached to the columns.

(U) The force from the hydrostatic pressure across the face of the thrust piston is transferred to the upper cross member, then through the columns to the lower structure which again reacts against the skirt. Testing with this test stand (1) simulates only the pressure loads on the aft dome that would result during motor firing, (2) allows complete freedom of case growth under pressure, (3) simulates static test loads on the segment joints, and (4) simulates thrust loads on the forward skirt.

(U) The portable pumping system and its operation were obtained from Haliburton Company, Vernal, Utah. The HT400 model pumping unit consists of two positive displacement piston type pumps which are driven by two Cummins diesel 600 hp engines. The pump flow rate capacity is 1,140 gpm at 1,500 psig. The pumping system is used only for pressurization. The main pumps were supplied with water at approximately 100 psig from a primer pumping unit (Figure 69) which in turn drew from storage tanks having a total storage capacity of 4,800 gallons.

(U) C. TEST PROCEDURES

(U) The test stand base and lower two column sections were in the test bay. The forward segment was received in the test area with the igniter cap and

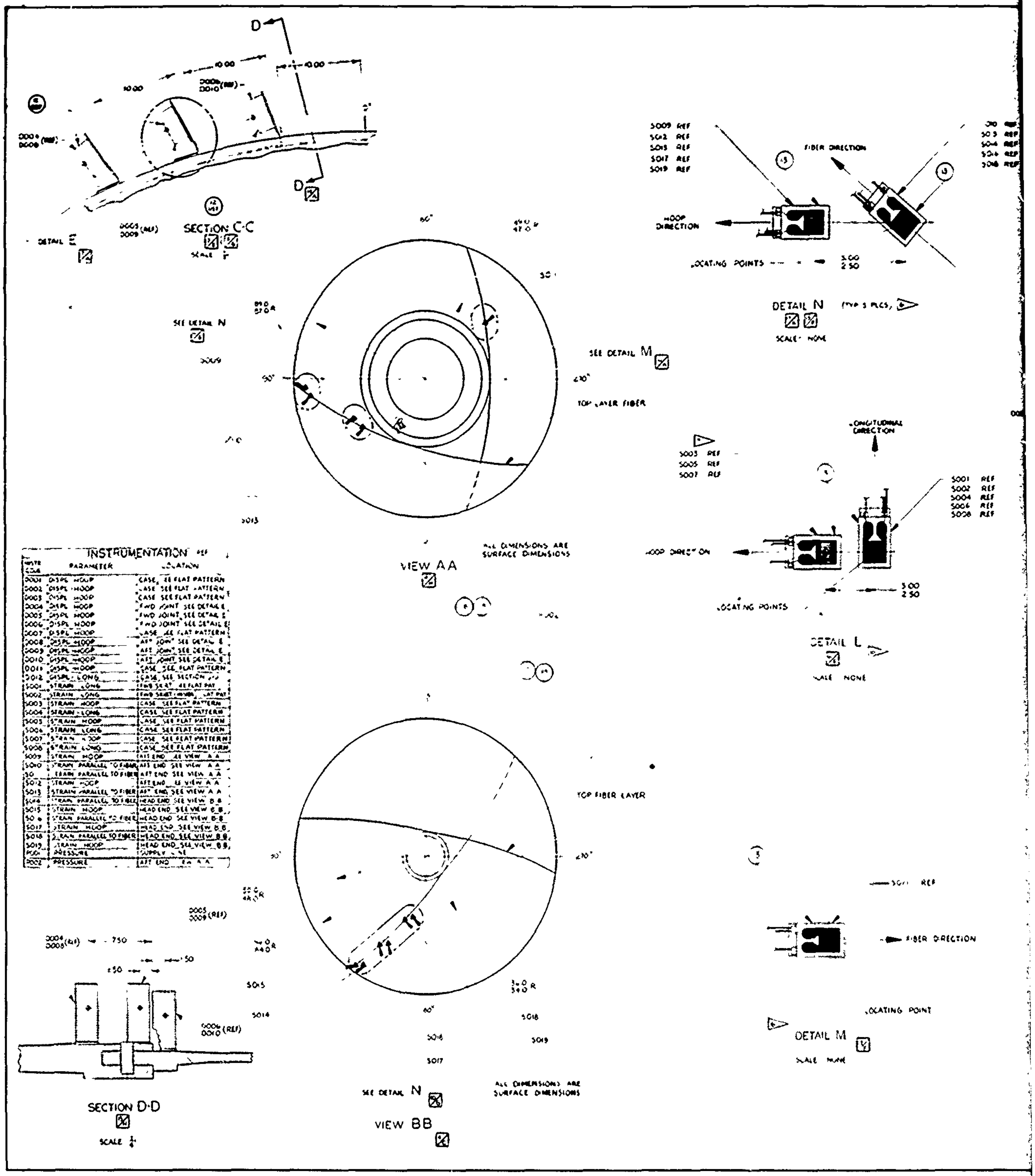

INSTRUMENTATION REF

NOTE CODE	PARAMETER	LOCATION
0001	DISPL HOOP	CASE, SEE FLAT PATTERN
0002	DISPL HOOP	CASE SEE FLAT PATTERN
0003	DISPL HOOP	CASE SEE FLAT PATTERN
0004	DISPL HOOP	FWD JOINT SEE DETAIL E
0005	DISPL HOOP	FWD JOINT SEE DETAIL E
0006	DISPL HOOP	FWD JOINT SEE DETAIL E
0007	DISPL HOOP	CASE SEE FLAT PATTERN
0008	DISPL HOOP	AFT JOINT SEE DETAIL E
0009	DISPL HOOP	AFT JOINT SEE DETAIL E
0010	DISPL HOOP	AFT JOINT SEE DETAIL E
0011	DISPL HOOP	CASE SEE FLAT PATTERN
0012	DISPL LONG	CASE, SEE SECTION [illegible]
5001	STRAIN LONG	FWD SKIRT SEE FLAT PAT
5002	STRAIN LONG	FWD SKIRT [illegible] FLAT PAT
5003	STRAIN HOOP	CASE SEE FLAT PATTERN
5004	STRAIN LONG	CASE SEE FLAT PATTERN
5005	STRAIN HOOP	CASE SEE FLAT PATTERN
5006	STRAIN LONG	CASE SEE FLAT PATTERN
5007	STRAIN HOOP	CASE SEE FLAT PATTERN
5008	STRAIN LONG	CASE SEE FLAT PATTERN
5009	STRAIN HOOP	AFT END SEE VIEW A A
5010	STRAIN PARALLEL TO FIBER	AFT END SEE VIEW A A
50[illegible]	STRAIN PARALLEL TO FIBER	AFT END SEE VIEW A A
5012	STRAIN HOOP	AFT END SEE VIEW A A
5013	STRAIN PARALLEL TO FIBER	AFT END SEE VIEW A A
5014	STRAIN PARALLEL TO FIBER	HEAD END SEE VIEW B B
5015	STRAIN HOOP	HEAD END SEE VIEW B B
50[illegible]	STRAIN PARALLEL TO FIBER	HEAD END SEE VIEW B B
5017	STRAIN HOOP	HEAD END SEE VIEW B B
5018	STRAIN PARALLEL TO FIBER	HEAD END SEE VIEW B B
5019	STRAIN HOOP	HEAD END SEE VIEW B B
P001	PRESSURE	SUPPLY LINE
P002	PRESSURE	AFT END [illegible] A A

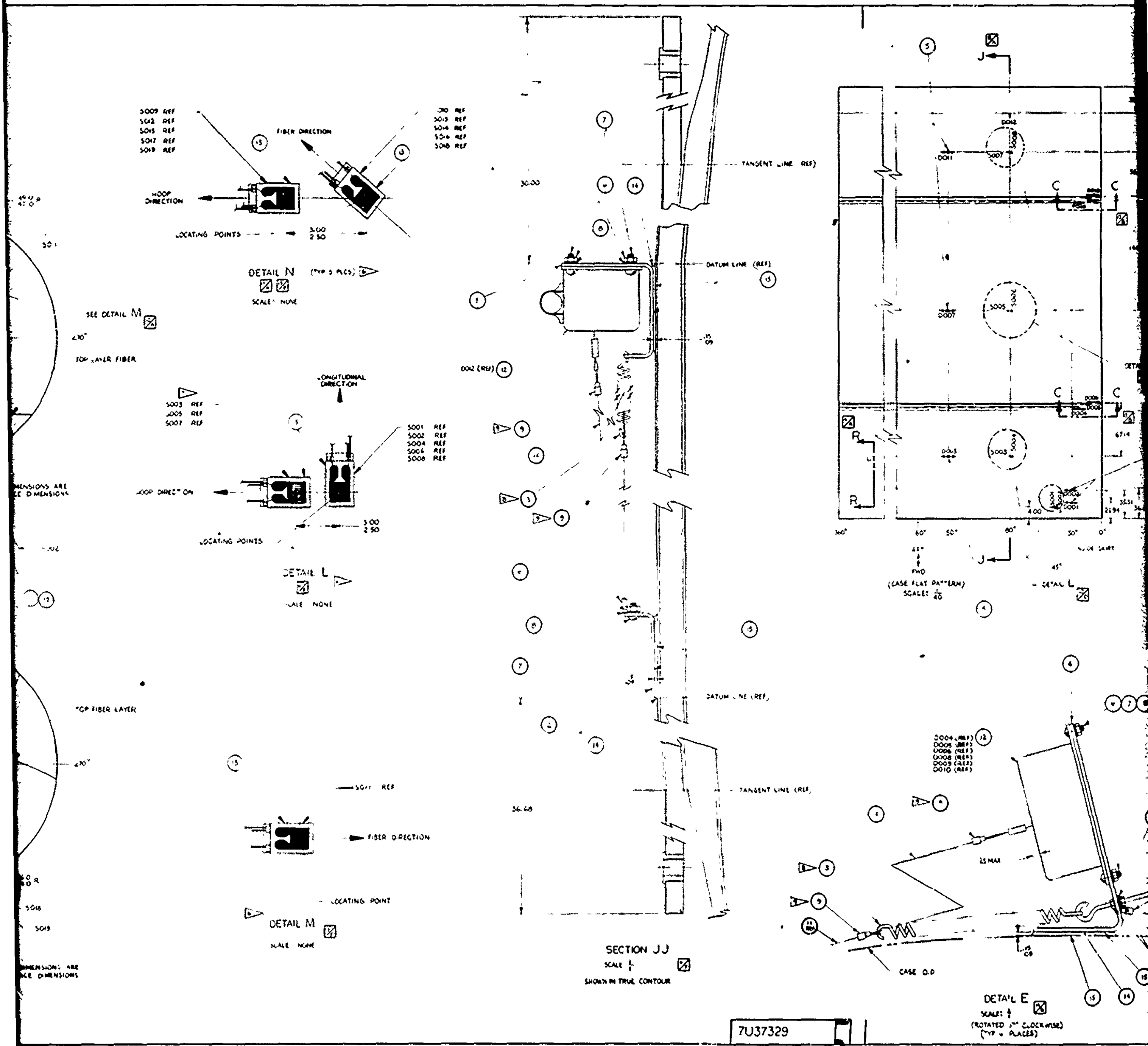

FIBER DIRECTION
HOOP DIRECTION
LOCATING POINTS
DETAIL N (TYP 5 PLCS)
SCALE: NONE
SEE DETAIL M
TOP LAYER FIBER
LONGITUDINAL DIRECTION
HOOP DIRECTION
DETAIL L
SCALE: NONE
TOP FIBER LAYER
LOCATING POINT
DETAIL M
SCALE: NONE
TANGENT LINE (REF)
DATUM LINE (REF)
SECTION JJ
SHOWN IN TRUE CONTOUR
(CASE FLAT PATTERN)
DETAIL E
(ROTATED CLOCKWISE)
CASE O.D
25 MAX
7U37329

2

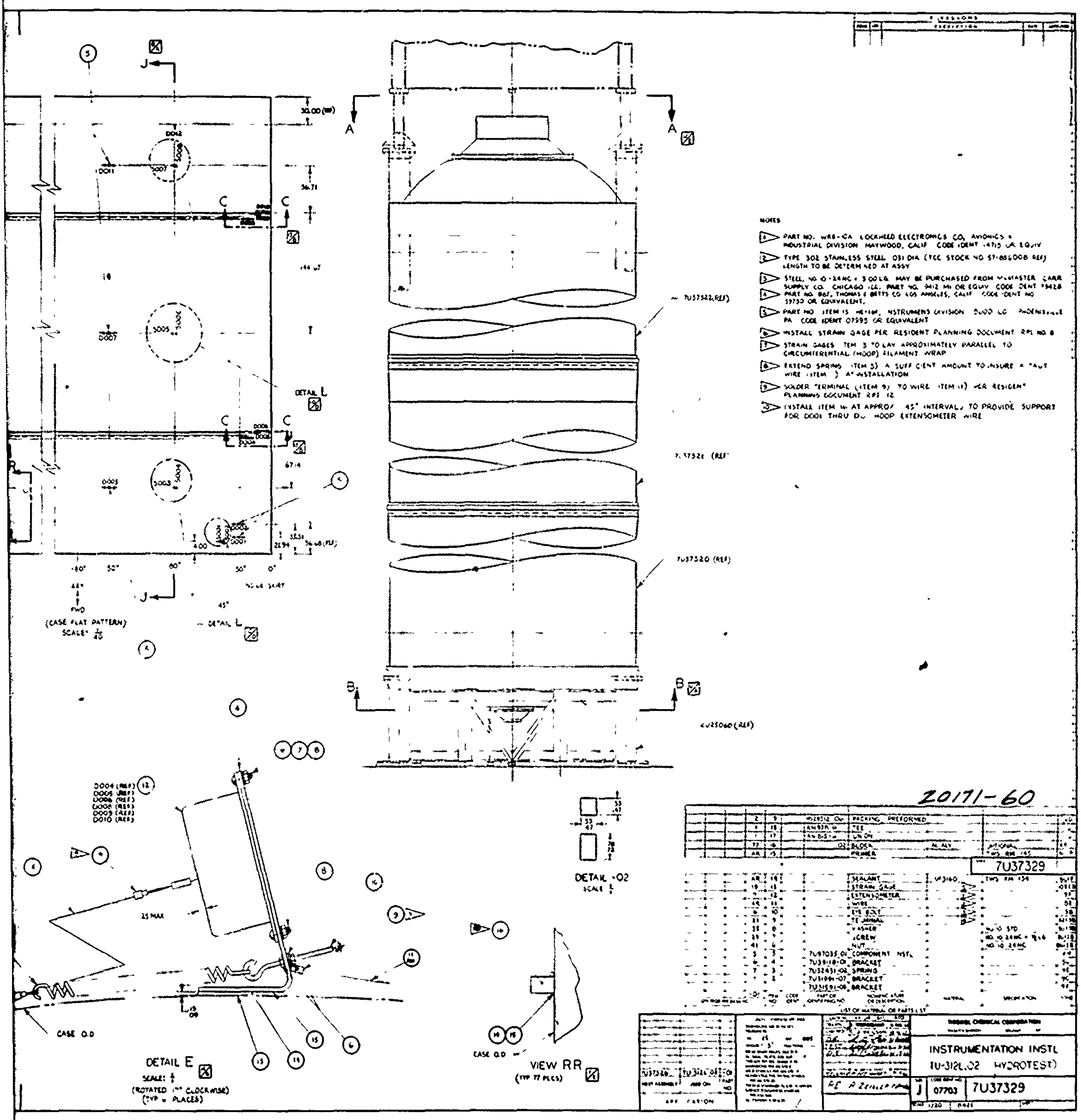

(U) Figure 67. 156-8 Instrumentation Installation

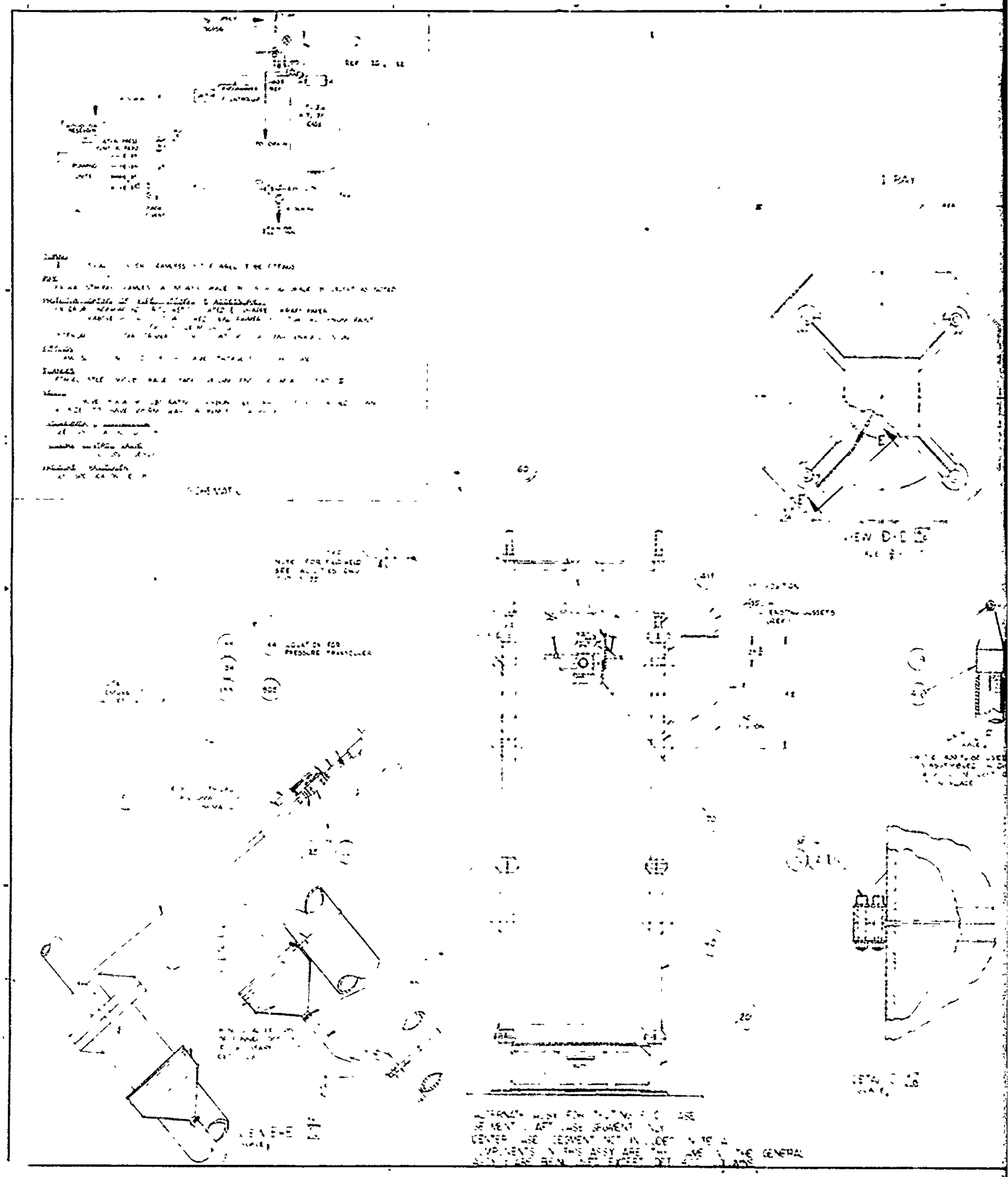
SCHEMATIC
VIEW D-D

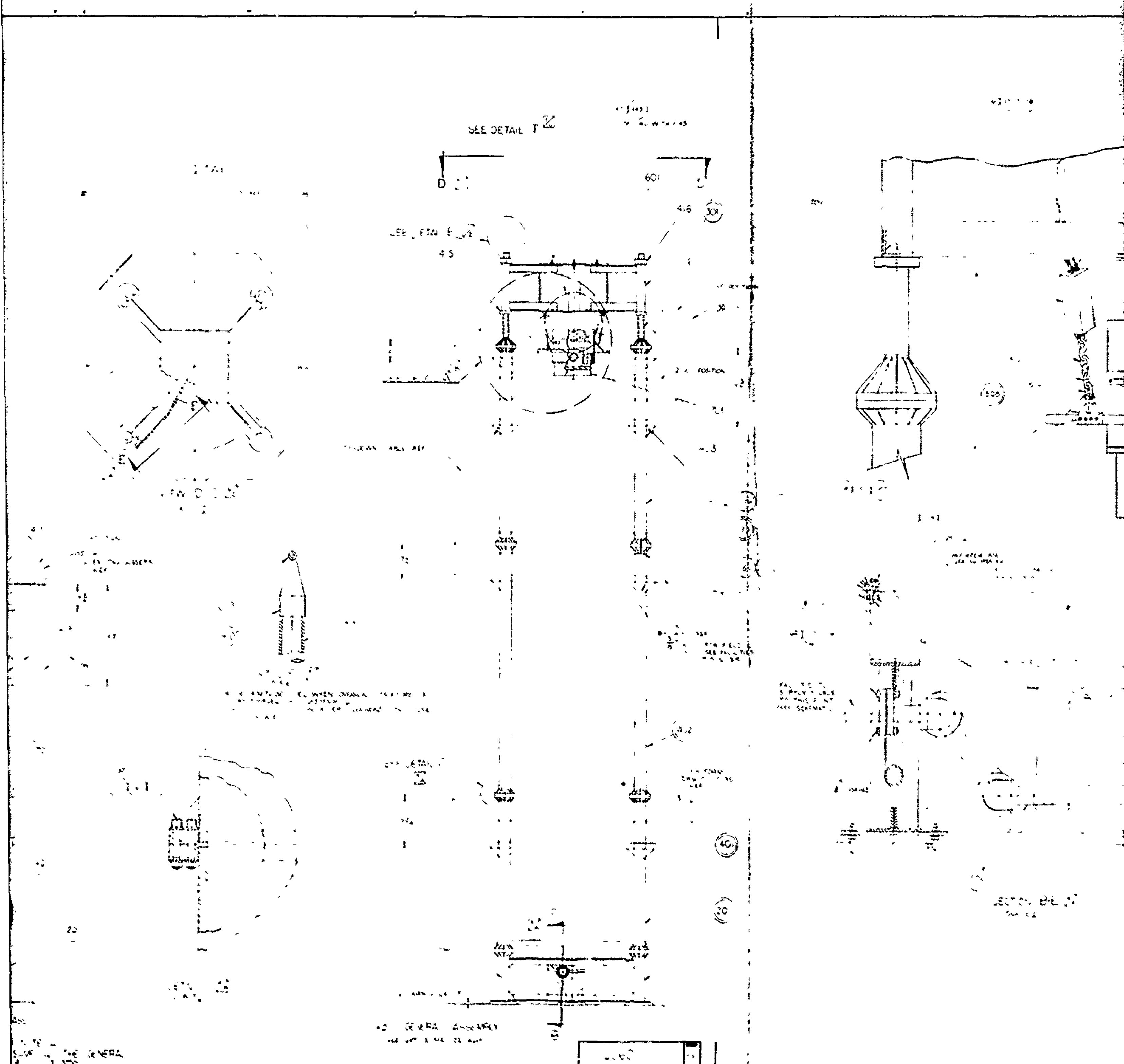

2

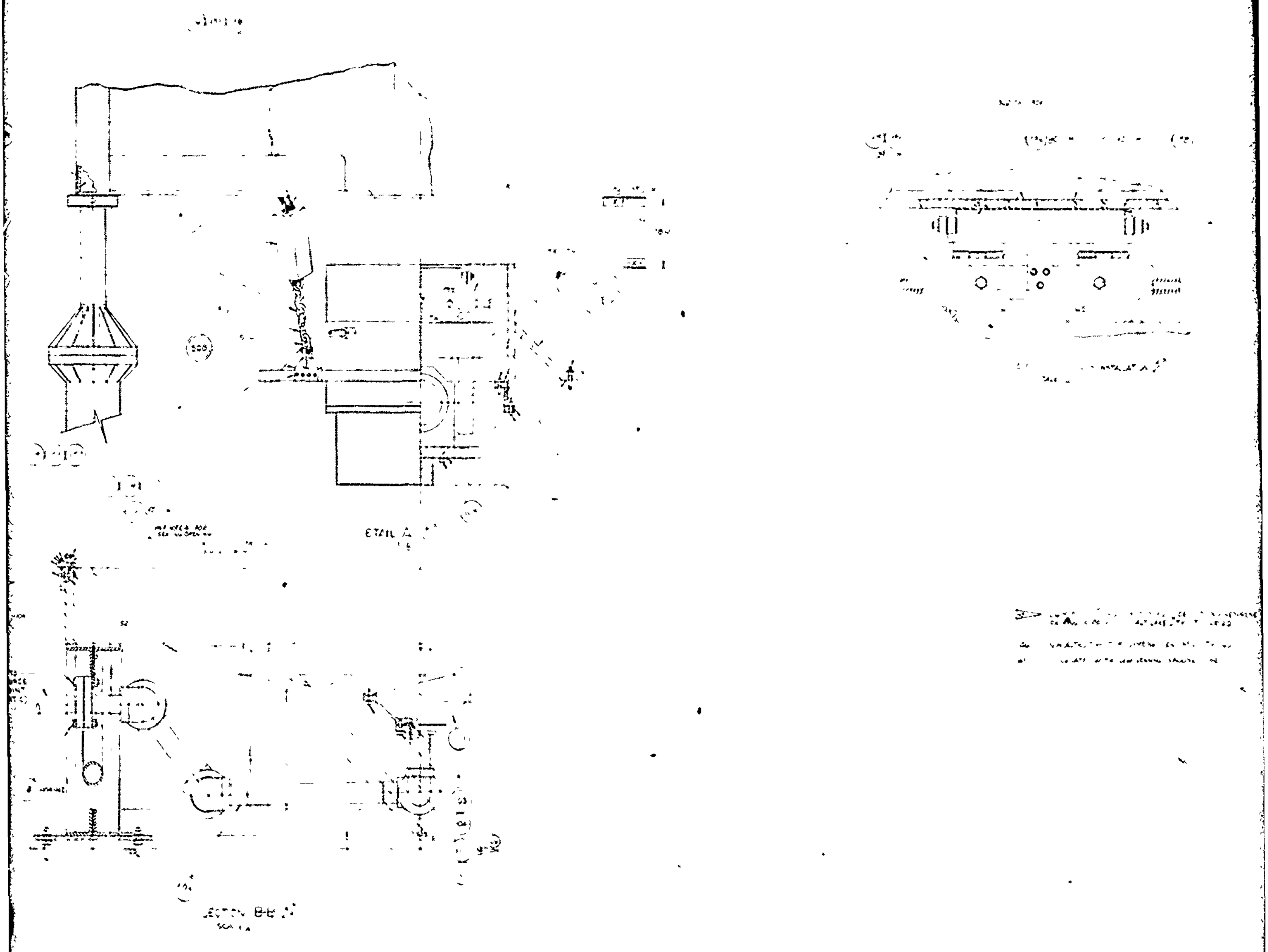

3

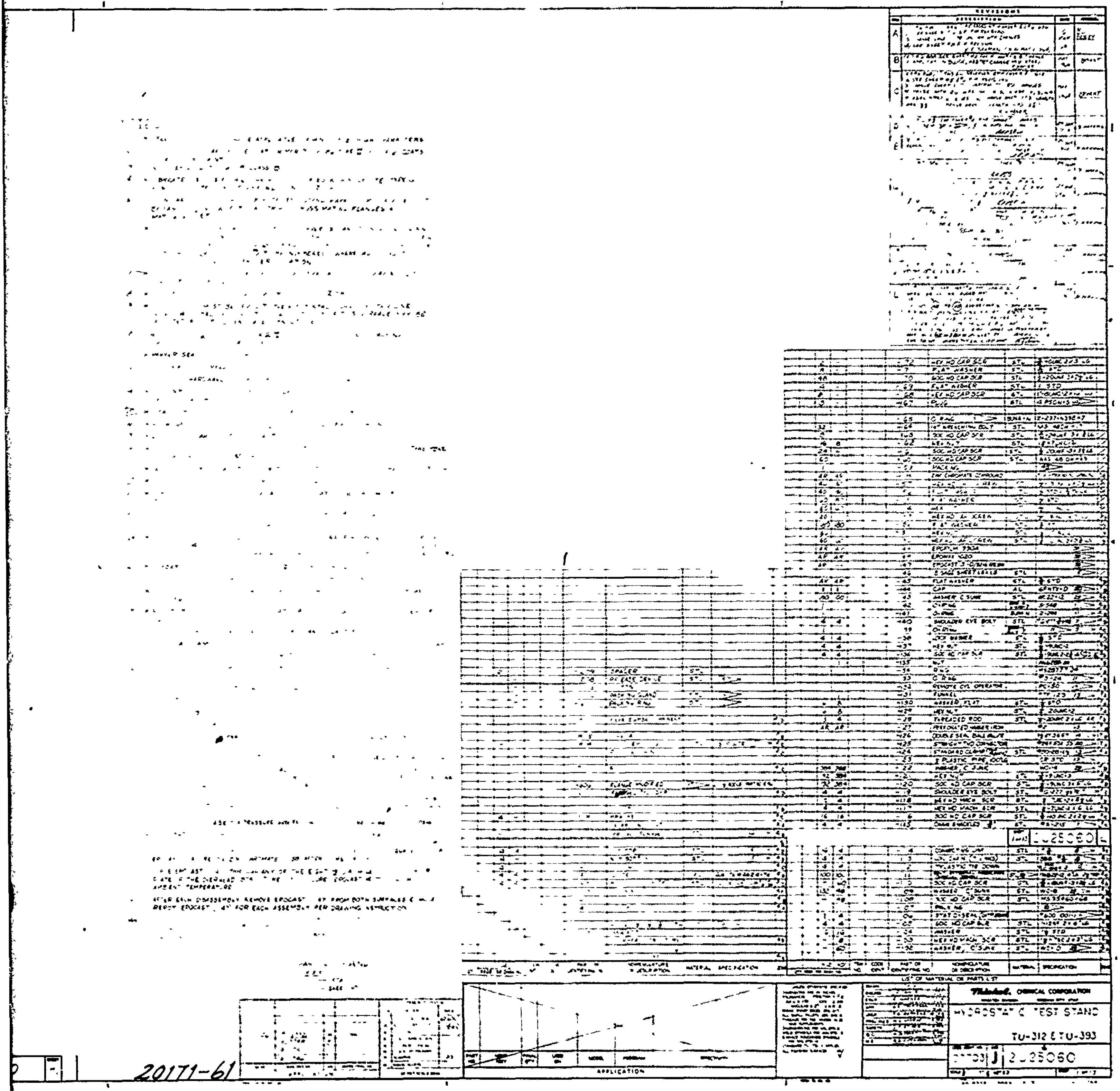

(U) Figure 68. Hydrostatic Test Stand

4

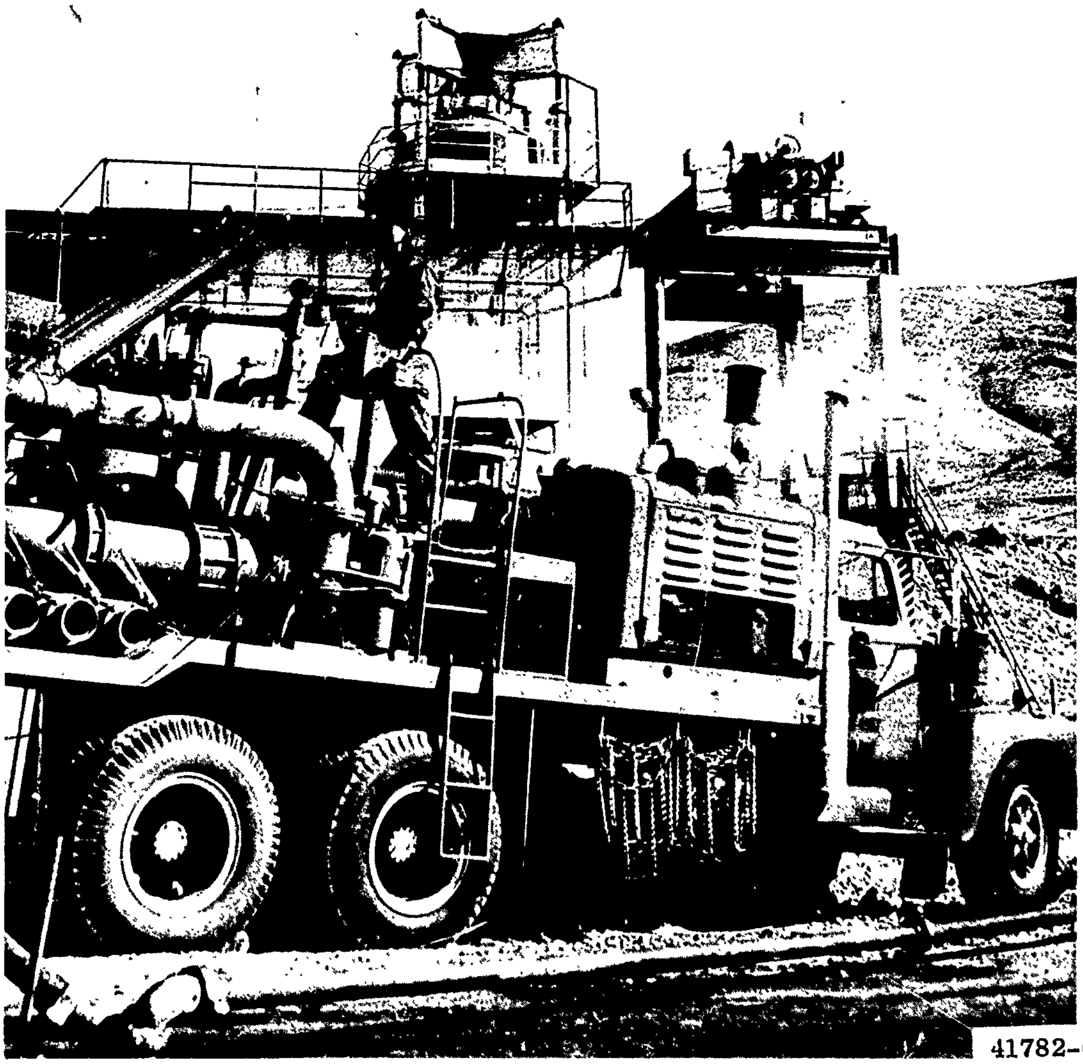

41782-6

(U) Figure 69. Portable Primer Pumping Unit case installed. It was removed from the transporter, broken over to the vertical attitude, and installed in the test stand (Figure 70). Epocast 31D was pumped under the skirt and allowed to cure to provide a complete bearing surface for the skirt. The segment joint seal was then lubricated with PBAA and installed in the seal groove. The female insulation joint on the forward segment was potted with extruded vacuum bag compound (Figure 71). Pneuma-Grip harness rings were installed on the aft end of the forward segment and the forward end of the center segment for handling and rounding operations. The center segment then was lowered onto the forward segment until its tongue engaged the clevis of the forward segment (Figure 72). The pins were installed and the harness rings removed. The test stand was assembled further during the operations to assemble the case.

(U) The aft segment was assembled to the center segment using the same procedure. After completion of the assembly, the interior of the joints was inspected to verify adequate squeezeout of the extruded vacuum bag compound. The thrust piston was installed to the aft end of the case and the upper cross members installed (Figure 73). Instrumentation was installed as required throughout the assembly operations. Following completion of the assembly, the case was filled with water and leak tested at 100 psig for 10 min using line pressure. No leakage occurred.

(U) Following the leak test, the thrust piston was seated against the thrust block on the upper cross member with 35 psig internal pressure, and the interface between the piston and thrust block was potted with Epocast 31D to provide for full bearing (Figure 73).

(U) Instrumentation systems were checked and calibrated.

(U) During the hydroproof pressurization, the pressure was gradually increased from 35 psig to 60 psig. At 60 psig, the instrumentation recording systems and slow speed motion movie cameras were started. Pressure was increased at an average rate of 2.3 psi per second to a maximum of 896.8 psig (Figure 74).

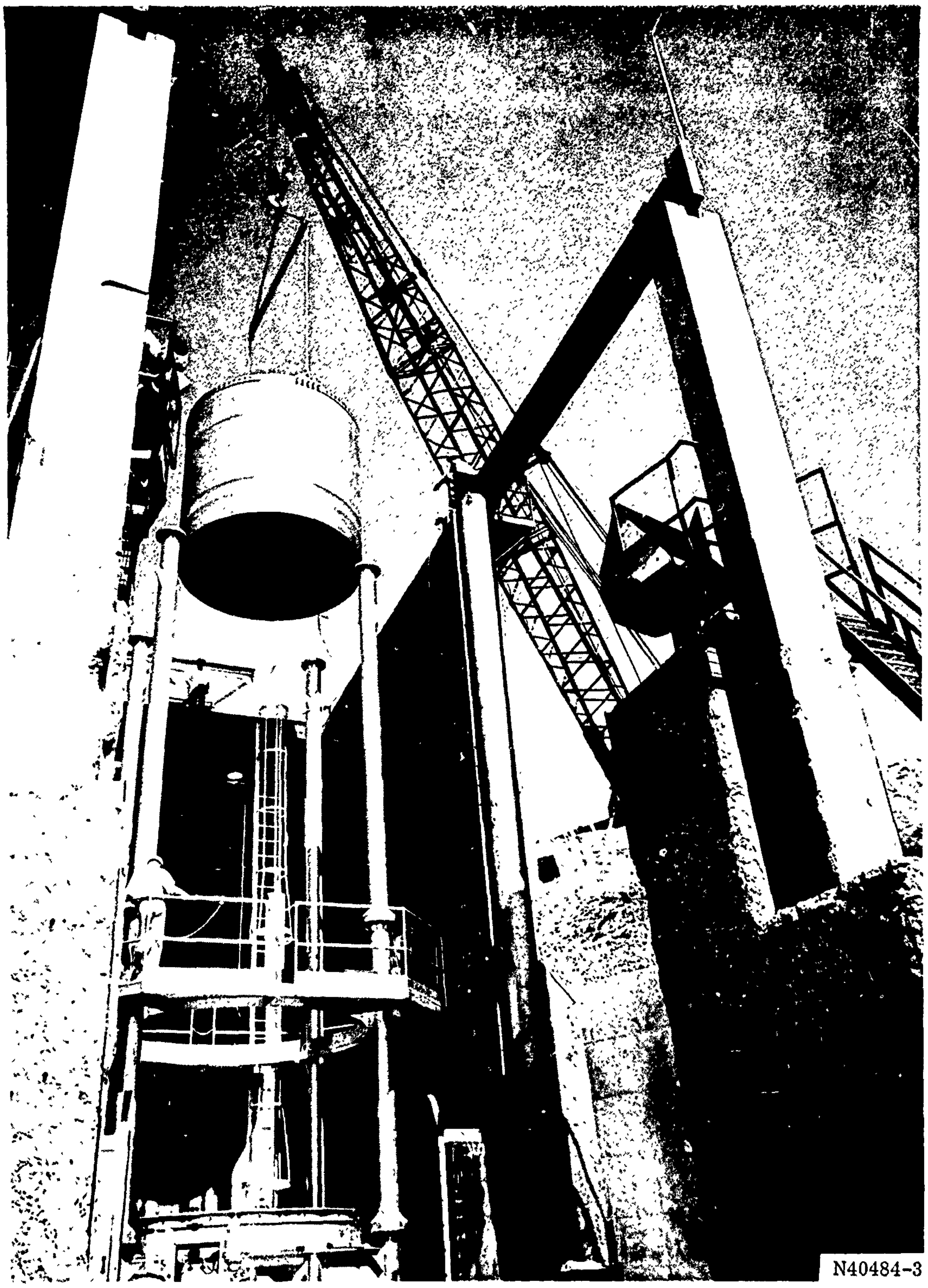

(U) Figure 70. Lowering Forward Segment into Place

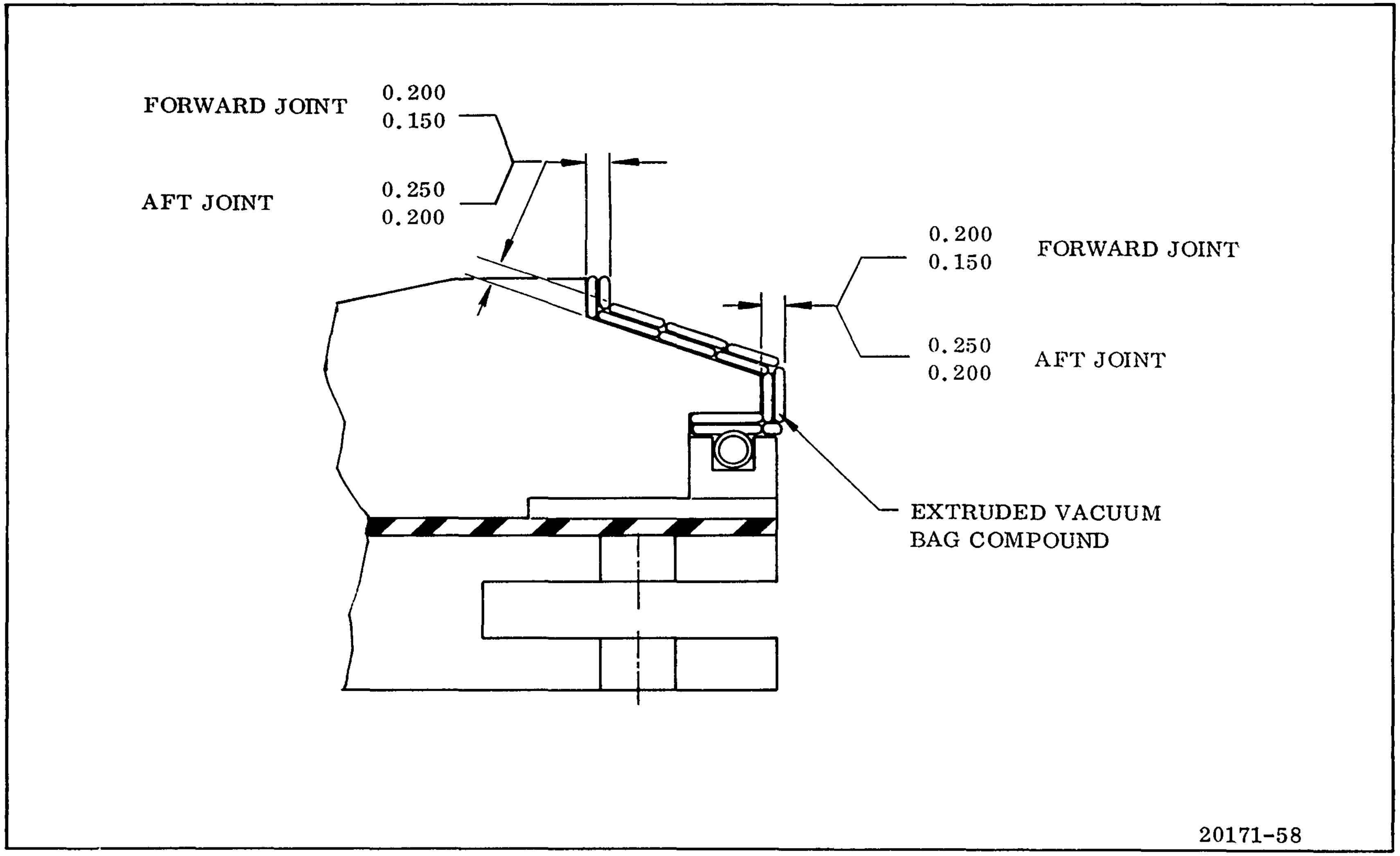

(U) Figure 71. 156-8 Joint Potting

(U) Figure 72. Lowering Center Segment into Place

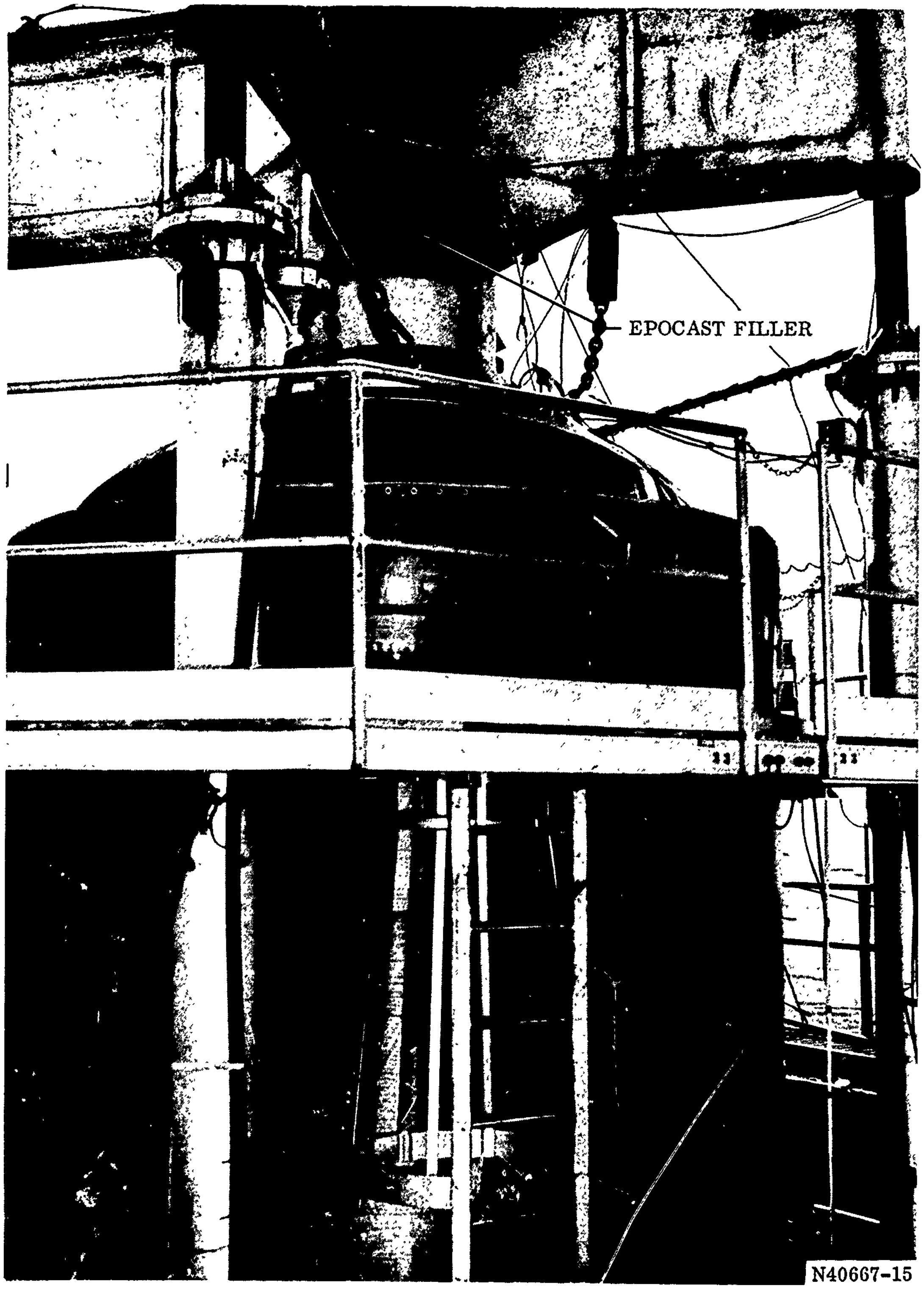

(U) Figure 73. Aft Closure, Thrust Piston, and Overhead Structure

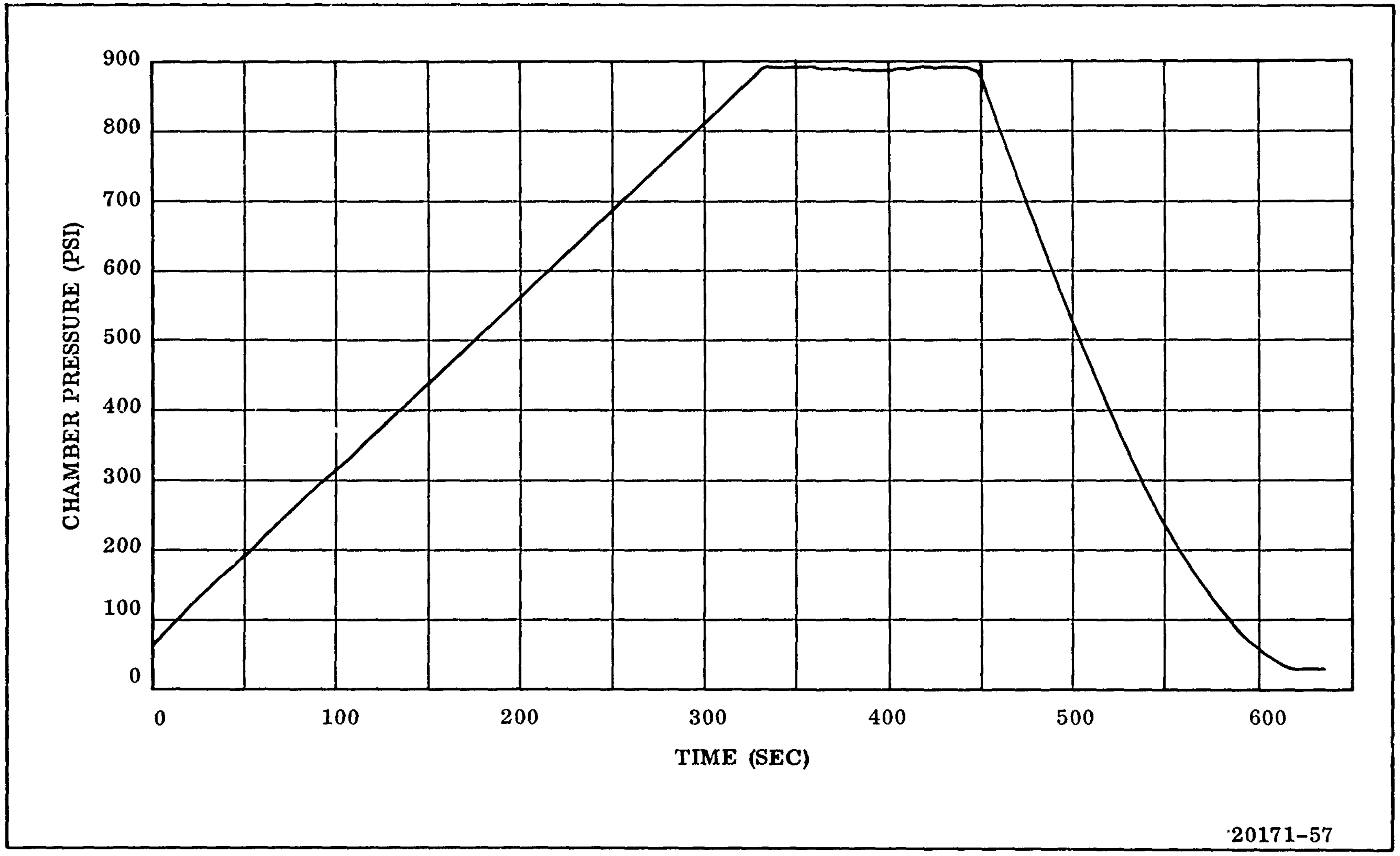

(U) Figure 74. 156-8 Case Hydrotest Pressure Trace

High speed cameras were started at 720 psig as the pressure was increased. Pressure was maintained within the 890 ($\pm$ 10) psig tolerance for 123 sec before being decreased at a rate of approximately 6.3 psi per second to 33 psig.

(U) The pressurization rates were attained by an operator following a preplotted graph and opening and closing bypass valves as necessary in the Haliburton portable pumping systems.

(U) D. TEST RESULTS

(U) The case withstood the pressurization cycle with no structural failure and no leakage whatsoever in the joint areas, forward segment dome, center segment, aft segment, and head end cap. Post-test inspection revealed a small amount of seepage from the case wall at the three degree position 42 in. forward of the forward joint in the cylindrical portion of the forward segment.

(U) Post disassembly inspection revealed a small cut in the bladder (Figure 75) and a circumferential area into which the water had been forced, unbonding the bladder. The area was cut open and dried and the unbonded area was bonded back into place and a patch of cured NBR bonded over the area.

(U) Data from the 29 Mar 1966 hydrotest and this test were comparatively analyzed with emphasis on the joints.

Relative gage locations and data separations are shown in Figures 67 and 76. Figures 77 and 78 depict forward and aft joint raidal deflections, respectively, and show excellent correlation of test results and anticipated deflections. Figure 79 shows forward skirt deflections. The 0.1 in. difference between D024 from previous hydrotest and D001 of this hydrotest at 900 psig did not result from any structural change. The difference is within the expected variation due to normal gage location error and normal instrumentation system error.

(U) Figure 80 shows deflection measured at the center of each segment. The greater deflections of the cylinder in this hydrotest when compared to those of

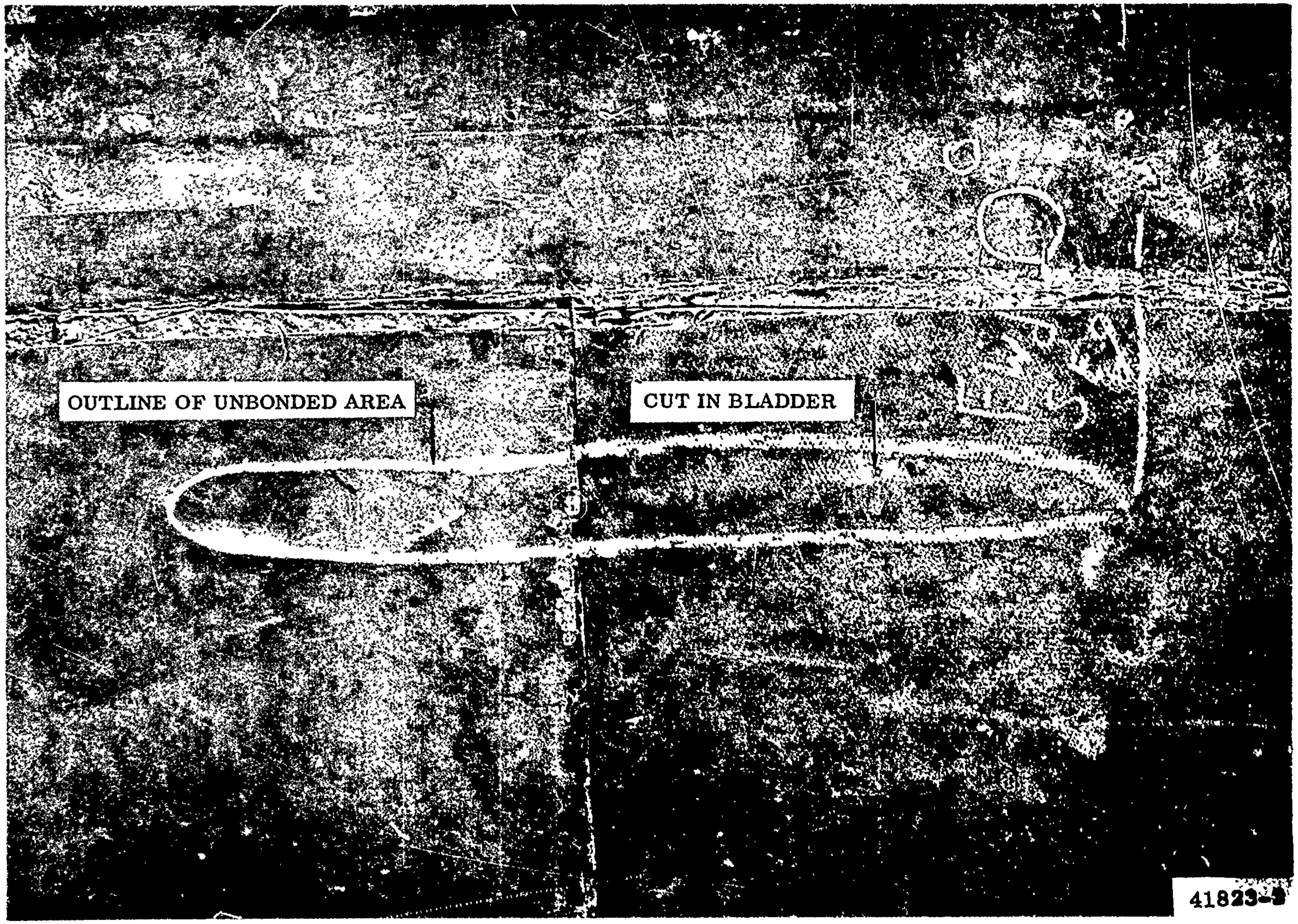

(U) Figure 75. Defect in Bladder

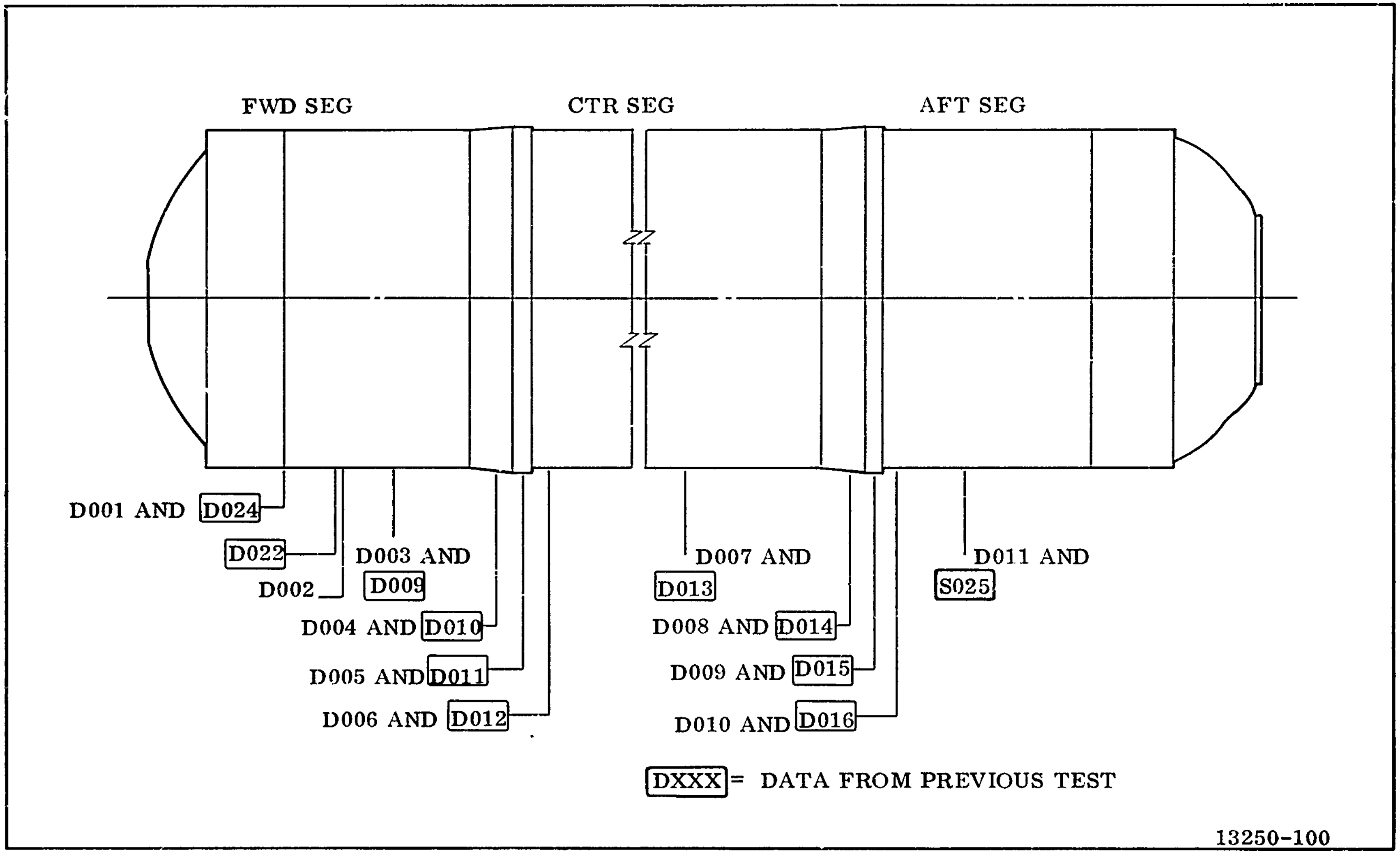

(U) Figure 76. Gage Locations

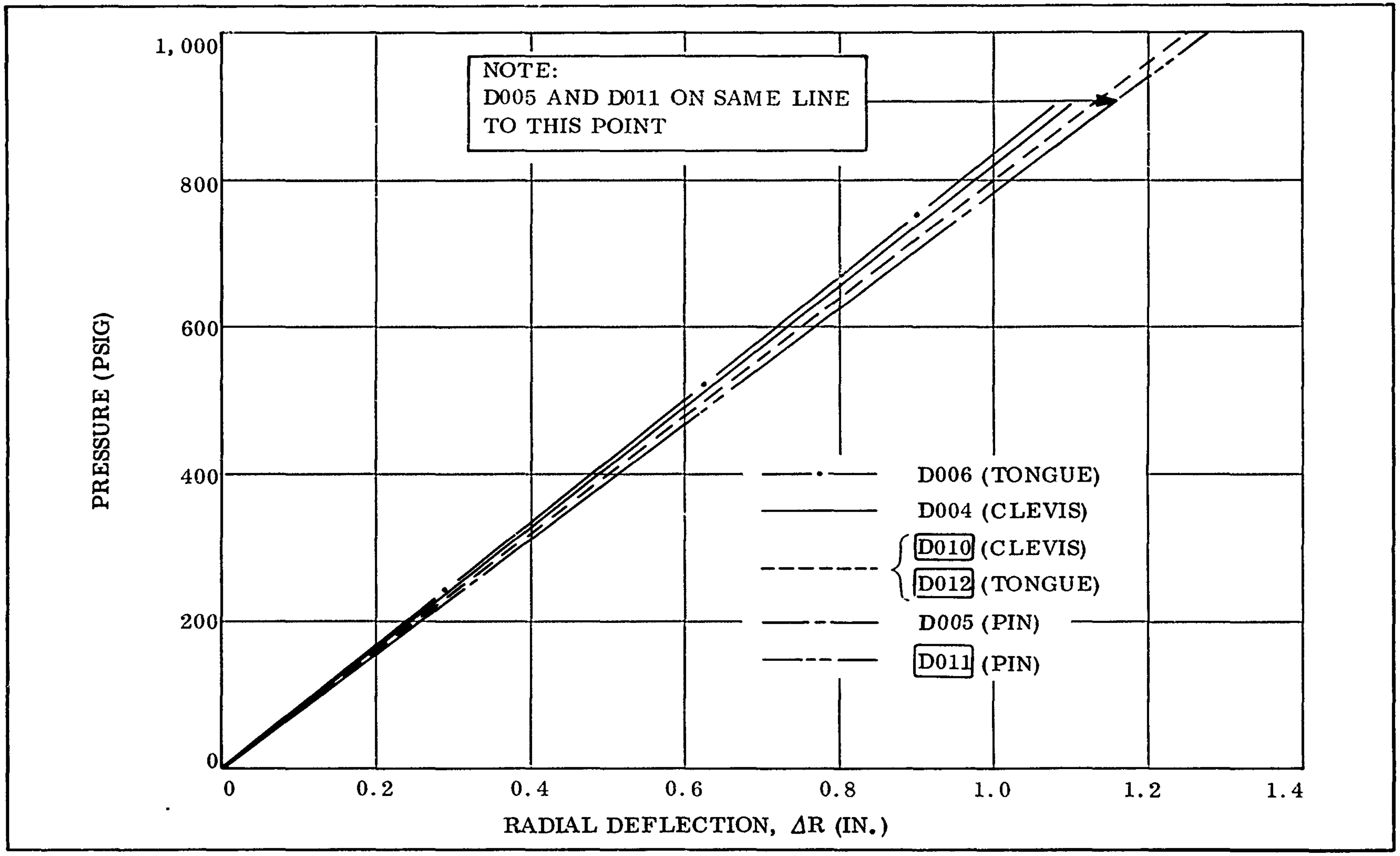

(U) Figure 77. Forward Joint Deflections

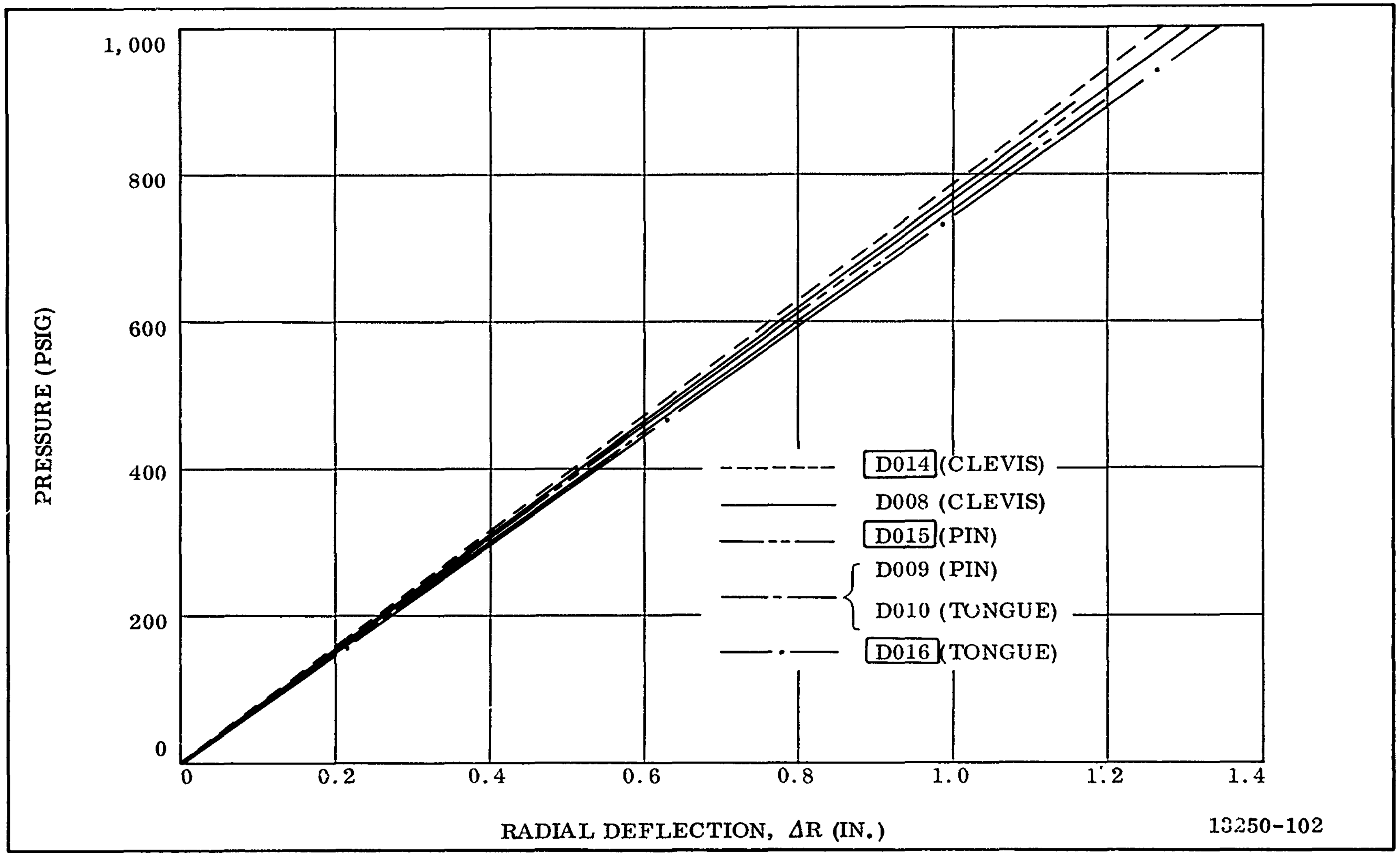

(U) Figure 78. Aft Joint Deflection

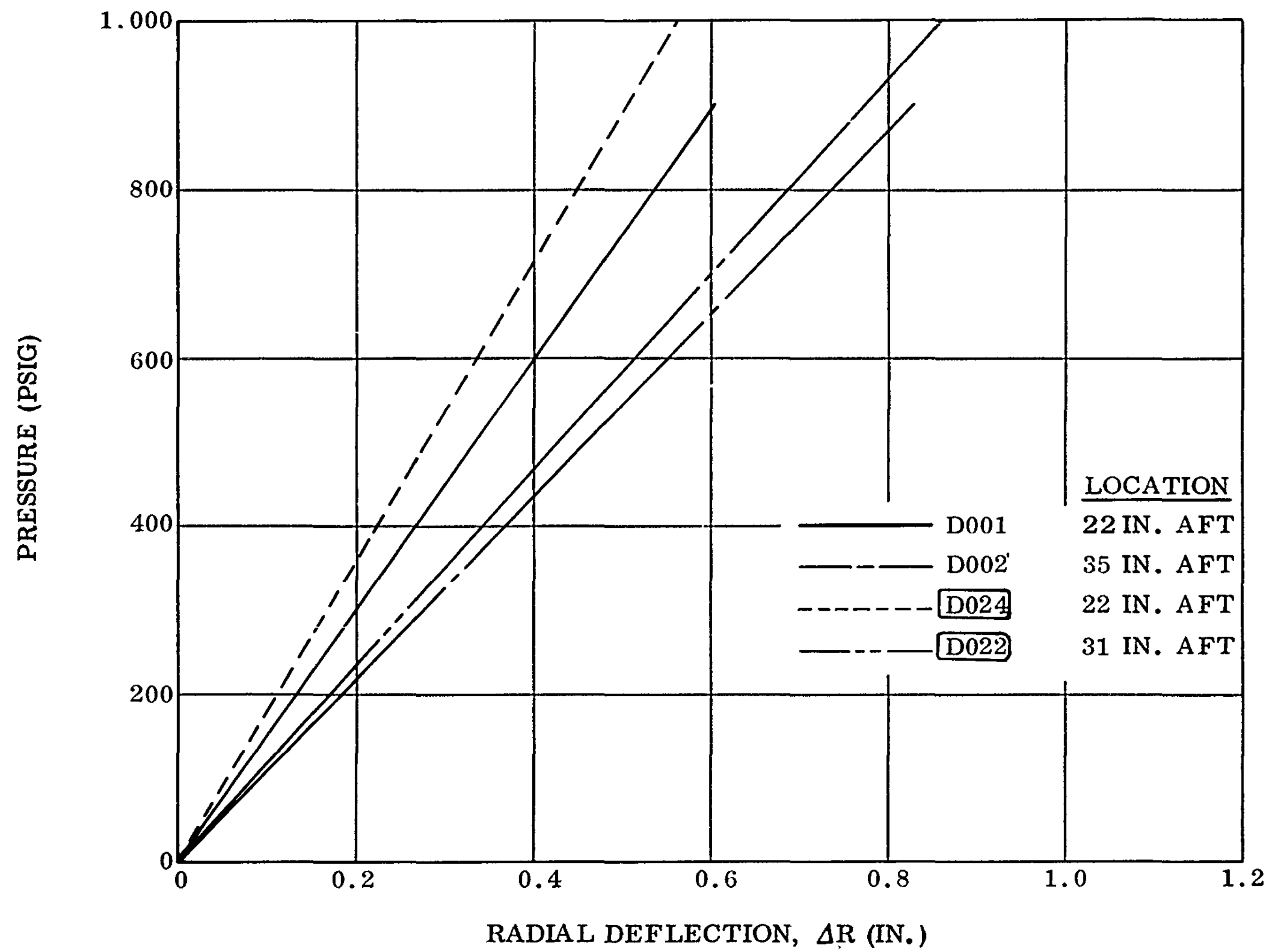

(U) Figure 79. Skirt Deflections

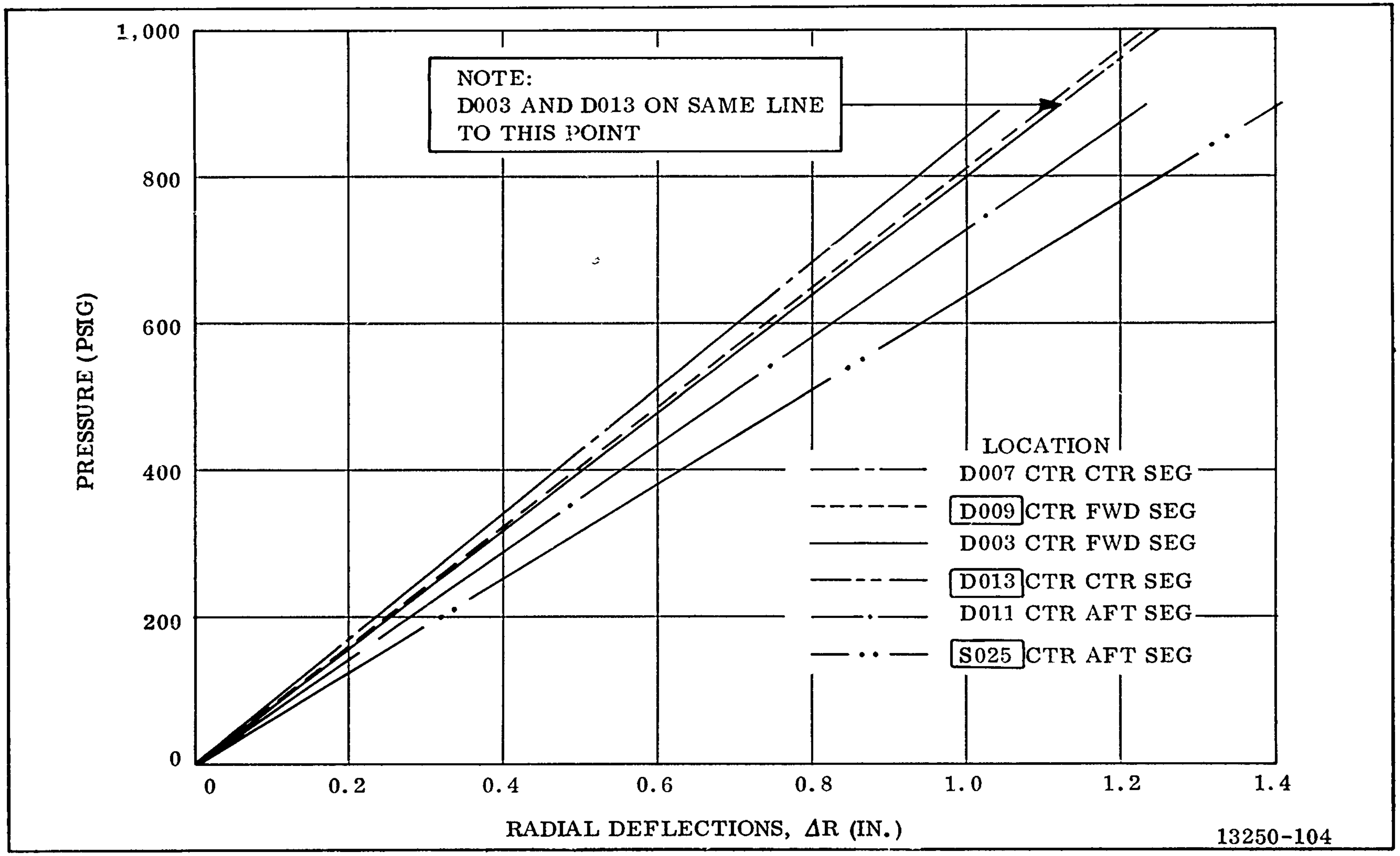

(U) Figure 80. Case Deflections

the same location of the previous hydrotest were attributed to the reduction of glass thickness during bladder removal. However, no quantitative conclusion can be reached since the difference again is within the expected range of error due to gage location and instrumentation system data acquisition.

(U) Strain gage data did not compare, in general, with that from the previous test. Since the extensometer data from this test correlate well with both the strain data and extensometer data from the previous test, the strain gage data for this test are considered erroneous. The erroneous data most likely resulted from inadequate bond between the strain patches and case sealant or between the case sealant and case.

(U) E. CONCLUSIONS

(U) The following conclusions were based on the test results.

1. The design and fabrication of the case seal resulted in a pressure tight seal. No leakage occurred during the extended low pressure or at the high pressure.
2. The structural integrity of the 156-8 case has been sufficiently maintained to withstand an internal pressure of 880 psig during static test. Extensometer data indicate that glass removal has had no greater effect than predicted and the predicted minimum factor of safety remains at 1.62.
3. The replacement bladder, although one leak did occur, is pressure tight after repair of the revealed hole. The repair was performed using the same process and material as used to install the bladder. In addition, this area will be covered with liner and propellant until the moment of motor burnout.

4. The igniter cap design and fabrication resulted in a part which would withstand a static test pressure of 880 psig.

SECTION VI

(U) LINER AND BONDING MATERIAL DESIGN AND FABRICATION

(U) A. <u>BONDING MATERIALS</u>

(U) 1. MATERIAL DESIGN AND SELECTION

(U) The selection of bonding material for use in the 156-8 motor was based on previous experience on other programs and test data generated in the 156-8 program.

(U) a. <u>Silica-Filled NBR Bladder Bond to Case</u>--The design criteria for the bonding material to bond the silica-filled NBR (Gen Gard V-45) bladder to the 156-8 case were based on insuring a safety factor of 7 on the propellant grain to case bond by having a tensile adhesion of at least 70 psi. UF-3119 was selected for this application as the more processible of two candidate materials tested. Testing details are covered in Section VI-C. The formulation and properties of UF-3119 are given in Table XIV.

(U) b. <u>Bond of Primary Insulation (Asbestos-Filled NBR)</u>--The criteria for selecting the material for bonding the asbestos-filled NBR (Gen Gard V-44) to both the remaining original and the new silica-filled NBR bladders and for bonding the joints between the pieces of insulation were:

1. Provide a tensile adhesion of at least 70 psi to withstand grain stresses.
2. Provide thermal protection approximately as good as V-44 in the stagnant flow areas of the case.

(U) UF-1149 was selected based on previous experience. The formulation and properties of UF-1149 are given in Table XV . Previous experience on the 156-1-C

TABLE XIV

(U) UF-3119 BONDING MATERIAL

Usage	
V-45 Bladder to Fiberglass Case	
Composition (%)	
Liquid Epoxy Resin (Type II)	35.00
Versamid 140	65.00
Cure	
24 hr at 80° F	
Physical Properties*	
Density (lb/cu ft)	65.8
Tensile Strength (psi)	65.8
Elongation (%)	106
Peel Strength, V-45 to Fiberglass (pli)	53
Tensile Adhesion, V-45 to Fiberglass (psi)	255
Thermal Properties	
Thermal Conductivity (Btu/sq ft-hr-° F/ft)	0.10
Adhesion Properties	
Silica-Filled NBR (to Gen Gard V-45) to 156-8 Fiberglass Case (psi)	>70

*Nominal values.

TABLE XV

(U) UF-1149 BONDING MATERIAL

Usage	
V-44 Insulation to Bladder	
V-44 Insulation to Silica Phenolic Insulation	
V-44 Insulation to V-44 Insulation	
Composition (%)	
Epon 838	29.16
Versamid 140	33.33
Genamid 2000	16.66
M-Floats (asbestos)	20.85
Cure	
24 hr at 80° F or	
5 hr at 135° F or	
3 hr at 170° F	
Pot Life	
2.5 hr in 100 gm quantities	
Physical Properties*	
Density (lb/cu ft)	63.4
Tensile Strength (psi)	580
Elongation (%)	89
Tensile Adhesion (psi)	
NBR to Steel	630
Steel to Steel	1,160
Adhesion Properties	
NBR to NBR (psi)	580

*Nominal values.

program indicated that erosion and char of UF-1149 in low gas velocity areas are approximately the same as for asbestos-filled NBR.

(U) c. Silica Cloth Phenolic Bond to V-45 Bladder--The criteria for selection of the bonding material between the silica cloth phenolic and the silica-filled NBR bladder were based on the requirement that the material simply hold the insulation piece in place and then prohibit separation during processing. The silica cloth phenolic ring was locked in place by the asbestos-filled NBR insulation and the aluminum polar piece.

(U) The material selected based on previous experience was UF-3195. The formulation and properties of UF-3195 are given in Table XVI.

(U) d. Bond of Nylon Seal Backup Ring to Silica-Filled NBR Bladder (B. F. Goodrich 39322)--The criteria for the selection of a material to bond the nylon backup ring to the silica-filled NBR bladder were based on the need to transfer the loads due to case growth into the nylon ring such that it would grow in diameter with the case during pressurization.

(U) The material selected was UF-3195. The properties and formulation are given in Table XVI. The bond strength to nylon, as verified by tests on this program, is covered in Section VI-C.

(U) B. LINER DESIGN

(U) UF-2121 liner is used for the primary bond between NBR insulation, bladder, and propellant and to thermally protect the cylindrical portion of the segments which are subjected only to tailoff heating. The NBR insulation surface is coated with an epoxy primer (Koropon), prior to application of UF-2121 liner. This primer prevents migration between the NBR and liner-propellant interface.

(U) The nominal thickness of the UF-2121 liner over the primed surface is 0.075 inch. The composition and physical properties of UF-2121 liner are given in Table XVII.

TABLE XVI

(U) UF-3195 BONDING MATERIAL

Usage	
Nylon Ring to V-45 Bladder	
Silica Phenolic Ring to V-45 Bladder	
Composition (%)	
Liquid Epoxy Resin (Type II)	27.52
Versamid 140	51.09
Asbestos Floats	20.40
Cab-O-Sil	0.99
Cure	
4 hr at 170° F or	
24 hr at 80° F	
Physical Properties*	
Density (lb/cu ft)	60.15
Tensile Strength (psi)	1,510
Elongation (%)	59
Modulus (psi x 10^4)	4.7
Peel Strength 180 deg (pli)	63
Adhesion Properties	
To NBR (psi)	799
To Silica Cloth Phenolic (psi)	684
To Nylon, Sandblasted (psi)	>290

*Nominal values.

TABLE XVII

(U) UF-2121 LINER

Usage	
Propellant to Insulation Bond	
Propellant to Bladder Bond	
Composition (%)	
HC Polymer	82.86
MAPO	2.42
ERLA-0500	1.67
Asbestos Floats	10.30
Thixcin "E"	1.75
Iron Drier Catalyst	1.00
Cure	
Precure: 19 hr at 135° F	
Full Cure: 96 hr at 135° F	
Physical Properties*	
Density (lb/cu ft)	62.4
Tensile Strength (psi)	198
Elongation (%)	160
Thermal Properties	
Thermal Conductivity (Btu/sq ft-hr-° F/ft)	0.10

*Nominal values.

(U) The UF-2121 liner has been used by Thiokol in the production of the Stage I Minuteman rocket motors, the Air Force large booster development program, and various other rocket motor development programs.

(U) The grain structural analysis (Section VII-D) reflects the loads and resulting safety factors of the liner propellant bond.

(U) The bond strength of the V-45 bladder-UF-2121 liner and TP-H1011 propellant was verified with the raw materials used in the motor (Section V-C).

(U) C. LINER AND BONDING MATERIAL VERIFICATION TESTING

(U) A series of tests was conducted to verify the propellant-liner-insulation case bonds. The original test plan called for eight phases. Later, a series was added to determine bond strengths and surface preparation for bonding in the nylon backup ring for the case joint seal. The eight phases are as follows:

Phases	
IA and IB	Silica-filled NBR bladder to case bond.
IIA and IIB	Insulation and bladder to liner to propellant bonds.
III	Igniter insulation to liner to propellant bonds.
	In-process verification of:
IVA	Bladder to case bond.
IVB	Insulation to liner to propellant bonds.
IVC	Igniter insulation to propellant to liner bonds.

(U) 1. PHASE IA

(U) Tests under Phase IA were established to determine what material would be suitable to bond the replacement V-45 bladder into the case segments after the original bladder was removed and the case surface was cleaned of loose glass. Since it would be very difficult to duplicate the condition of the glass composite in the 156-8 case segments, it was decided to perform these tests directly on the interior of the segments. A conservative minimum acceptance limit of 70 psi tensile adhesion was established to test the bond to avoid further damage to the glass surface through specimen failure.

(U) Two of Thiokol's most reliable bonding materials (UF-3119 and UF-3177) were chosen. Both materials have been used extensively in past programs.

(U) A special test apparatus was designed and fabricated (Figures 81 and 82). This apparatus adapted an air piston to the conventional tenshear plate which is normally used on the Instron testing machine. The tenshear plate test uses a 7 to 8 sq in. bond area. The air piston was mounted in a frame which reacted the load back to the segment wall to apply direct tension to the specimen. Accurate loading was applied to the tenshear plate through accurately controlled air pressure. V-45 bladder material was bonded to the tenshear plate on one side with a standard adhesive. The other side of the V-45 was bonded to the case wall with the test materials where it was cured for 16 hr (min).

(U) Two UF-3119 samples and two UF-3177 samples were bonded to each of the aft and center segments and tested. These tests showed UF-3119 to be superior and therefore only UF-3119 samples were tested in the forward segment. The tensile force was applied to each bond in 10 lb increments. The load was held at each level for one minute.

(U) Of the 10 samples tested, only one failed. This sample used UF-3177 as a bonding material and failed at the final loading. Examination of this specimen revealed that it had not seated properly and that a fraction of the area had been bonded. Measurement of the effective bond area and calculation of the load applied revealed that the actual bond stress was approximately 120 psi at failure.

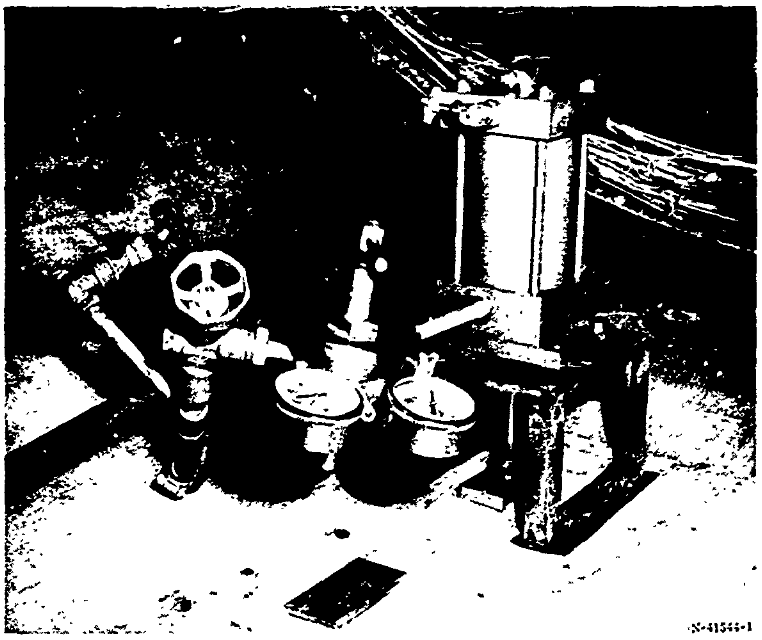

(U) Figure 81. Bond Test Apparatus Connected to Specimen

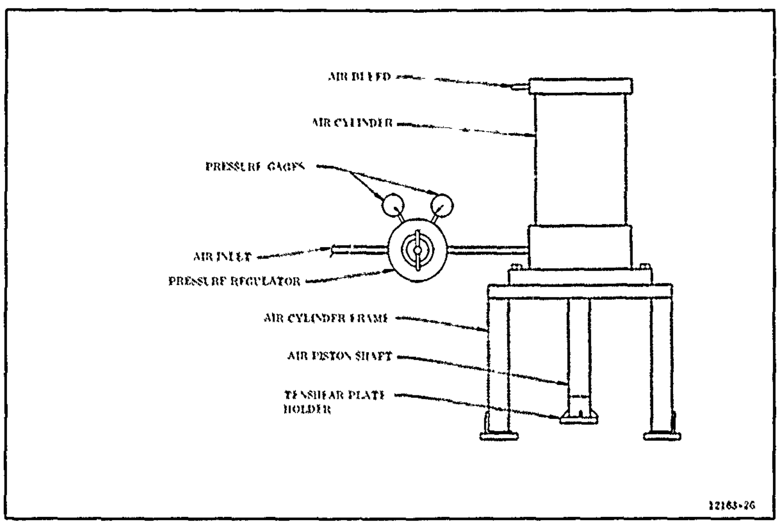

(U) Figure 82. Apparatus for Testing Tenshear Plates Bonded in 156-8 Case

(U) Although both of the test materials met the bond requirements, UF-3119 was selected because of its better processibility due to longer pot life.

(U) 2. PHASE IB

(U) Phase IB was designed to determine the effect of the silicone dioxide release agent from Trevarno cloth on bonds to the V-45 and possible methods of removing this release agent. In past programs, insulations and bladders have been cured with Trevarno cloth containing silicone dioxide release agent; however, these items have also been buffed on the surface following cure. Since buffing of the 0.060 in. thick bladder of the 156-8 would produce thin spots and possible holes, another method of cleaning required development.

(U) Tenshear samples consisting of two tenshear plates bonded together with V-45 (cured with Trevarno cloth) between the plates were prepared. The surfaces of the V-45 used in the specimens were prepared by various test methods. The methods used are shown in Table XVIII. Three samples for each condition were prepared and tested.

(U) The results of the test showed no effect of the release agent in that all samples failed at a minimum of seven times the established minimum acceptable bond to the case.

(U) The MEK wipe method was originally chosen because this is necessary to remove any other contaminants.

(U) An additional series of tests was designed and conducted to determine the relative bond strength of the UF-2121 liner to clean buffed V-45 bladder material as opposed to unbuffed cleaned V-45 bladder material. Actual raw materials and processes simulating those planned for the manufacture of the 156-8 motor were utilized in these tests. Table XIX shows the test details and results.

(U) The results of these tests showed that both the buffed and unbuffed V-45 bladder material produced acceptable bond strengths to UF-2121 liner, with the unbuffed material showing slightly higher strength.

TABLE XVIII

(U) V-45 (CURED WITH TREVARNO CLOTH) ADHESION TO UF-3119
(PHASE IB)

Sample: Steel

Adhesive: UF-3195

Insulation: V-45

Cleaning Method		MEK Wipe	Soap and Water	Trichloro-ethylene Wipe	Soap and Water (H_2O) Rinse	Sandblast	Wire Brush
Adhesive	UF-3119	UF-3119	UF-3119	UF-3119	UF-3119	UF-3119	UF-3119
Number of Tenshear Tensile Adhesion Samples	3	3	3	3	3	3	3
Tensile Adhesion Values (psi)	534	551	525	526	420	636	581
Failure Mode	All samples failed in the UF-3119						

TABLE XIX

(U) BOND STRENGTH OF UF-2121 LINER TO BUFFED AND UNBUFFED V-45 BLADDER MATERIAL

Insulation	V-45	
Barrier	Koropon	
Liner	UF-2121	
Liner Cure	16-24 hr at ambient 26 hr at 135°F	
V-45 Preparation	Buffed and MEK Wipe	Unbuffed and MEK Wipe
RESULTS		
ASTM 180 deg Peel	5	5
Test Values (pli)	10.4	14.1
Primary Failure Mode	100 Percent Koropon to V-45	25 Percent Koropon to UF-2121 75 Percent Koropon to V-45
Tenshear Tensile	5	5
Adhesion Values (psi)	166	163
Primary Failure Mode	100 Percent UF-2121	100 Percent UF-2121

(U) Two tensile adhesion tests were performed by applying Koropon to the inner bladder surface of the case in the local areas of the center segment. Then two tenshear plates were bonded directly to the Koropon with UF-3195 adhesive. These plates were tested to 70 psi tensile force and held for one minute at this force. The bond of both samples held and the tests were discontinued.

(U) 3. PHASE IIA

(U) Phase IIA verification testing was designed to verify the compatibility of the bond system materials between the insulation and the propellant, using the actual raw materials and the processes simulating those planned for the manufacture of the 156-8 motor. These tests would reveal any possible deficiency in the raw materials or planned processes. Bond system samples were prepared consisting of V-44 insulation, Koropon primer, UF-2121 liner, and TP-H1011 propellant (Table XX). This system has been highly reliable in the past.

(U) Two types of specimens, tenshear and peel, were prepared and tested. The tenshear specimens were used to determine the tensile adhesion strength of the TP-H1011 propellant to UF-2121 liner bond. The samples were tested on the Instron testing machine in direct tension. Figure 83 shows the apparatus and test sample. Each specimen had a seven square inch bond area.

(U) ASTM 180 deg peel test specimens were used to determine the ability of the bond to withstand peeling action. The specimens were one inch wide and the average peel strength was determined during three inches of peel. Figure 84 shows a typical specimen and the apparatus.

(U) Five samples were prepared for each of three conditions of UF-2121 liner cure for each type of test simulating the minimum and maximum liner cure for each segment of the 156-8 motor.

(U) The results of these tests (Table XX) indicate no deficiencies in the raw materials or planned processes.

TABLE XX

(U) PHASE IIA COMPATIBILITY TEST OF PROPELLANT TO INSULATION BOND

Insulation		V-44	
Barrier		Koropon	
Liner		UF-2121	
Liner Cure	Minimum All Segments 16-24 hr ambient 26 hr at 135°F	Maximum Forward and Aft Segment 16-24 hr ambient 48 hr at 135°F	Maximum Center Segment 16-24 hr ambient 66 hr at 135°F
Propellant	TP-H1011	TP-H1011	TP-H1011
RESULTS			
ASTM 180 deg Peel, No. of Samples	5	5	5
Test Values (pli)	15.0	13.8	12.0
Primary Failure Mode	Propellant Film	Propellant Film	Propellant Film
Tenshear (Tensile) No. of Samples	5	5	5
Adhesion Values (psi)	85.4	109.1	111.6
Primary Failure Mode	Propellant	Propellant	Propellant

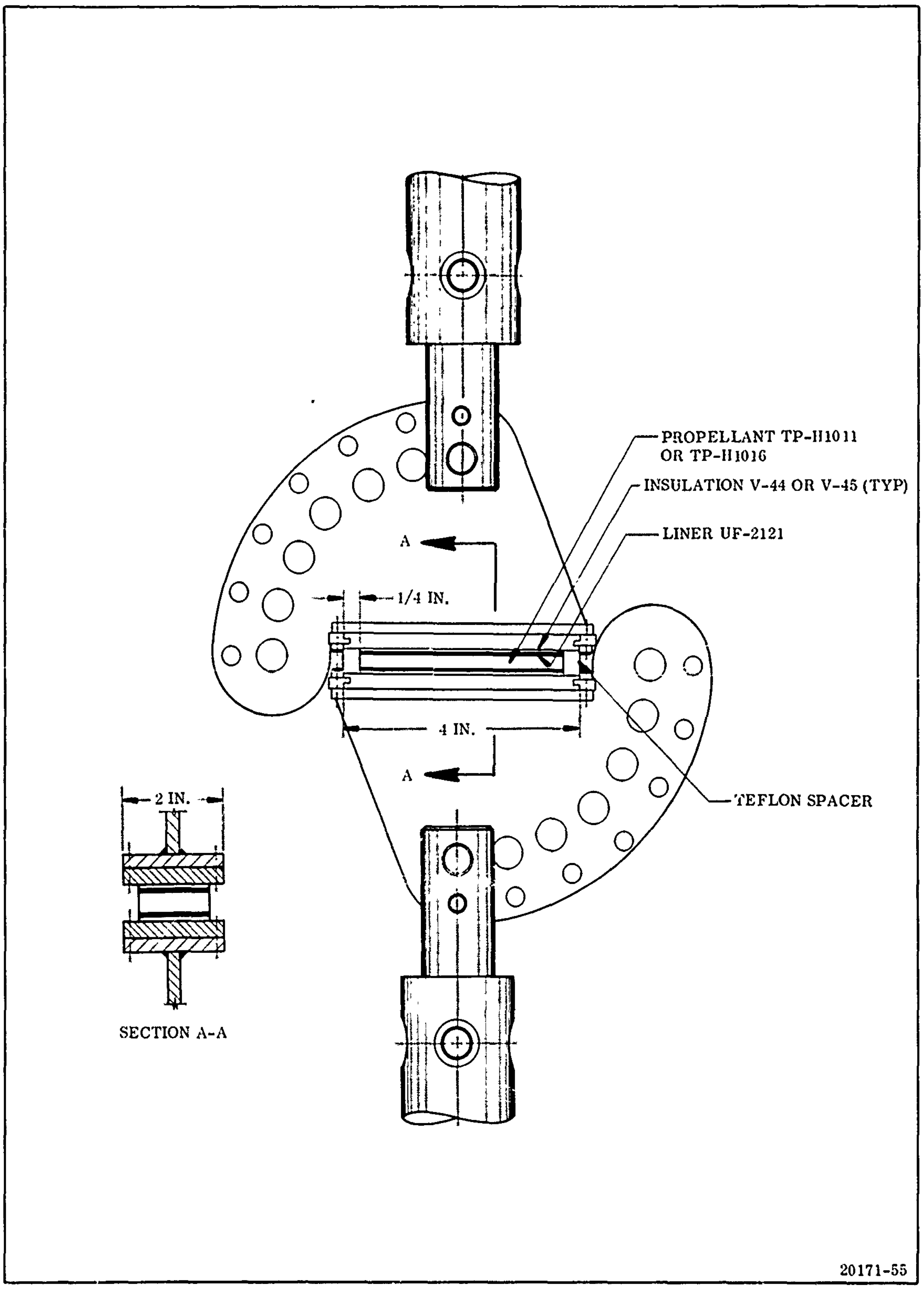

(U) Figure 83. Tenshear Test Apparatus

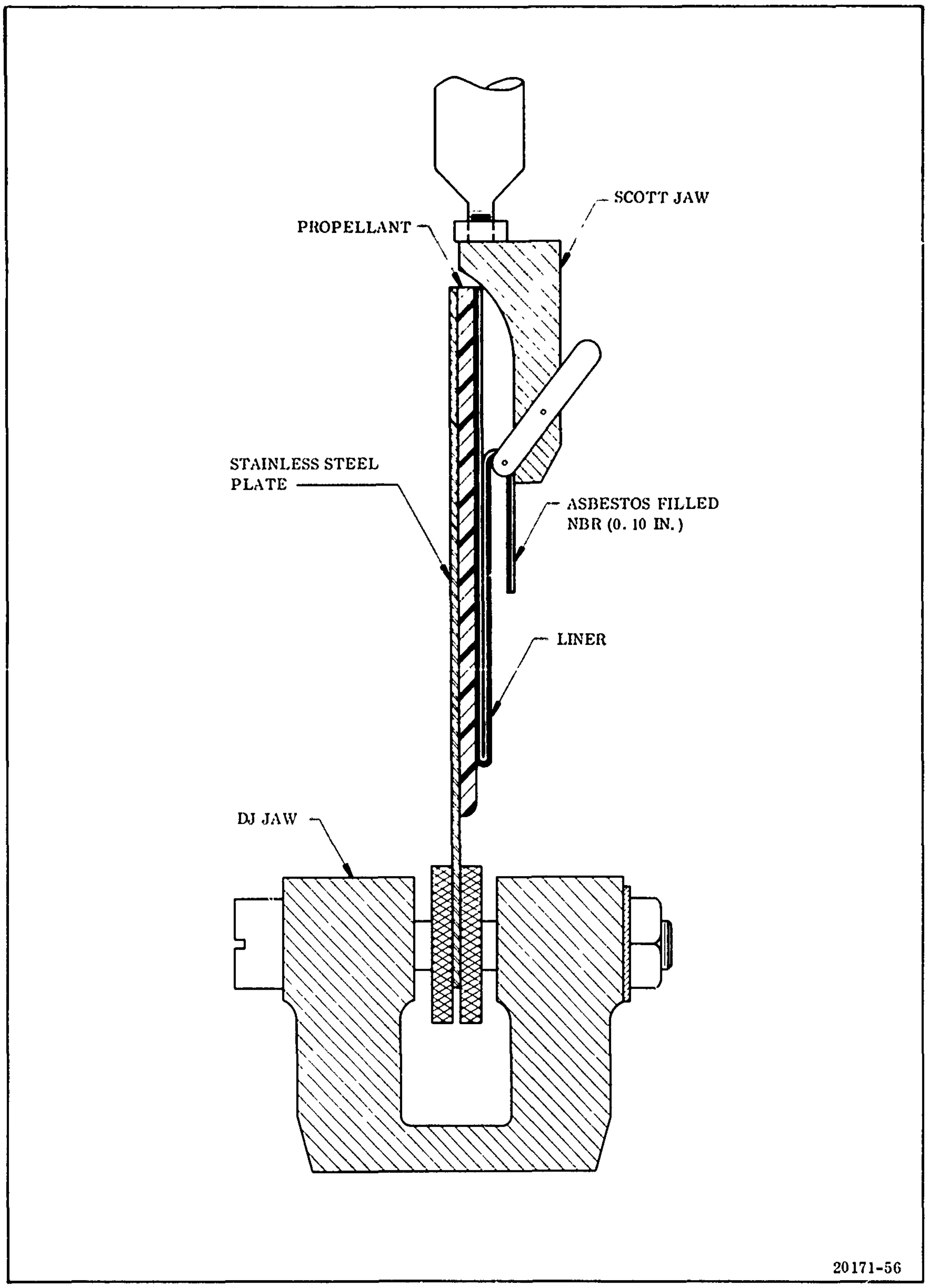

(U) Figure 84. 180 Deg Peel Test Specimen and Arrangement

(U) 4. PHASE IIB

(U) Phase IIB verification testing was designed to verify the compatibility of the bond system materials adjacent to the V-45 bladder. Since the bladder was in the center of the segment and the UF-2121 liner is cured for an intermediate time, liner cure variations were not considered. Table XXI shows the tests details and the results.

(U) A set of five samples was tested for peel in addition to those specified in the test plan. These samples were prepared without propellant to isolate the bond strength of UF-2121 liner to the Koropon surface of the V-45 bladder.

(U) The results of these tests (Table XXI) indicate no deficiencies in the raw materials or planned processes.

(U) 5. PHASE III

(U) The Phase III tests were designed to verify the compatibility of the bond of the igniter propellant to the igniter internal insulation.

(U) The test specimens were prepared using the raw materials and manufacturing processes simulating those planned for the igniter. The number and detailed makeup of these test specimens are shown in Table XXII. The results of these tests, also shown in Table XXII, indicate no deficiencies in the raw materials or the planned processes.

(U) 6. PHASE IVA

(U) Phase IVA verification testing was designed to verify the integrity of the bonds achieved when installing the V-45 bladder in the 156-8 motor case. Two tenshear plates were bonded to the installed bladder at random locations in each case segment. The specimens were then tested to 70 psi bond load using the apparatus shown in Figures 81 and 82. All specimens successfully withstood the 70 psi bond load.

TABLE XXI

(U) PHASE IIB UF-2121 TO MEK WIPED V-45 BLADDER MATERIAL TESTS

Insulation	V-45
Clean	MEK Wipe
Barrier	Koropon
Liner	UF-2121
Liner Cure	16-24 hr ambient 26 hr at 135° F

Propellant	TP-H1011	None
RESULTS		
ASTM 180 deg Peel No. of Samples	5	5
Avg Test Value (pli)	12.9	12.0
Primary Failure Mode	Propellant Film	50 Percent Koropon to UF-2121 50 Percent Koropon to V-45
Tenshear Tensile No. of Samples	5	0
Adhesion Values (psi)	92.3	
Primary Failure Mode	Propellant	

TABLE XXII

(U) PHASE III IGNITER COMPATIBILITY TESTS AT TP-H1016 TC UF-2121 INTERFACE

Insulation	V-44
Barrier	Koropon
Liner	UF-2121
Liner Cure	16-24 hr ambient 26 hr at 135°F
Propellant	TP-H1016
RESULTS	
ASTM 180 deg Peel No. of Samples	5
Test Values (pli)	14.5
Primary Mode of Failure	Propellant Film
Tenshear Tensile No. of Sampies	5
Adhesion Values (psi)	127.0
Primary Failure Mode	Propellant Film

(U) 7. PHASE IVB

(U) Phase IVB was designed to verify the bond strength between the 156-8 insulation and propellant grain. Past history has reflected no appreciable difference in bonds to the asbestos-filled NBR (V-44) versus bonds to silica-filled NBR (V-45); consequently, only V-44 from the same rolls of material used in the segments was vulcanized to the propellant relief flaps of the 156-8 motor. This material was considered representative of the V-44 installed in the segments. The V-44 specimen material was processed along with the case segments through ali significant phases of processing including hydrotest and buffing, cleaning and Koropon applications, and cure.

(U) When each segment was lined, the liner was also applied to the samples then cured with the segment. During casting of each segment, propellant was cast on the samples from the first and last mixes cast into the segment. The samples were then placed in the curing pit and cured with the segment.

(U) The test results are given in Table XXIII. The lowest values were on the 180 deg peel samples from the last mix cast in the center segment. These samples had an average value of 4.0 pli and 100 percent bond failure. The liner had been cured 121 hr before the samples were cast with propellant. These values were considered lower than desirable but acceptable. Also, the propellant used had cooled considerably more prior to casting the sample than that cast into the motor. Therefore, samples were taken from the trim of the propellant relief flap to which the last mix was cast in the motor and tested. These samples gave the high values of 10.3 pli given in Table XXIV.

(U) All other values were well within acceptable limits.

TABLE XXIII

(U) 156-8 MOTOR AND IGNITER INPROCESS SAMPLES

Segment	Propellant Mix No.		Tenshear Adhesion (psi)	Failure* (%)	180 deg Peel (lb/in.)	Failure (%)
Forward	4690001		131	60	9.4	100**
	(1st mix)		118	90	10.0	100**
			121	95	9.4	100**
			129	95	9.3	100**
			118	80	9.1	100**
		Avg	123		9.4	
Forward	4690023		112	85	7.8	100**
	(last mix)		116	95	7.2	100**
			117	95	7.5	100**
			121	100	7.5	100**
			107	80	7.5	100**
		Avg	115		7.5	
Center	4690048		126	100	8.0	100**
	(1st mix)		126	100	8.0	100**
			126	100	8.0	100**
			121	100	9.0	100**
			124	100	8.0	100**
		Avg	125		8.2	
Center	4690088		109	100	2.8	100 Bond
	(last mix)		104	100	3.0	100 Bond
			111	100	3.8	100 Bond
			108	100	5.6	100 Bond
			110	100	5.0	100 Bond
		Avg	108		4.0	
Aft	4690024		125	100	9.0	100**
	(1st mix)		122	100	8.8	100**
			124	100	9.0	100**
			122	100	9.0	100**
			124	100	9.6	100**
		Avg	123		9.1	
Aft	4690046		114	100	9.8	100**
	(last mix)		110	100	10.0	100**
			120	100	10.4	100**
			104	100	10.4	100**
			107	100	10.2	100**
		Avg	111		10.2	

*Indicates percentage failure in propellant.
**Indicates percentage failure in propellant film.

TABLE XXIV

(U) 156-8 CENTER SEGMENT TEST VALUES
SAMPLES CUT FROM RELIEF FLAP

<u>180 Deg Peel (pli)</u>

10.8

10.0

10.0

Average 10.3

<u>Adhesion Cup (psi)</u>

108

106

110

Average 110

Data from flap sample.

(U) 8. PHASE IVC

(U) Phase IVC was designed to verify the bonds achieved during processing of the 156-8 igniter motor. These samples were prepared using material from the actual processing of the 156-8 igniter and accompanied the igniter motor through all processing. The tests all gave results well within acceptable limits and are given in Table XXV.

(U) 9. TESTING OF BONDING OF NYLON BACKUP RING

(U) A series of tests was used to determine the bond strength and surface preparation required to bond nylon to the original bladder, which was made of B. F. Goodrich 39322 silica-filled NBR. Samples were fabricated to test:

1. UF-3195 adhesion to nylon.
2. Shear strength of nylon bonded to B. F. Goodrich 39322 NBR with UF-3195.
3. Shear strength of UF-3195 to nylon.
4. Peel strength of B. F. Goodrich 39322 NBR bonded to nylon with UF-3195.

(U) The results of these tests are given in Table XXVI. The samples were originally prepared by cleaning the nylon with MEK and buffing the NBR prior to application of the UF-3195. All results were acceptable except the 180 deg peel samples. The average 180 deg peel values as reported from the Instron test trace were adequately high; however, on several samples there were short distances over which the bond was negligible. Examination of the nylon stock revealed intermittent areas of glassy finish. These areas correlated with the areas of negligible bond.

(U) Additional tests were conducted by grit blasting the nylon to a dull rough finish then cleaning and applying the UF-3195.

(U) These samples gave a higher peel value (62.5 pli average versus 21.7 pli average) as well as a consistent bond. The failure actually occurred in the NBR in many places.

TABLE XXV

(U) 156-8 IGNITER INPROCESS VERIFICATION TEST RESULTS

Segment	Propellant Mix No.	Propellant Type	Tenshear Adhesion (psi)	Failure (%)	180 Deg Peel (pli)	Failure (%)
Igniter	4780002	TP-H1016	123	100 Propellant Film	6.8	100 Propellant Film
			120	100 Propellant Film	6.8	
			126	100 Propellant Film	6.9	
			124	100 Propellant Film	6.8	
			125	100 Propellant Film	6.8	
		Average	124		6.8	

TABLE XXVI

(U) NYLON BACKUP RING BONDING TESTS

Sample Make-up	Test	Resulting Value
UF-3195 to Nylon Cleaned with MEK	Tensile Adhesion cup	812 psi
		602
		644
		798
		672
		705 Average
Nylon Cleaned with MEK Bonded to Buffed B. F. Goodrich 39322 NBR	Tenshear Pulled in Shear	177.5 psi
		195.0
		272.5
		247.5
		83.75
		195.2 Average
Buffed B. F. Goodrich NBR Bonded to MEK Cleaned Nylon with UF-3195	180 deg Peel	21.0 pli
		19.9
		24.3
		21.7 Average
Nylon to Nylon, Cleaned with MEK and Bonded with UF-3195	Lapshear	305 psi
Buffed B. F. Goodrich NBR Bonded to Grit Blasted Nylon with UF-3195	180 deg Peel	71 pli
		38
		78.5
		62.5 Average

It was therefore concluded that an adequate bond could be achieved through grit blasting the nylon prior to bonding.

(U) D. LINER APPLICATION

(U) Liner application was accomplished on all three segments with the segment positioned vertically in the casting pit. The UF-2121 liner used has been extensively applied in the Minuteman Stage I rocket motor and other large motors.

(U) Prior to application of the UF-2121 liner, all internal surfaces of the segments were prepared by solvent cleaning and application of a Koropon coating over the rubber insulation and bladder. UF-2121 liner was applied by hand brushing the insulation flap and polar boss areas of the segments with a specified amount of liner and then by applying the remaining liner utilizing the Thiokol designed 2U18000 Sling Lining Machine. The sling liner was originally developed on the Minuteman Program for the application of UF-2121 liner to Minuteman motor cases. The sling lining machine applies the mastic liner by pumping the liner through feed lines onto a rotating disc where the material is centrifugally thrown off the disc and onto the segment wall. The following weights of UF-2121 liner were applied to the forward, center, and aft segments:

Forward	211 lb
Center	359 lb
Aft	235 lb

(U) Cure of the liner was accomplished by allowing the material to gel at 80 $\pm$ 20°F for a period of 6-8 hr and then by high temperature curing for 24-26 hr at 135 $\pm$ 5°F.

SECTION VII

(U) GRAIN DESIGN AND FABRICATION

(U) A. GRAIN DESIGN

(U) Design criteria affecting the propellant grain configuration were specified in Exhibit A, "Technical Requirements," to Contract AF 04(611)-11603. These criteria included:

1. The Contractor shall design the required motor in accordance with the design criteria in the statement of work and the specifications shown in Table XXVII.
2. The motor shall be designed so that the headend pressure-time trace shall be essentially neutral during the steady state portion of motor operation. Neutrality is desirable. Limited regressivity is acceptable, but full duration progressivity is not acceptable.
3. The grain design for the 156-8 motor will be a segmented configuration. Structural and ballistic analyses of the grain will be performed. These analyses will assure case/grain compatibility with loads induced by (a) cure and thermal shrinkage, (b) transportation and handling, (c) motor operation (pressure), (d) erosive burning characteristics, and (e) ignition shock.

TABLE XXVII

(U) MOTOR PARAMETERS AND SPECIFICATIONS

Propellant Weight (lbm)	As required
Mass Fraction (minimum)	0.91
Burning Time Average Thrust, Sea Level (lbf)	900,000
Burning Time (sec)	115-120
Total Impulse, Sea Level, Maximum (lbf-sec)	120,000,000
Tailoff Impulse, Sea Level, Maximum (lbf-sec)	6,000,000
MEOP (psi)	880 (Maximum)
Motor Diameter, Nominal (in.)	156
Nozzle Throat Diameter (in.)	32.96
Nozzle Expansion Ratio	7:1

(U) The 156-8 motor used a segmented cylindrical perforate (CP) grain configuration (0.503 cured web fraction). The grain consisted of three segments separated by two 4-in. wide radial slots. The segments (distributed into forward, central, and aft portions) accounted for a net grain length of approximately 590 inches. Nominal web thickness of the grain configuration was 38.74 in. after cure and thermal shrinkage.

(U) Selection of a cylindrical perforate grain configuration was based upon many considerations. The first of these was burning surface neutrality. The grain design had a maximum-to-average surface area ratio over burning time of 1.065. To obtain the required burning time (115 - 120 sec), a large propellant web and low burning rate were needed. This requirement was best accomplished by use of a CP configuration. Another consideration governing grain configuration selection was strain concentration in the propellant. For the low cross sectional loading density required (75 percent), a CP grain design yielded an acceptable level of propellant strain. Ease of manufacturing and effects of erosive burning were also considered. The CP grain configuration was considered easier and less expensive to manufacture than the alternate propellant grain designs considered. The selected CP design had an initial port-to-throat area ratio of 5.38, thus assuring that erosive burning would not significantly affect motor performance.

(U) B. DESIGNED MOTOR PERFORMANCE

(U) The determination of propellant weight required to meet the impulse requirements (Table XXVII) was based upon an assumed one percent variation (3σ) in the design total impulse. This was necessary to assure that the delivered impulse would not exceed the maximum specified value.

(C) Empirical performance data from a variety of large rocket motor firings at Thiokol* indicate that in a motor the size of the 156-8, an efficiency equal to or greater than 94.5 percent could be anticipated. Therefore, based upon an efficiency of 94.5 percent and a theoretical specific impulse** of 262.5 lbf-sec/lbm for the selected propellant, a delivered reference specific impulse of 248.0 lbf-sec/lbm was predicted.

(U) The CP core was sized at 76.5 in. in diameter. The hardware for this configuration could be acquired economically by adding 4 in. of foam plastic on the radius of the existing 156-1C casting core. This core allowed use of properly sized slots between the segments and created a predicted pressure-thrust trace of excellent shape. The low web fraction (0.503) and low bore gas velocity motor inherently added to the reliability of the 156-8 motor.

*Thiokol motors TU-402 (50,413 lbm propellant), TU-412 or 156-1C (690,491 lbm propellant), TU-455 (51,840 lbm propellant).

**Chamber pressure = 1,000 psia; expansion ratio = optimum for P_a = 14.7 psia; divergence angle = 0 deg.

(C) The propellant weight required in the 156-8 motor was fixed by the impulse requirements and the specific impulse of the selected propellant. The neutrality of the selected grain design allowed the motor to operate at an average action time pressure of 732 psia at 70°F while complying with the MEOP of 880 psia maximum at 100°F. At this pressure, a delivered (Utah conditions) specific impulse of 243.0 lbf-sec/lbm was predicted with a 6.67:1 expansion ratio nozzle. Based on the above criteria, 494,442 lbm of propellant were required to produce the predicted Utah impulse of 120,124,600 lbf-sec (or sea level impulse of 118,609,100 lbm). The propellant weight listed above was re-evaluated as data pertaining to motor mass properties (insulation, cured propellant density, and case liner thicknesses, etc.) became available. The 156-8 propellant weight was re-predicted to be 493,826 lbm on the basis of the most current information. This discrepancy in propellant weights (-616 lbm) was not considered large enough to warrant a re-prediction of the ballistic parameters listed in Table XXVIII.

(U) Predicted performance traces, including chamber pressure, vacuum thrust, vacuum specific impulse and pressure and vacuum thrust decay rates versus time, are presented in Figures 85 thru 93.

(U) It should be noted that the technical requirements listed a maximum MEOP of 880 psia. This was assumed to be for 100°F which would result in an MEOP of 860 psia at 70°F. The refinement of the ballistics calculations later in the program gave an MEOP of 854 psia. However all previous calculations used 860 psia and it was not considered feasible to change over to 854 psia.

(U) C. PROPELLANT

(U) 1. SELECTION CRITERIA

(U) Design criteria for propellant, specified in "Technical Requirements," included the following:

1. The propellant shall be one of the polybutadiene/AP/AL family of propellants. Use of staples is specifically prohibited.

TABLE XXVIII

(C) 156-8 PREDICTED BALLISTIC PERFORMANCE
(Utah, 70° F)

<u>Web Time Performance</u>	
Web Time (sec)*	117.8
Average Pressure (psia)	744
Maximum Pressure (psia)	806
MEOP (psia)	854
Average Thrust (lbf)	1,006,500
Maximum Thrust (lbf)	1,077,700
Impulse (lbf-sec)	118,518,400
<u>Action Time Performance</u>	
Action Time (sec)**	121.3
Average Pressure (psia)	732
Average Thrust (lbf)	990,400
Impulse (lbf-sec)	120,124,600
Tailoff Impulse (lbf-sec)	1,606,200
Specific Impulse (lbf-sec/lbm)	243.0
Measured Thrust Coefficient, cfm	1.512

*Web time is defined as the interval from 75 percent of maximum pressure during rise to the point of pressure-time trace which lies on the line bisecting the angle formed by the tangents to the trace prior to and immediately after the beginning of tailoff.

**Action time is defined as the interval from 75 percent of maximum pressure during rise to 10 percent of maximum pressure during tailoff.

TABLE XXVIII (Cont)

(C) 156-8 PREDICTED BALLISTIC PERFORMANCE
(Utah, 70° F)

Propellant Configuration	
Port Diameter, Nominal (in.)	76.49
Web Thickness (in.)	38.741
Web Fraction	0.503
Propellant Weight (lbm)	494,442
Port Area/Throat Area (initial)	5.38
Propellant Mass Fraction	0.926
Nozzle Parameters	
Initial Throat Diameter (in.)	32.96
Initial Exit Diameter (in.)	87.20
Initial Throat Area (sq in.)	853.2
Initial Exit Area (sq in.)	5,972.4
Half Angle (deg)	17.5
Propellant Data	
Configuration	TP-H1011, Type II
Burning Rate at 744 psia (in./sec)	0.332
Burning Rate Exponent (300 to 900 psia)	0.21

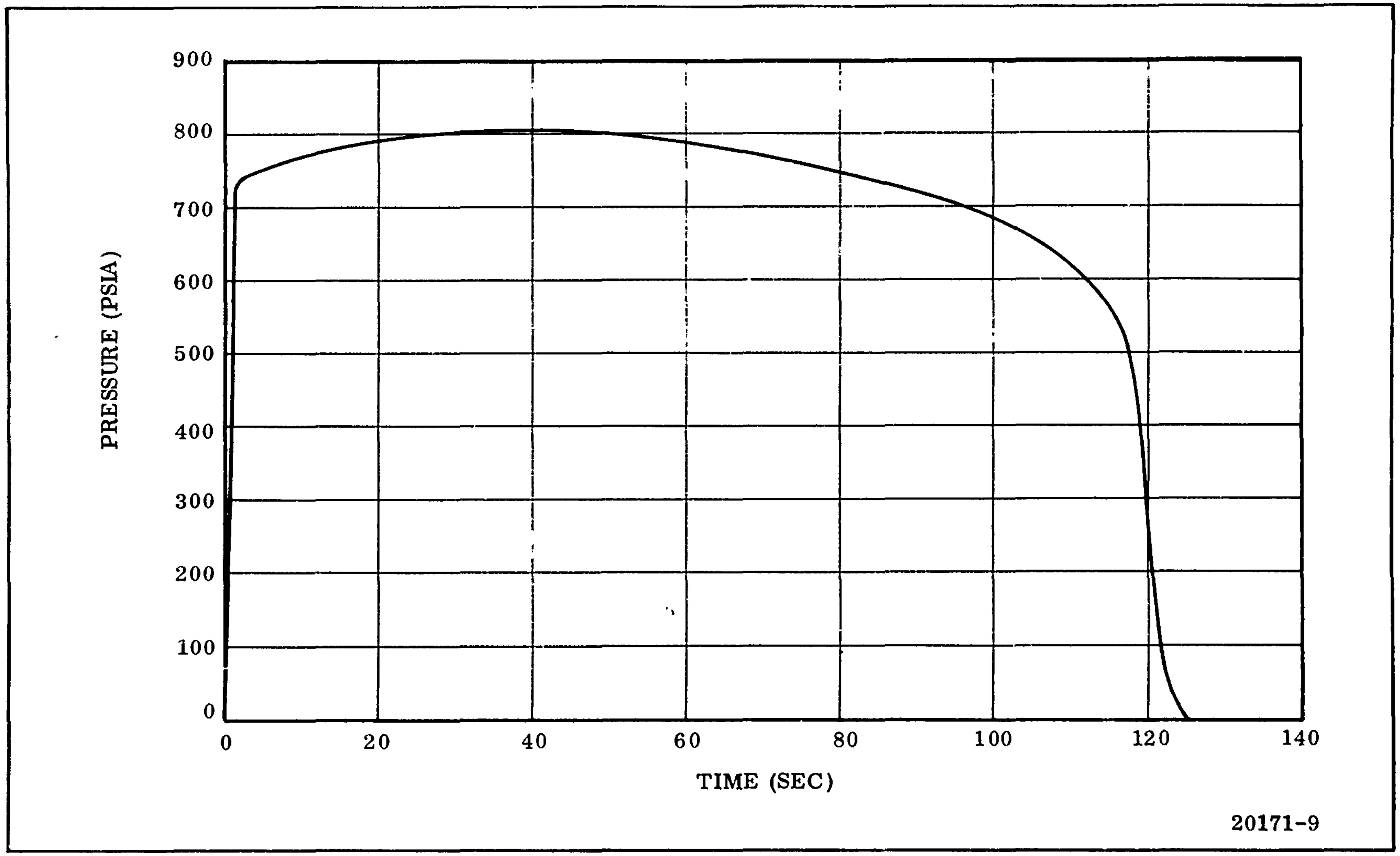

(U) Figure 85. 156-8 Predicted Chamber Pressure at 70° F

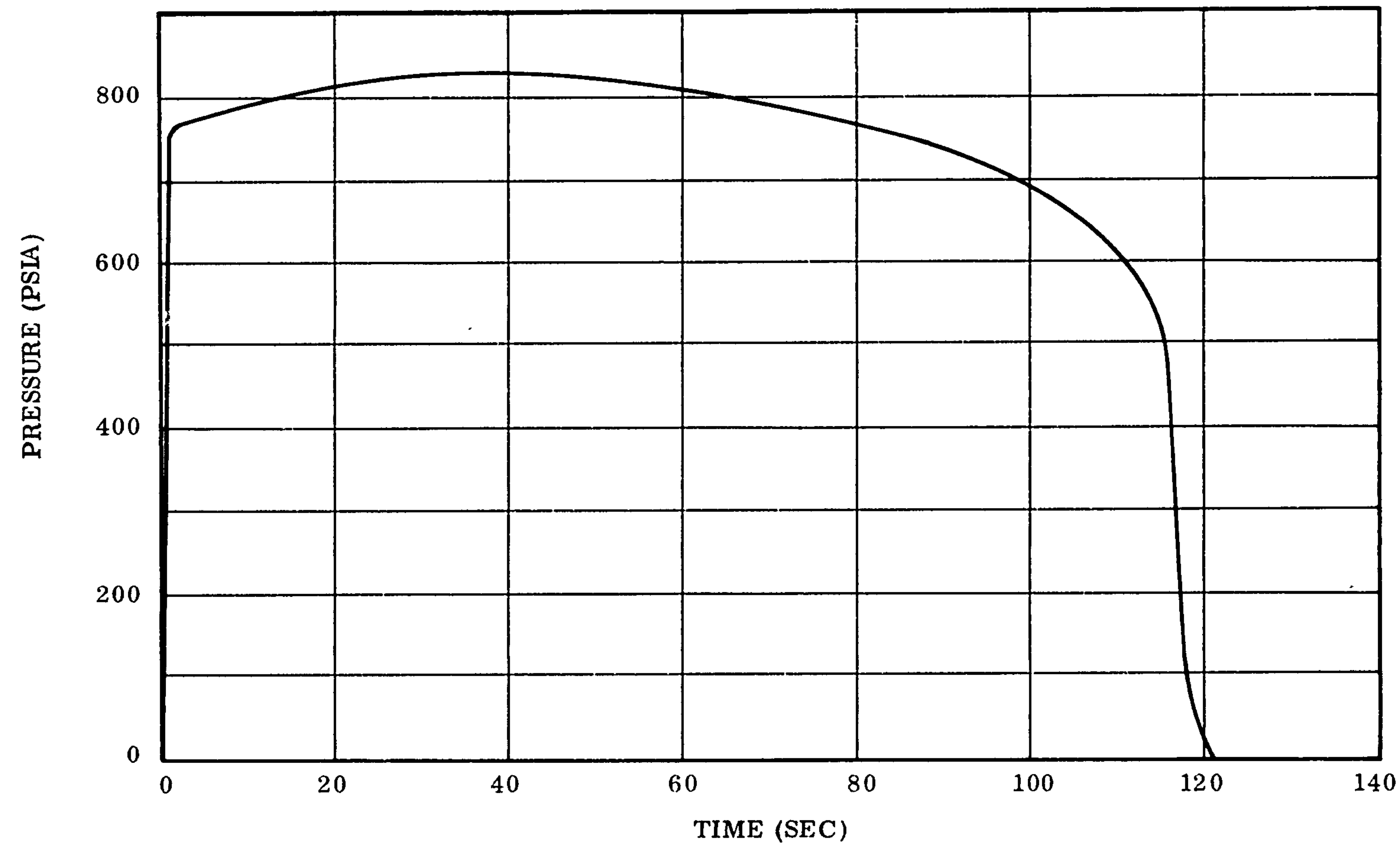

(U) Figure 86. 156-8 Predicted Chamber Pressure at 100° F

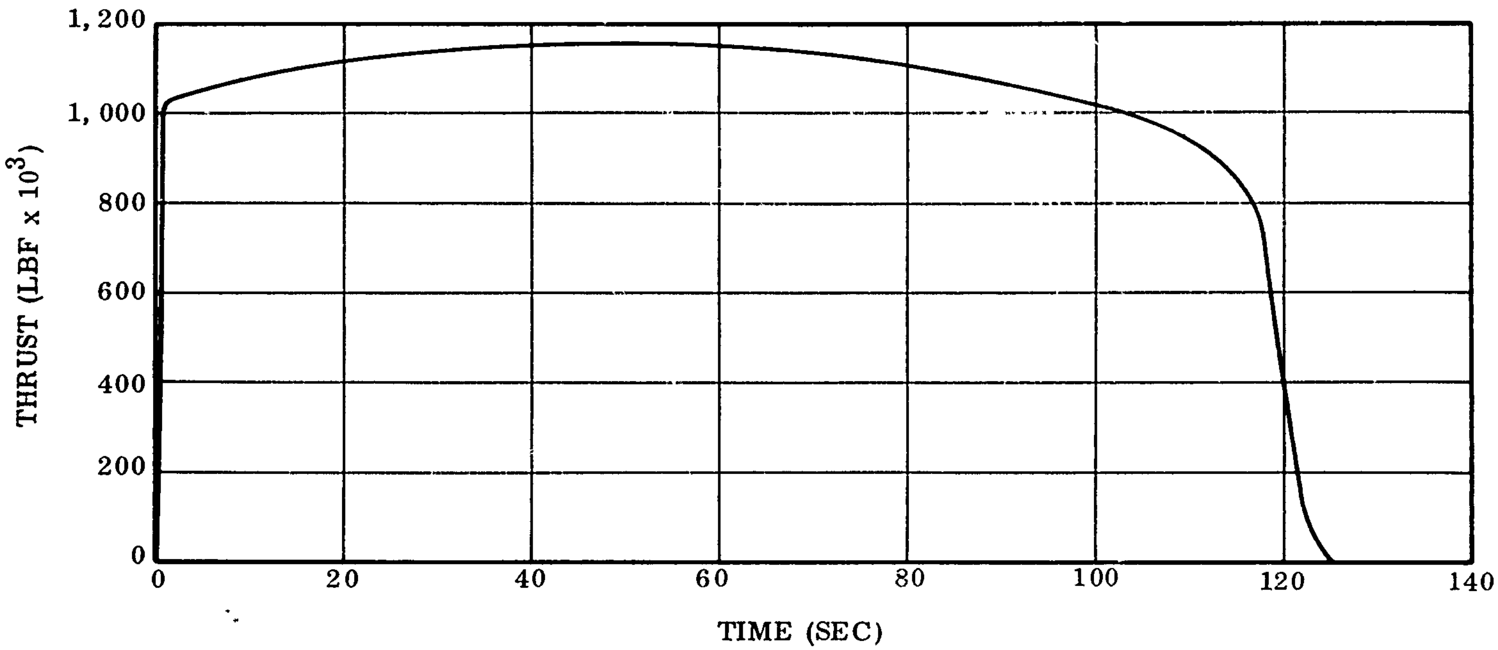

(U) Figure 87. 156-8 Predicted Vacuum Thrust at 70° F

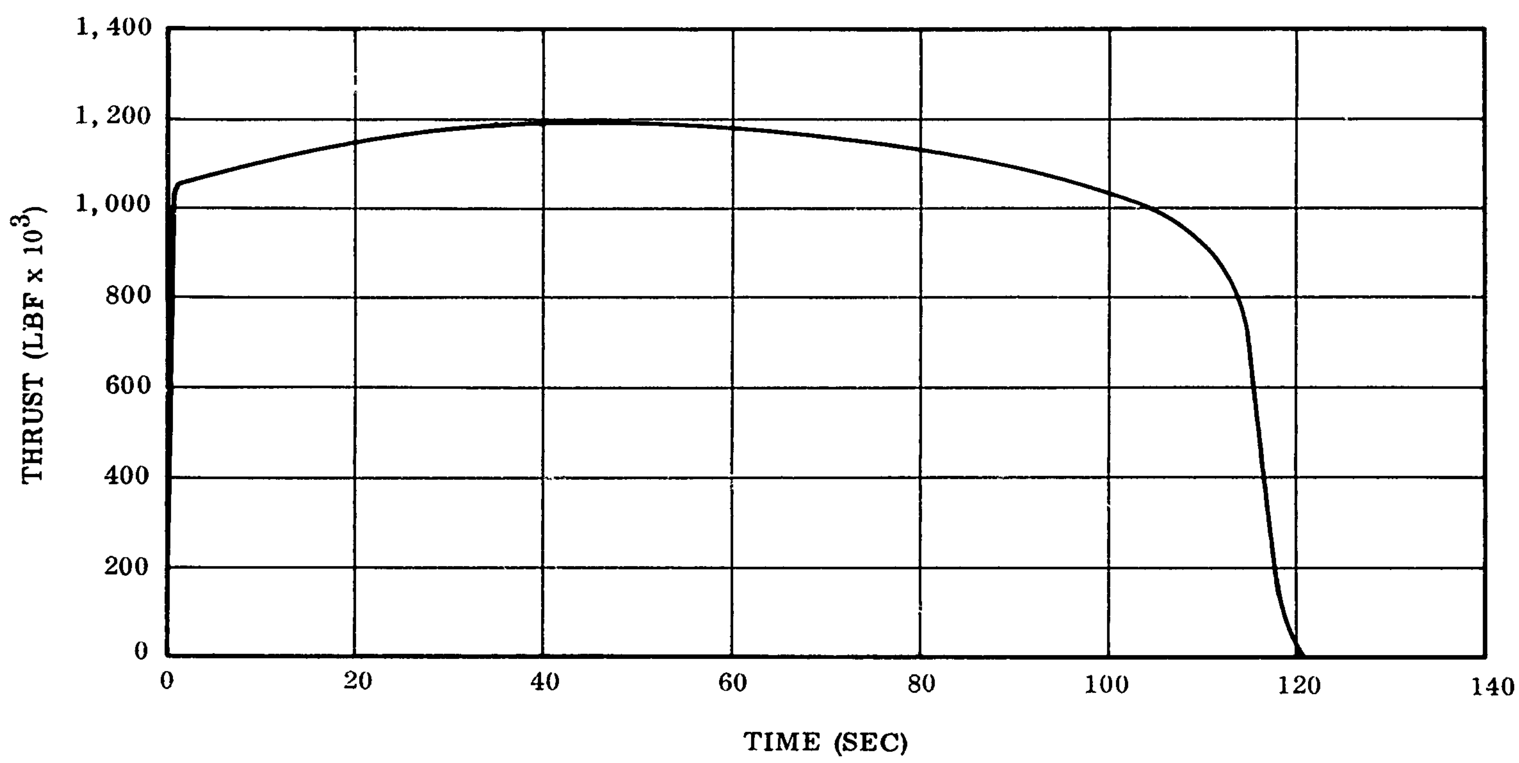

20171-6

(U) Figure 88. 156-8 Predicted Vacuum Thrust at 100° F

20171-5

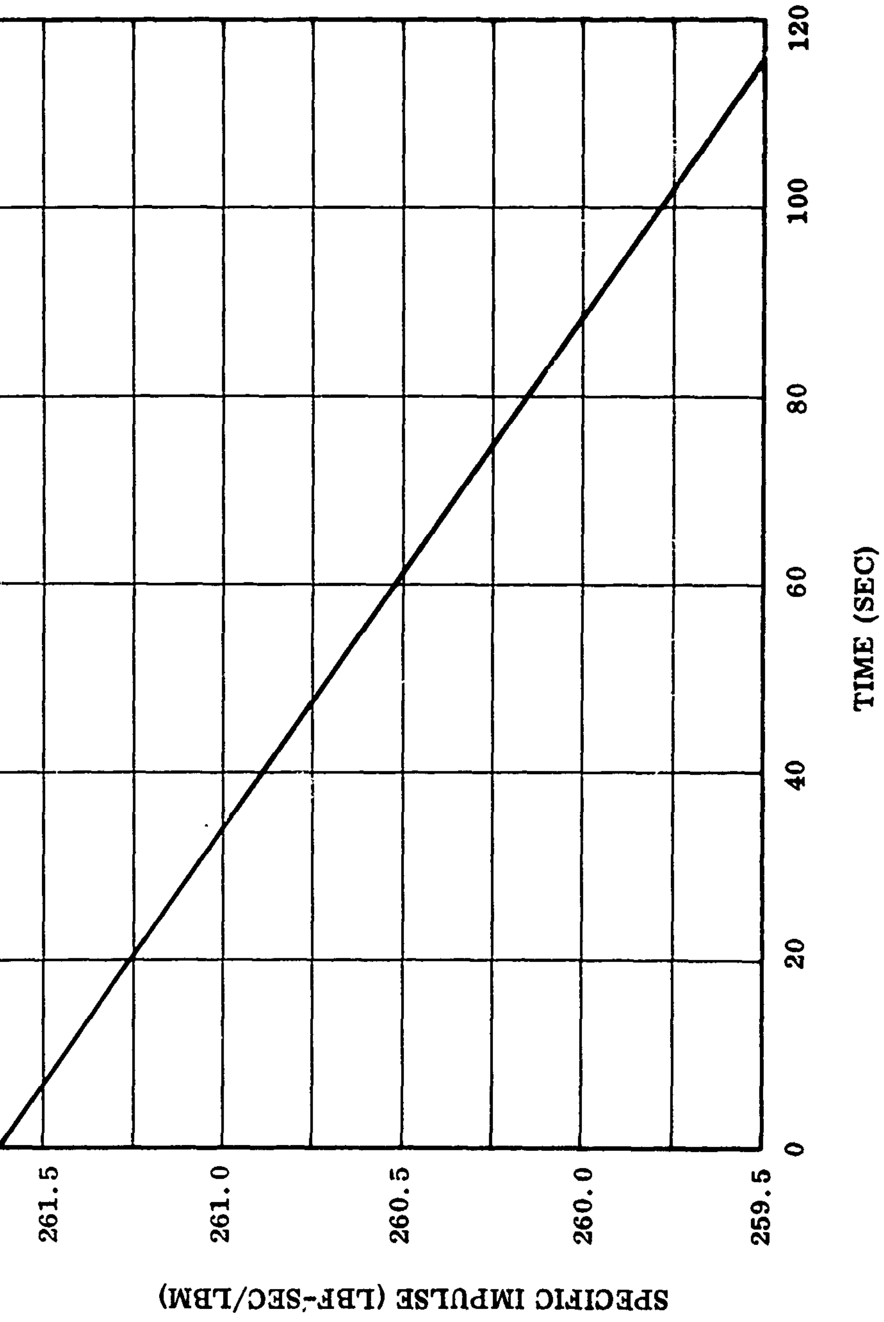

(C) Figure 89. 156-8 Predicted Vacuum Specific Impulse at 70-100° F

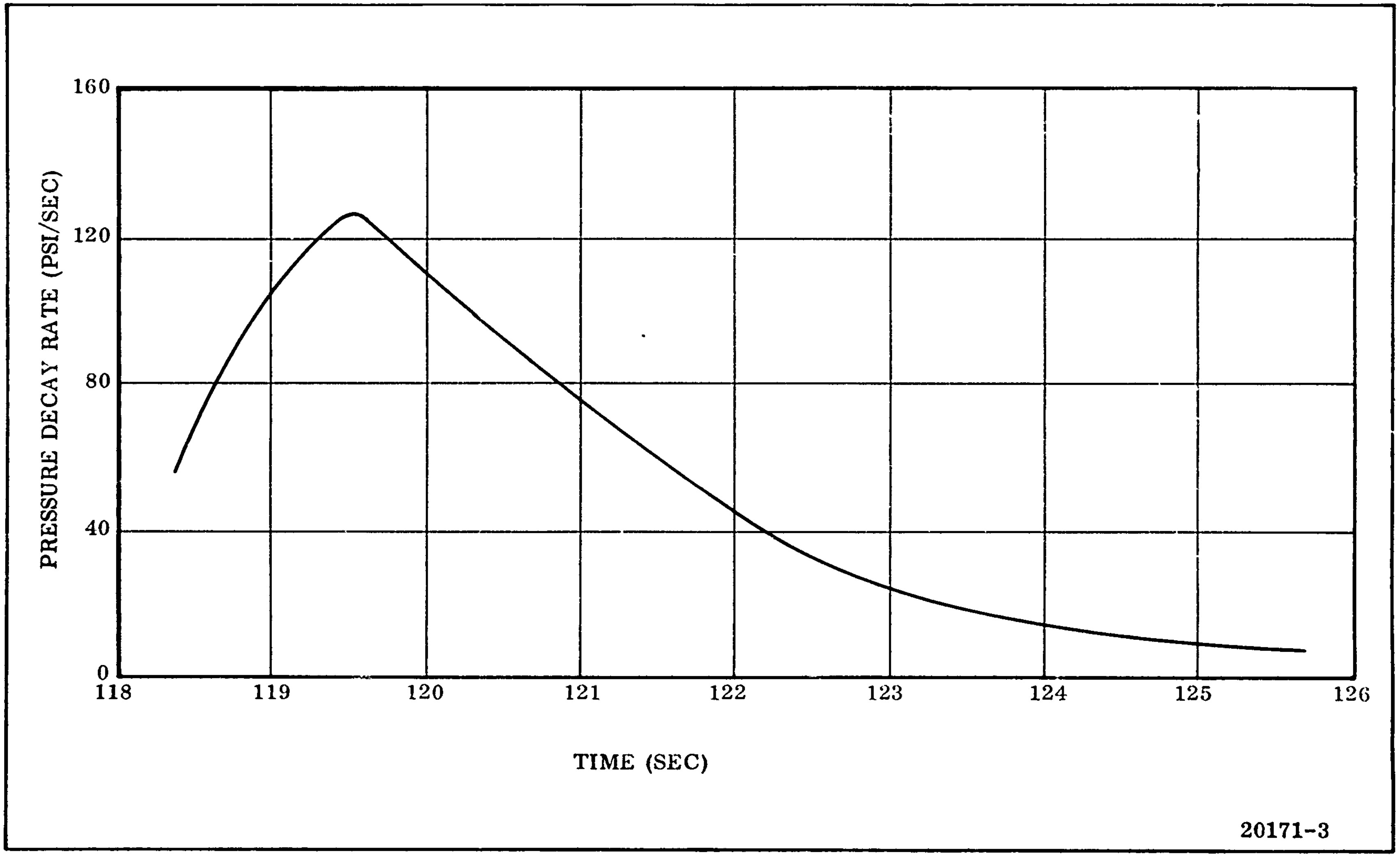

(U) Figure 90. 156-8 Predicted Pressure Decay Rate at 70° F

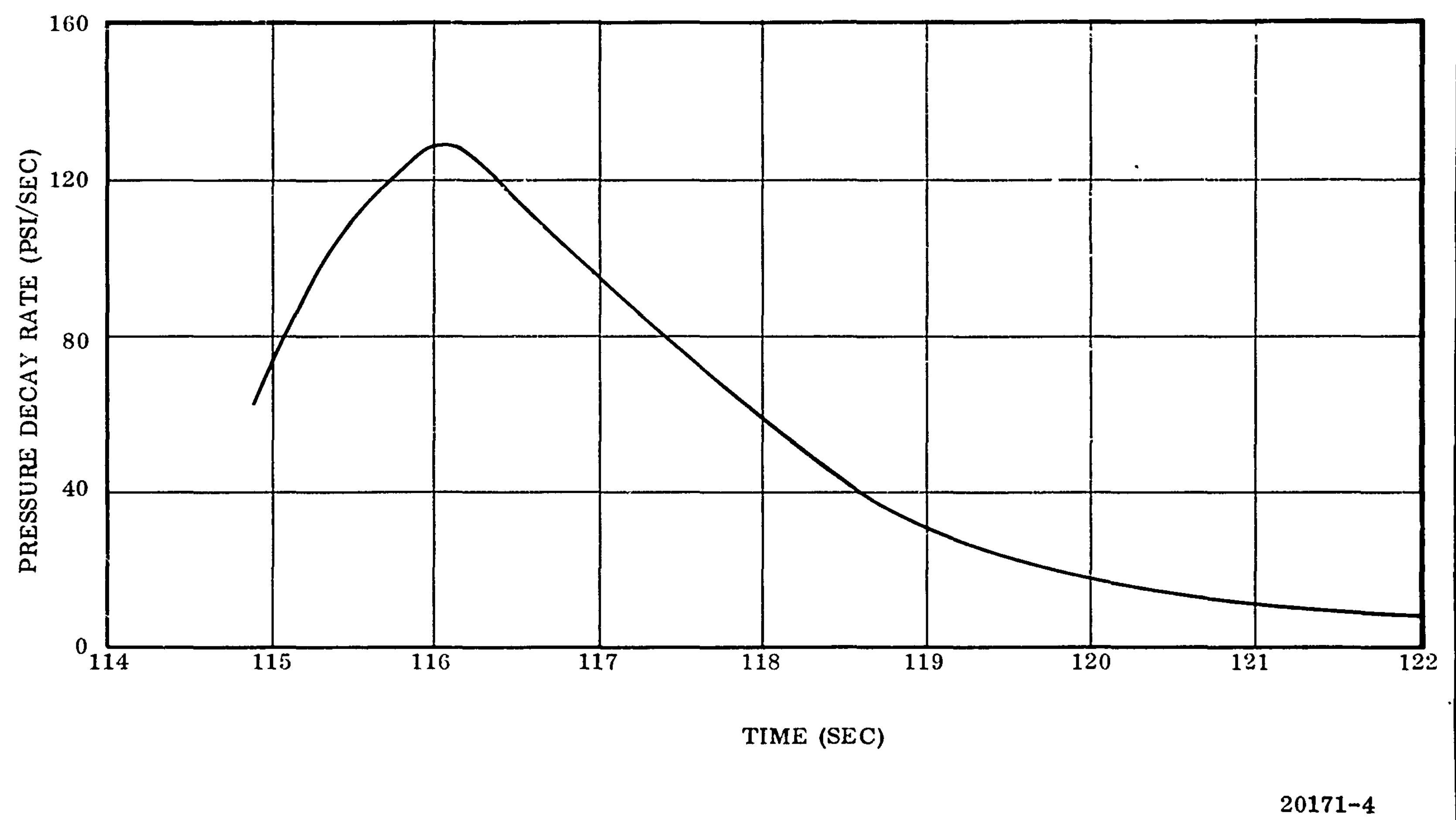

(U) Figure 91. 156-8 Predicted Pressure Decay Rate at 100° F

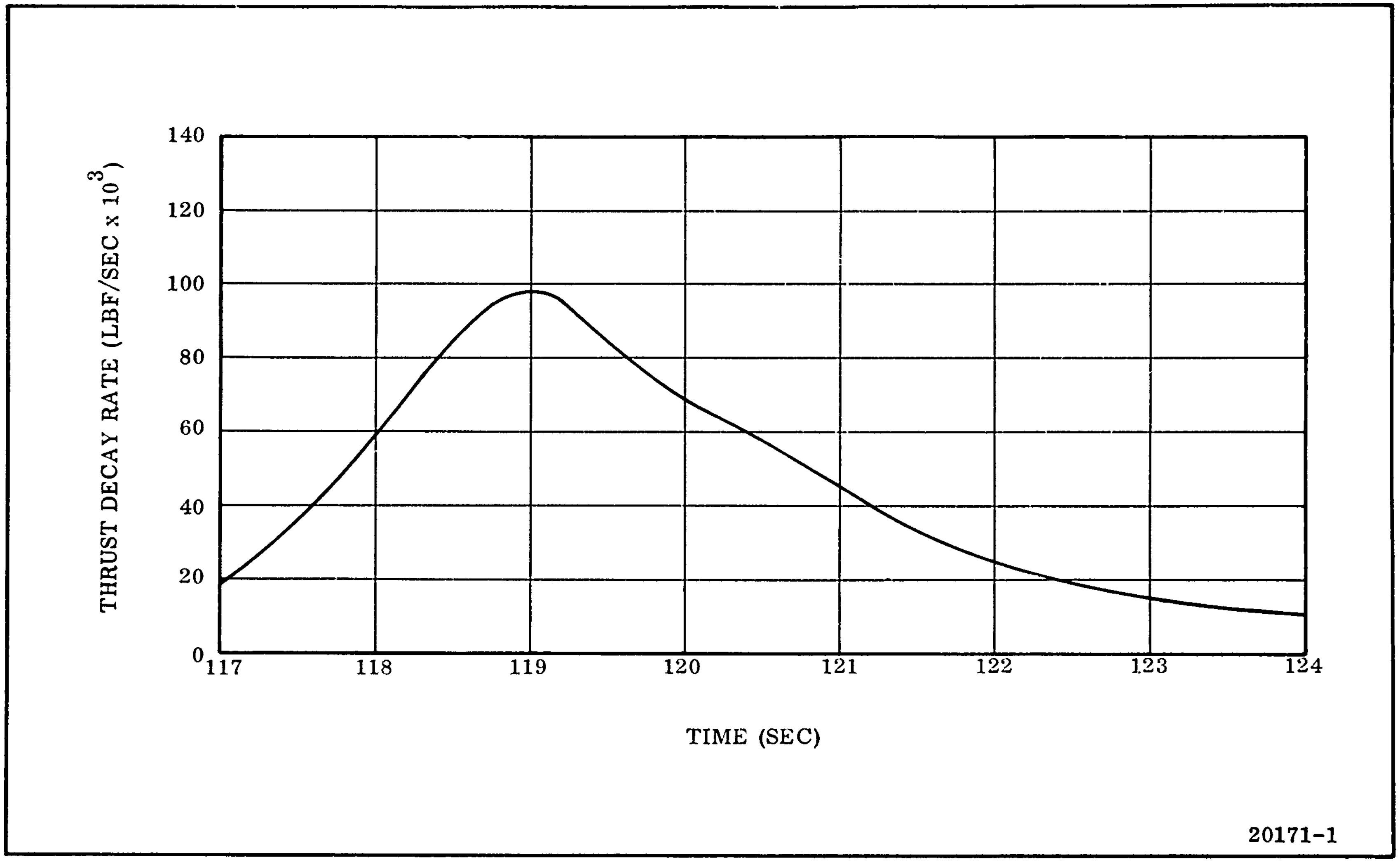

(U) Figure 92. 156-8 Predicted Vacuum Thrust Decay Rate at 70° F

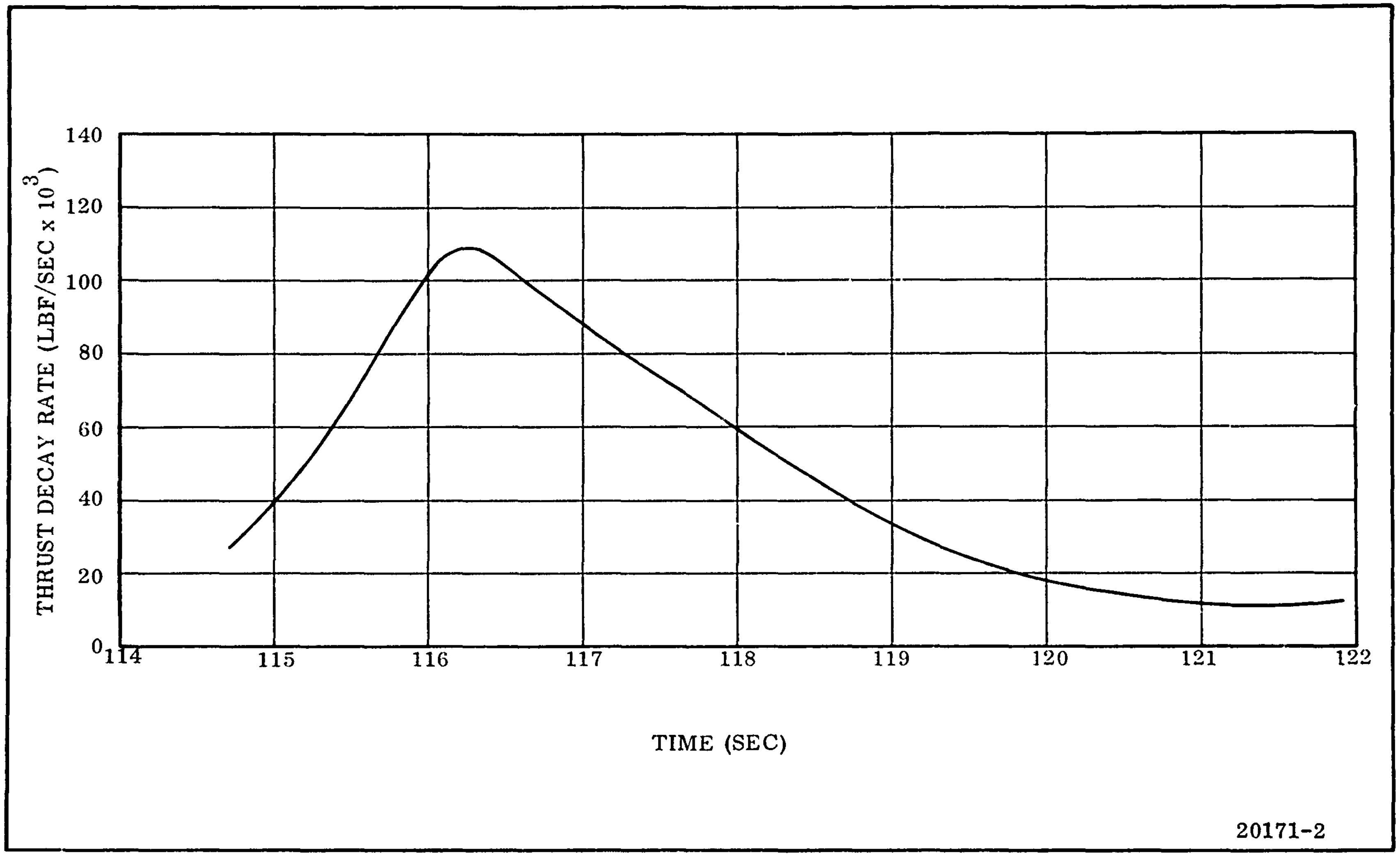

(U) Figure 93. 156-8 Predicted Vacuum Thrust Decay Rate at 100° F

2. The propellant shall exhibit an acceptable degree of reproducibility of both physical and ballistic properties.
3. The propellant formulation shall have a Class 2 explosive characteristic.

(U) 2. BALLISTIC AND PERFORMANCE PROPERTIES

(C) The propellant used in the 156-8 rocket motor is designated as TP-H1011, Type II (Stage I Minuteman propellant), in accordance with Specification STW5-472. This propellant contains 86 percent solids, a trimodal oxidizer distribution, and a polybutadiene acrylic acid acrylonitrile terpolymer with epoxy curing agent. The formulation for TP-H1011 as standardized for the 156-8 motor is presented in Table XXIX. The propellant has a Class 2 explosive classification. Propellant ballistic characteristics are presented in Table XXX.

(C) Cost and reliability considerations for the 156-8 motor test dictated the use of a conventional PBAN/AP/AL propellant well characterized as to physical and ballistic properties and processing characteristics. The greatest experience with PBAN/AP/AL propellant in the solid propellant rocket industry has been with 84 to 86 percent solids formulations containing from 14 to 16 percent aluminum. Formulations of this type can be expected to produce reference specific impulse values of approximately 248 lbf-sec in a motor the size of 156-8. The propellant selected for use in the 156-8 motor, TP-H1011, had been well characterized in the Minuteman program and provided proven reliability, with respect to strain capability and ability to withstand handling, for the 156-8 motor test. For these reasons, TP-H1011 propellant containing 86 percent solids and 16 percent aluminum was selected.

(U) 3. STANDARDIZATION

(C) The propellant was standardized for burning rate using TU-131 (7 lbm) batch check motors. The propellant has a burning rate of 0.306 in./sec at a pressure of

TABLE XXIX

(C) TP-H1011 PROPELLANT FORMULATION

Constituent	Composition (percent by weight)
Ammonium Perchlorate	70
Special Coarse and Ground[1]	
Unground[2]	
Aluminum	16
HB and ECA[3]	14

TABLE XXX

(C) THEORETICAL PERFORMANCE CHARACTERISTICS

Density (lbm/cu in.)	0.064
Characteristic Velocity (ft/sec)	5,180
Effective Specific Heat Ratio	1.18
Reference Specific Impulse[4] (lbf-sec/lbm)	248.0

[1] The amount of ground oxidizer is 35.5 percent.

[2] The amount of unground ammonium perchlorate is fixed at 45 plus or minus 2 percent.

[3] The ratio of HB to ECA is 86.8/13.2.

[4] Chamber pressure = 1,000 psia, optimum expansion to sea level conditions, 15 deg nozzle half angle.

700 psia when tested in a 5 in. CP (TU-131) and 0.332 in./sec at a pressure of 744 psia when tested in the full size motor. The selected formulation utilized a ground oxidizer fraction of 35.5 percent. The percent ground oxidizer selected is lower than normal Minuteman (TP-H1011) propellant (normal 38.0 - 41.0). The lower than normal percent ground oxidizer was expected due to the percent iron contained in the HB polymer.

(U) Data from two verification mixes of the required propellant are summarized in Tables XXXI and XXXII.

(U) 4. ANALYSIS OF DEFECT REPAIRS

(U) During the propellant casting operation in January 1967, folding occurred in the forward segment propellant resulting in numerous randomly oriented voids, details of which are described in Section VIII. Analysis of the effects of these voids upon motor operation indicated that a case burnthrough would result if corrective measures were not taken. A repair plan was initiated by which approximately 20,000 lbm of propellant were removed by a mechanical cutting operation, and propellant was recast into the void to reconstruct the original grain configuration. The propellant removed was formed by an 80 in. dia circular arc cut into the web to a depth of 36 in. and extending from the most forward slot toward the head end for a length of 133 inches. A decrease of approximately 450 lbm of propellant was noted after the repair measure, however, this loss of propellant was not considered to appreciably affect the ballistic performance predictions presented in Table XXVIII.

(U) Due to the vertical movement of the cutting tool and the smaller internal case diameter at the aft end of the case, the propellant could be removed only to within 6 in. of the case wall in the cylindrical section of the case. Some of the larger voids in this area were removed by individually cutting the voids from the propellant. Remaining voids in this area of the grain were not considered detrimental to motor performance.

TABLE XXXI

(U) TP-H1011 BATCH CONTROL DATA
(156-8 Verification Mixes)

Standard Mix No.		Modulus (psi)	Percent Ground Oxidizer	TU-131 r_b (in./sec)	5 In. Strand r_b (in./sec at 1,500 psi)
4696001	86.8	445	31.4	0.289	0.390
4696002	86.8	440	35.5	0.304	0.402

TABLE XXXII

(U) TP-H1011 BATCH CONTROL PHYSICAL PROPERTIES
(156-8 Verification Mixes)

Mix No.	Stress (psi)	Strain (in./in.)	Strain at Max Stress (in./in.)	Modulus (psi)
4696001-1	91	0.46	0.32	433
-2	91	0.44	0.31	436
-3	91	0.44	0.32	440
-4	91	0.43	0.30	453
Average	91	0.44	0.31	440
4696002-1	91	0.41	0.31	442
-2	91	0.39	0.31	437
Average	91	0.40	0.31	440

(C) Results of batch check data obtained from test firing TU-131 motors containing samples of the reloaded propellant portion (Table XXXIII) showed a slightly lower burning rate than the target. The reloaded portion showed a burning rate of 0.321 in./sec at 1,000 psia (scaled up from 0.296 at 682) as compared to 0.326 in./sec at 1,000 psia (scaled up from 0.303 at 701) for the remainder of the propellant in the forward segment. The difference in burning rate was not predicted to affect ballistic performance due to the limited amount of propellant involved (approximately 4 percent of total propellant weight).

(U) D. GRAIN STRESS ANALYSIS

(U) A comprehensive stress analysis of the propellant structure of the 156-8 motor grains was performed. The analysis was based on an axisymmetric, elastic, stiffness matrix method developed at Thiokol and programed for the IBM 7040 computer.

(U) The calculated stress and strain patterns for conditions of cure, thermal shrinkage, and pressurization were calculated and compared to the failure criteria. The failure criteria used was the Smith failure boundary derived from biaxial and uniaxial propellant tests. The analysis showed satisfactory margins between the calculated imposed loads and the failure boundary in all cases.

(U) The grain web thickness of all three segments is 52 percent (as cast) and from fore to aft, the length to diameter ratios are 0.714, 1.37, and 0.693. Since the forward and aft segments have nearly identical geometric constraints, only the former was analyzed. The 156-8 grains are of TP-H1011 propellant, which is also used in the Stage I Minuteman. The loading conditions considered in this study were cure and thermal shrinkage, pressurization, and 1g lateral slump.

(U) In general, the 156-8 studies conducted defined (1) deformations caused by stress inducing loads, and (2) worst stress-strain conditions in the motor compared to the capability limits.

TABLE XXXIII

(C) TU-131 BATCH CHECK DATA, 156-8 FORWARD SEGMENT
(Repair Propellant)

Batch No.			Burning Rate (in./sec)	Pressure (psia)
Sampled Original Mixes	5		0.305	702
	10		0.301	702
	15		0.303	702
	20		0.303	699
		Average	0.303	701
Reloaded Mixes	89		0.299	690
	92		0.294	674
		Average	0.296	682

(U) The grid boundary and the actual grains are not precisely the same, as can be seen by comparing Figures 94 and 95 to Figure 1 . From a structural standpoint, no significant differences will be found.

(U) The cure and thermal shrinkage deformations of the center and dome segments at + 60° F are presented, respectively, in Figures 96 and 97. The worst stress-strain conditions for each of these grains due to the + 60° F soak temperature are tabulated in Table XXXIV along with the 1g lateral slump.

(U) The deformation patterns due to pressure are not significantly different than those shown for the cure and thermal shrinkage as can be seen in Figures 98 and 99. Note that the pressure case was superimposed on the cure and thermal shrinkage deformed grid. The worst stress-strain conditions for each grain pressurized condition are also tabulated in Table XXXIV.

(U) Computation of the failure criteria is very straightforward and requires only superposition of the above tabulated stresses and strains on the proper failure boundary. Figure 100 presents the dilatational failure boundary. Since the failure boundary is independent of path, only the end points for each case are shown. As can be seen in Figure 100, dilatational load conditions do not approach the boundary limit. Figure 100 presents the distortional failure boundary, where pressure effects are considered independently of shrinkage effects. Again, no point reaches the boundary. Finally, the distortional and dilatational effects are accumulated and presented in Figure 100.

(U) As has been seen above in Figure 100, the 156-8 grains do not approach the failure boundary for any specific loading conditions. Further, even the accumulated loading effects do not approach the boundary. To illustrate the excellent structural characteristics of the 156-8 grains, margins of safety were compiled for the various loads (Table XXXV). As can be seen, the least margin is greater than 1.79; hence, it must be assumed that no deleterious propellant structural conditions will occur in the 156-8 motor.

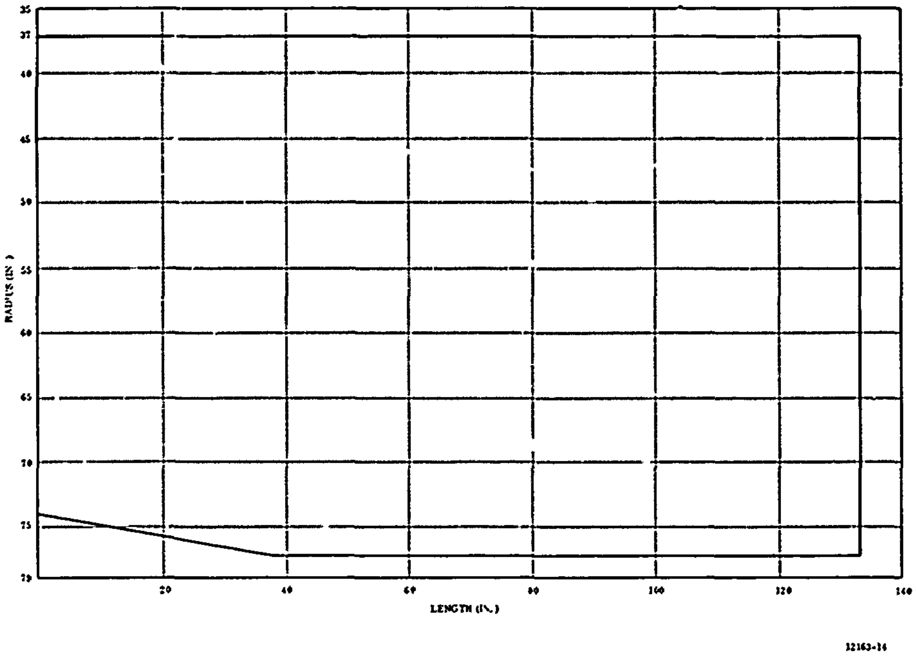

(U) Figure 94. Stress Analysis Grid Boundary of 156-8 Center Segment (Half Grain)

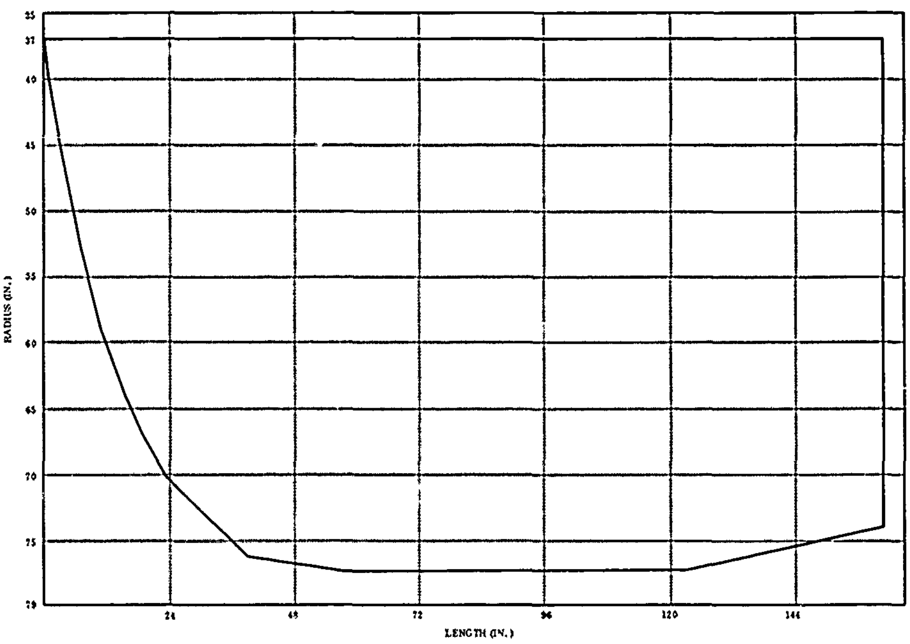

(U) Figure 95. Stress Analysis Grid Boundary of 156-8 Dome Segment Grain

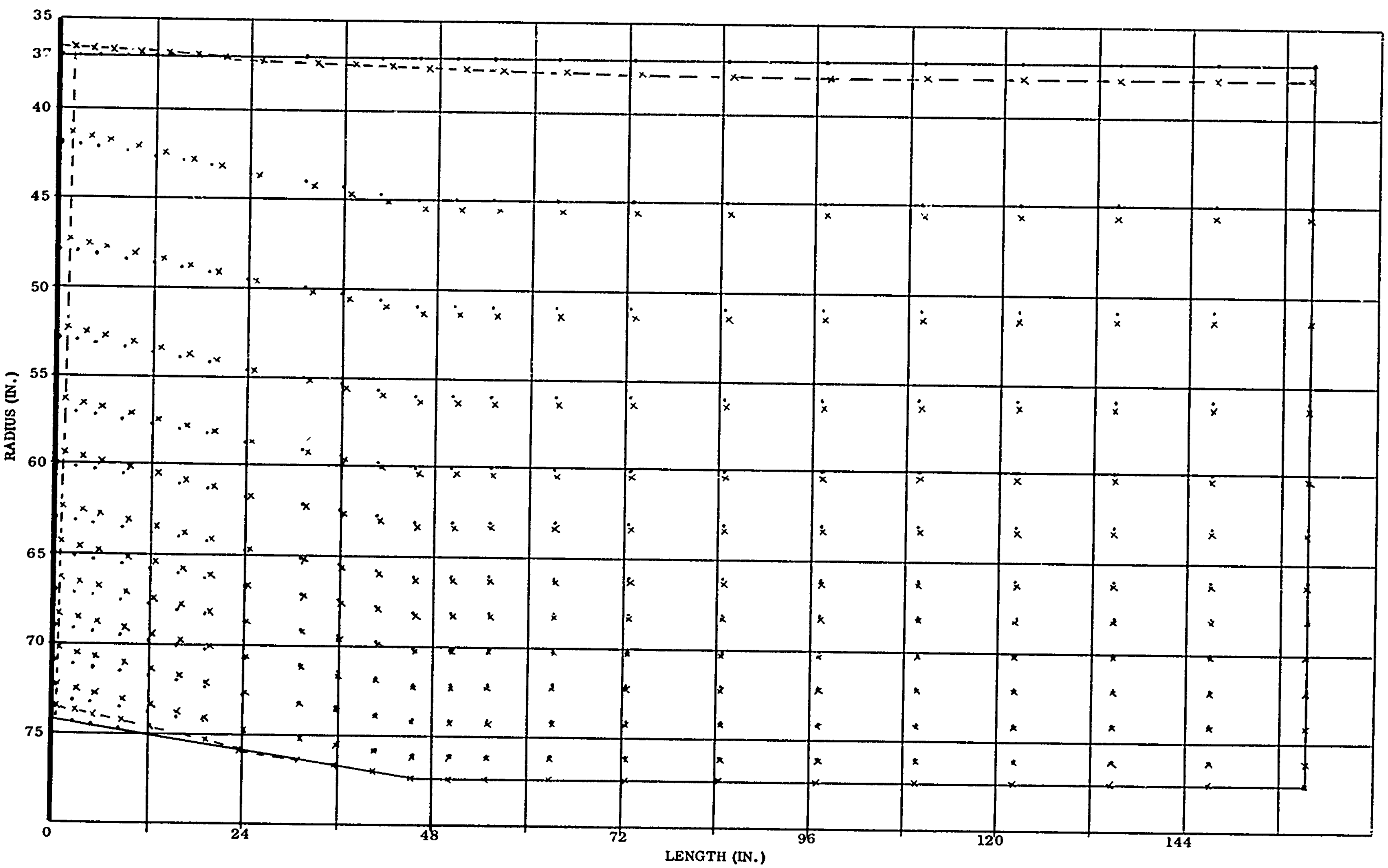

(U) Figure 96. Deformation of 156-8 Center Grain at 60° F

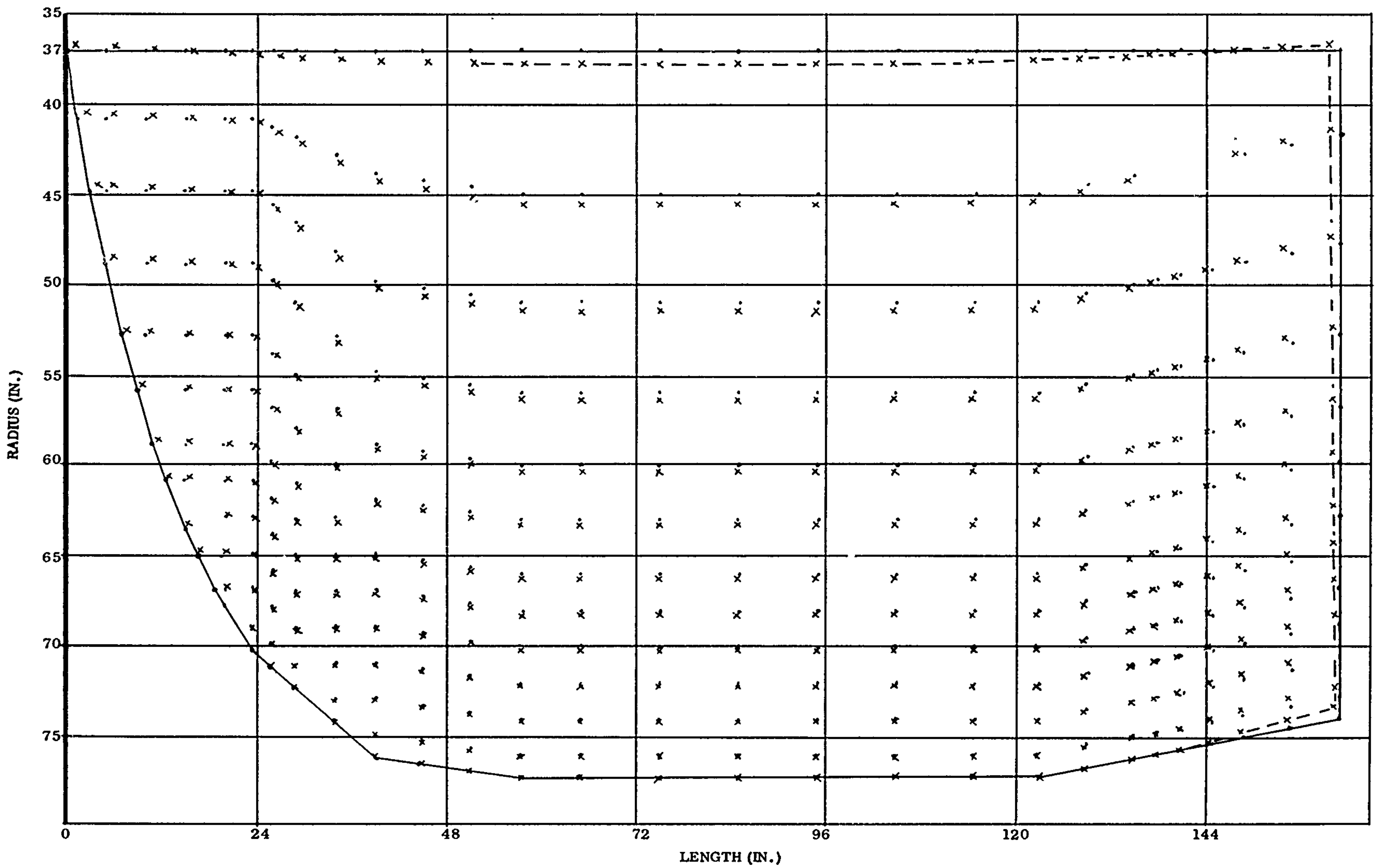

(U) Figure 97. Deformation of 156-8 Forward Dome Grain at 60° F

TABLE XXXIV

(U) WORST STRESS-STRAIN CONDITIONS IN THE 156-8 GRAINS

		Center Segment	Dome Segment
A.	Cure and Thermal Shrinkage (to + 60° F)		
	Inner Bore Hoop Strain (in./in.)	0.027	0.021
	Sum of Principal Stress (psi)	15.8	8.8
	Maximum Principal Strain at Case Interface (in./in.)	0.033	0.031
	Sum of Principal Stress at Case Interface (psi)	20.4	23.0
B.	Lateral Siump (1g)		
	Inner Bore Hoop Strain (in./in.)	0.0222	0.0222
	Sum of Principal Stress (psi)	6.16	6.16
	Maximum Principal Strain at Case Interface (in./in.)	0.002	0.002
	Sum of Principal Stress at Case Interface (psi)	6.66	6.66
C.	Pressure (at 750 psi)		
	Inner Bore Hoop Strain (in./in.)	0.0632	0.0542
	Maximum Deviatoric Stress (psi)	17.0	14.0
	Maximum Principal Strain at Case Interface (in./in.)	0.0565	0.096
	Maximum Deviatoric Stress at Case Interface (psi)	17.5	34.0

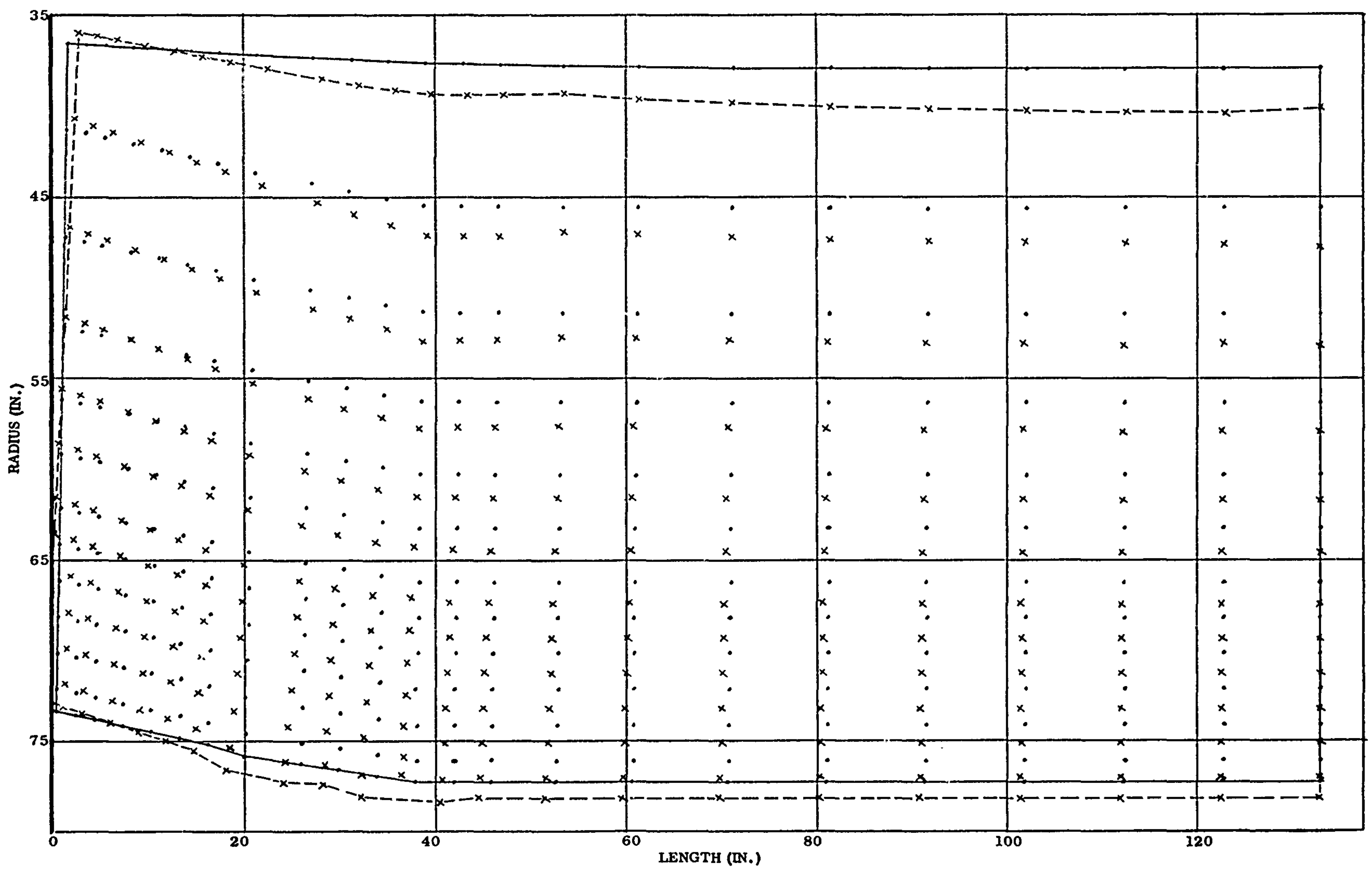

(U) Figure 98. Deformation of 156-8 Center Grain at 750 psi

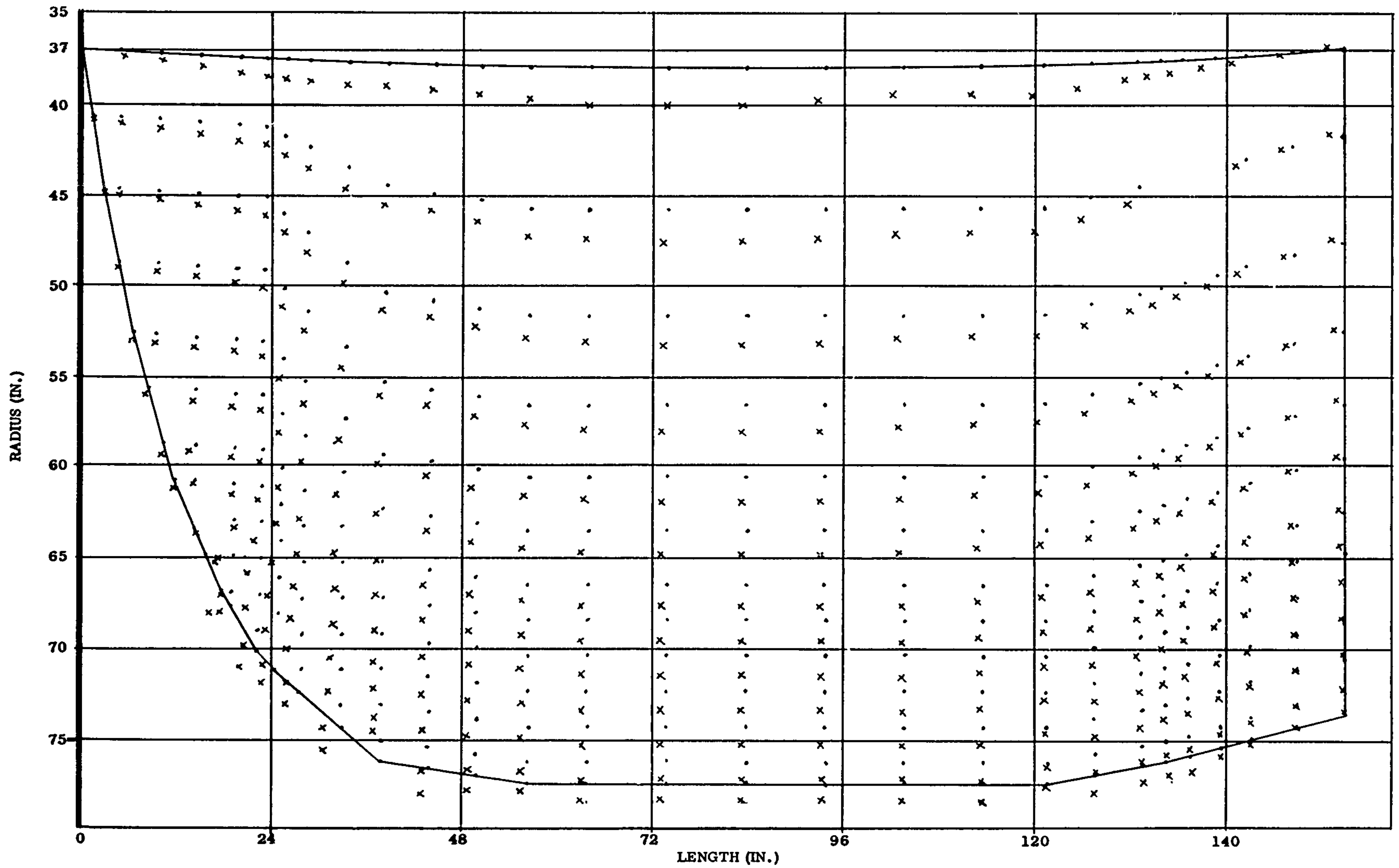

(U) Figure 99. Deformation of 156-8 Forward Dome Grain at 750 psi

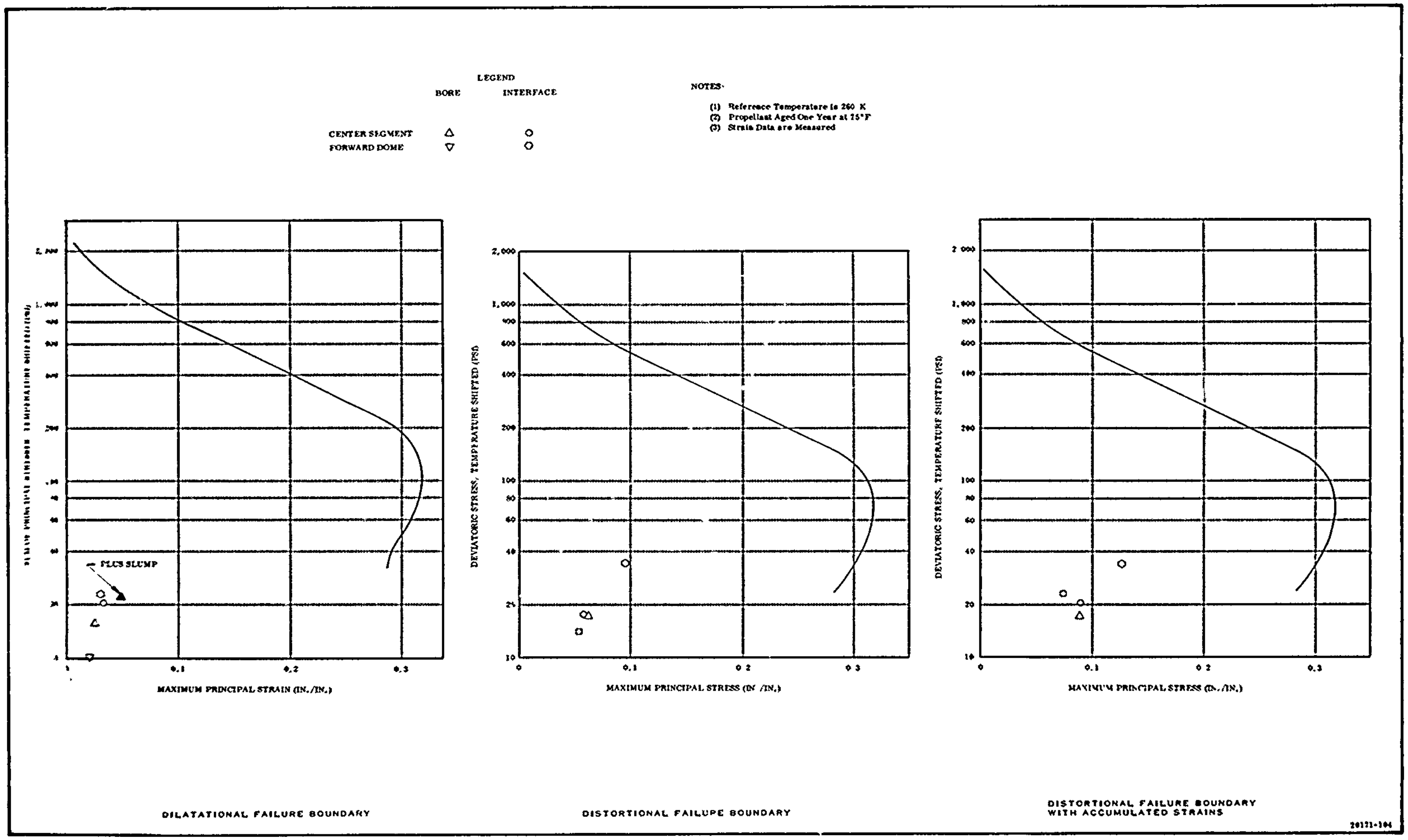

(U) Figure 100. Failure Criteria for 156-8 Grains

TABLE XXXV

(U) SAFETY MARGINS FOR 156-8 LOADING CONDITIONS
(Worst Conditions Only)

Load	Failure Criteria	Maximum Tensile Stress and/or Strain	Propellant Stress/Strain Capability*	Margin of Safety
Cure and Thermal Shrinkage (60° F)	Sum of Principal Stress (psi)	23.0	41.1	1.79
	Maximum Strain (in./in.)	0.033	0.238	7.2
Slump	Sum of Principal Stress (psi)	6.7	41.1	6.13
	Maximum Strain (in./in.)	0.022	0.238	10.8
Cure and Thermal Shrinkage plus Pressurization to 750 psi	Sum of Principal Stress (psi)	34	476	14.0
	Maximum Strain (in./in.)	0.127	0.238	1.875

*Propellant capability has been reduced by 17.6 and 21.8 percent for strain and stress, respectively, which represent the three sigma coefficients of variation for these parameters.

REFERENCES

1. Cook, W. A., "A Finite Element Formulation for Axisymmetric Bodies Having Incompressible and Near Incompressible Materials," TWR-1749, Thiokol Chemical Corporation, Brigham City, Utah. March 1966.

2. Becker, E. B. and Brisbane, J. J., "Application of the Finite Element Method to Stress Analysis of Solid Propellant Rocket Grains," Vol I and II, Report No. S-76 Rohm and Haas Company, Huntsville, Alabama. November 1965.

3. Macbeth, A. W., "Stress Analysis of the TU-465 Propellant Grain Rev A," TWR-1577, Thiokol Chemical Corporation, Brigham City, Utah. 10 Nov 1965.

4. Nelson, J. M., Special Report, "Improvement of the Elastic Analysis Method of Predicting Low Temperature Operation of Capability of Solid Propellant Motors (U)," Thiokol Chemical Corporation - Alpha Division, Huntsville Plant. 27 Nov 1963.

(U) E. LOADED SEGMENT FABRICATION

(U) The loading of the 156-8 segments with TP-H1011 propellant consisted of propellant raw materials preparation, preparation of segment for casting, propellant mixing, and propellant casting.

(U) The ammonium perchlorate oxidizer was prepared in three fractions: special coarse (400 micron), unground (200 micron) and ground (25-30 micron). The oxidizer for the ground fraction was passed through a Mikro-Bud grinder to achieve the 25-30 micron size. The oxidizer was then preweighed for each mix unblended into a "Tote Bin" where it was sealed and stored in a controlled environment.

(U) The premix was prepared by mixing the HB polymer and aluminum. The premix was then preweighed and separated into the proper amounts for each mix.

(U) The TP-H1011 propellant for the 156-8 motor was remotely mixed in a 600 gal. vertical planetary type Baker-Perkins mixer (Figures 101 and 102). The procedure used was to place the premix and curing agent (ECA) into the mixer bowl just prior to mixing. The mixing cycle was then started, the bowl charged with oxidizer and mixed for 50 minutes.

(U) The following number of 6,300 lb mixes was required to complete the casting.

Segment	Number of Mixes
Forward	23
Center	41
Aft	24

(U) After completion of propellant mixing, the mix bowl was transported to a dump station where the propellant was deaerated into two 300 gal. casting cans (Figures 103 and 104). Deaeration was accomplished by pulling the propellant through a slotted plate into the casting can by maintaining a vacuum in the casting can. This process forms the propellant into thin ribbons, allowing the entrapped air to be flashed off as it enters the vacuum chamber in the casting can.

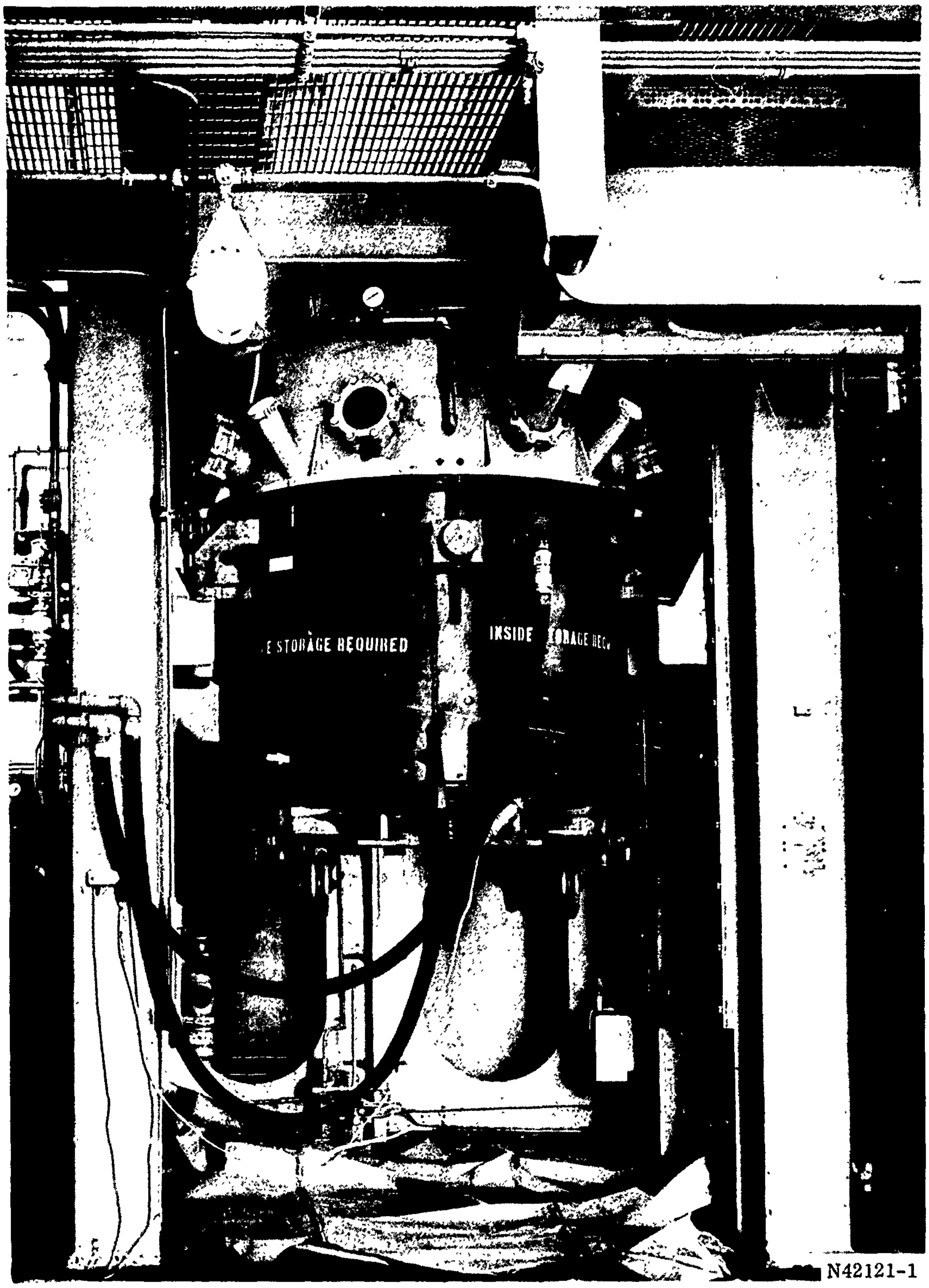

(U) Figure 101. 600-Gal. Mixer (View A)

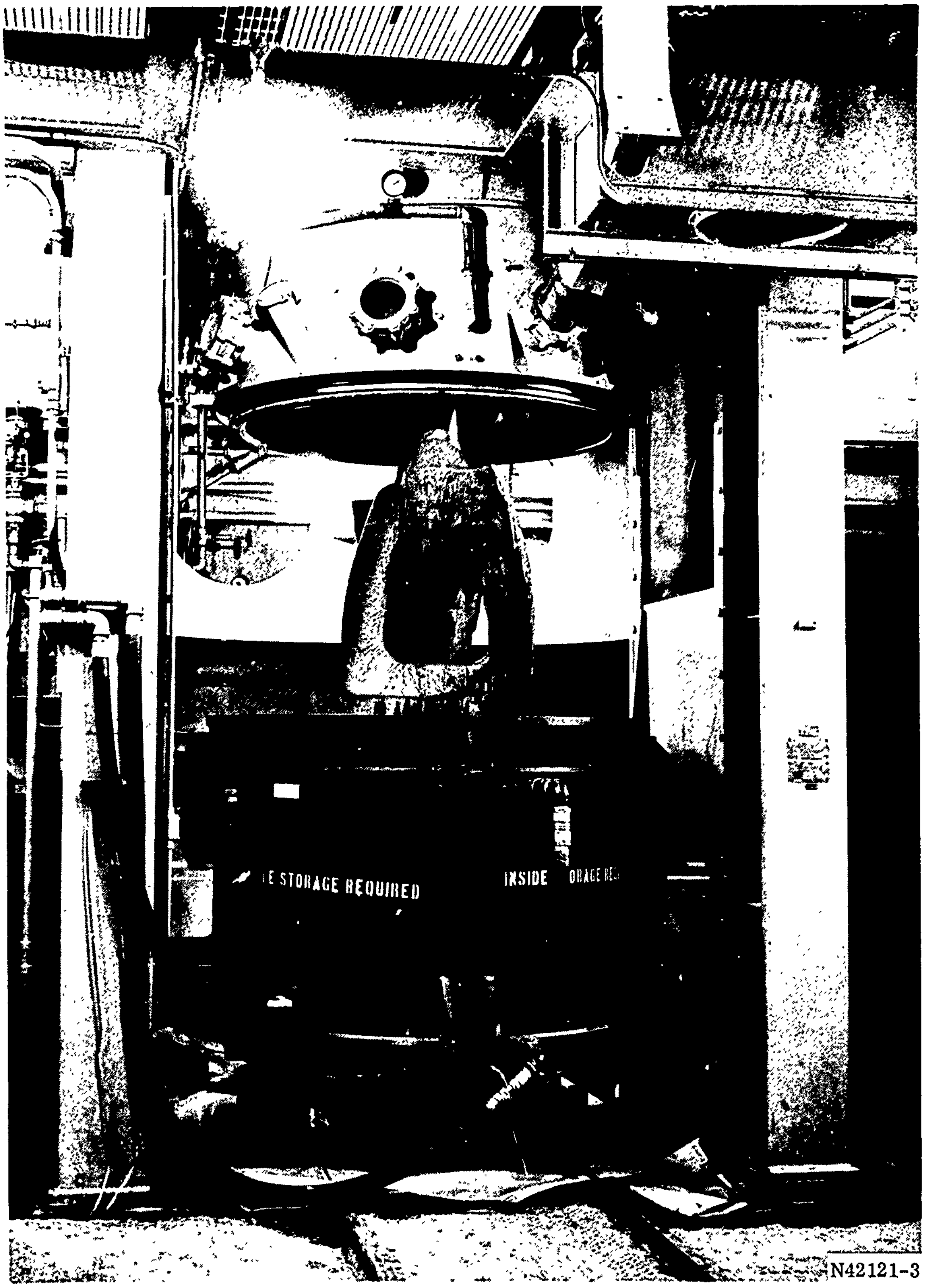

(U) Figure 102. 600-Gal. Mixer (View B)

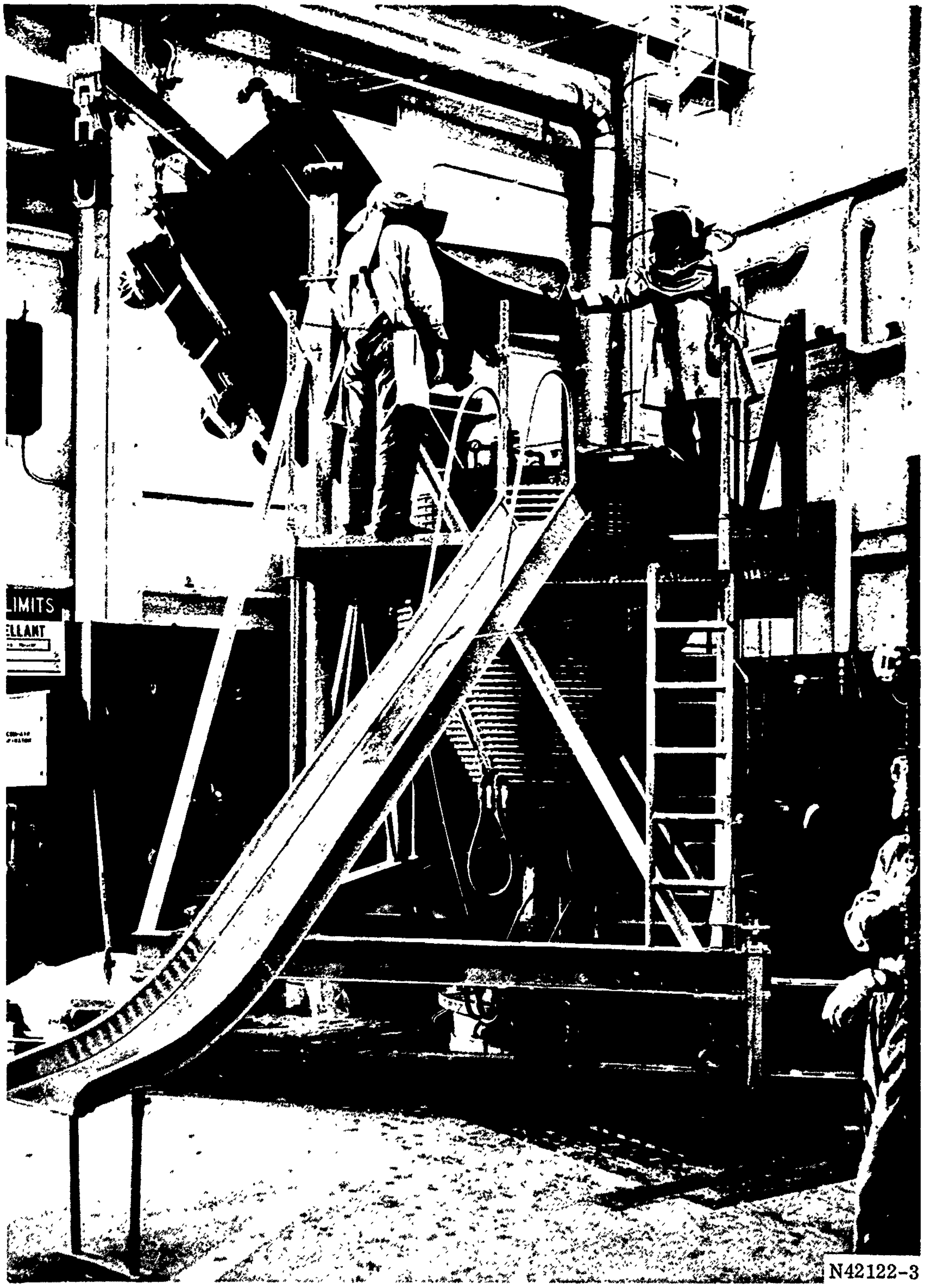

(U) Figure 103. 600-Gal. Mix Bowl Dump Station

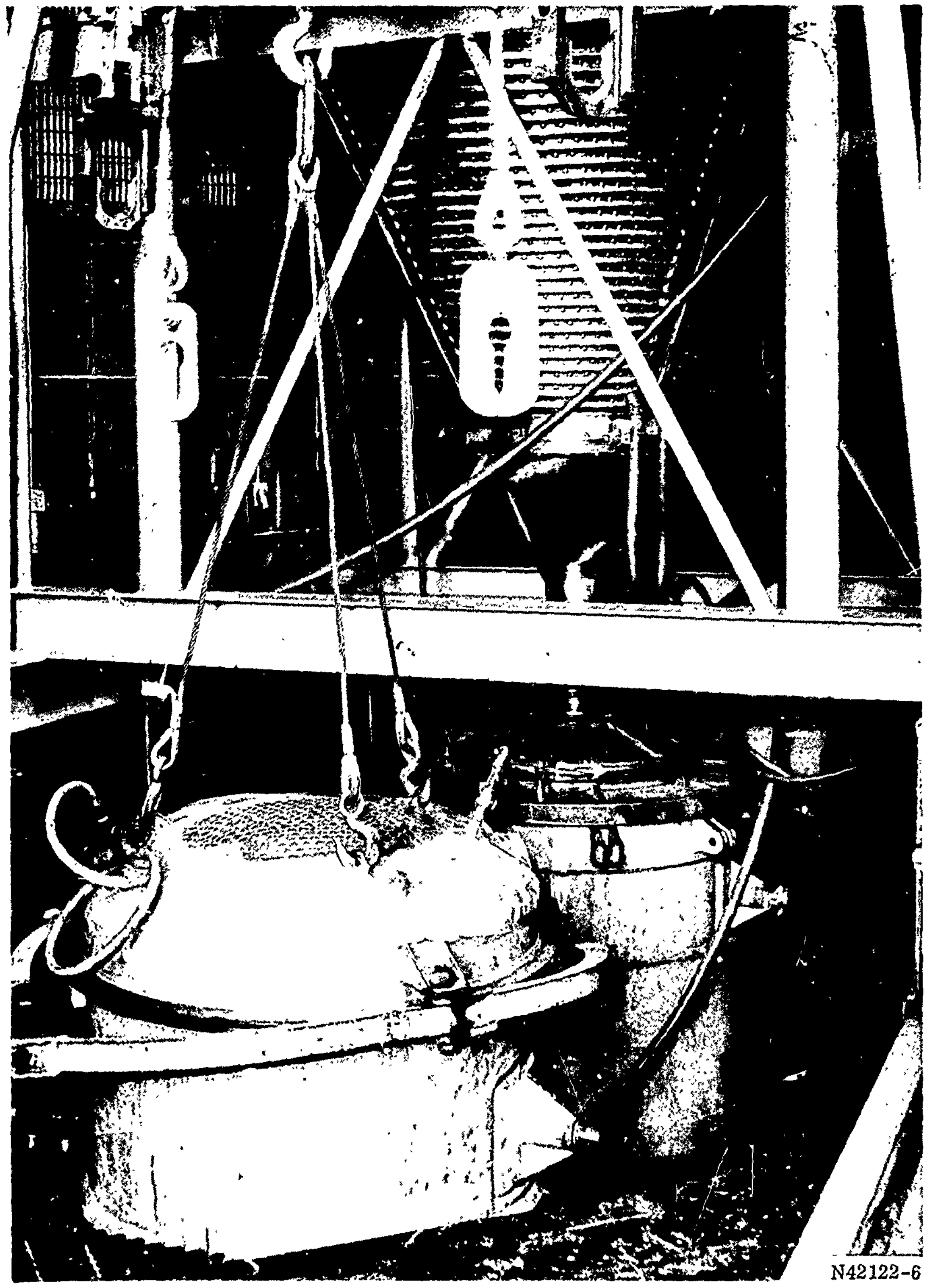

(U) Figure 104. Propellant Deaeration Assembly

(U) The segments were assembled for casting (forward segment per 2U27769, center segment per 2U27770, and aft segment per 2U27771). The forward and aft segments were cast dome end down with the core sealing against forward dome insulation. The center segment was cast aft end down. The aft end was fitted with a flat plate casting dam which sealed the vessel on that end and formed the aft end of the propellant grain. The casting arrangement was preheated to a minimum of 115°F prior to the start of casting.

(U) After being charged with propellant, the casting cans were transported to the casting site and coupled to the casting arrangment. The casting arrangement consisted of two 8 in. flexible hoses connected to a single line containing two hand operated Keystone valves, which were in turn connected to the casting can (Figures 105 and 106). The casting can was then pressurized to maintain the desired flow into the motor. The bayonets were retracted to keep the ends submerged approximately 6 in. below the propellant surface as the propellant surface rose. The propellant was cast to the desired level and hand finished in the uncured state.

(U) During casting of the forward segment, the propellant surface did not rise evenly. The two bayonets entered the motor at approximately 240 and 300 deg locations. This arrangement forced the propellant to flow around the motor (approximately 17 ft) to the 90 deg location. The propellant (due to the long deaeration process and flowing this extensive distance) folded in the 90 deg area. The details of this problem and the details of the resulting defects are covered in Section VIII. As a result of these problems, a duplicate casting arrangement was added for the center and aft segments with the two additional bayonets entering the motor at approximately 70 and 120 deg locations.

(U) The segments were then cured at 135°F for 96 hours.

(U) Following cure the pit heat was shut off, the pit opened, and the blowers turned on to circulate air. The segment was allowed to cool one day prior to core

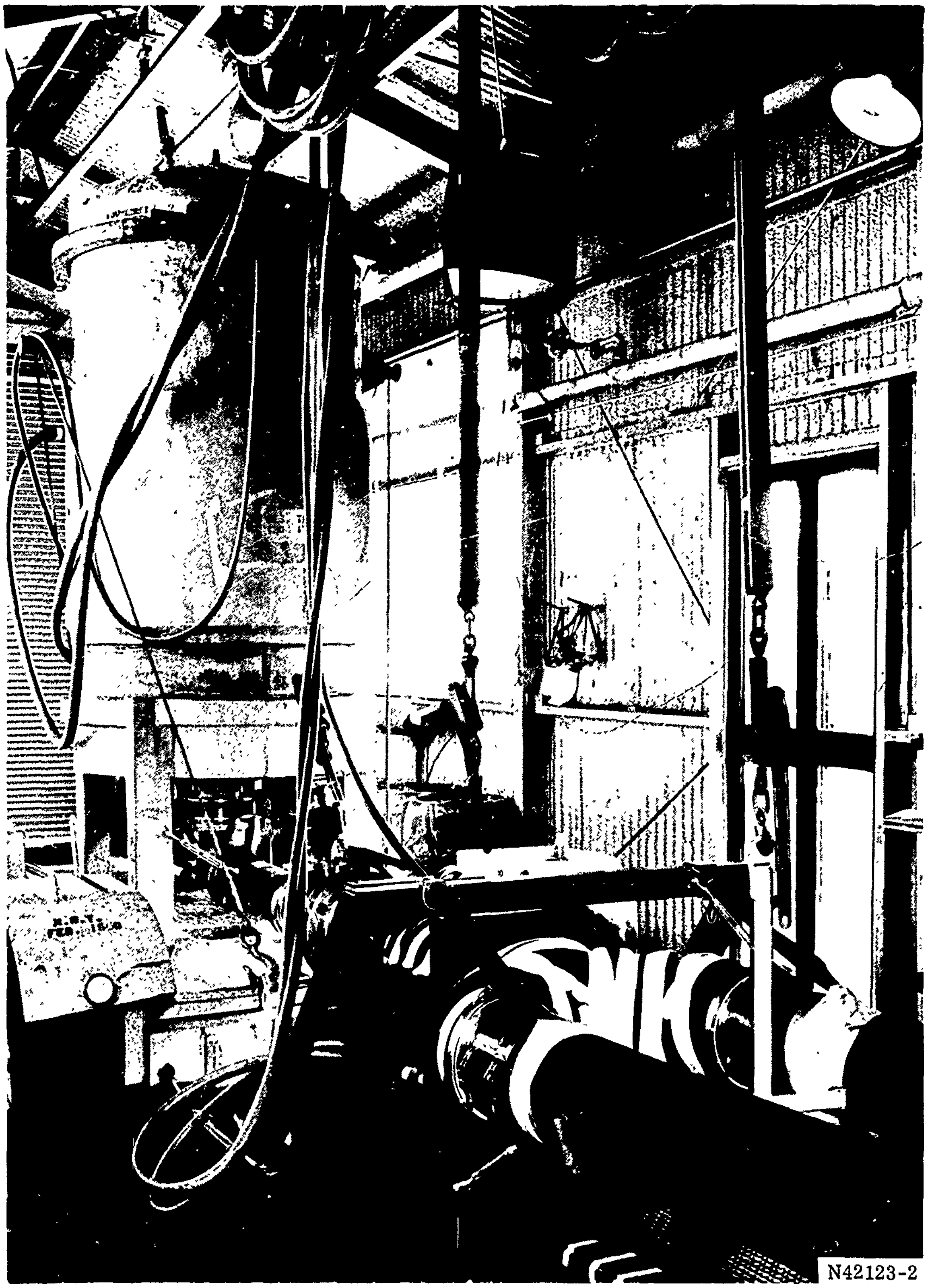

(U) Figure 105. Bayonet Casting Arrangement (View A)

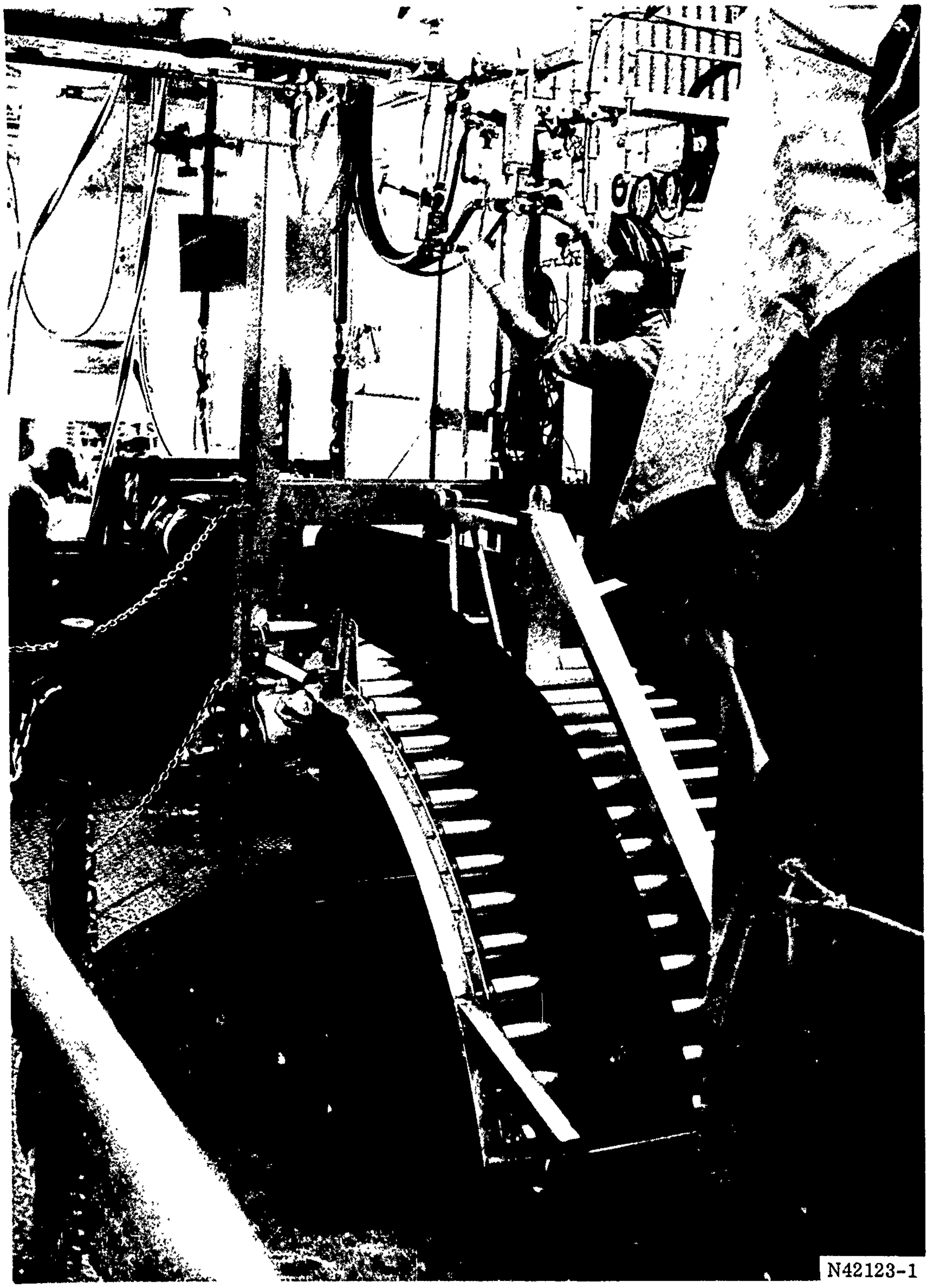

(U) Figure 106. Bayonet Casting Arrangement (View B) pop and removal. The core was popped remotely using a hydraulic jack. The core popping forces required were as follows.

Segment	Force (tons)
Forward	36
Center	45
Aft	28

(U) F. MASS PROPERTIES SUMMARY AND ANALYSIS

(U) The theoretical mass properties based on the motor design are presented in Tables XXXVI thru XXXIX and Figures 107 thru 110. The actual weights throughout the program were measured and accounted for. Table XL shows (1) the design weight as reported in the motor data book, (2) the measured weight of the "as-built" motor, (3) the difference in pounds, and (4) the difference as a percent of the measured weight. The design and measured mass fractions are also reported, and both exceed the minimum requirement of 0.91 specified in the work statement.

(U) None of the differences reported in Table XL are considered discrepant since each could occur without building any part outside of its specified tolerances.

(U) Table XLI shows the effects to the theoretical propellant weight of the known differences between the design reported in the design data book and the "as-built" design. The resulting theoretical weight is then compared with the measured weight, apparently showing the difference to be within the capabilities of the measuring system.

(U) TABLE XXXVI

MASS PROPERTIES DATA

156-8 MOTOR ASSEMBLY MASS PROPERTIES SUMMARY

	WEIGHT (LBS)	CENTER OF GRAVITY LONG.	LAT.	VERT.	MOMENT OF INERTIA PITCH	ROLL	YAW
FORWARD SEGMENT	139925.777	166.043	100.000	100.000	113.340	109.601	113.340
CASE	7182.455	166.846	100.000	100.000	8.759	8.297	8.759
INSULATION	1892.639	156.961	100.000	100.000	2.761	1.859	2.761
LINER	242.710	156.853	100.000	100.000	.260	.279	.260
PROPELLANT	130607.975	166.148	100.000	100.000	101.521	99.166	101.521
CENTER SEGMENT	250862.207	376.575	100.000	100.000	423.245	204.810	423.245
CASE	10410.438	381.502	100.000	100.000	24.189	14.215	24.189
INSULATION	1894.874	371.483	100.000	100.000	6.654	2.241	6.654
LINER	379.653	376.280	100.000	100.000	.718	.481	.718
PROPELLANT	238267.242	376.399	100.000	100.000	391.618	187.872	391.618
AFT SEGMENT	135379.902	584.812	100.000	100.000	106.270	105.646	106.270
CASE	7488.566	599.539	100.000	100.000	9.073	7.891	9.073
INSULATION	2707.143	613.376	100.000	100.000	3.521	2.173	3.521
LINER	233.569	592.606	100.000	100.000	.242	.269	.242
PROPELLANT	124950.626	583.296	100.000	100.000	92.543	95.312	92.543
TOTAL SEGMENT ASSEMBLY	526533.703	374.165	100.000	100.000	3249.569	420.526	3249.569
CASE	25081.459	385.131	100.000	100.000	190.222	30.403	190.222
INSULATION	6404.656	410.334	100.000	100.000	63.838	6.273	63.838
LINER	855.933	373.091	100.000	100.000	6.099	1.030	6.099
PROPELLANT	493825.840	373.141	100.000	100.000	2985.192	382.350	2985.192
CASE SEALANT	16.417	376.074	100.000	100.000	.073	.020	.073
CASE ATTACHMENT PROVISIONS	349.412	373.582	100.000	100.000	1.574	.450	1.574
IGNITION SYSTEM	680.913	84.929	99.999	99.998	.022	.000	.022
IGNITER	657.254	85.328	100.000	100.000	.021	.000	.021
SAFETY AND ARMING DEVICE	4.780	69.301	99.905	99.714	.000	.001	.000
IGNITER ATTACH PROVISIONS	17.282	74.697	100.000	100.000	.000	.001	.000
IGNITER TO CASE SEALANT	1.358	78.819	100.000	100.000	.000	.000	.000
IGNITER TO CASE O RING	.239	75.132	100.000	100.000	.000	.000	.000
TOTAL NOZZLE ASSEMBLY	6501.157	704.982	100.000	100.000	2.035	1.318	2.035
NOZZLE	6211.123	706.440	100.000	100.000	1.932	1.240	1.932
NOZZLE ATTACH PROVISIONS	283.850	673.805	100.000	100.000	.039	.077	.039
NOZZLE TO CASE SEALANT	6.183	671.756	100.000	100.000	.001	.001	.001
TOTAL MOTOR	533715.766	377.826	100.000	100.000	3415.945	421.854	3415.945
MASS FRACTION	.925						

MOMENT OF INERTIA IS IN SLUG-FEET SQUARED DIVIDED BY 1000

(U) TABLE XXXVII

MASS PROPERTIES DATA

156-8 MOTOR ASSEMBLY EXPENDED - UNEXPENDED MASS PROPERTIES SUMMARY

	WEIGHT (LBS)	CENTER OF GRAVITY LONG.	LAT.	VERT.	MOMENT OF INERTIA PITCH	ROLL	YAW
FORWARD SEGMENT	139925.777	166.043	100.000	100.000	113.340	109.601	113.340
CASE - UNEXPENDED	7182.455	166.846	100.000	100.000	8.759	8.297	8.759
INSULATION	1892.639	156.961	100.000	100.000	2.761	1.859	2.761
EXPENDED	336.190	153.683	100.000	100.000	.526	.284	.526
UNEXPENDED	1556.449	157.669	100.000	100.000	2.234	1.575	2.234
LINER	242.710	156.953	100.000	100.000	.260	.279	.260
EXPENDED	136.407	153.378	100.000	100.000	.178	.146	.178
UNEXPENDED	106.302	161.377	100.000	100.000	.082	.133	.082
PROPELLANT	130607.975	166.148	100.000	100.000	101.521	99.166	101.521
EXPENDED PAT*	349.557	159.607	100.000	100.000	.218	.105	.218
EXPENDED DAT*	130212.029	166.169	100.000	100.000	101.267	99.002	101.267
UNEXPENDED EAT*	46.388	155.963	100.000	100.000	.031	.059	.031
CENTER SEGMENT	250862.207	376.575	100.000	100.000	423.245	204.810	423.245
CASE - UNEXPENDED	10410.438	381.502	100.000	100.000	24.189	14.215	24.189
INSULATION	1804.874	371.483	100.000	100.000	6.654	2.241	6.654
EXPENDED	355.628	364.985	100.000	100.000	1.333	.432	1.333
UNEXPENDED	1449.246	373.078	100.000	100.000	5.317	1.808	5.317
LINER	379.653	376.280	100.000	100.000	.718	.481	.718
EXPENDED	105.937	375.498	100.000	100.000	.354	.132	.354
UNEXPENDED	273.717	376.582	100.000	100.000	.364	.350	.364
PROPELLANT	238267.242	376.399	100.000	100.000	391.618	187.872	391.618
EXPENDED PAT	567.729	376.695	100.000	100.000	.796	.170	.796
EXPENDED DAT	237292.137	376.348	100.000	100.000	390.310	187.183	390.310
UNEXPENDED EAT	407.375	405.653	100.000	100.000	.437	.519	.437
AFT SEGMENT	135379.902	584.812	100.000	100.000	106.270	105.645	106.270
CASE - UNEXPENDED	7488.566	599.539	100.000	100.000	9.073	7.891	9.073
INSULATION	2707.143	613.376	100.000	100.000	3.521	2.173	3.521
EXPENDED	917.690	633.928	100.000	100.000	.930	.530	.930
UNEXPENDED	1789.453	602.837	100.000	100.000	2.464	1.643	2.464
LINER	233.569	592.606	100.000	100.000	.242	.269	.242
EXPENDED	121.889	595.934	100.000	100.000	.151	.129	.151
UNEXPENDED	111.680	588.974	100.000	100.000	.090	.140	.090
PROPELLANT	124950.626	583.296	100.000	100.000	92.543	95.312	92.543
EXPENDED PAT	324.944	588.065	100.000	100.000	.182	.097	.182
EXPENDED DAT	124474.675	583.276	100.000	100.000	92.254	95.023	92.254
UNEXPENDED EAT	151.006	590.080	100.000	100.000	.104	.192	.104
TOTAL SEGMENT ASSEMBLY	526533.703	374.165	100.000	100.000	3249.569	420.526	3249.569
CASE - UNEXPENDED	25081.459	385.131	100.000	100.000	190.222	30.403	190.222
INSULATION	6404.656	410.334	100.000	100.000	63.838	6.273	63.838
EXPENDED	1609.508	474.192	100.000	100.000	16.212	1.247	16.212
UNEXPENDED	4795.147	388.990	100.000	100.000	45.734	5.026	45.734

(U) TABLE XXXVII (Cont)

MASS PROPERTIES DATA

156-8 MOTOR ASSEMBLY EXPENDED - UNEXPENDED MASS PROPERTIES SUMMARY

	WEIGHT (LBS)	CENTER OF GRAVITY LONG.	LAT.	VERT.	MOMENT OF INERTIA PITCH	ROLL	YAW
LINER	855.933	373.091	100.000	100.000	6.099	1.030	6.099
EXPENDED	364.234	366.062	100.000	100.000	3.408	.407	3.408
UNEXPENDED	491.699	378.297	100.000	100.000	2.694	.623	2.694
PROPELLANT	493825.840	373.141	100.000	100.000	2985.192	382.350	2985.192
EXPENDED PAT	1242.230	370.898	100.000	100.000	7.876	.372	7.876
EXPENDED DAT	491978.836	373.074	100.000	100.000	2974.643	381.208	2974.643
UNEXPENDED EAT	604.769	432.551	100.000	100.000	2.210	.770	2.210
CASE ATTACHMENT PROVISIONS	365.829	373.634	100.000	100.000	1.648	.469	1.648
HARDWARE - UNEXPENDED	349.412	373.532	100.000	100.000	1.574	.450	1.574
SEALANT	16.417	376.074	100.000	100.000	.073	.020	.073
EXPENDED	1.686	375.190	100.000	100.000	.008	.002	.008
UNEXPENDED	14.732	376.176	100.000	100.000	.066	.018	.066
IGNITION SYSTEM	680.913	84.929	99.999	99.998	.022	.009	.022
IGNITER	657.254	85.328	100.000	100.000	.021	.009	.021
EXPENDED PAT	133.146	91.282	100.000	100.000	.003	.001	.003
EXPENDED DAT	44.748	93.451	100.000	100.000	.001	.001	.001
UNEXPENDED EAT	479.360	82.916	100.000	100.000	.015	.007	.015
SAFETY AND ARMING DEVICE	4.780	69.301	99.905	99.714	.000	.000	.000
IGNITER ATTACH PROVISIONS	18.879	74.990	100.000	100.000	.000	.001	.000
HARDWARE - UNEXPENDED	17.521	74.693	100.000	100.000	.000	.001	.000
SEALANT	1.358	78.819	100.000	100.000	.000	.000	.000
EXPENDED	.481	79.847	100.000	100.000	.000	.000	.000
UNEXPENDED	.878	78.256	100.000	100.000	.000	.000	.000
TOTAL NOZZLE ASSEMBLY	6501.157	704.982	100.000	100.000	2.035	1.318	2.035
NOZZLE	6211.123	706.440	100.000	100.000	1.932	1.240	1.932
EXPENDED	854.896	727.019	100.000	100.000	.247	.177	.247
UNEXPENDED	5356.227	703.155	100.000	100.000	1.594	1.063	1.594
NOZZLE ATTACH PROVISIONS	290.034	673.762	100.000	100.000	.039	.078	.039
HARDWARE - UNEXPENDED	283.850	673.835	100.000	100.000	.039	.077	.039
SEALANT	6.183	671.756	100.000	100.000	.001	.001	.001
EXPENDED	2.952	672.380	100.000	100.000	.000	.000	.000
UNEXPENDED	3.232	671.186	100.000	100.000	.000	.001	.000
TOTAL MOTOR	533715.766	377.826	100.000	100.000	3415.945	421.854	3415.945
EXPENDED PAT	1375.376	343.829	100.000	100.000	9.909	.373	9.909
EXPENDED DAT	494857.328	373.986	100.000	100.000	3021.924	383.042	3021.924
UNEXPENDED EAT	37483.064	429.776	100.000	100.000	360.361	38.438	360.361
MASS FRACTION	.925						

MOMENT OF INERTIA IS IN SLUG-FEET SQUARED DIVIDED BY 1000

*PAT MEANS PRIOR TO ACTION TIME, DAT MEANS DURING ACTION TIME, AND EAT MEANS AT END OF ACTION TIME

(U) TABLE XXXVIII

MASS PROPERTIES DATA

SEQUENTIAL MASS PROPERTIES DATA FOR THE 156-8 MOTOR AT 70 DEGREES F.

	WEIGHT (LBS)	CENTER OF GRAVITY LONG.	LAT.	VERT.	MOMENT OF INERTIA PITCH	ROLL	YAW
1 LAUNCH TIME = 0.00	533715.766	377.826	100.000	100.000	3415.945	421.954	3415.945
2 BEGINNING OF ACTION TIME TIME = 0.62	532340.383	377.914	100.000	100.000	3405.693	421.480	3405.693
3 4 PERCENT TIME = 5.00	513110.059	378.116	100.000	100.000	3297.696	412.502	3297.696
4 20 PERCENT TIME = 24.26	433447.461	379.073	100.000	100.000	2836.775	372.137	2836.775
5 40 PERCENT TIME = 48.52	331349.508	380.717	100.000	100.000	2221.445	311.300	2221.445
6 MAXIMUM THRUST TIME = 50.00	325051.680	380.844	100.000	100.000	2182.792	307.142	2182.792
7 60 PERCENT TIME = 72.78	228040.145	383.777	100.000	100.000	1576.128	234.370	1576.128
8 80 PERCENT TIME = 97.04	127972.268	390.996	100.000	100.000	937.218	141.640	937.218
9 90 PERCENT TIME = 109.17	80609.511	400.927	100.000	100.000	631.784	90.286	631.784
10 END OF ACTION TIME TIME = 121.30	37483.064	429.776	100.000	100.000	360.361	38.438	360.361

(U) TABLE XXXIX

MASS PROPERTIES DATA

SEQUENTIAL MASS PROPERTIES DATA FOR THE 156-8 MOTOR AT 100 DEGREES F.

		WEIGHT (LBS)	CENTER OF GRAVITY LONG.	LAT.	VERT.	MOMENT OF INERTIA PITCH	ROLL	YAW
1	LAUNCH TIME = 0.00	533715.766	377.826	100.000	100.000	3415.945	421.854	3415.945
2	BEGINNING OF ACTION TIME TIME = 0.60	532340.383	377.914	100.000	100.000	3405.693	421.481	3405.693
3	4 PERCENT TIME = 4.85	513110.059	378.116	100.000	100.000	3297.696	412.502	3297.696
4	20 PERCENT TIME = 23.54	433447.461	379.073	100.000	100.000	2836.775	372.137	2836.775
5	40 PERCENT TIME = 47.08	331349.508	380.717	100.000	100.000	2221.445	311.300	2221.445
6	MAXIMUM THRUST TIME = 48.52	325051.680	380.844	100.000	100.000	2182.792	307.142	2182.792
7	60 PERCENT TIME = 70.62	228040.145	383.777	100.000	100.000	1576.128	234.370	1576.128
8	80 PERCENT TIME = 94.16	127972.268	390.996	100.000	100.000	937.218	141.640	937.218
9	90 PERCENT TIME = 105.93	80609.511	400.927	100.000	100.000	631.784	90.286	631.784
10	END OF ACTION TIME TIME = 117.70	37483.064	429.776	100.000	100.000	360.361	38.438	360.361

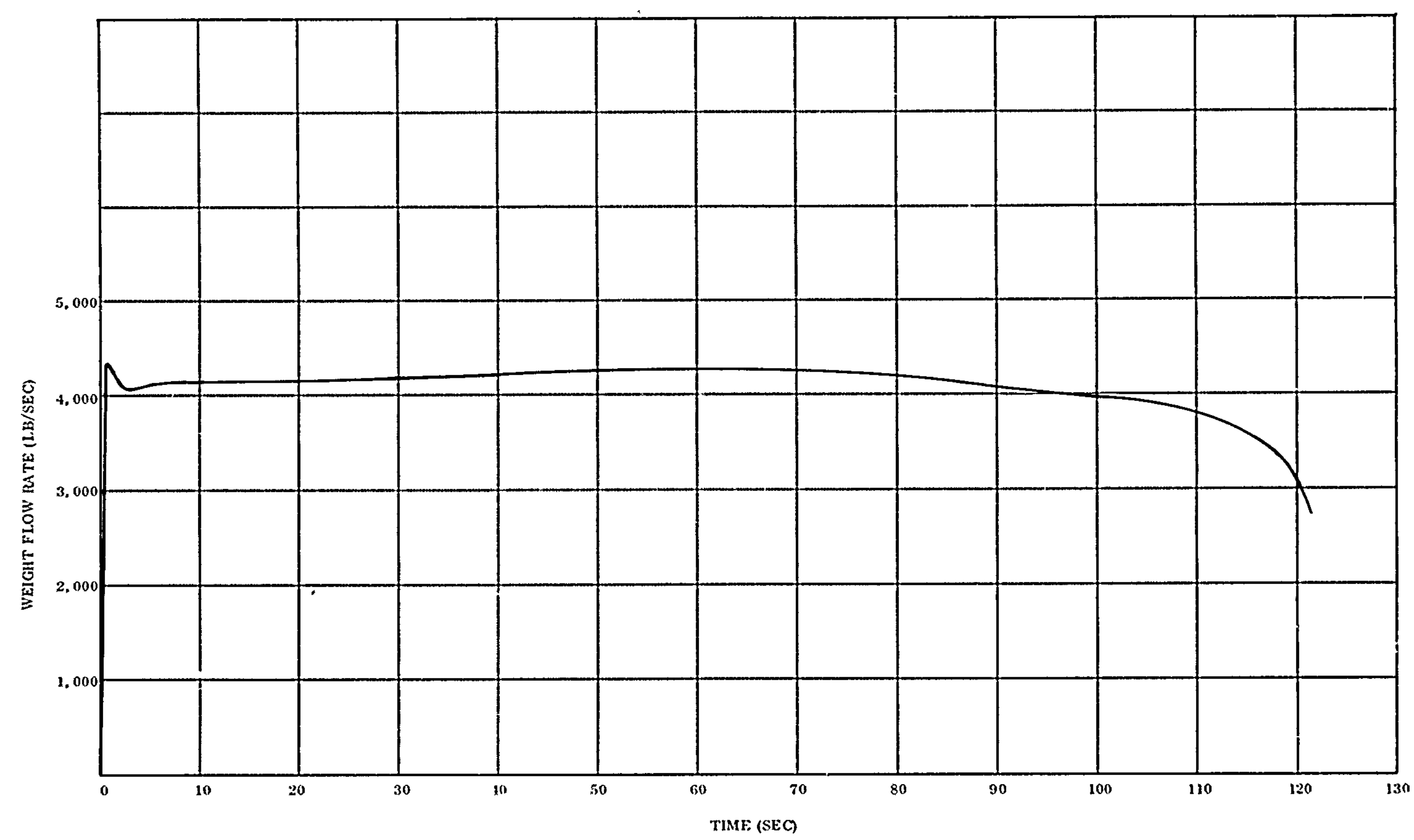

(U) Figure 107. Total Motor Weight Flow Rate vs Time at 70°F

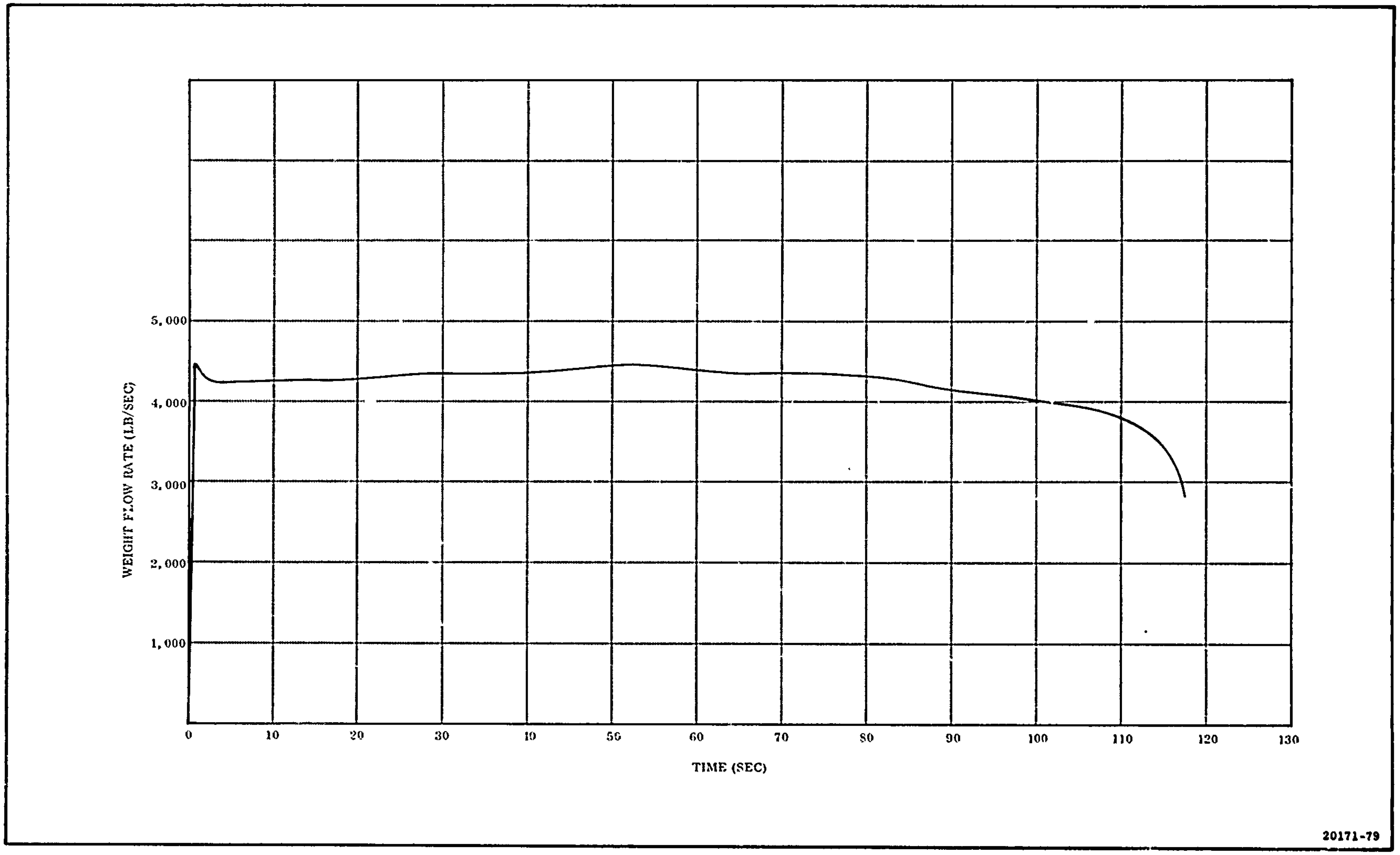

(U) Figure 108. Total Motor Weight Flow Rate vs Time at 100°F

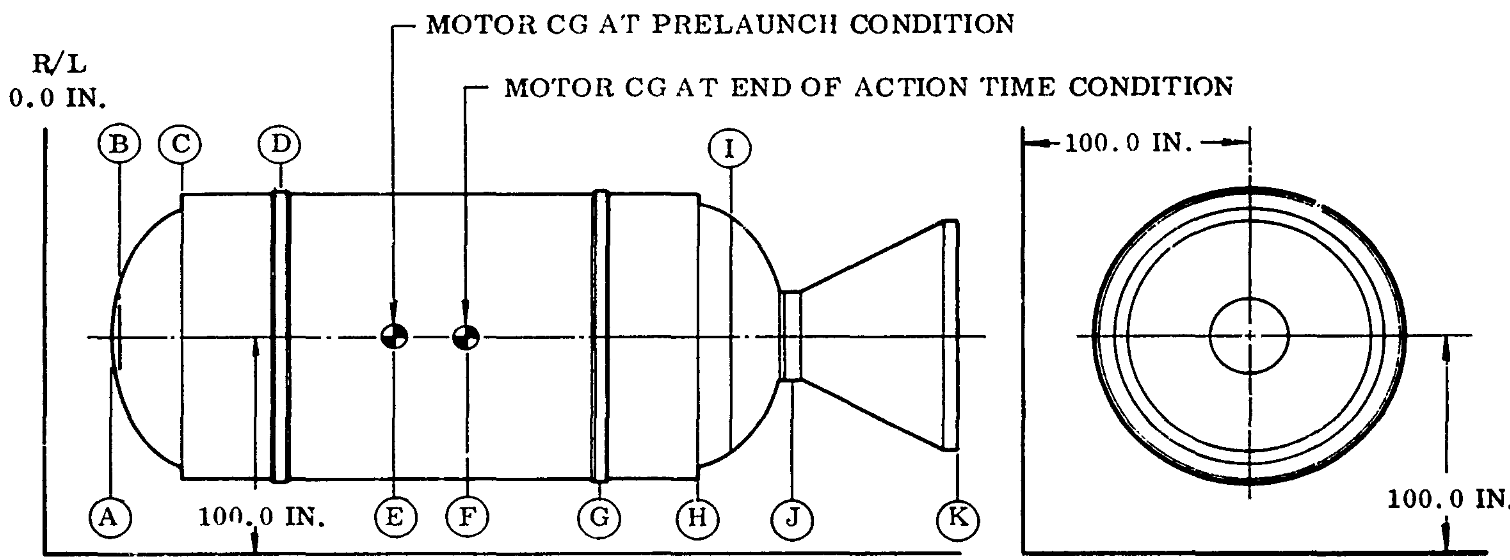

MOTOR STATION		MOTOR STATION	
A	68.238	F	
B	75.029	LONGITUDINAL	429.776
C	100.000	LATERAL	100.000
D	242.810	VERTICAL	100.000
E		G	510.579
LONGITUDINAL	377.848	H	647.670
LATERAL	100.000	I	673.329
VERTICAL	100.000	J	686.240
		K	675.132

20171-77

(U) **Figure 109.** 156-8 Motor Center-of-Gravity Reference System

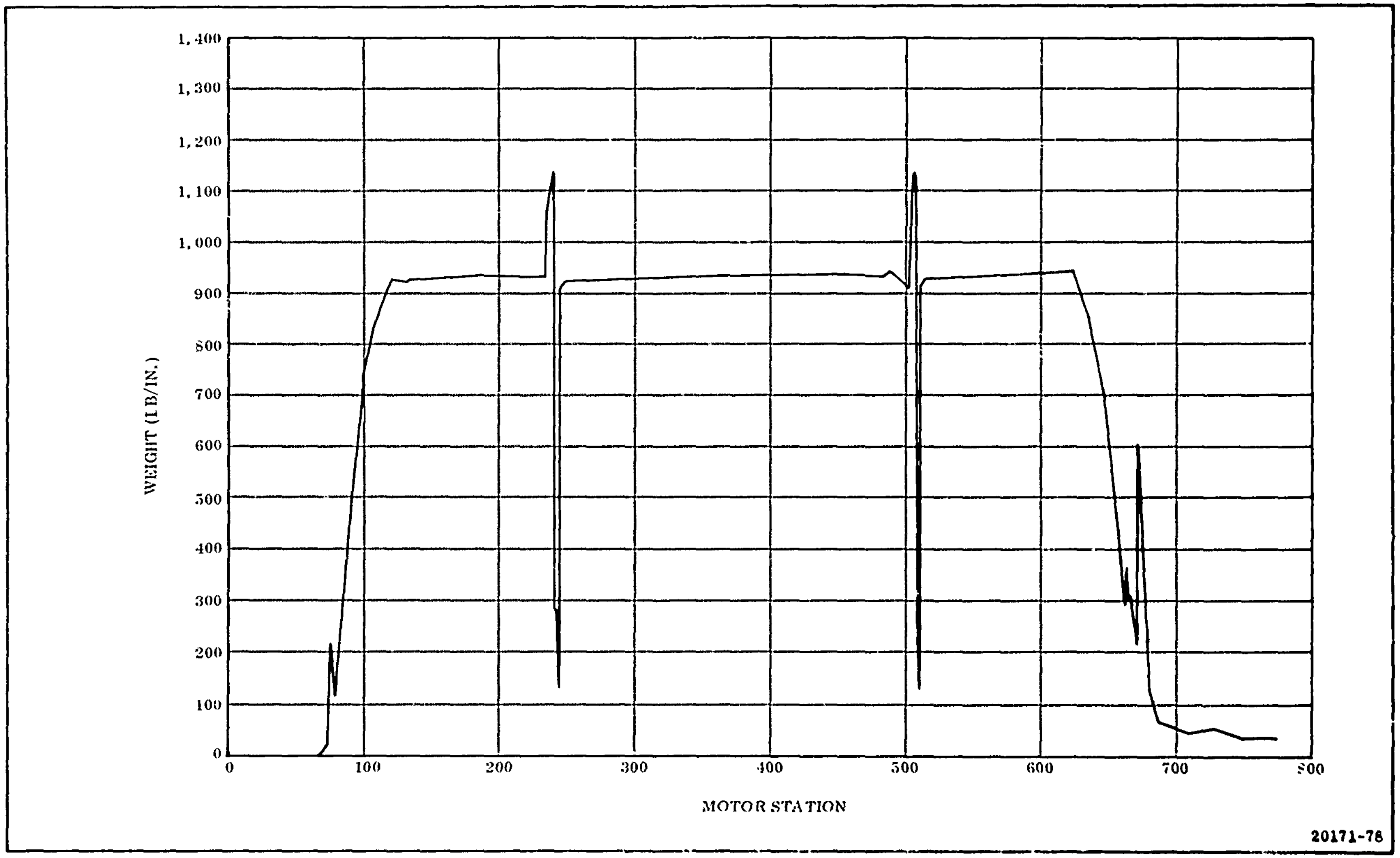

(U) Figure 110. 156-8 Motor Mass Distribution

TABLE XL

(U) 156-8 MOTOR WEIGHT COMPARISON SUMMARY

Component	Weight (lb) Design	Measured	Difference	Difference (percent)
Forward Segment Assembly	139,926	139,252	674	0.48
Case	7,182	7,385	203	2.75
Insulation	1,893	1,686	207	12.28
Liner	219	211	8	3.79
Koropon Primer	24	24*	--	--
Epon 812	--	4	4	--
Propellant	130,608	129,942	666	0.51
Center Segment Assembly	250,862	249,907	955	0.38
Case	10,410	10,137	273	2.69
Insulation	1,805	1,692	113	6.68
Liner	342	359	17	4.74
Koropon Primer	38	38*	--	--
Propellant	238,267	237,681	586	0.25
Aft Segment Assembly	135,380	135,367	13	0.01
Case	7,489	7,572	83	1.10
Insulation	2,707	2,541	166	6.53
Liner	210	235	25	10.64
Koropon Primer	23	23*	--	--
Propellant	124,951	124,996	45	0.04
Total Segment Assembly	526,534	524,912	1,627	0.31
Case	25,081	25,095	14	0.06
Insulation	6,405	5,919	486	8.21
Liner	771	805	34	4.22
Koropon Primer	85	85*	--	--
Epon	--	4	4	--
Propellant	493,826	492,619	1,207	0.25
Segment Assembly Provisions	366	389	23	5.91
Ignition System	681	705	24	3.40
Igniter	657	683	26	3.81
Safety and Arming Device	5	5	0	0
Igniter Attach Provisions	19	17	2	11.8
Nozzle Assembly	6,501	6,176	325	5.26
Nozzle	6,211	6,100	111	1.82
Nozzle Attach Provisions	290	76	214	281.58
Total Motor	533,716	531,793	1,923	0.36
Mass Fraction	0.925	0.926**	0.001	0.11

*Theoretical Weight
**Work Statement Required Minimum Mass Fraction is 0.91.

TABLE XLI

(U) PROPELLANT DESIGN ADJUSTMENTS REFLECTING MOTOR "AS-BUILT" CONDITION

Item	Forward Segment (lb)	Center Segment (lb)	Aft Segment (lb)
Design Propellant	130,608	238,267	124,951
Actual Density Correction	-245	-446	-234
Actual Liner Correction	+14	-30	-43
Actual Insulation Correction	+281	+154	+227
Actual Slot Length Correction	-439	N/A*	N/A*
Propellant Removed to Allow Core to be Reinstalled	-10	0	0
Propellant Repair Bonding Material	-7	0	0
Adjusted Design Propellant	130,202	237,945	124,901
Measured Propellant	129,942	237,681	124,996
Difference	-260	-264	+95
Difference (percent of measured weight)	0.20	0.11	0.08

*N/A means slot measurements not available.

SECTION VIII

(U) FORWARD SEGMENT CASTING PROBLEM

(U) A. CASTING PROBLEM

(U) During casting of the 13th mix into the forward segment a folding condition appeared from approximately the 45 to 135 deg positions. Figure 111 exhibits how the lowest portion and deepest folds centered at exactly the 90 deg position. This is the point of farthest flow where the propellant met as it flowed around from the two bayonets at the 300 and 240 deg locations. The low point at 90 deg was actually 16 in. below the propellant level near the bayonets. It was evident that the propellant in this area had a high viscosity. Temperature measurements indicated the propellant was 135 to 140°F, thus the high viscosity probably resulted from partial curing, not low temperature.

(U) The propellant flow into the segment raised the surface in the area near the bayonets. The propellant from each mix did not flow around the core as anticipated. Apparently, propellant from the earlier mixes, which had started to cure, was forced or displaced upward in the 45 to 135 deg area.

(U) The distance from the bayonets to the 90 deg position was 17 ft at the outer periphery. This apparently was too far considering the propellant had a higher than normal viscosity due to abnormally longer deaeration cycle and casting through long bayonets.

(U) When the folding condition was noticed, arrangements were immediately made to cast from a single 6 in. bayonet at the 90 deg location. The existing bayonets were raised to the propellant surface in an attempt to allow the propellant flow across the surface rather than down into the cast propellant.

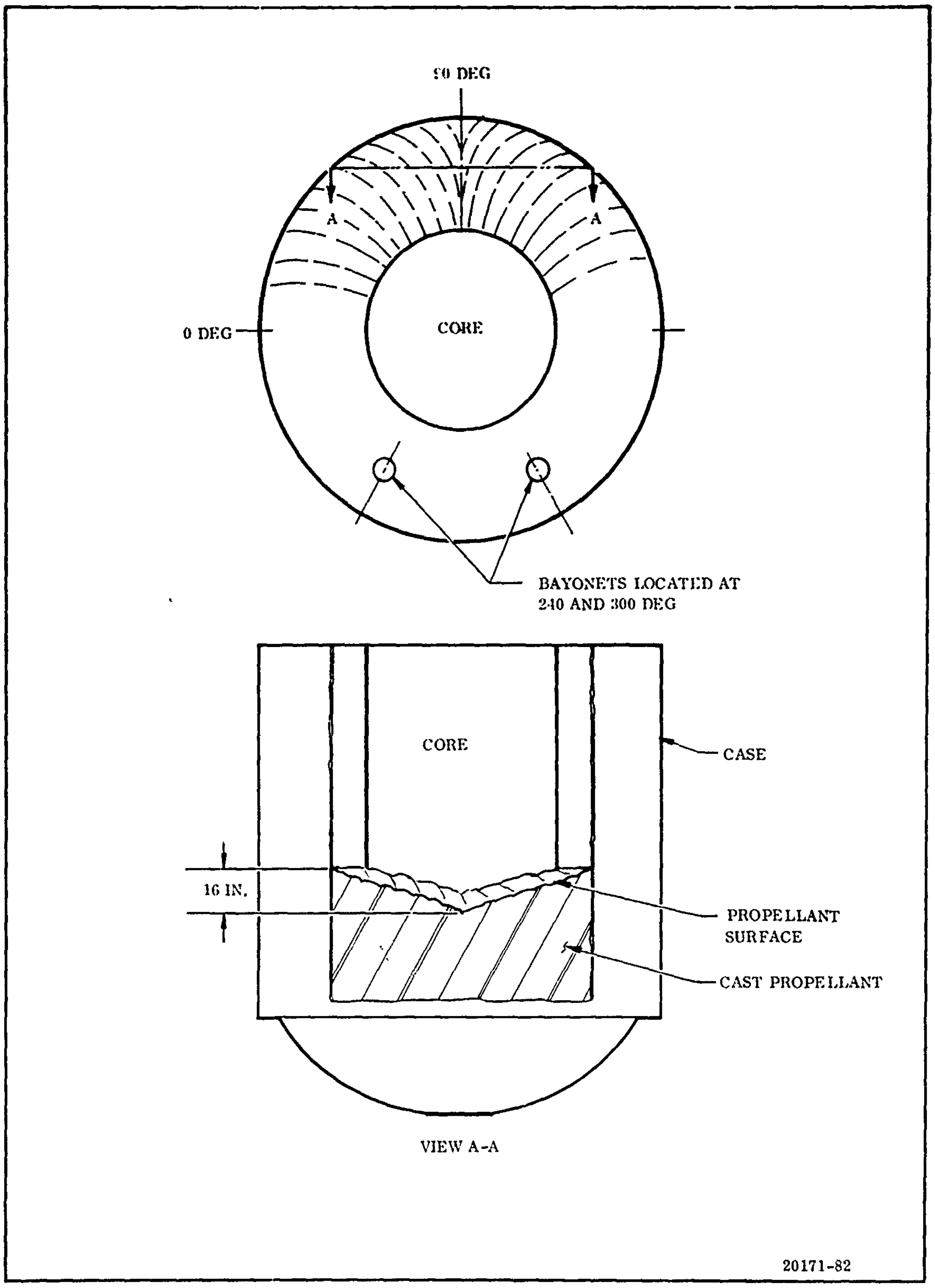

(U) Figure 111. Schematic of Propellant Folding Condition in Forward Segment

(U) As the 13th and 14th mixes were cast, the propellant near the 90 deg location actually appeared to fracture and then to melt, and the folds and fractures appeared to heal and flow together.

(U) During the 15th mix, propellant from the two 8 in. bayonets flowed over the still somewhat rough surface of the folded area. At this same time casting was started from the single bayonet. This propellant appeared to flow into all folds without air entrapment except against the case wall where one fold appeared to entrap air. The resulting void in this area would not be highly detrimental to the motor since it would not be exposed until burnout.

(U) Casting of the segment was continued and completed without further recurrence of folding.

(U) B. INSPECTION

(U) Upon removal of the core from the cured grain, the propellant surface of the core cavity was inspected. Flowlines having small long angular surface voids were observed. The flowline and surface voids farthest aft corresponded exactly in shape and position to the folded propellant surface as it existed in the 13-14-15 mix casting. Two other less prominent flowlines were evident farther forward in the segment (lower as cast). These flowlines aroused suspicion that folding had occurred prior to casting the 13th mix. The segment had been covered during casting with periodic inspections of the propellant surface. Folding could have been covered by low viscosity propellant flowing over the top of the surface during the time between inspections.

(U) The flowlines and voids were concentrated at the 45 to 135 deg area with one very minor flowline at the 270 deg location.

(U) The flowlines were hand trimmed and the void cut out until a complete knitting of the propellant was noted (Figure 112). The deepest void was 3-7/8 inches. It was a small angular hole varying in cross sectional area as it progressed into the propellant. It should be noted that in Figure 112 there are many longitudinal lines caused by wrinkling of the polyethylene core cover. These shallow and rounded lines were not considered detrimental to the motor.

(U) Based on the above events and findings it was decided to radiographically inspect the forward segment grain although radiography of grains was not planned in the program. The first set of X-rays was taken at the 90 deg location with the segment in the horizontal position. Since the segment could not be handled in the X-ray facility, it was positioned on the large motor transporter in front of the door such that it was positioned 40 ft from the Arco 8 mev, 1,000 Rankins/minute radiographic linear accelerometer. Two rows each of Kodak AA and T film were placed in the core cavity to account for variations in the propellant thickness. The two rows of film were exposed simultaneously to a 2.0 H & D nominal density at a source to film distance of 40 feet.

(U) A 1-1 T penetrometer demonstrated a 0.7 percent radiographic sensitivity on each exposure. The X-ray films gave excellent resolution. Many angular voids were evident in the area of the folding observed in mixes 13, 14, and 15 (160 to 170 in. from the aft grain surface). Also voids were evident further forward in the segment to 126 in. from the aft grain surface. These voids were concentrated in areas which corresponded to the previously noted surface defects.

(U) The segment was then inspected in the vertical position, taking shots at 45, 135 and 270 degrees. The X-rays taken at 270 deg revealed only one 1/2 in. diameter circular void; those at 45 and 135 deg substantiated those at 90 degrees. The radiographs also indicated that the voids decreased in number and size in relation to distance from the 90 deg location. Most voids were impossible to triangulate because of the irregular shape of the voids, thickness of propellant, and distance of the source from the film. However, one void was identifiable in two views and is shown in Figure 113.

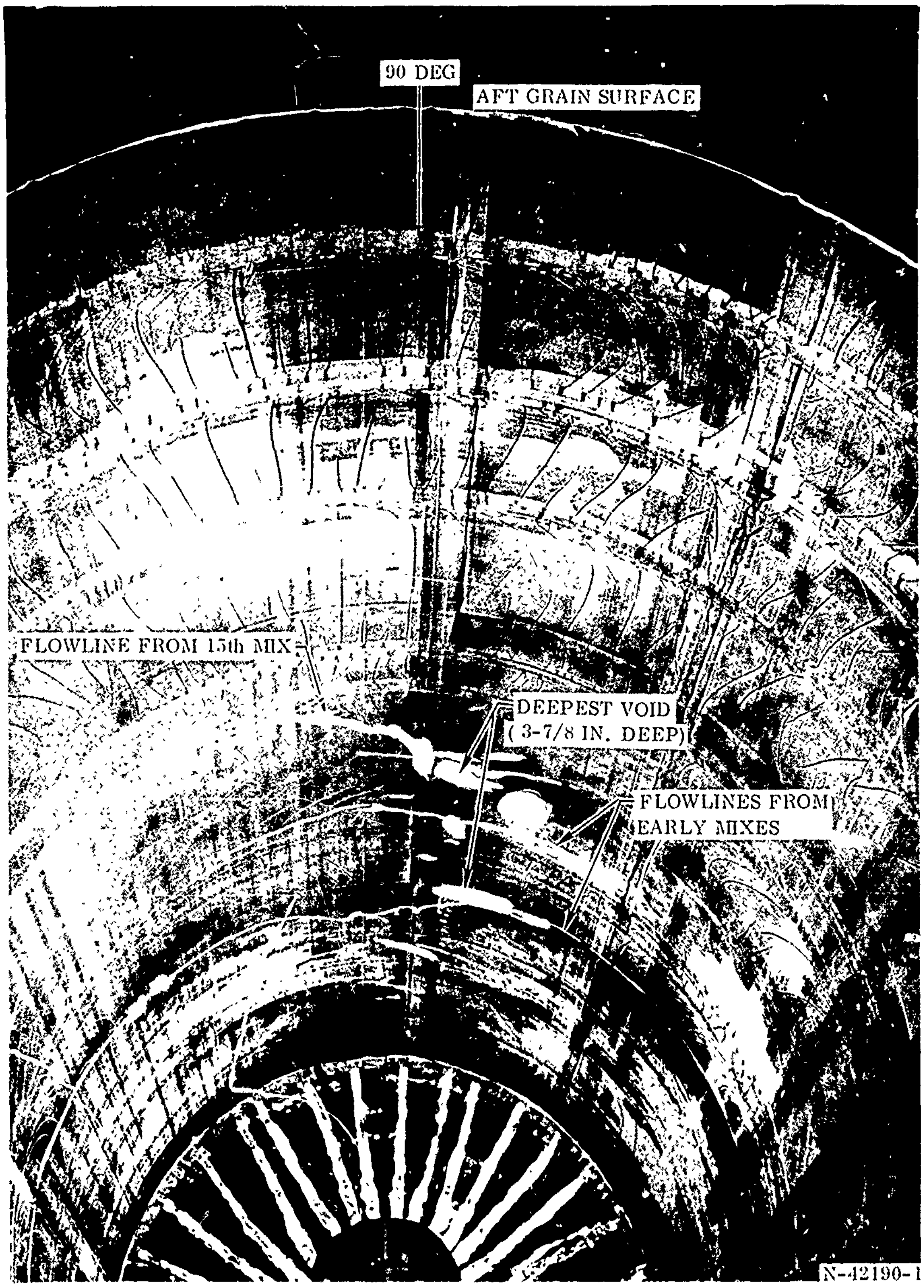

(U) Figure 112. Propellant Surface of Core Cavity Showing Trimmed Flowlines

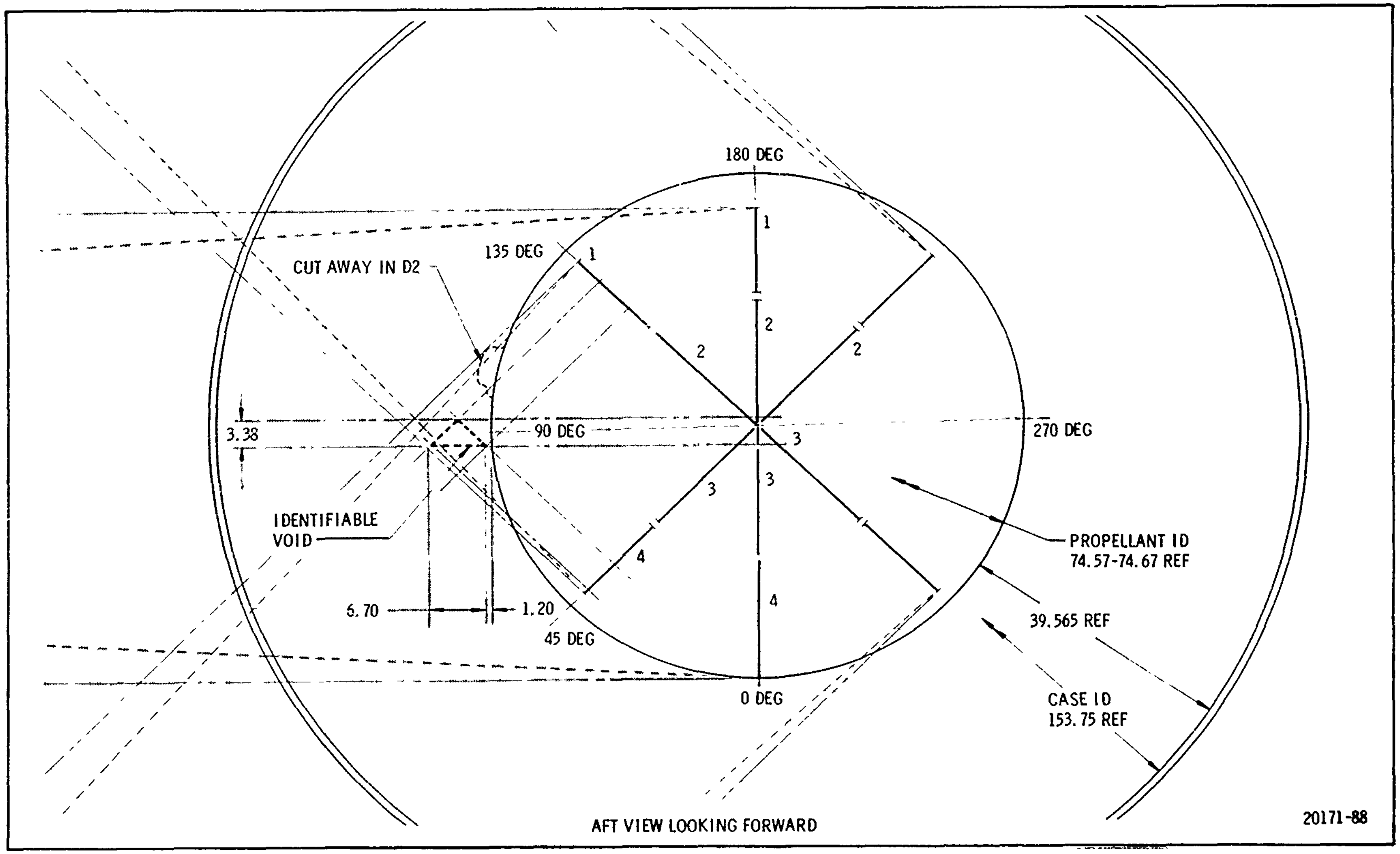

(U) Figure 113. X-ray Triangulation, 156-8 Forward Segment

(U) The nature of the voids and fold prompted the conclusion that a flame path could occur in which the case wall could be exposed prematurely and result in a burnthrough. It was also concluded that pressure would not likely rise significantly due to increased burning surface in the void area.

(U) Studies were then conducted to determine the best method of rework. The two prime considerations were:

1. Cut out the defect area and recast with propellant.
2. Inhibit the 90 deg area on the core cavity.

These studies indicated that propellant removal and recast was the most feasible since inhibition of the grain posed problems of case heating during a long tailoff and of the possibility of the inhibitor burning off and momentarily plugging the nozzle.

(U) C. TESTING

(U) The major concern of the grain repair was achieving a bond between the existing propellant and the recast propellant. A study was conducted to determine how to achieve a bond between the new propellant to be cast and the existing propellant. Thiokol had used Epon 812 to cast live grains against inert grains and also to activate partially cured propellant surfaces when long casting delays had occurred in previous large motors. Also, UF-2121 liner was considered as a candidate.

(U) A series of tests were conducted by cutting loaf samples cast from the mixes used in the 156-8 forward segment. Two types of cut surfaces were evaluated, wire cut and knife cut. The cut surfaces were treated with UF-2121 liner and Epon 812. New TP-H1011 propellant was then cast onto the surface and cured. Dogbone tensile samples were then cut across the interface and tested. The results indicated a superior bond using Epon 812 on a knife cut surface. In these samples no failures occurred in the interface. All failures occurred in the old propellant, which had a lower modulus. It was therefore concluded that a knife cut should be used to remove the propellant and the surface should be activated with Epon 812 prior to casting.

(U) D. PROPELLANT REMOVAL

(U) The propellant was removed by making a circular cut from the aft end of the propellant grain and progressing along the longitudinal axis through the void area in accordance with Figure 114. The longitudinal cut was made with the segment in the vertical position. There were known voids outside of this area next to the case wall. However, these voids would be exposed only at tailoff and would result in only a few seconds premature exposure of the liner and bladder. Machine cutting exactly to the case wall would be risky and very expensive. It was therefore concluded to leave these voids when unexposed.

(U) The cut was made with a modified Minuteman cutback machine (WTAB1001) attached to a tripod. The tripod consisted of three "H" beams welded together. The tripod was bolted to a framework arrangement and secured to the aft harness ring in three places. The tripod had bolt holes and could be lowered in 6 in. increments. Figure 115 shows the cutback machine in position prior to starting the cutting operation.

(U) The cutback machine was powered by two air motors, one turning the shaft and cutting blade, and one to raise and lower the shaft. The shaft had a vertical travel of 18 in. and was geared to make a 1/12 in. cut per revolution. The machine had dual controls with an interlock system so it could be operated remotely.

(U) The cutting blade had a long arm with a short cutting edge and a short arm with a long cutting edge to balance torque. The trailing edges of the cutting blades had scoops to push the 1/12 in. thick propellant slices into the scrap catcher (Figure 116) in the core cavity. The end of the cutting blade making the outer periphery cut was curved with a 2 in. radius to eliminate the stress rising effect of a sharp corner in the cutout cavity.

(U) All machine cutting operations were conducted remotely and monitored by television and audio systems.

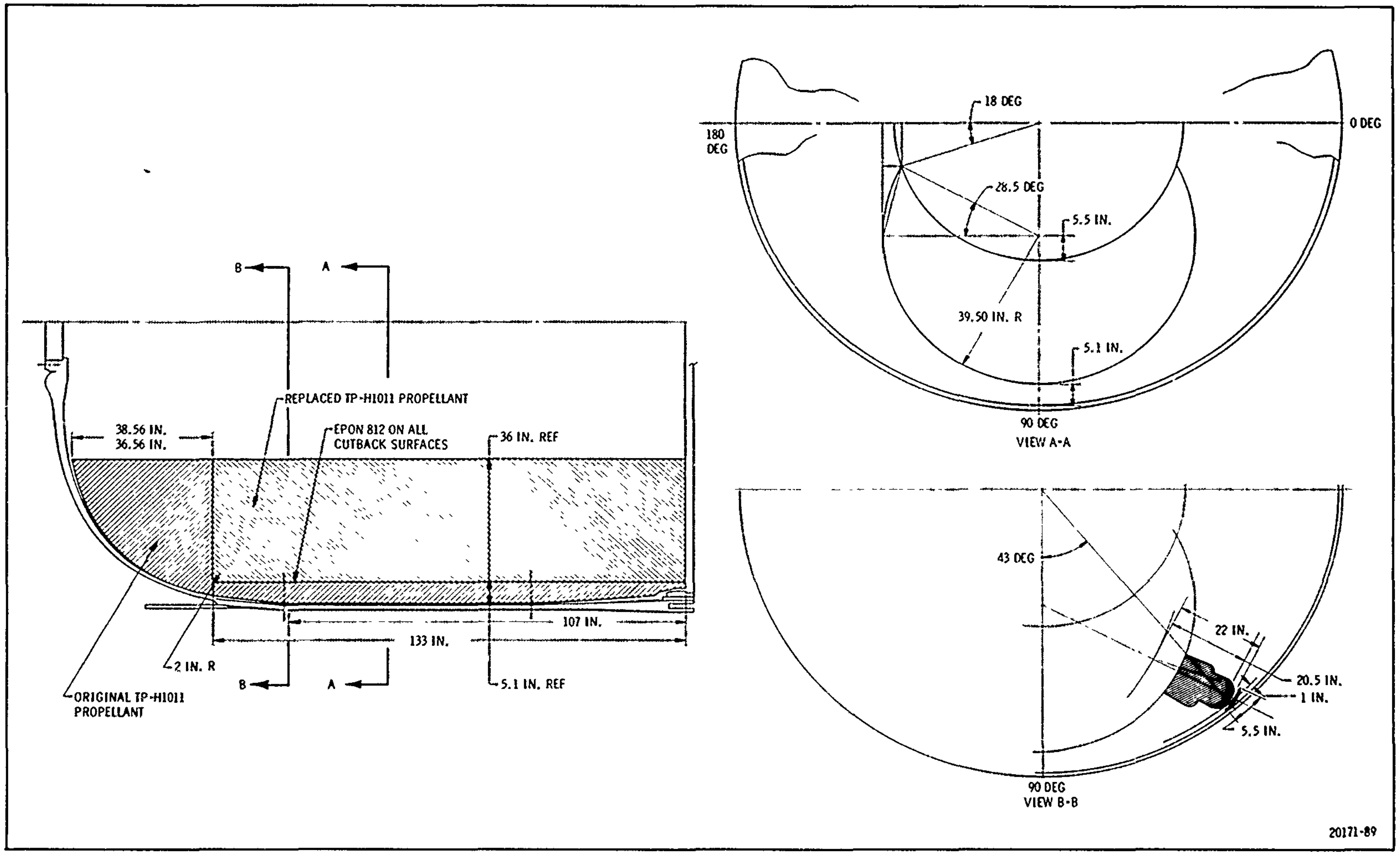

(U) Figure 114. Forward Segment Rework

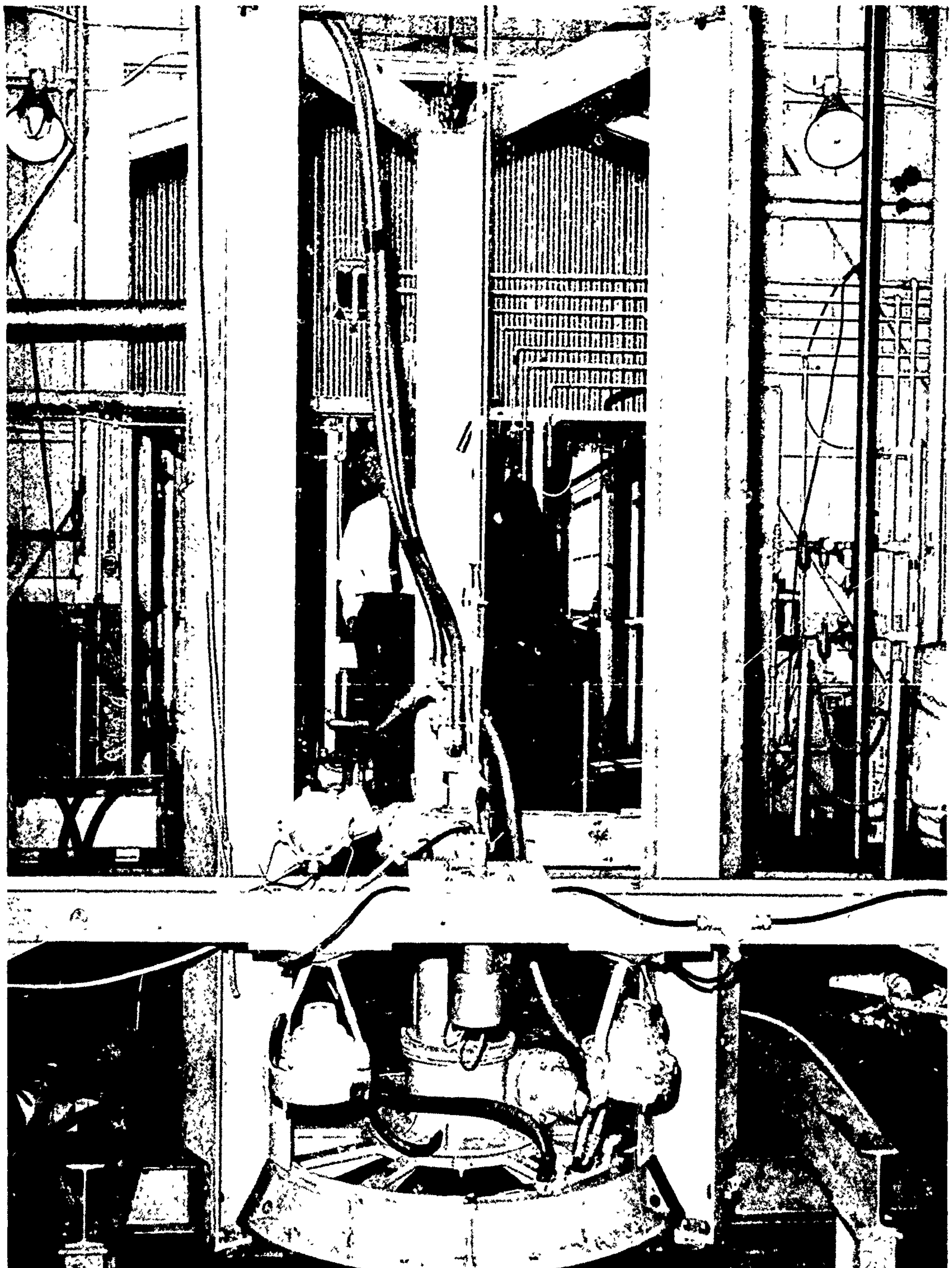

(U) Figure 115. Cutback Machine in Position over Segment

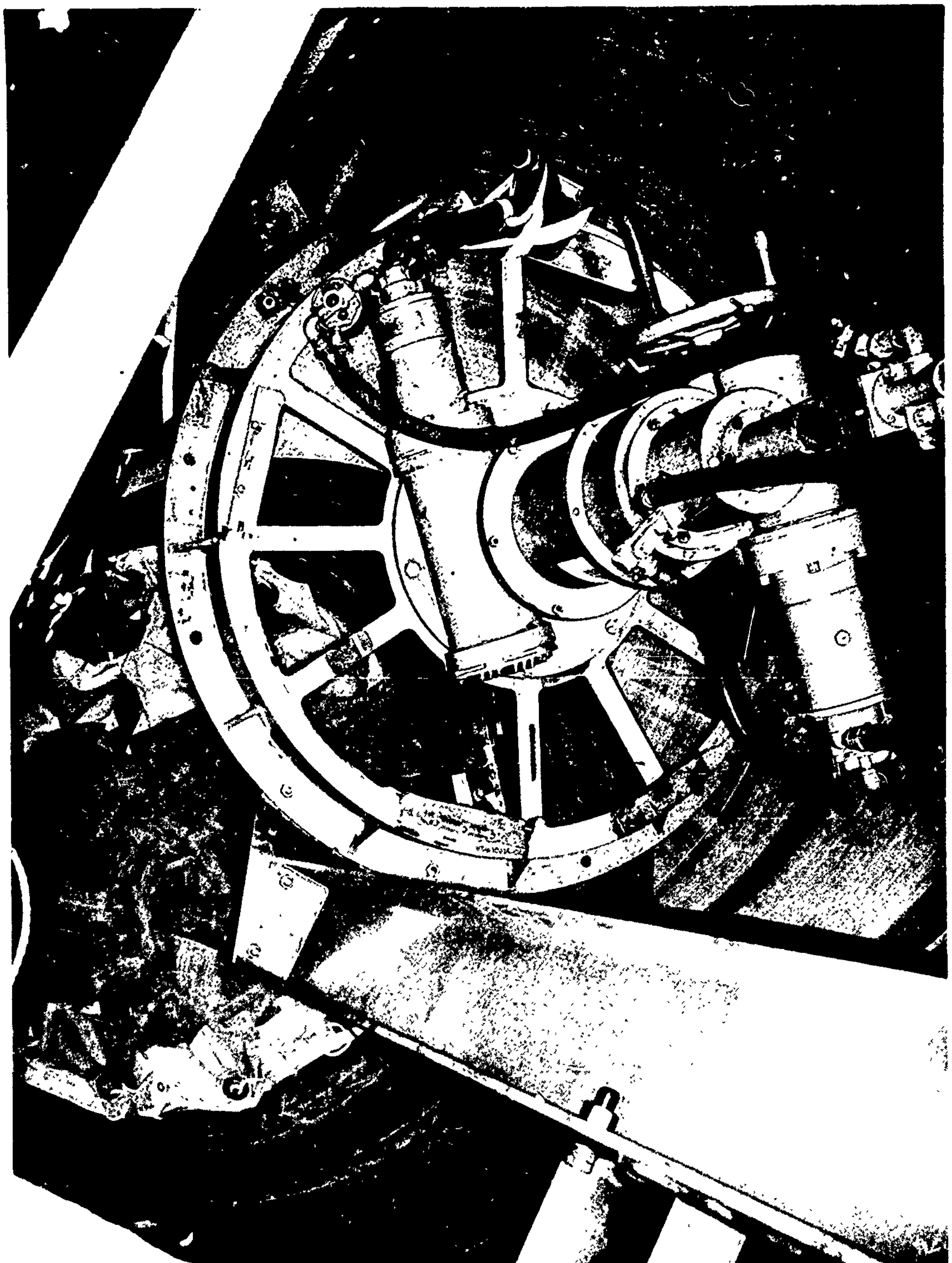

(U) Figure 116. Cutback Machine During Operation (With Scrap Catcher)

The cutting operation was conducted by a series of 6 in. longitudinal cuts. The machine was set to cut 6 in. and then operated remotely. Following completion of 6 in. of cutting, the controls were locked out. The cutback machine was then removed from the cavity, the scrap propellant removed and all propellant contamination removed from the working area. The machine was then reinstalled on the tripod and set for another cut.

The initial cutting in the nonvoid area near the aft end of the grain was accomplished in full 6 in. cuts. In the area of the voids, the distance of longitudinal cut was reduced as desired to as little as 1/2 in. so that the nature and frequency of the voids could be studied. When a cut of less than 6 in. was made, the cleanup and resetting of the machine was not performed, only the examination of the propellant surface and scraps was performed.

It was found that the voids corresponded very closely to those interpreted in the X-rays. Figures 117 and 118 show typical voids in the slices of propellant removed from the defect area. Figure 119 shows a series of voids and unknitted flowlines at 111-1/2 in. from the aft end of the grain which could have led to case wall exposure shortly after ignition.

The cutting was stopped at 126 in. from the aft end of the grain. The cutback machine was removed and the area forward of the cutout area was X-rayed. Several small voids were detected in the next 4 in. of propellant which were not next to the case wall and therefore this additional propellant was removed with the cutback machine.

(U) The outer periphery of the cavity exposed several irregular voids. These were hand trimmed until no visible evidence of the void remained (Figure 120). One of these voids extended to the case wall.

(U) Following this operation, skim cuts were made on all machine cut surfaces to remove contamination from the previous cutting operations and to insure a good bond of the recast propellant. X-rays had revealed a large 7 in. long void at 46 deg and 107 in. from the aft end of the propellant grain surface. This void lay outside the cutout area and was judged to be up to 7 in. from the case wall. The decision was

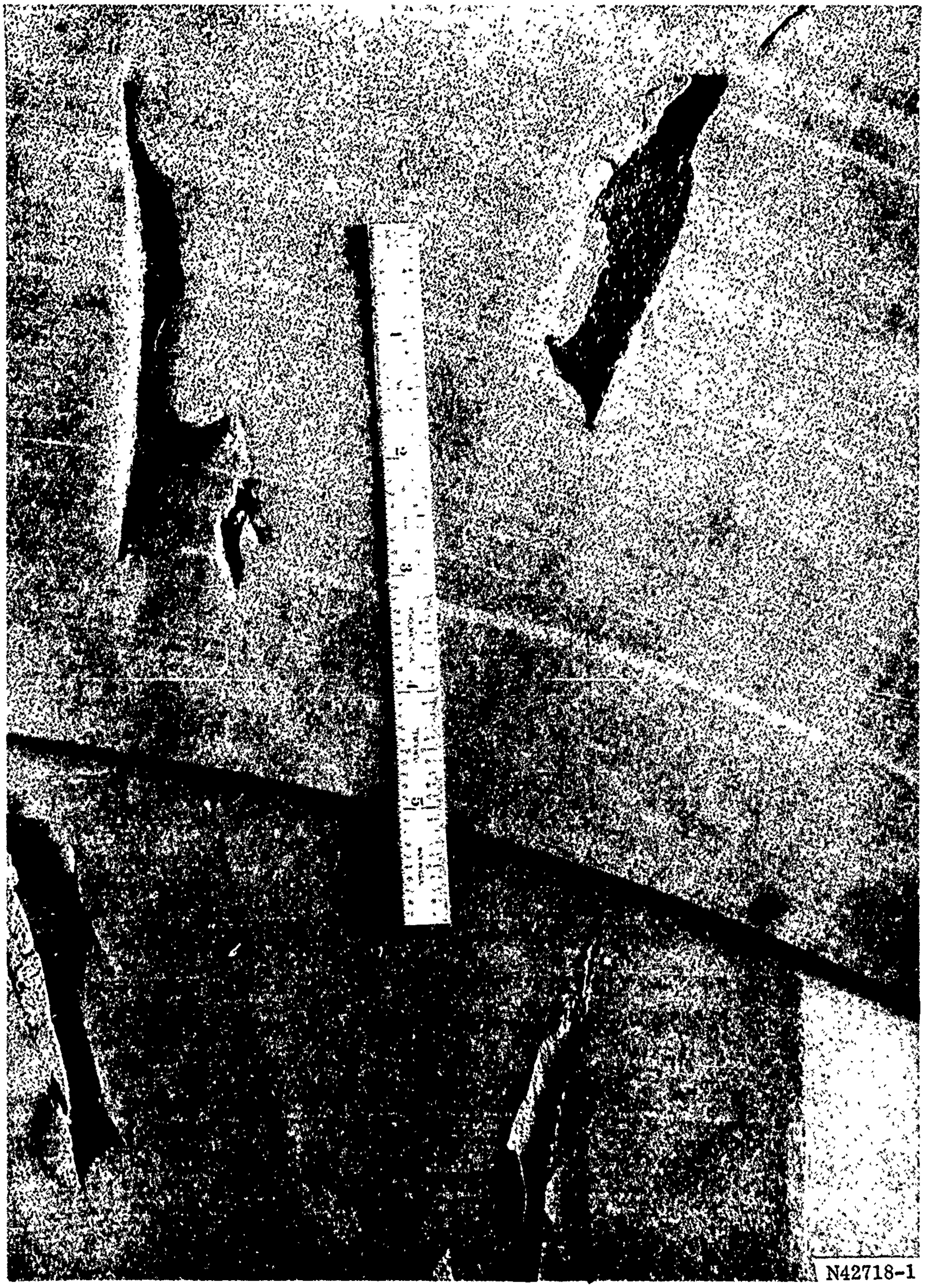

(U) Figure 117. Typical Voids in Propellant Slices Removed from Defect Area (View A)

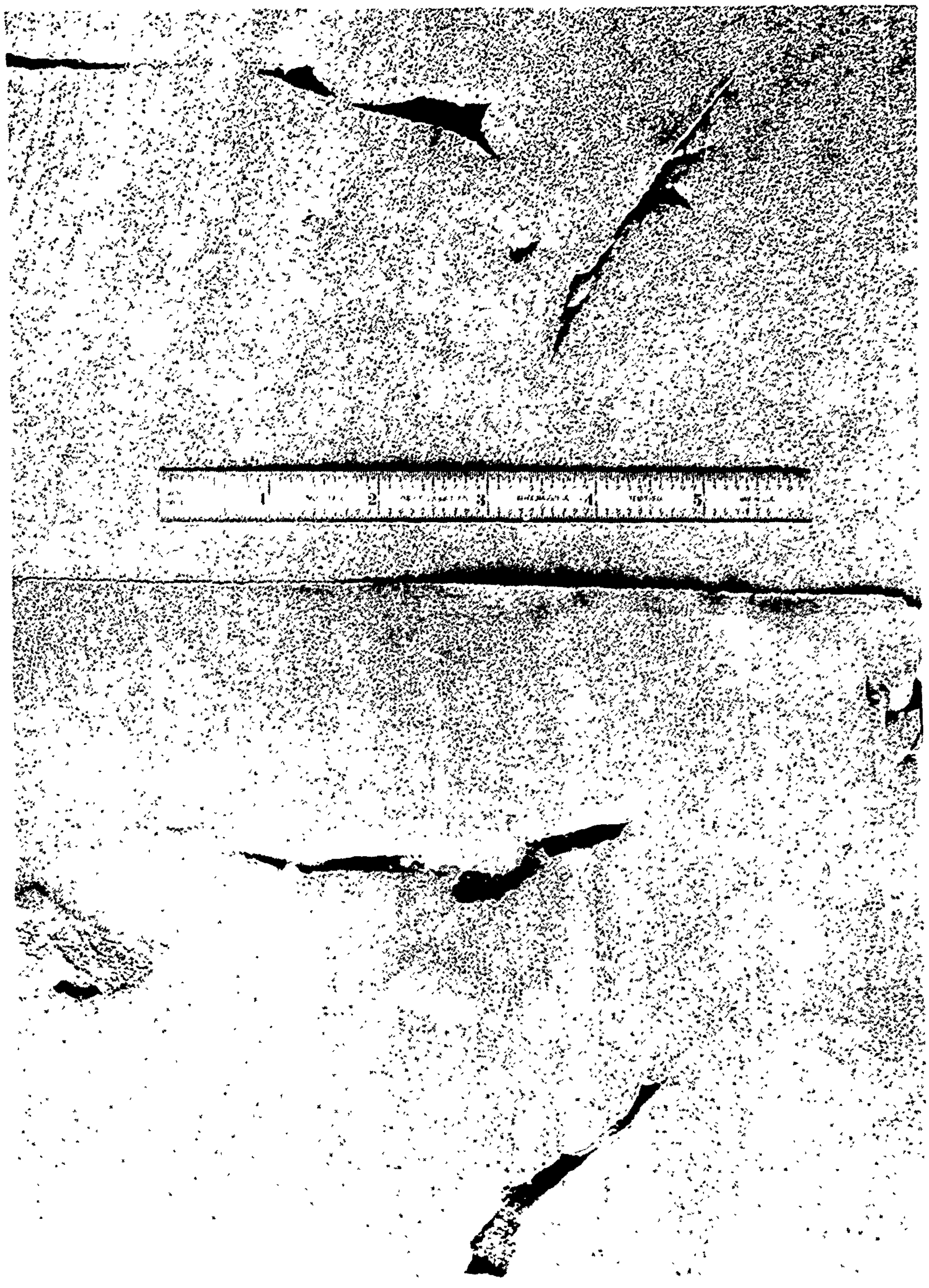

(U) Figure 118. Typical Voids in Propellant Slices Removed from Defect Area (View B)

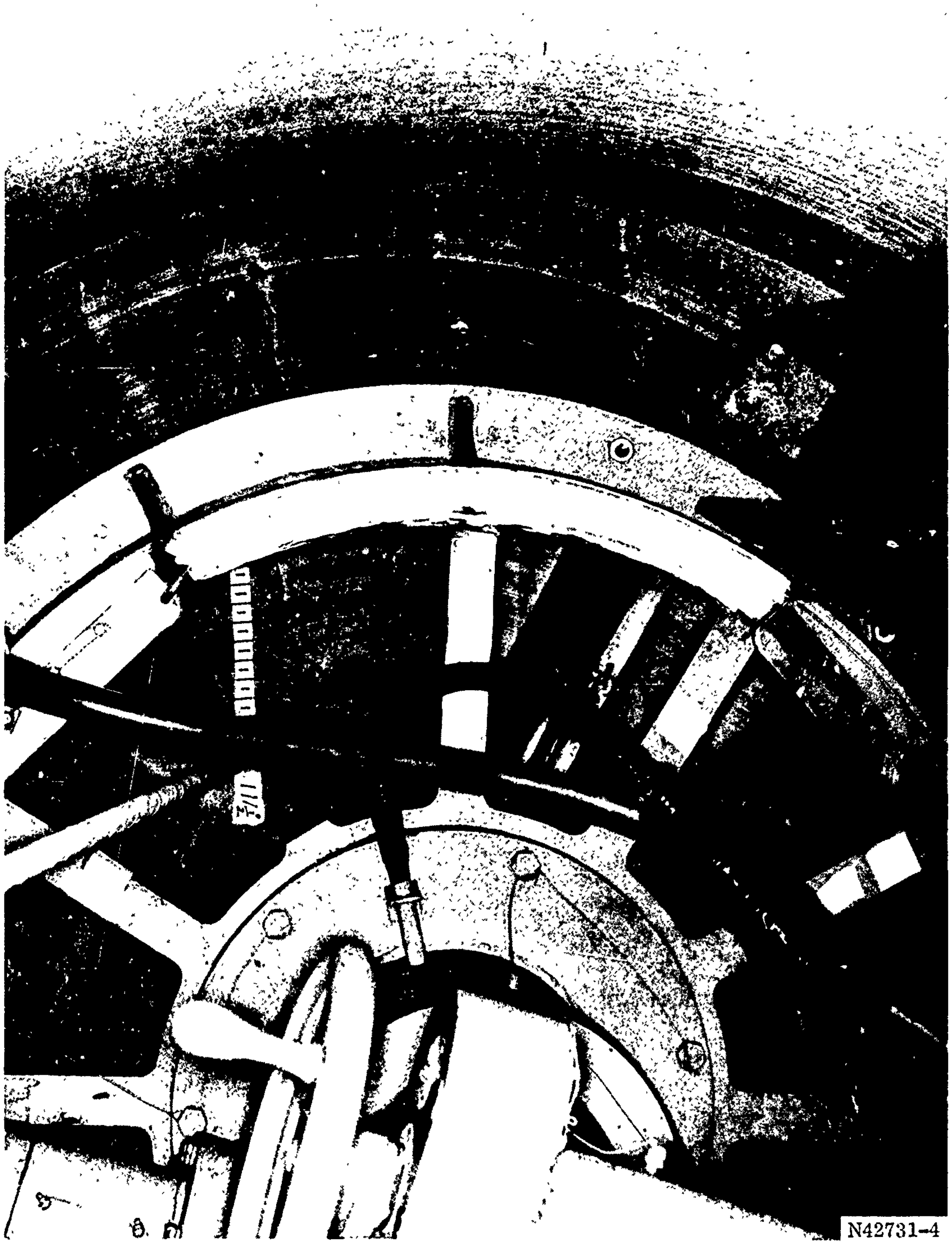

(U) Figure 119. Cut Surface Showing Voids and Unknitted Flow Lines

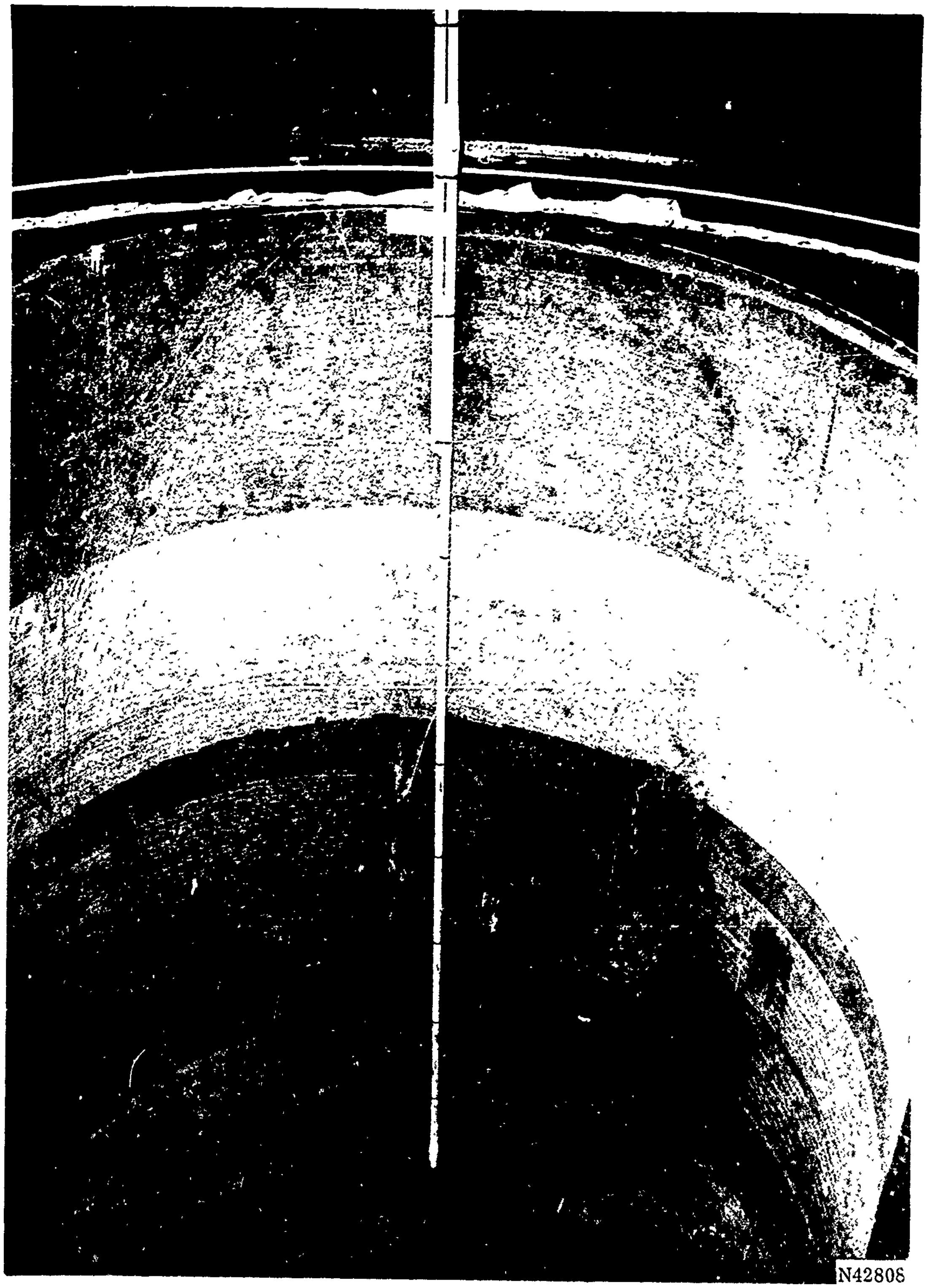

(U) Figure 120. Propellant Cavity Surface Showing Hand Blended Voids made to remove this void by using remote machine cutting, since there was too much propellant to be removed to hand trim to the void.

(U) To remove the void, a single stroke cutout tool (2U26385) was designed and fabricated. The tool connected to the bottom of the tripod in the same way as the rotary cutout machine. The cutting blades were "U" shaped with edges which cut an area 3 in. wide, and 1-1/2 in. deep. There were a series of these blades which were incrementally longer.

(U) The blades cut the propellant in a vertical plane rotating on a pivot point between the two ends of the blade. The blade was operated with a hydraulic piston connected to the end opposite the cutting edge. The hydraulic ram was operated remotely with a hand pump. The cavity depth was increased using the rotary cutback machine to 133 in. from the aft propellant surface to provide clearance for "U" shaped cutting blades.

(U) A series of cutting operations were conducted using the incrementally longer "U" shaped blades. X-rays were taken using a portable 12 Curie CO 60 source. The source was placed in the cutout cavity and the film on the outside of the case. The series of cuts carried to within 1-1/2 in. of the case wall. One small defect (1 by 1-1/2 by 1/8 in.) had been removed; however, an X-ray taken after the last cut revealed the large void still existed. At this point it was concluded that the void lay along the case wall and did not warrant further cutting and the risk of engaging the case wall with the machine operated blades. The inherent inaccuracies in the triangulation had precluded precise determination of the orientation of the void.

(U) Since the cutout tool tore the propellant quite badly, the side cavity surfaces were hand trimmed to provide a smooth cut surface for bonding. Figure 121 shows the completed side cavity.

(U) It should be noted that several large circumferential voids existed on the opposite side of the semicircular cavity at the 107 in. level; however, they appeared to lie along the case and no attempt was made to remove them.

(U) A total calculated weight of 23,400 lb of propellant had been removed from the segment.

(U) Figure 121. Hand Trimmed Side Cavity

(U) E. RECASTING AND CURE

(U) The casting arrangement used was per drawing 2U26202. This arrangement used the original steel core (ref Section VII-E) with 4 in. thick foam segments covering 120 deg of the core in this area of the cutout cavity. This allowed the core to be installed in the offset position and also allowed it to be inserted in the core cavity which was smaller due to cure and thermal shrinkage of the propellant. A foam rubber seal (1/2 in. thick by 2 in. wide) was attached to the core to match the vertical and horizontal edges of the cutout cavity.

(U) Before the core could be inserted into the cavity, an area at the aft end of the grain required trimming 6 in. wide by 24 in. long by 1 in. deep. This was required because the cured propellant had experienced greater than predicted slumpage due to the cutout.

(U) The core was inserted offset then forced against the propellant using hydraulic pistons. Initially a good seal was not accomplished. However, as the propellant modulus lowered during precasting heatup, the propellant conformed and an excellent seal was effected.

(U) The segment was preheated for seven days at 135 $\pm$ 5°F with the warm air circulating around the segment into the cutout cavity and in the space between the core and core cavity. Twelve hours prior to casting, Epon 812 was sprayed on the surfaces of the propellant in the cutout area.

(U) Two 8 in. bayonets were used to recast the segment. Six 4,400 lb mixes and one 2,200 lb mix was used to recast the cutout cavity. These mixes were mixed in the 400 gal. Baker-Perkins multiwing mixers. The propellant had been restandardized to account for aging of the raw materials and to account for use of the horizontal mixer.

(U) The segment was cured for 96 hr at 135°F. After a 24 hr cooldown, the core was removed. The edges of the recast area required cleanup by hand trimming.

(U) Inprocess samples were processed using loaf samples from the previous mixes cast into this segment, the Epon 812 used to activate the grain surface and new propellant. These were preheated and cured with the segment. Test results again indicated a bond of the new to old propellant better than the propellant tensile strength. Figures 122 and 123 show the completed repair.

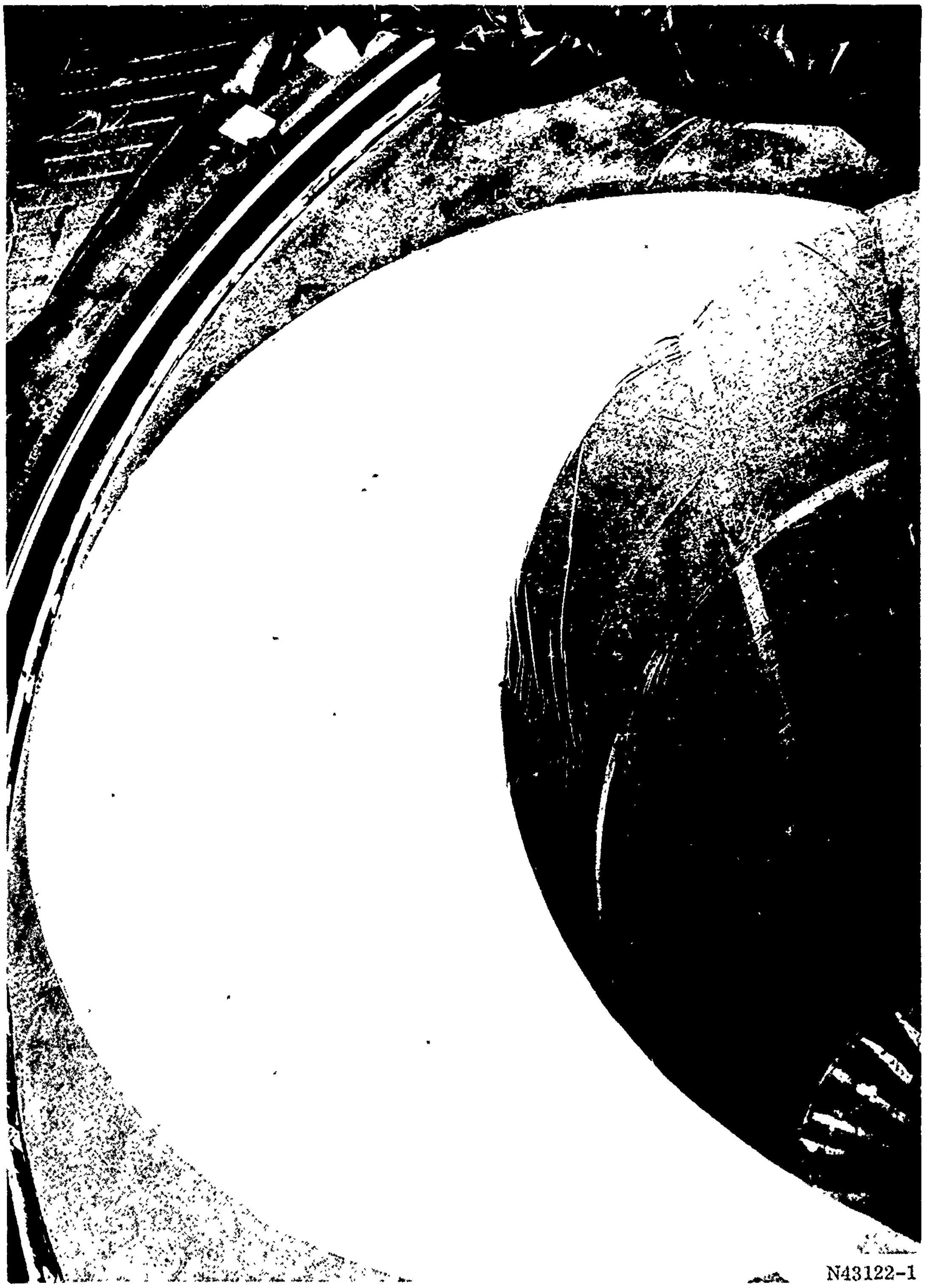

(U) Figure 122. Aft View of Completed Forward Segment Repair

(U) Figure 123. View from Core Cavity of Completed Forward Segment Repair

SECTION IX

(U) IGNITION SYSTEM DESIGN AND FABRICATION

(U) A. IGNITION SYSTEM DESIGN

(U) The ignition system for the 156-8 motor was designed as a headend ignition system (Figure 124) in accordance with the contract work statement. The design criteria were: (1) use of existing hardware and tooling to the greatest extent possible, (2) loaded case designed such that one design could be used for both the 156-8 and the 156-9 motors so that common verification testing and tooling could be used, and (3) use of a proven design requiring no development.

(U) The system was composed of the following four main subassemblies.

1. Safety and arming device.
2. Initiating system.
3. Booster Pyrogen igniter.
4. Adapter.

(U) 1. SAFETY AND ARMING (S & A) DEVICE

(U) The S & A device selected for the 156-8 ignition system is currently being used on the Stage I, II, and III Minuteman motors. Thiokol developed this device for the Stage I motor ignition system and later it was standardized for all three stages. The S & A has been qualified to the latest Air Force requirements and over 2,500 have been produced for various development, qualification, flight test, and production programs.

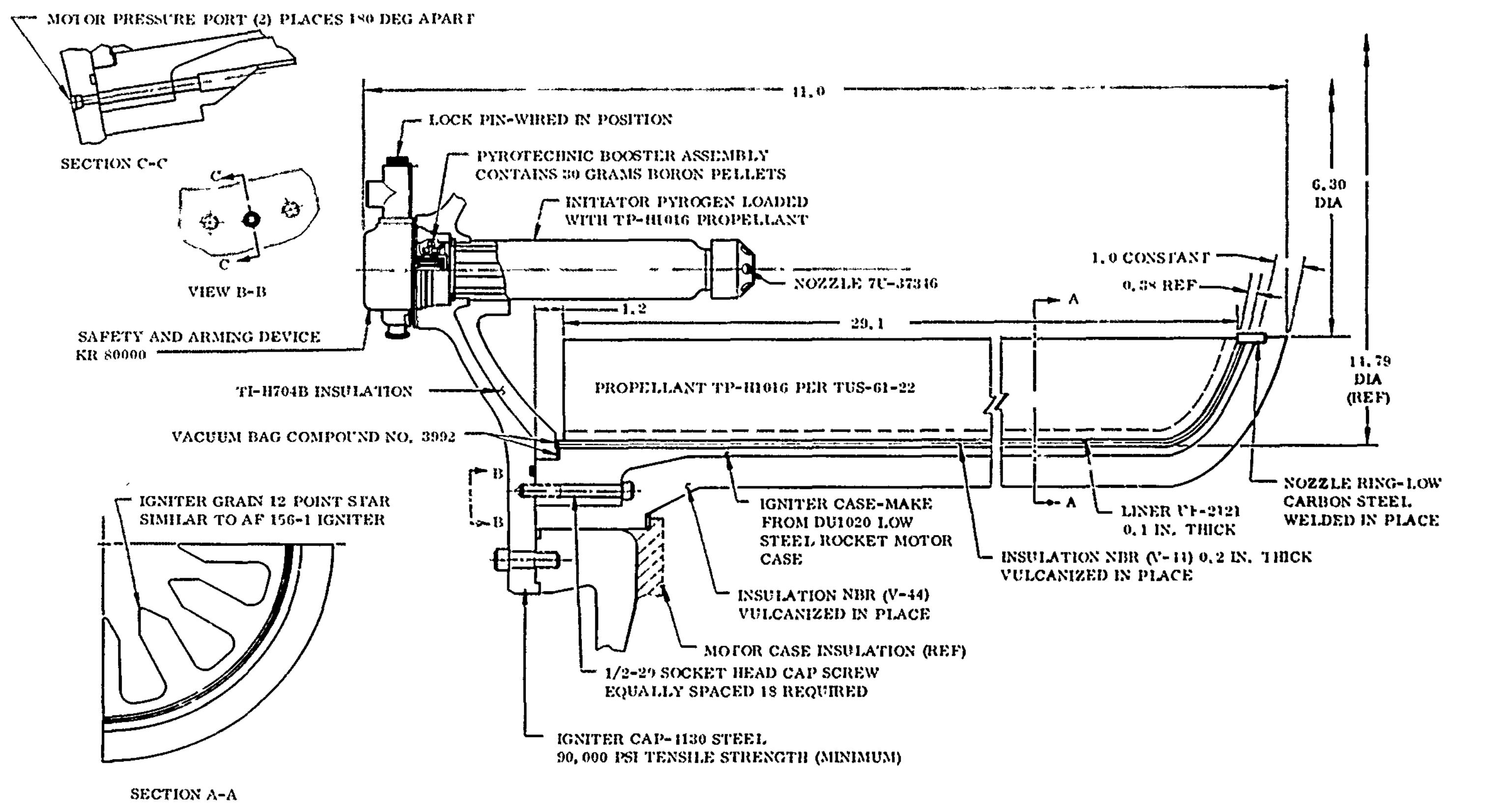

(U) Figure 124. 156-8 Ignition System

(U) Upon initiation, two ES-003 electrical squibs (initiated with 4.5 amps) started the ignition train for the motor ignition sequence. In the safe position, the squibs were electrically shorted and mechanically isolated from the ignition train. The S & A device had a visual indicator, mechanical lockpin, separate connectors for the control and firing circuits, hermetic seals, and other safety features to minimize the possibility of inadvertent firing. A lockwire secured the lockpin in place to insure assembly of the S & A device to the Pyrogen igniter in the unarmed (safe) condition. The lockwire and lockpin had to be removed manually before the device could be armed electrically with the required 24 volts. This feature satisfied the requirement that the S & A device not be installed in the motor while in the armed condition.

(U) 2. INITIATING SYSTEM

(U) The initiating system consisted of an adapter, pyrotechnic booster assembly, and an initiating Pyrogen igniter.

(U) a. Adapter--The adapter, made from low carbon steel, adapted the Pyrogen igniter, pyrotechnic booster, and the S & A device into one integral assembly. This assembly was installed in the motor adapter and held in place with a beveled retaining ring.

(U) b. Pyrotechnic Booster--The pyrotechnic booster was the link in the ignition train between the S & A device and the initiating Pyrogen igniter. It contained 30 gm of size 2A boron-potassium nitrate pellets, and the container was identical to the design used on the Stage I Minuteman.

(U) c. Pyrogen Igniter--The initiating Pyrogen igniter, loaded with TP-H1016 propellant (Stage I Minuteman igniter propellant), ignited the booster Pyrogen igniter. It produced a mass discharge rate for booster Pyrogen ignition of 3.5 lb/sec for approximately 0.3 second. A multiple port nozzle diffused the flame for a fast smooth ignition of the booster Pyrogen igniter. The case and grain designs had previously been demonstrated in ~~the 156-1 and 156-9~~ motor static tests and in the Mace program for which this design was originally developed.

(U) 3. BOOSTER PYROGEN IGNITER

(U) The booster Pyrogen igniter assembly consisted of a mild steel case, NBR external and internal insulation, UF-2121 liner, and TP-H1016 propellant. The grain was the same 12 point star configuration used in the booster Pyrogen igniter for the 156-1 and 156-9 motors. The igniter operated at an average pressure of 820 psia, having a maximum pressure of 1, 005 psia, and provided a mass discharge rate of 158 lb/sec for approximately 0. 6 second. Pressure and mass flow then dropped. The total burning time was approximately 1. 1 second (Figure 125).

(U) At 1, 005 psi the booster Pyrogen igniter case had a design structural safety factor greater than 2. The low carbon steel igniter case was 32 in. long and 14. 79 in. in diameter. A 6. 3 in. ID steel ring was welded in the aft end to serve as the nozzle throat. The selection of a steel case for the 156-8 and 156-9 igniters was based upon economic considerations rather than weight performance.

(U) The steel case was insulated internally and externally to prevent melting during the motor firing. Thermodynamic calculations indicated that 0. 03 in. of insulation would prevent melting from the inside; however, to protect the bond of the external case insulation to the steel case, additional internal insulation was necessary. The final design used 0. 20 in. of NBR layup, vulcanized in place, and 0. 10 in. of UF-2121 liner. The thickness of the internal insulation controlled the propellant web thickness and provided more than enough insulation on the internal surfaces to prevent bond failure of the external insulation.

(U) 4. ADAPTER

(U) a. Booster Igniter to Motor--The booster igniter adapter facilitated installation of the igniter loaded case assembly to the motor head end. Made from low carbon steel, this adapter permitted installation of the booster igniter at the head end of the motor. The booster igniter adapter had ports to monitor igniter pressure,

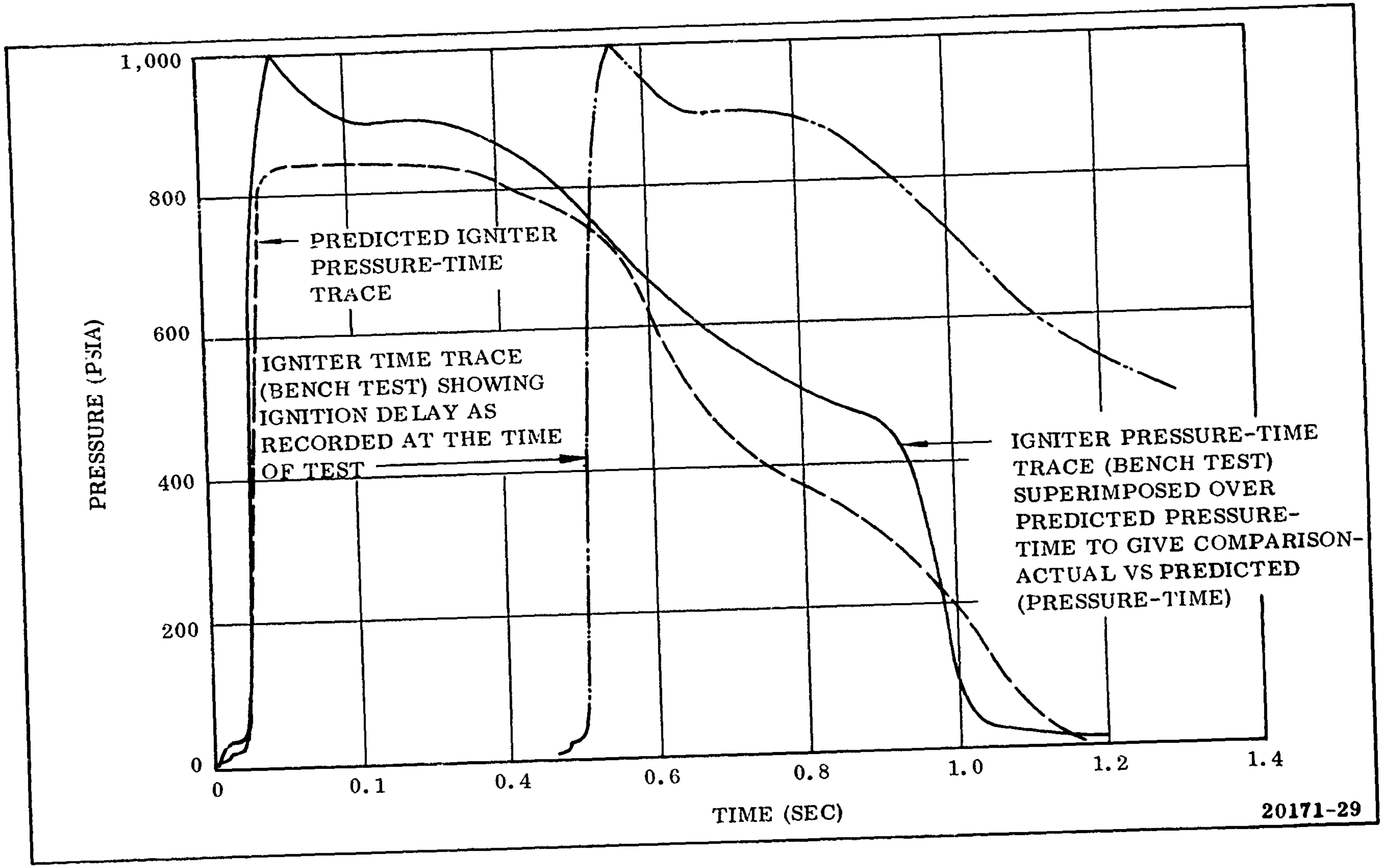

(U) Figure 125. Igniter Pressure Time Trace motor pressure, and provide passage for the carbon dioxide quench system. The initiating system was attached to the igniter adapter with a beveled retaining ring.

(U) B. IGNITER BALLISTIC DESIGN AND MOTOR IGNITION TRANSIENT

(U) The empirical Pyrogen igniter coefficient is the primary parameter used for determining the required size of a booster Pyrogen igniter. When the ratio of igniter mass flow rate (lb/sec) to the motor throat area (sq in.) is in the range of 0.15 to 0.25, satisfactory ignition will result. Thus, an approximate Pyrogen igniter motor mass flow rate can be established for a motor having specified nozzle dimensions. Usually, the values selected for the Pyrogen igniter coefficient have been in the range of 0.17 to 0.20. The 156-8 igniter had a mass flow rate of 158 lb/sec, which resulted in a coefficient of 0.185.

(U) Motor ignition occurred through the sequential action of a pyrotechnic charge and two Pyrogen igniters. The S & A device was electrically armed and two electrical squibs were initiated; the flame and pressure created by the squibs ruptured two diaphragms and ignited the pyrotechnic booster charge; the flame from the booster charge ignited the initiating Pyrogen igniter; and the initiating Pyrogen igniter exhaust gases ignited the booster Pyrogen igniter.

(U) Prior to the motor test, the motor ignition transient had been predicted. The igniter mass flow was entirely adequate for this motor, but the grain port diameter was large and the impingement point of the igniter plume against the grain port was far downstream from the igniter nozzle. This latter factor led to the prediction of a long (0.250 sec) lag time, that is time from beginning of igniter output to the first ignition of motor propellant.

(U) C. IGNITER INSULATION DESIGN

(U) 1. CASE INTERNAL INSULATION

(U) The case internal insulation provided thermal protection and controlled the web thickness of the propellant grain. The internal insulation consisted of two 0.1 in. thick plies of asbestos filled NBR laid up and vulcanized in place. The insulation was sealed with Koropon prior to the application of a 0.1 in. coating of UF-2121 liner. The UF-2121 liner provided a high strength bond to the TP-H1016 propellant. The insulation-liner-propellant bond system has historically resulted in propellant bonds of 120 psi tensile adhesion and 6.8 pli for the 180 deg peel test.

(U) 2. CASE EXTERNAL INSULATION

(U) The igniter case external insulation prevented the steel case from melting during the motor firing, precluding the ejection of igniter case fragments. The external insulation consisted of 0 in. of asbestos filled NBR laid up and vulcanized in place. The insulation thickness calculated for the 156-8 motor was based on an action time of 122 sec, compared to 70.51 sec for the 156-9 motor. To facilitate use of the same design without excessive engineering and manufacturing changes, the same external igniter insulation thickness was used for both motors. The insulation thickness was calculated for the 156-8 motor based on a char rate of 5.5 mil/sec with a 1.5 safety factor.

(U) 3. IGNITER CAP INSULATION

(U) The insulation applied to the adapter (Figure 12 i) was TI-H704B (the same as the 156-9 motor case insulation). The insulation was a mastic material containing primarily HC binder, asbestos, and carbon black. This material is most effective in areas of low gas velocity, and was selected as the Pyrogen igniter insulation because of its relatively low cost, ease of application to any configuration, and ability to cure at ambient temperature.

(U) D. IGNITER WEIGHT ANALYSIS

(U) The component weights for the Pyrogen igniter are listed below.

	Weight (lb)
Loaded Case Booster Pyrogen Igniter	
Case	262.8
External Insulation	87.6
Internal Insulation	13.3
UF-2121 Liner	4.1
TP-H1016 Propellant	131.9
Initiating Pyrogen Igniter	
Liner	0.029
Case	3.9
TP-H1016 Propellant	1.2
Nozzle	0.6
Booster Assembly	0.481
S & A Device	4.8
Insulated Adapter	145.154
Miscellaneous	6.118
Total	662.034

(U) E. IGNITION SYSTEM PROPELLANT

(U) The propellant selected for use in the ignition system is designated TP-H1016. The composition, ballistic and physical properties of this propellant are shown in the following tabulations.

(C) TP-H1016 Propellant Composition

Constituent	Composition by Weight (Percent)
Ammonium Perchlorate	77
Aluminum Powder	2
HB and ERL*	18
Ferric Oxide	3

(C) Ballistic Properties

Characteristic Velocity, C* (ft/sec)	4,945
Density (lb/cu in.)	0.0605
Exponent Burn Rate, n	0.35
Burn Rate at 1,000 psi and 80°F (in./sec)	0.86 (Actual)
Flame Temperature (°R)	4,770
Ratio of Specific Heats (γ)	1.23

(U) Physical Properties

	Minimum	Maximum
Density (lb/cu in.)	0.0599	0.0611
Maximum Strain (psi)	140	227
Strain at Maximum Stress (in./in.)	0.20	0.33
Modulus of Elasticity (psi)	600	1,200

*The ratio of HB to ERL is determined from raw material standardization to achieve the desired physical properties.

(U) F. IGNITION SYSTEM STRUCTURAL ANALYSIS

(U) The 156-8 ignition system was structurally analyzed to determine its compatibility with the forward polar boss and surrounding areas. Structural components of the system which were subjected to analysis included the forward polar boss, igniter cap, igniter case, and attachment bolts. To determine the most severe loading, two conditions were investigated.

1. Ignition-booster igniter case pressurized to MEOP (1,000 psia) 156-8 motor unpressurized.
2. 156-8 main stage motor pressurized to MEOP (860 psia), booster igniter case at 70° F and equilibrium pressure.

(U) Analytical results of these conditions are summarized in Figures 126 and 127. Safety margins shown were calculated from stresses existing at the appropriate MEOP and ultimate material strengths. Structural materials and their mechanical properties are presented in Table XLII. A minimum safety factor of 1.32 occurs in the igniter cap during Condition 2. Safety factors throughout all igniter structural components are shown in Figures 126 and 127.

(U) G. IGNITER FABRICATION, ASSEMBLY, AND INSTALLATION

(U) The igniter case was fabricated from a TU-121 motor case. The lifting lugs, Pyrogen igniter boss and headend skirt were removed, the Pyrogen igniter port was opened to 7 in., and a nozzle ring welded in place. The weld area was stress relieved and the nozzle ring finish machined. Each igniter case was hydrotested to 1,100 psig. Four igniter cases were fabricated: two for the 156-8 program and two for the 156-9 program. One of the 156-8 igniter cases was used as a bench test for both the 156-8 and 156-9 programs.

(U) After machining, the interior and exterior surfaces were grit blasted and vapor degreased. V-44 NBR insulation was applied to both the interior and exterior surfaces of the case, using a Chemlok 203 and 220 bonding system, and vulcanized in an autoclave at 100 psig and 250° F for 3 hr, 310° F for 3 hr, then cooled for 6 hours. The external surface and nozzle area insulation were then final machined.

(U) The internal insulation was abraded, and cleaned with MEK. Koropon was applied to the internal insulation and cured for 5 hr at ambient temperature. UF-2121 liner was then applied and cured for 3 hr at ambient temperature and 40 hr at 135° F.

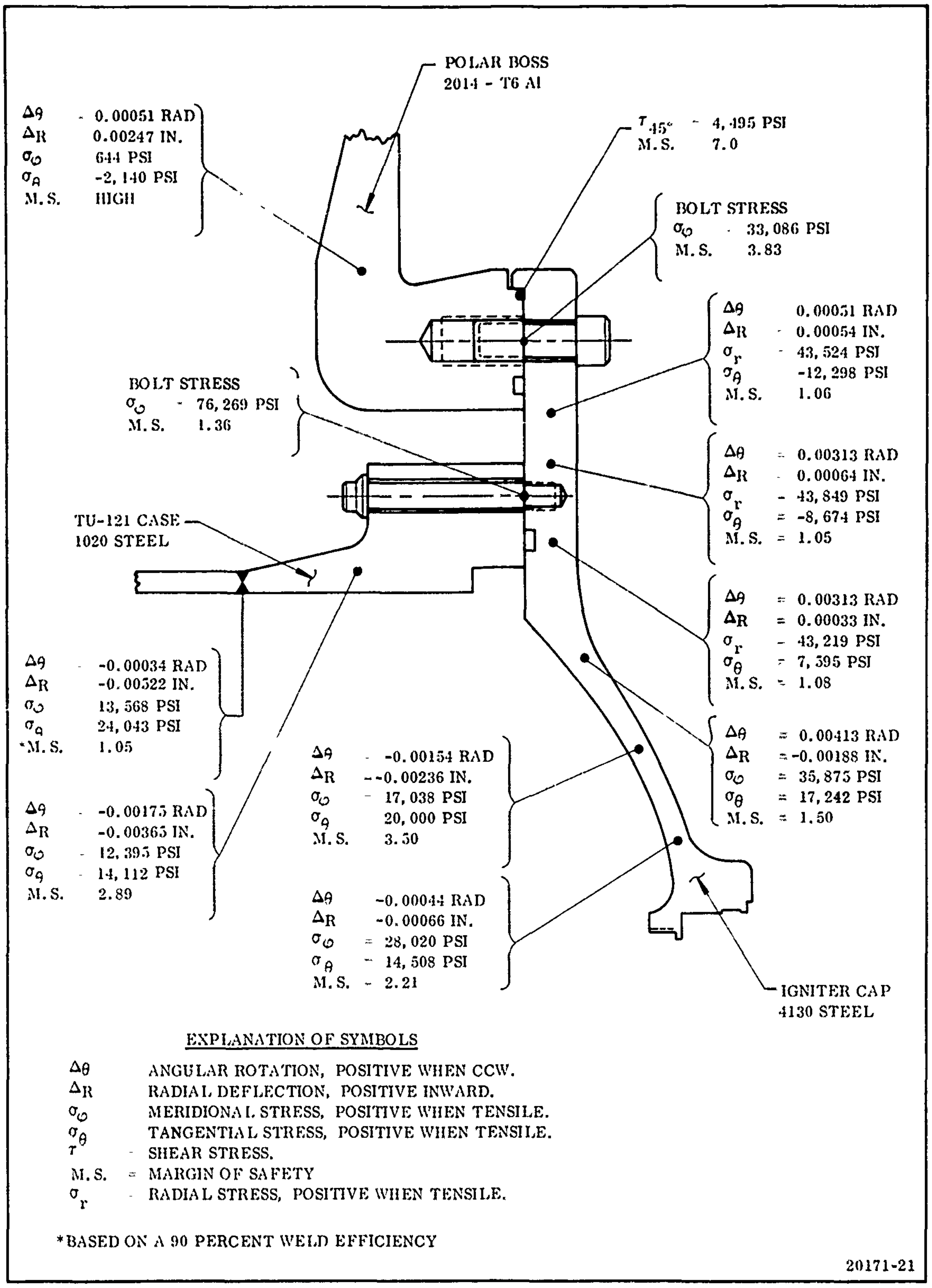

(U) Figure 126. Summary of Structural Analysis on 156-8 Igniter Case, Headend Adapter, and Pole Piece. Condition I (Igniter Only Pressurized to 1,000 psi)

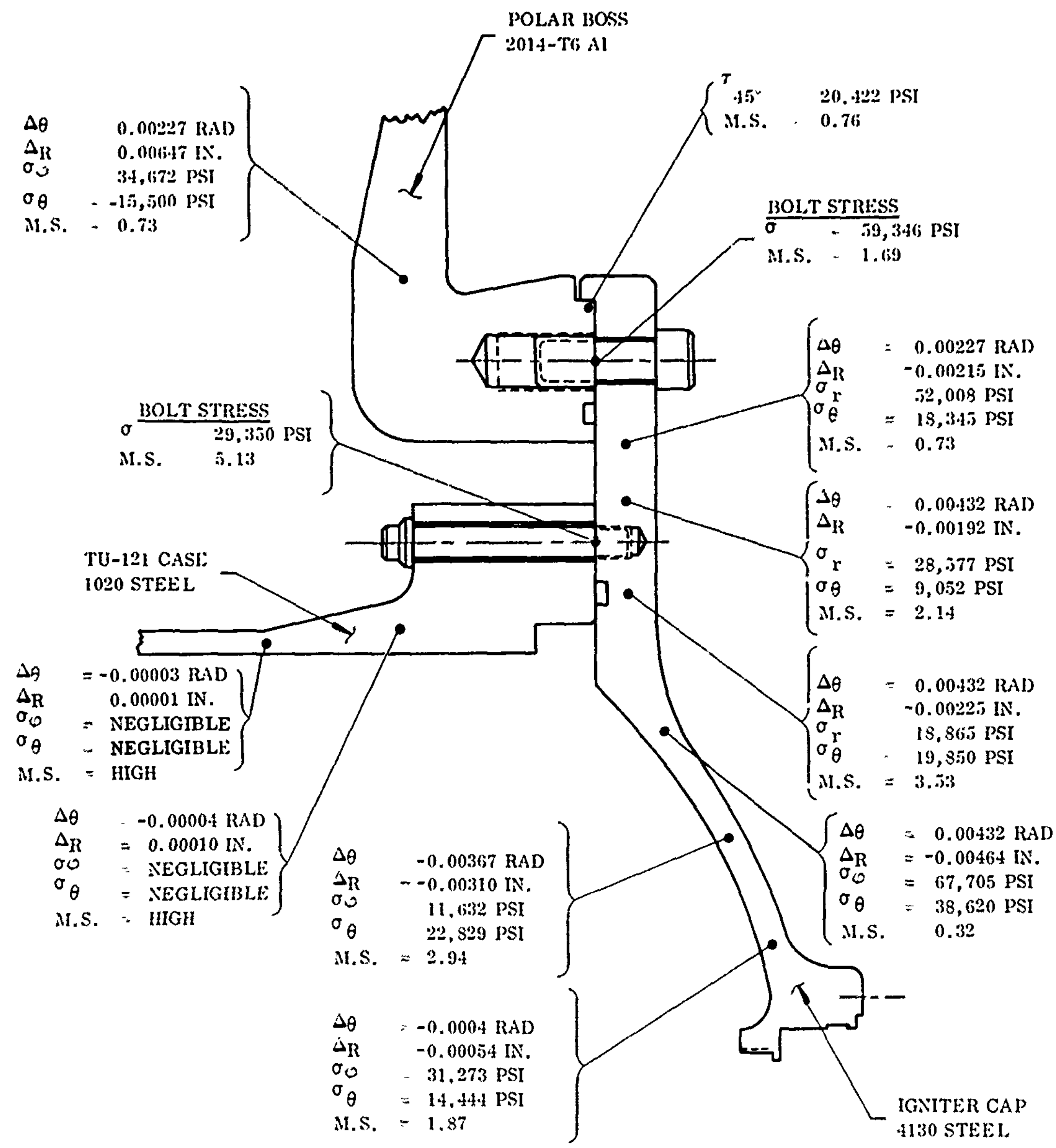

EXPLANATION OF SYMBOLS

$\Delta\theta$	-	ANGULAR ROTATION. POSITIVE WHEN CCW.
Δ_R	-	RADIAL DEFLECTION. POSITIVE INWARD.
σ_ϕ		MERIDIONAL STRESS. POSITIVE WHEN TENSILE.
σ_θ	-	TANGENTIAL STRESS. POSITIVE WHEN TENSILE.
σ_r		RADIAL STRESS. POSITIVE WHEN TENSILE.
M.S		MARGIN OF SAFETY.
τ		SHEAR STRESS.

20171-22

(U) Figure 127. Summary of Structural Analysis on 156-8 Igniter, Headend Adapter, and Pole Piece, Condition II (Rocket Motor Pressurized to MEOP of 860 psi)

TABLE XLII

(U) IGNITION SYSTEM STRUCTURAL MATERIALS

2014-T6 Aluminum	Component
F_{tu} = 60,000 psi	
F_{ty} = 55,000 psi	Polar Boss
F_{su} = 36,000 psi	(Ref Drawing 9U37466)
E = 10.5×10^6 psi	
4130 Steel	
F_{tu} = 90,000 psi	Igniter Cap
F_{ty} = 70,000 psi	(Ref Drawing 7U37344)
F_{su} = 54,000 psi	
E = 29×10^6 psi	
1020 Steel	
F_{tu} = 55,000 psi	Igniter Case
F_{ty} = 36,000 psi	(Ref Drawing DU1020)
F_{su} = 35,000 psi	
E = 29×10^6 psi	
Bolt (NAS 1351-10)	
5/8 - 18UNF	Igniter Cap to Polar
F_{tu} = 160,000 psi	Boss Attachment
E = 30×10^6 psi	
Bolt (NAS 628-44)	
1/2 - 20UNF	Igniter Cap to Case
F_{tu} = 180,000 psi	Attachment
E = 30×10^6 psi	

(U) Casting fixtures were assembled in the case and the igniter was vacuum cast with TP-H1016 propellant. After a propellant cure of 96 hr at 135° F and 24 hr cool-down at ambient, the core was removed and the propellant cut back to print configuration.

(U) Final assembly of the igniter was accomplished by bolting the insulated adapter to the igniter and filling over the bolts, which were countersunk in the NBR, with UF-1155 insulation. The UF-1155 insulation was cured for 2 hr at ambient temperature.

(U) The initiator assembly, a modified TU-P140 (MACE) Pyrogen igniter, was also cast with TP-H1016 propellant after degreasing and lining with UF-2109 liner. The liner was cured for 18 hr and the propellant for 96 hr at 135° F. After propellant cure and casting fixture removal, the nozzle and adaptor were installed on the loaded initiator case using UF-3131 sealant. The booster was installed and the assembly painted.

(U) The igniter was installed in the motor after the motor was in the test bay with the motor in the horizontal position. Attachment to the motor case was accomplished by bolts through the igniter adapter into the case boss. After installation, all bolts were lock wired.

(U) H. IGNITION SYSTEM FUNCTIONAL VERIFICATION (BENCH TEST)

(U) The ignition system consisted of components previously demonstrated in the AF 156-1 motor test. The only modification to the AF 156-1 igniter is that the booster Pyrogen igniter is somewhat shorter. Consequently, only minimal bench testing was required to verify components and performance. This testing included the static firing of one complete igniter assembly with a rebuilt S & A device and without external insulation. This test was conducted under the AF 156-8 program since 156-8 and 156-9 ignition systems were identical except for motor adapting arrangements. The primary objective of this test was to evaluate performance parameters such as igniter response time, igniter ignition delay, and booster Pyrogen ignition lag time, and pressures. Instrumentation consisted of pressure gages on the booster Pyrogen igniter.

(U) The 156-9 ignition system was successfully tested during the week ending 13 Jan 1967 in the TU-121 delta test stand (Figure 128 before test and Figure 129 after test) and fired when the igniter grain temperature was at 74° F. The igniter had been temperature conditioned for a minimum of 12 hr at a temperature of 85 $\pm$ 5° F. The igniter ballistic characteristics (Table XLIII) and the pressure time trace (Figure 125) verified that satisfactory ignition of the 156-8 motor would occur, resulting in a smooth transient through ignition without an excessive pressure spike.

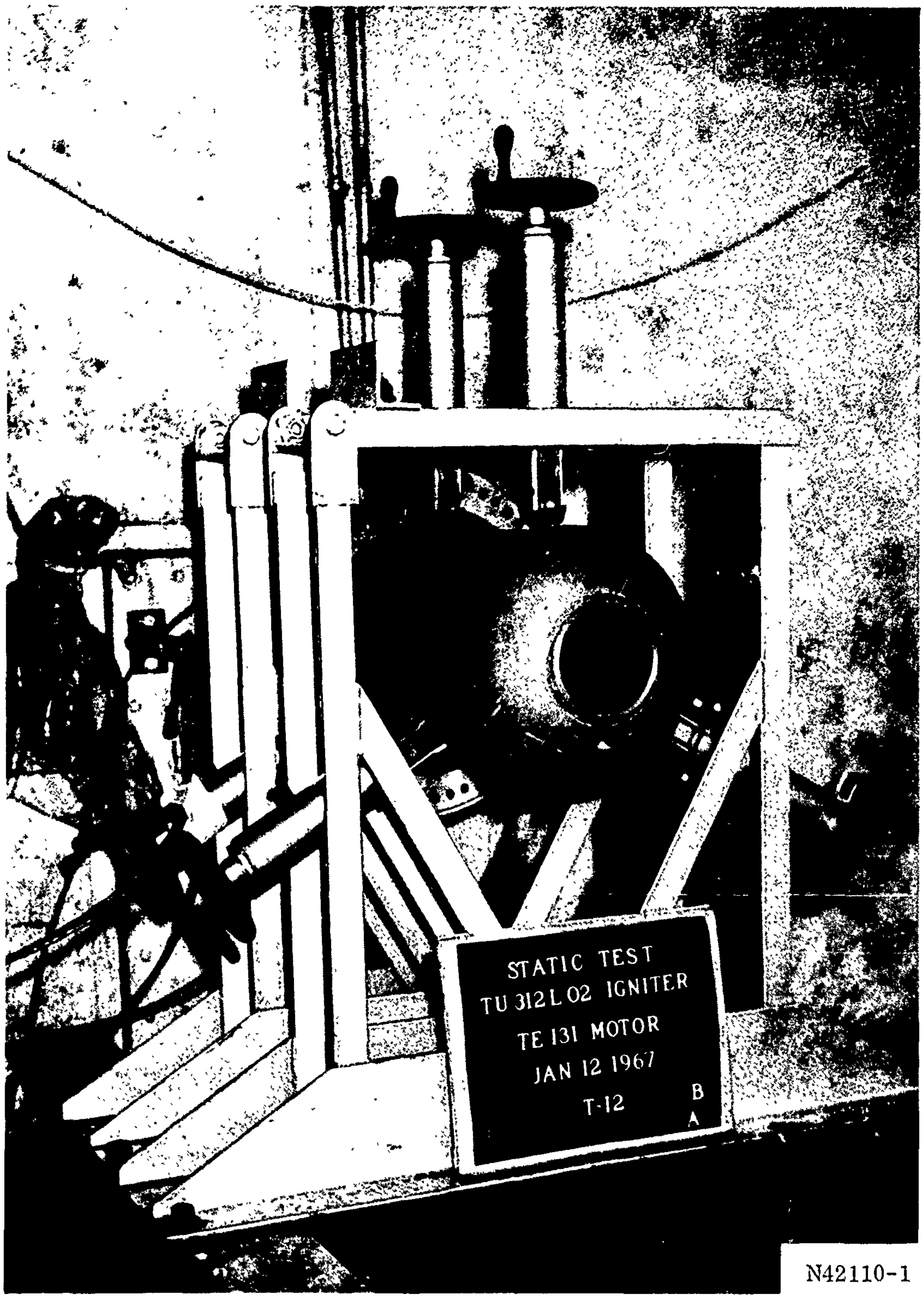

Figure 128. 156-9 Igniter in Test Stand (Before Firing)

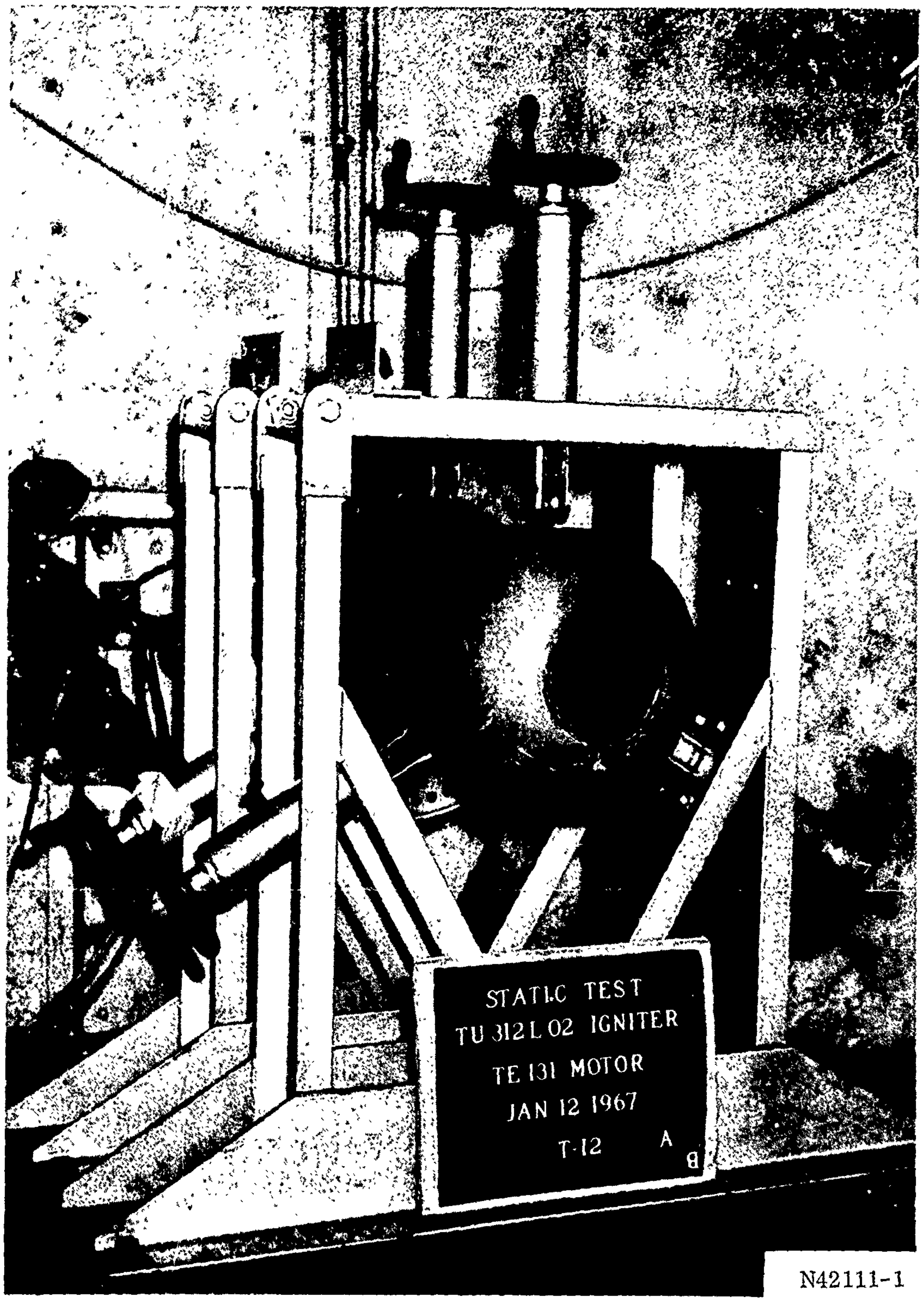

N42111-1

Figure 129. 156-9 Igniter in Test Stand (After Firing)

TABLE XLIII

(C) 156-8 IGNITION DATA

Characteristics	Actual Igniter Bench Test Data
Mass Flow Rate, First Level 0.56 sec (lb/sec)	170
Burning Time, 10 percent P_{max} to 10 percent P_{max} (sec)	0.95
Maximum Operating Pressure (psia)	1,005
Average Operating Pressure, First Level (psia)*	840
Average Operating Pressure, Second Level (psia)**	529
Ignition Delay T_0 to 10 percent P_{max} for Booster Pyrogen Igniter (sec)	0.040***
Ignition Interval Booster Pyrogen Igniter T_0 to 90 percent P_{max} (sec)	0.069**
156-8 Igniter Coefficient (lb/sec/sq in.)	0.199
Toial Impulse (lbm-sec)	24,200
Specific Impulse (lbm-sec/lbf)	184.5
	Predicted Motor Ignition Data
156-8 Ignition Delay Time T_0 to 75 percent P_{max} (sec)	0.56
156-8 Maximum Motor Pressure at Ignition (psia)	748

*First level is the integral of pressure from 10 percent of maximum pressure during pressure rise to the knee of first pressure drop divided by time.

**Second level is the integral of pressure from the knee of the first pressure drop to the knee of the second pressure drop divided by time.

***Based on first pressure indication being T_0. The time T_0 as recorded at time of test appears to be erroneous.

SECTION X

(U) NOZZLE DESIGN AND FABRICATION

(U) A. NOZZLE DESIGN SUMMARY

(U) 1. DESCRIPTION

(U) The nozzle for the 156-8 motor was a fixed, external, ablative plastic nozzle of the convergent-divergent type. The nozzle was designed and fabricated by TRW under Contract AF 33(657)-11301 (Development of Manufacturing Processes for Reinforced Plastic Solid Propellant Rocket Nozzles). Design was complete in 1964 and fabrication was complete in 1965.

(U) 2. NOZZLE CONFIGURATION

(U)

Throat Diameter, Initial (in.)	32.96
Expansion Ratio, Ae/A_t, Initial	7:1
Conical Exit Section	
Downstream Radius Ratio	0.6
Exit Half Angle (deg)	17.5
Length	
Throat to Exit, Nominal (in.)	87.597
Flange Forward Face to Exit, Nominal (in.)	101.803

(U) 3. NOZZLE DRAWING

(U) A drawing of the nozzle showing the major dimensions and identifying the materials of construction is shown on Figure 130.

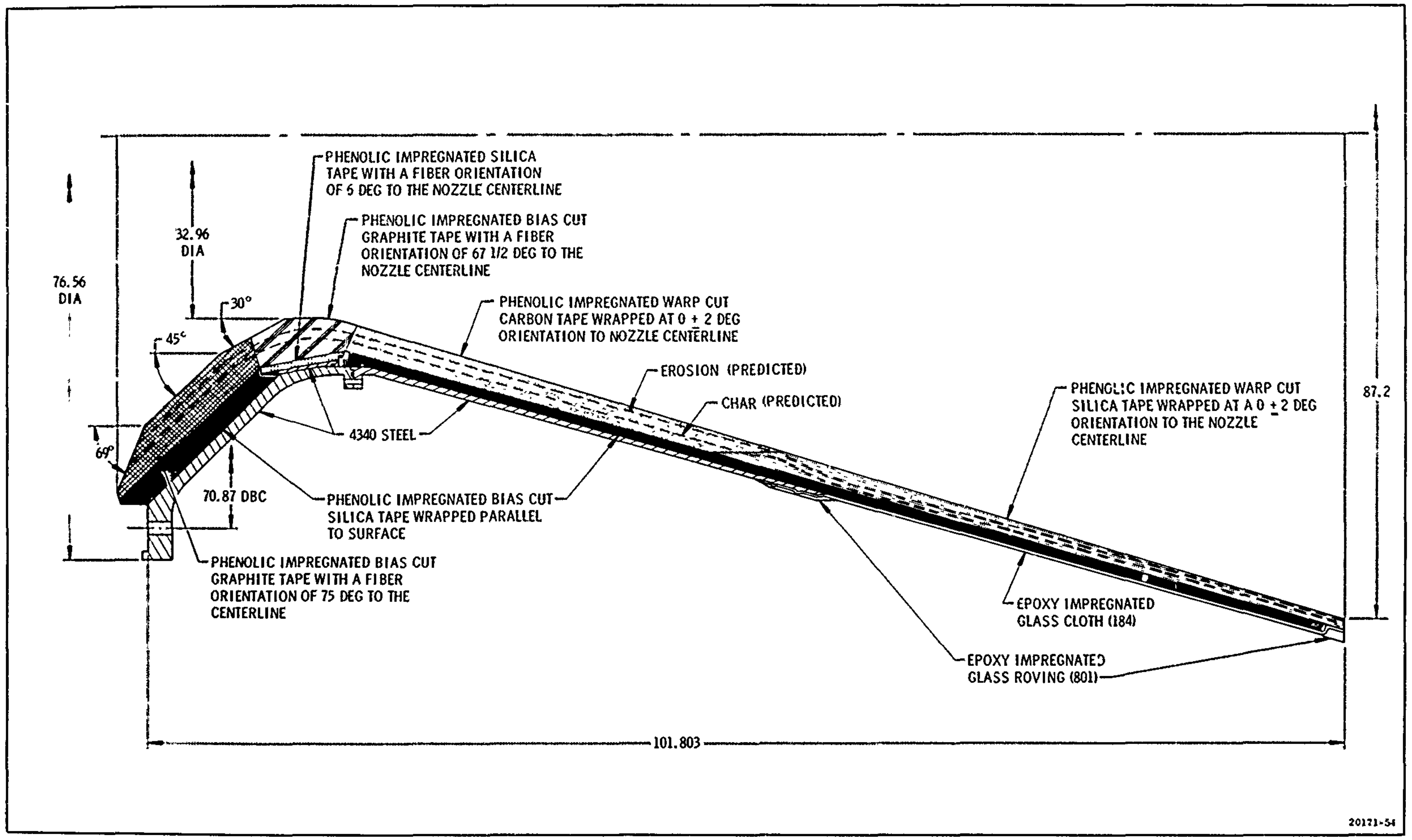

(U) Figure 130. 156-8 Nozzle Design

(U) 4. DESIGN REQUIREMENTS

Throat Diameter, Initial (in.)	32.96
Expansion Ratio, Ae/A_t, Initial	7:1
Chamber Pressure, Maximum (psia)	1,200
Dynamic Forces (g's)	
Lateral	3
Longitudinal	5
Burning Time (sec)	120

(U) 5. STRUCTURAL CHARACTERISTICS

(U) Details of the structural analyses of the nozzle performed by TRW and the structural characteristics resulting from these analyses are given in the Manufacturing Process Development Program Final Report AFML-TR-65-345, pages 11-1 thru 11-18. Structural characteristics of the motor case-nozzle interface resulting from analyses performed by Thiokol are shown in Figure 131. Original stress analysis on this interface was based on an MEOP of 880 psia and was not corrected to the refined MEOP of 854 psia.

(U) 6. INSULATION MATERIALS

(U) Vendor materials and properties are given in Table XLIV.

Graphite Cloth Phenolic	Throat approach Throat insert
Carbon Cloth Phenolic	Throat extension
Silica Cloth Phenolic	Throat approach insulator Throat insert insulator Exit cone extension Exit cone overwrap

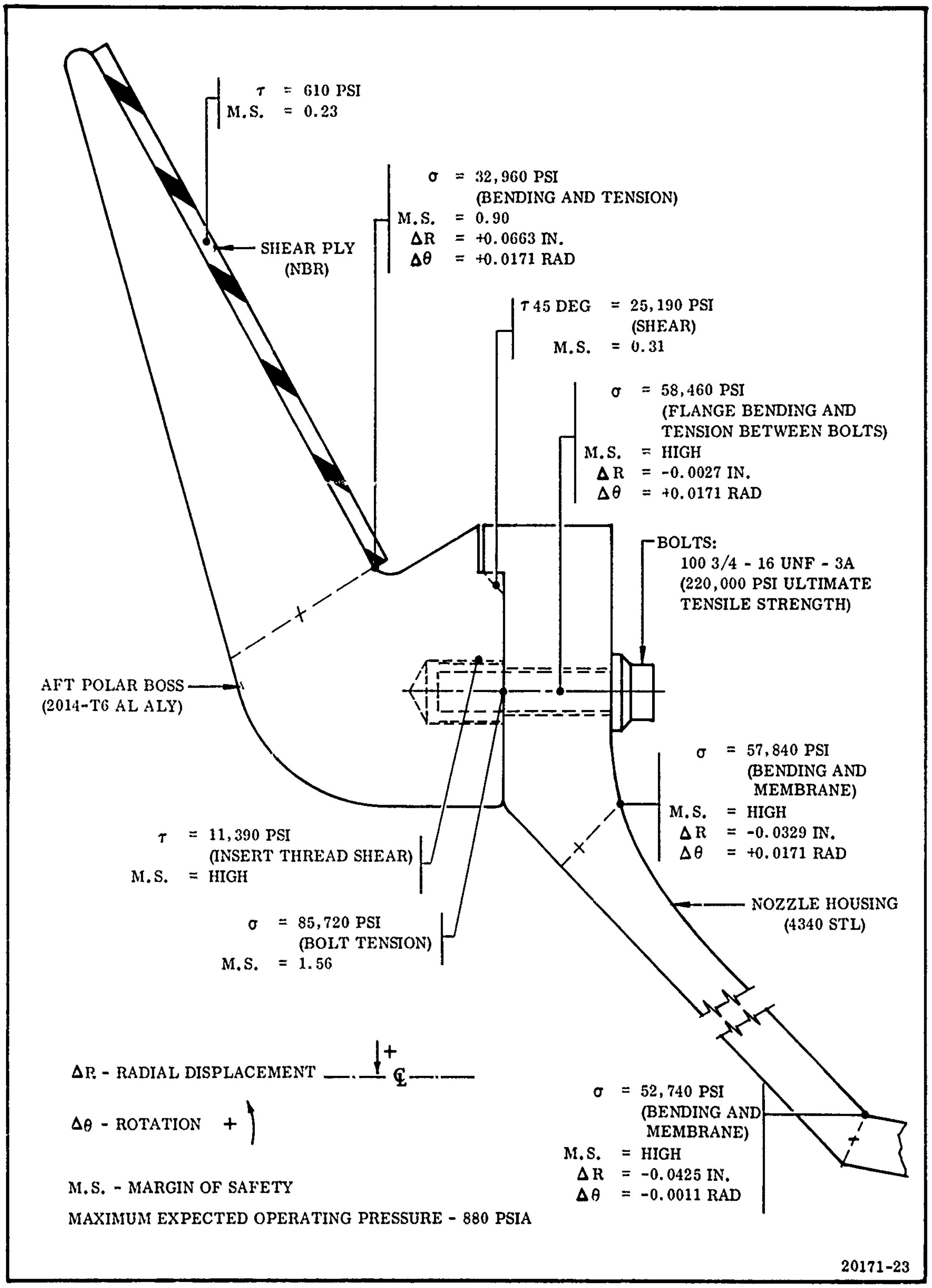

(U) Figure 131. 156-8 Stress and Deflection at Nozzle Attachment

TABLE XLIV

(U) PHYSICAL PROPERTY TEST RESULTS FOR FULL SCALE NOZZLE COMPONENTS

Nozzle Component	Material	Specific Gravity	Acetone (%)	Volatile (%)	Edgewise Compression
Throat Insert	FM5014G* with Basic	1.430	0.05	2.17	14,493
	Carbon Graphite Fabric	1.440	0.16	2.58	22,700
Throat Insert	FM5131* Silica Phenolic	1.730	0.14	2.89	--
Insulator		1.760	0.24	4.00	--
Throat Approach	FM5014G* with Basic	1.430	0.01	2.37	16,470
	Carbon Graphite Fabric		0.09	2.39	17,990
Throat Approach	FM5131* Silica Phenolic	1.740	0.24	0.22	--
Insulation			0.29	0.41	--
Throat Extension	Fiberite** MX4926 Carbon	1.415	0.26	1.37	46,200
	Phenolic	1.417	0.27	1.54	49,600
Exit Cone	FM5131* Silica Phenolic	1.690	0.37	2.20	23,400
Extension		1.740	0.55	2.37	23,900
Exit Cone	FM5131* Silica Phenolic	1.690	0.50	3.11	13,700
Insulator		1.740	0.65	5.30	14,480

*U.S. Polymeric, Santa Ana, California.
**Fiberite Corp., Winona, Minnesota.

Bonding Materials and Usage

Fabrication adhesive (Cured components to uncured wraps)	Narmco 2034
Bonding (Cured plastic components to each other and to steel)	Steel Epon 913 and 919 Adhesives
(Throat module to exit cone module)	RTV Silicone Rubber

Potting Material

(Between inlet and throat insert)	RTV Silicone Rubber

(U) 7. STRUCTURAL MATERIALS

AMS4340 Steel (Ultimate tensile 200,000 psi)	Inlet throat housing Throat support housing
MIL-S-16216 (HY-100) Steel (Ultimate tensile 128,000 psi)	Exit cone (throat extension) housing
Epoxy impregnated glass roving (Tensile strength of control specimens (ASTM-D-638) = 28,300 psi to 30,100 psi warp direction)	Exit cone structural overwrap

(U) 8. MATERIAL PROPERTY SUMMARY

(U) The design review of the nozzle by Thiokol covers the physical and thermal properties of the nozzle materials.

(U) Predicted nozzle erosion and char layer profiles are based primarily on empirical data obtained on large motor firings.

(U) Thiokol data on nozzle ablative and insulation material properties are given in Table XLIV. A summary of the physical property test results reported by TRW on nozzle components are given in Table **XLV** . Prediction of the temperature profiles at the nozzle throat are given on Figure 132.

(U) The convective heat transfer coefficient vs nozzle area ratio is given on Figure 133. The erosion rate vs the convective heat transfer coefficient for graphite or carbon cloth phenolic and for silica cloth phenolic are given on Figures 134 and 135, respectively.

(U) B. NOZZLE FABRICATION

(U) Fabrication of the 156-8 nozzle was accomplished in two modules: a throat module and an exit cone module. The two modules were bonded and bolted together to form the nozzle assembly.

(U) The nozzle was produced by processes which did not require the use of hydroclave, autoclave, or matched die facilities during the curing operation. This was accomplished by using a pretensioned nylon overwrap over uncured components which generated a pressure on the layup during the curing process simulating the hydrostatic pressure obtained during hydroclave cure. (Axial strips were placed over the uncured components as part of the overwrap process before they were wrapped with pretensioned nylon.)

(U) The throat housing and the throat support ring were machined from 4340 steel forgings and then heat treated. The throat extension housing was machined from HY-100 steel.

(U) The inlet contour of the nozzle consists of a series of truncated cones and was apparently developed to facilitate fabrication of the ablative plastic parts. Phenolic impregnated graphite cloth was used in the entrance, throat, and throat extension sections. The graphite cloth entrance and throat section components

TABLE XLV

(U) NOZZLE ABLATIVE AND INSULATION MATERIAL PROPERTIES AT ROOM TEMPERATURE

Property	Graphite Cloth Phenolic	Carbon Cloth Phenolic	Silica Cloth Phenolic	Glass Cloth Phenolic
Thermal Conductivity, (Btu/in./ft^2/°F)	6.0 to 8.0	3.2	2.1	1.97
Specific Heat (Btu/lb/°F)	0.26	0.25	0.24	0.22
Linear Coefficient Thermal Expansion (in./in./°F x 10^6)	4.5 to 7.5	4.5 to 8.0	4.6 to 6.0	6.0
Ultimate Flexural, Minimum (psi)	20,000	25,000	20,100	55,000
Flexural Modulus, Minimum (psi x 10^6)	1.8	2.35	2.25	3.5
Ultimate Tensile, Minimum (psi)	10,000	15,000	12,000	45,000
Tensile Modulus, Minimum (psi x 10^6)	1.60	2.0	2.0	3.5
Compressive Modulus, Minimum (psi x 10^6)	1.75	2.0	2.0	3.0
Compressive Strength, Minimum (psi)	10,500	25,000	20,000	35,000
Specific Gravity, Minimum	1.40	1.37	1.70	1.80
Tape Breaking Strength, Minimum (lb)	50	40	50	250
Organic Resin Solids, Maximum (%)	36	36	36	36
Volatiles Range, Maximum (%)	2.0	2.0	2.0	2.0
Poisson's Ratio	0.26	0.25	0.25	0.23

NOTE: U.S. Polymeric No. 39 Resin was used in all four materials.

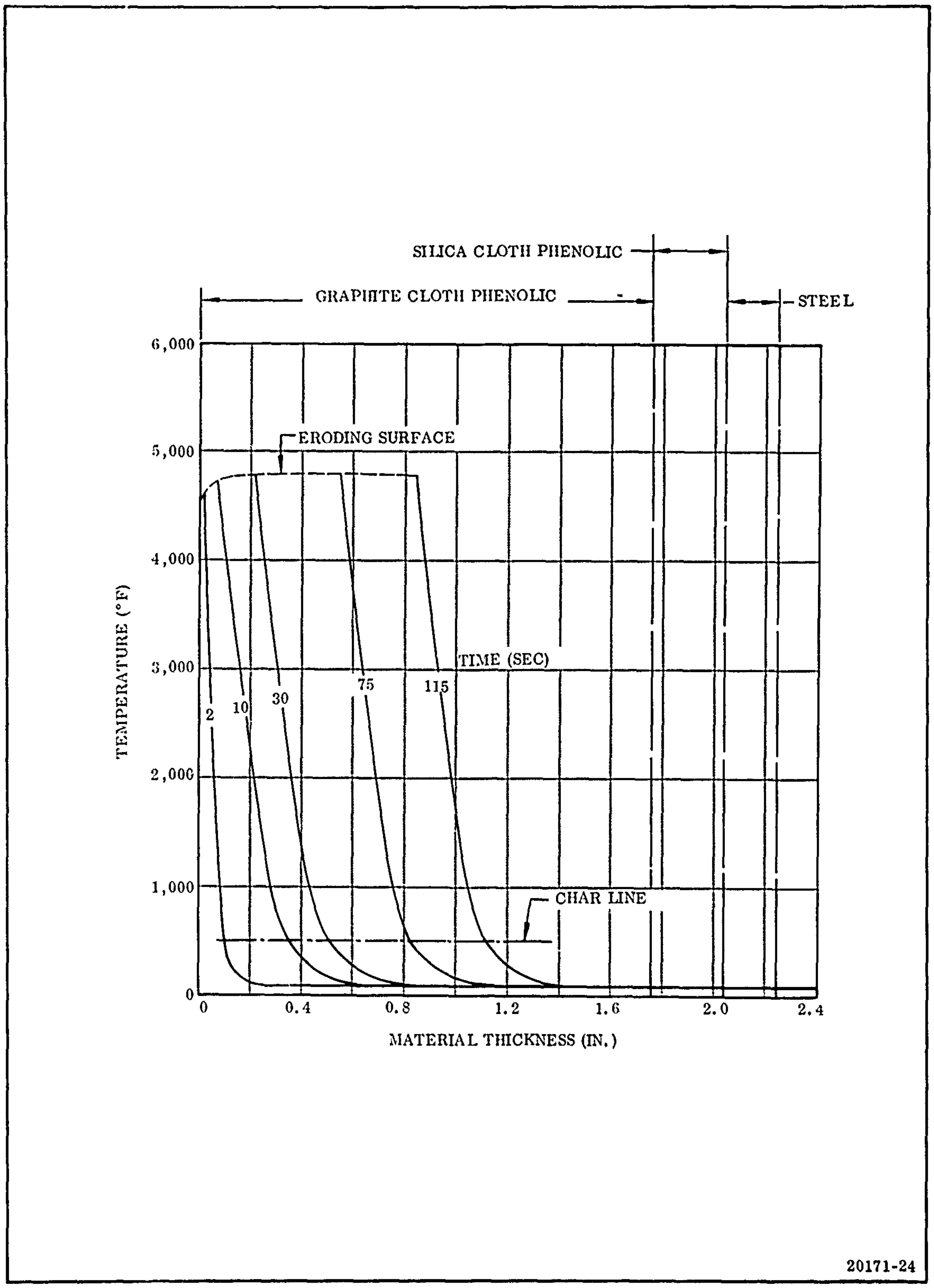

(U) **Figure 132. Temperature Profiles at 156-8 Nozzle Throat Centerline**

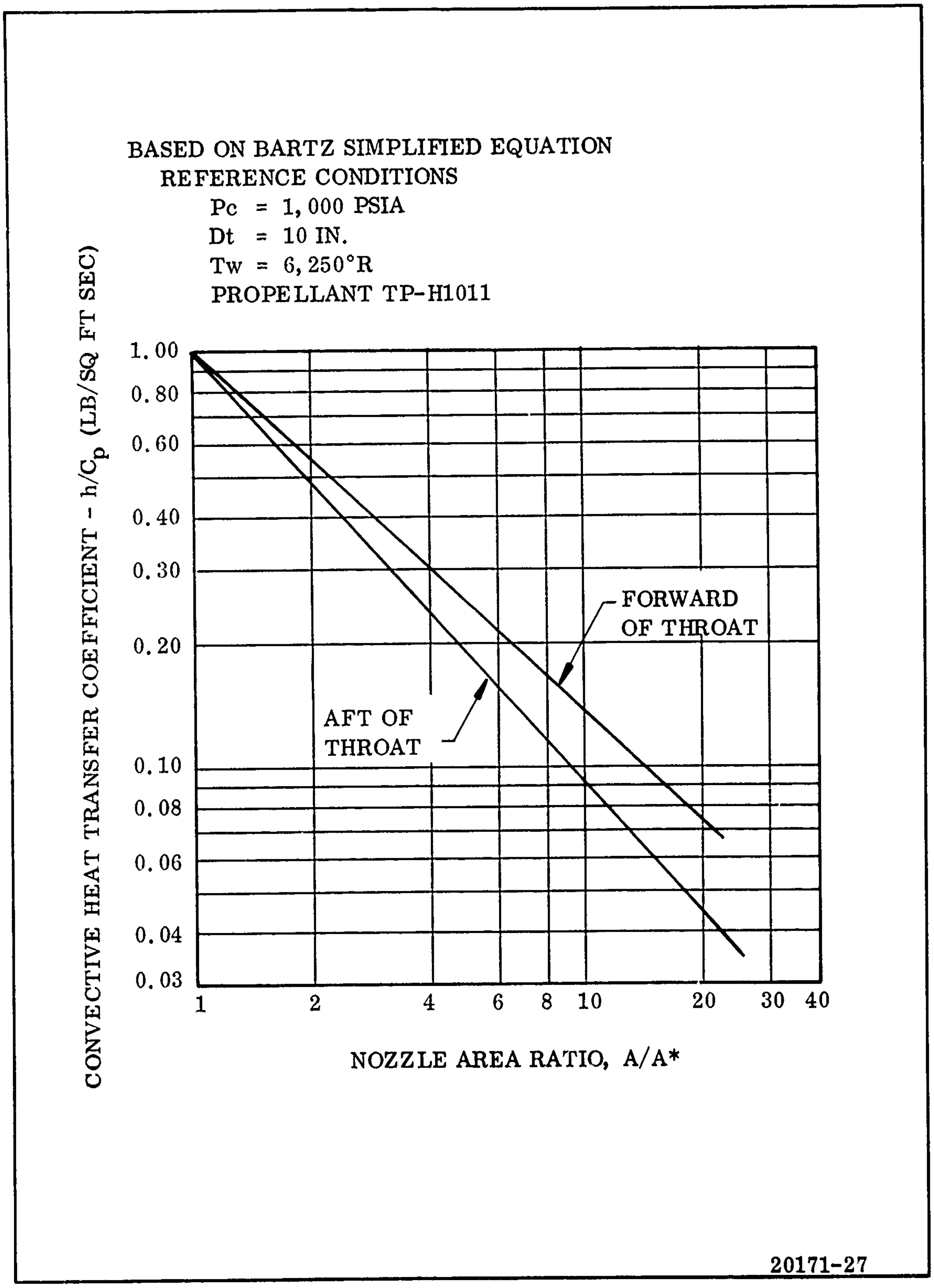

(U) Figure 133. Convective Heat Transfer Coefficient vs Nozzle Area Ratio

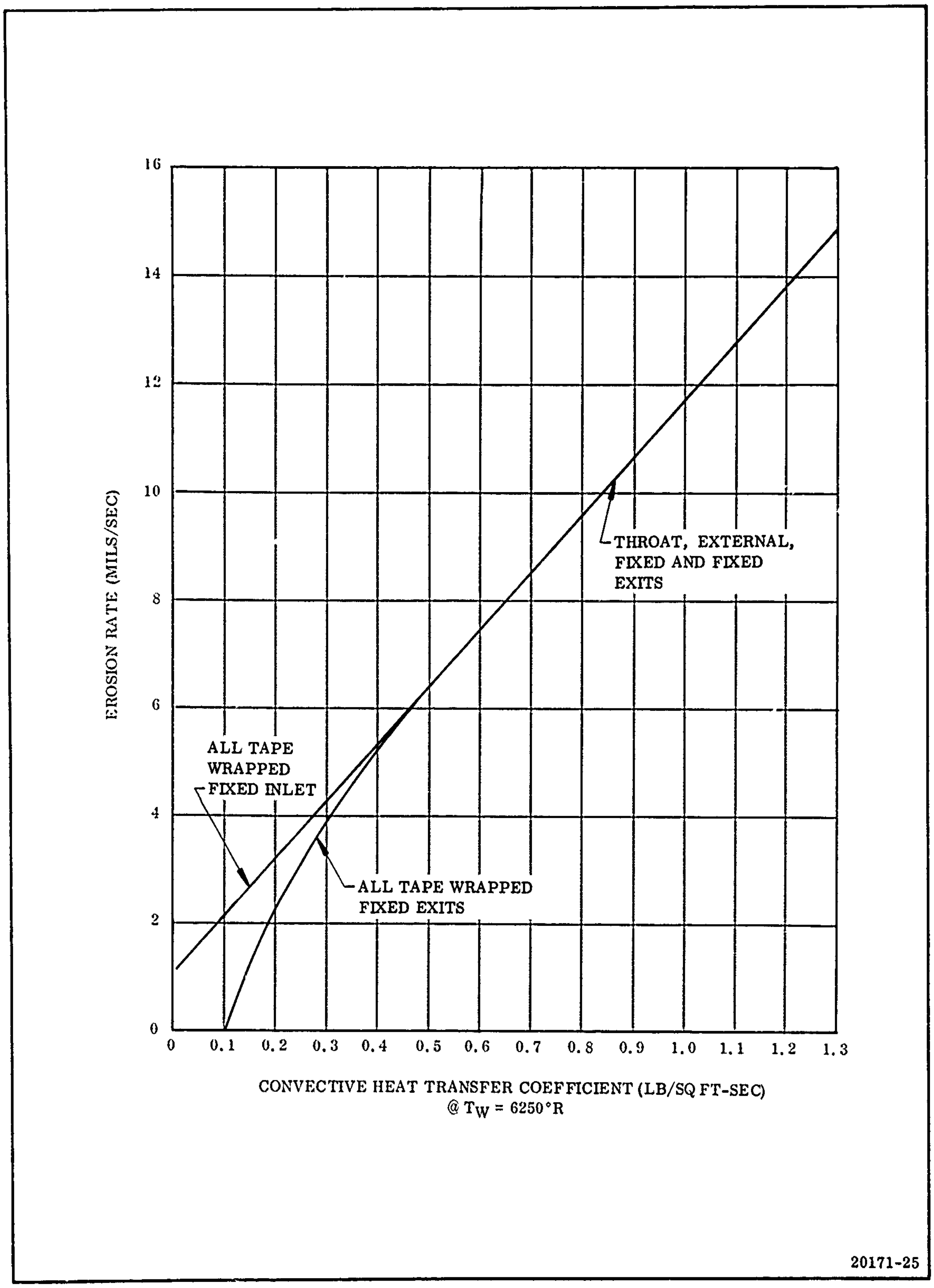

(U) **Figure 134. Relationship of Erosion Rate to Convective Heat Transfer Coefficient for Graphite or Carbon Cloth Phenolic**

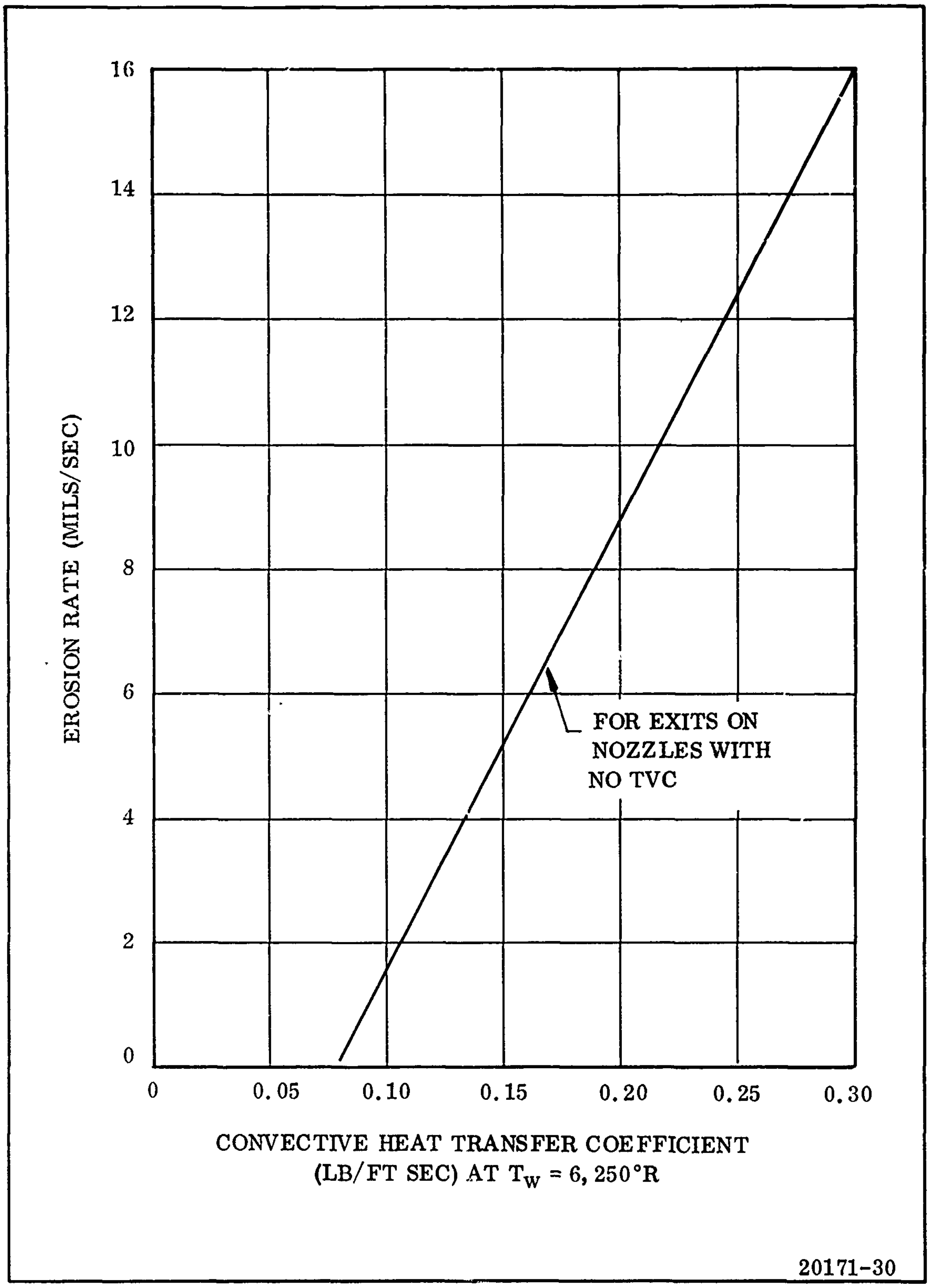

(U) Figure 135. Silica Cloth Phenolic Erosion Rate vs Convective Heat Transfer Coefficient were insulated with phenolic impregnated silica fabric tape components which are supported and retained by a high strength 4340 steel forging.

(U) The throat support sleeve was bonded to the throat insert with Epon 913 adhesive and the aft face machined. This subassembly was then bonded into the inlet housing with Epon 919 adhesive. The forward face and internal diameter of the throat and the aft face of the inlet plastic were machined. The inlet plastic assembly was molded to contour, dry stacked, and bonded in place with Epon 913 adhesive. The joint between the inlet and throat insert was potted with RTV silicone rubber.

(U) The exit cone plastic assembly fabrication was performed in two principal operations. The liner portion of the exit cone was laid up parallel to the nozzle centerline for the complete liner from phenolic impregnated warp cut carbon tape for the throat extension portion and from phenolic impregnated warp cut silica tape for the exit cone extension portion of the liner. The liner component was overwrapped with pretensioned nylon and oven cured. The cured liner assembly was then machined and overwrapped parallel to the machined surface with epoxy impregnated glass cloth. The glass cloth was overwrapped with pretensioned nylon and oven cured.

(U) The exit cone plastic assembly was bonded to the steel throat extension housing with Epon 913. A structural overwrap was applied to the exit cone as shown on the nozzle drawing using 801 glass roving and a room temperature curing resin.

(U) The completed throat and exit cone modules were joined together by bonding and sealing the plastic interfaces with RTV silicone rubber and by bolting together the steel mating flanges.

(U) C. NOZZLE PERFORMANCE ANALYSIS

(U) In the review of previous analyses of case nozzle insulation at the motor/ nozzle interface, it was felt that case insulation thickness at this point was marginal and therefore additional thickness was added. This additional thickness resulted in a hump or sharper change in contour of the flow surface at the case/nozzle interface. A flow analysis was made of the aft case to nozzle throat section utilizing the computerized flow net program to obtain convective heat transfer coefficients, predicted erosion profiles, and local wall Mach number profiles. Computer runs were made for zero burning time and 100 percent burning time. The results (Figures 136 and 137) show some variation in the heat transfer coefficient and wall Mach number for 0 percent burning time and reflect the flow acceleration-decelerations and change in boundary layer thickness along the changing contour. The 100 percent burning time plots show a smoothing or reduction in variation reflecting the eroding of abrupt surface contour changes into a smoother contour form. No discontinuities are evident in the plots, therefore showing that flow separation and reattachment would not occur and that satisfactory flow conditions would be maintained. The erosion profile predicted from the flow net results is shown superimposed on the figures.

(U) Erosion and char depths throughout the nozzle were calculated using methods developed by Thiokol from the study and analysis of a large number of materials and nozzle tests. The Thiokol predictions of erosion vary somewhat from those of TRW but are generally in good agreement. The TRW values and Thiokol calculated values, tabulated for comparison, are shown in Table XLVI.

(U) Depth of char into the exit cone liner material and the depth below char to ambient temperature point were also calculated and profiles drawn (Figure 138). As can be seen, adequate material thicknesses existed in the design to withstand the erosion and thermal environment with ample margins of safety.

(U) The analysis shows that no heating should be experienced on the exterior of the nozzle exit cone through transfer of heat from the exhaust gases and; therefore, temperatures registered by the exterior thermocouples along the cone should remain at or very near ambient levels.

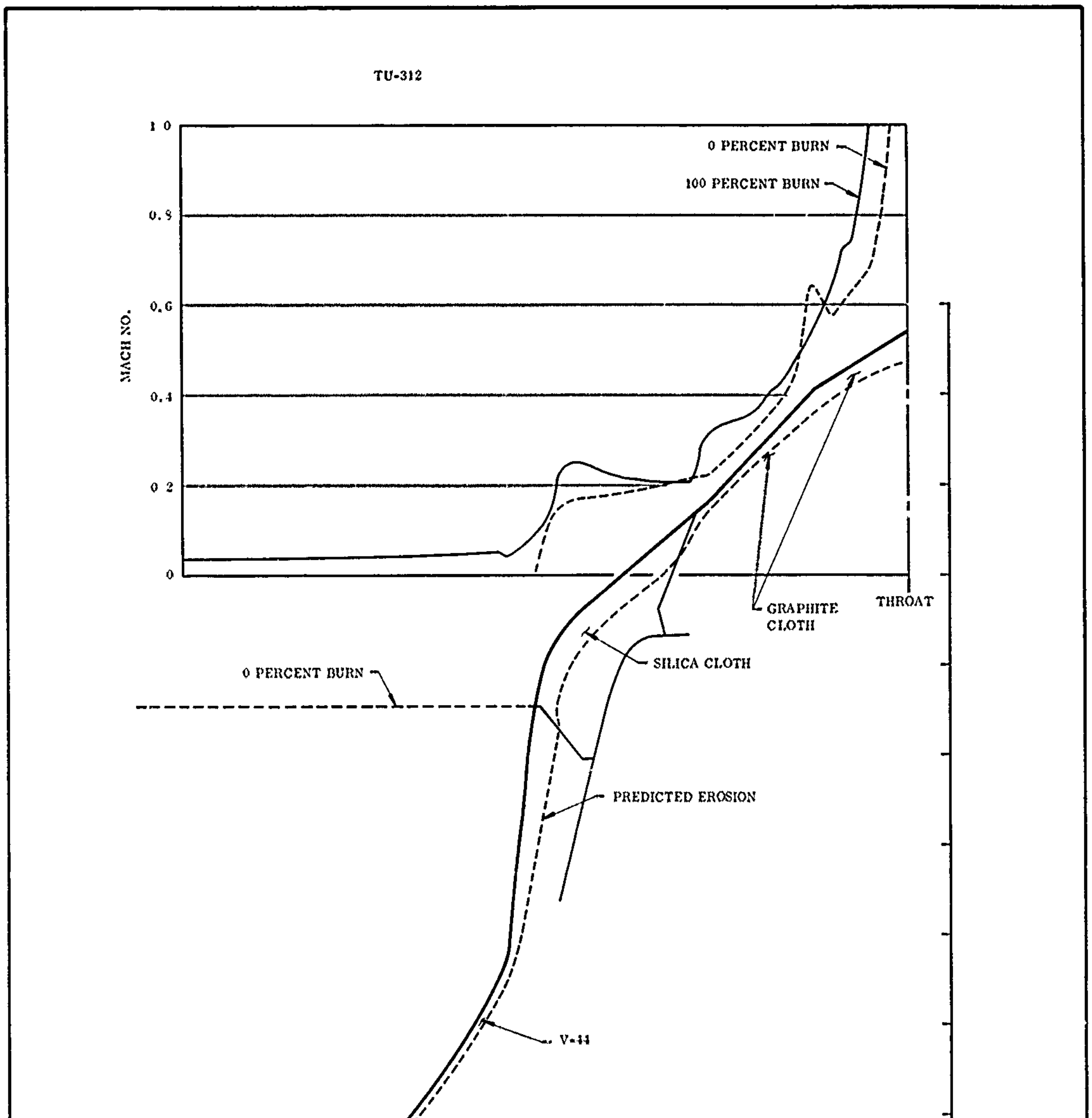

(U) Figure 136. Wall Mach Number vs Axial Position, Aft Case and Nozzle Inlet

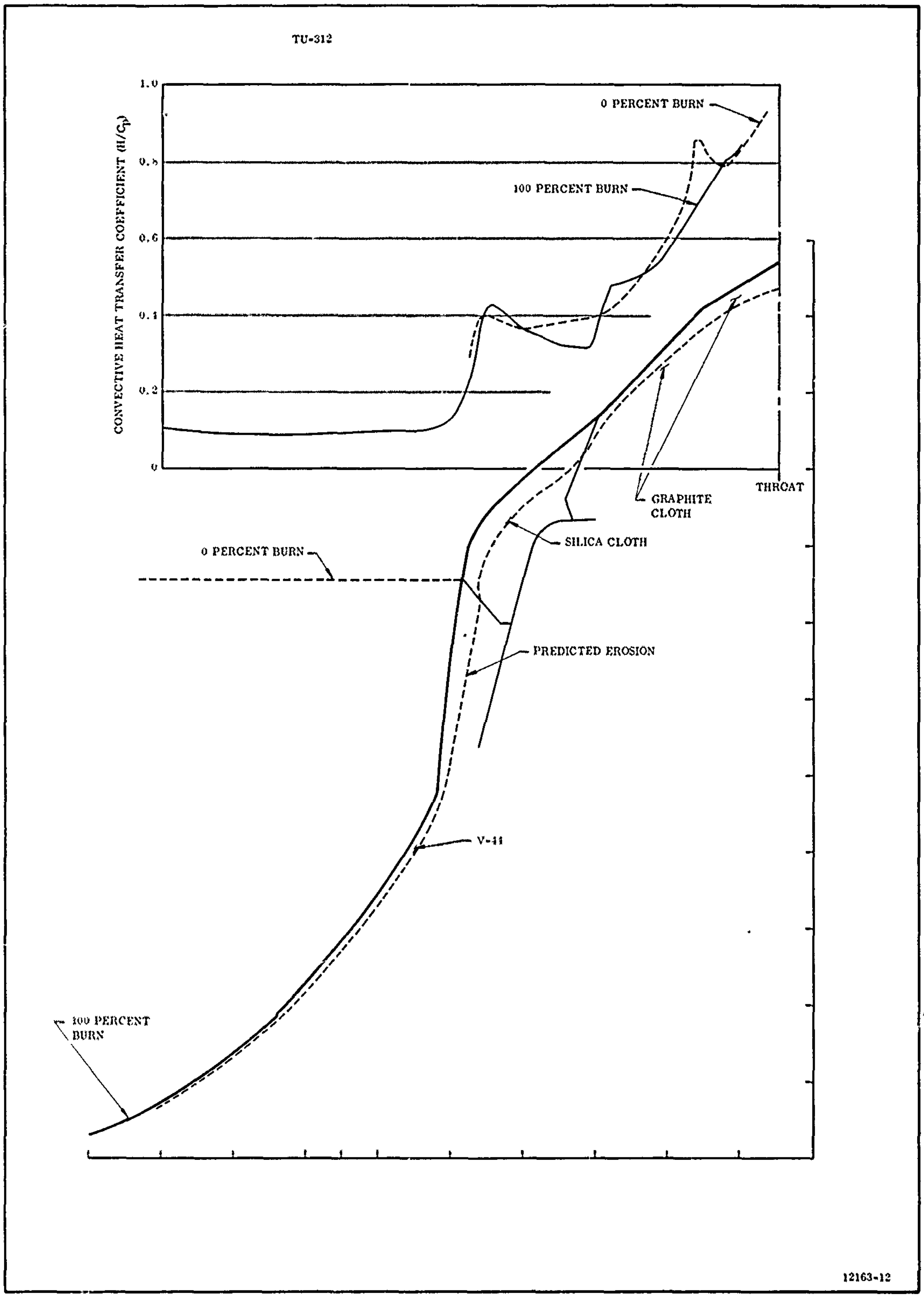

(U) Figure 137. Convective Heat Transfer Coefficient vs Axial Position, Nozzle Inlet

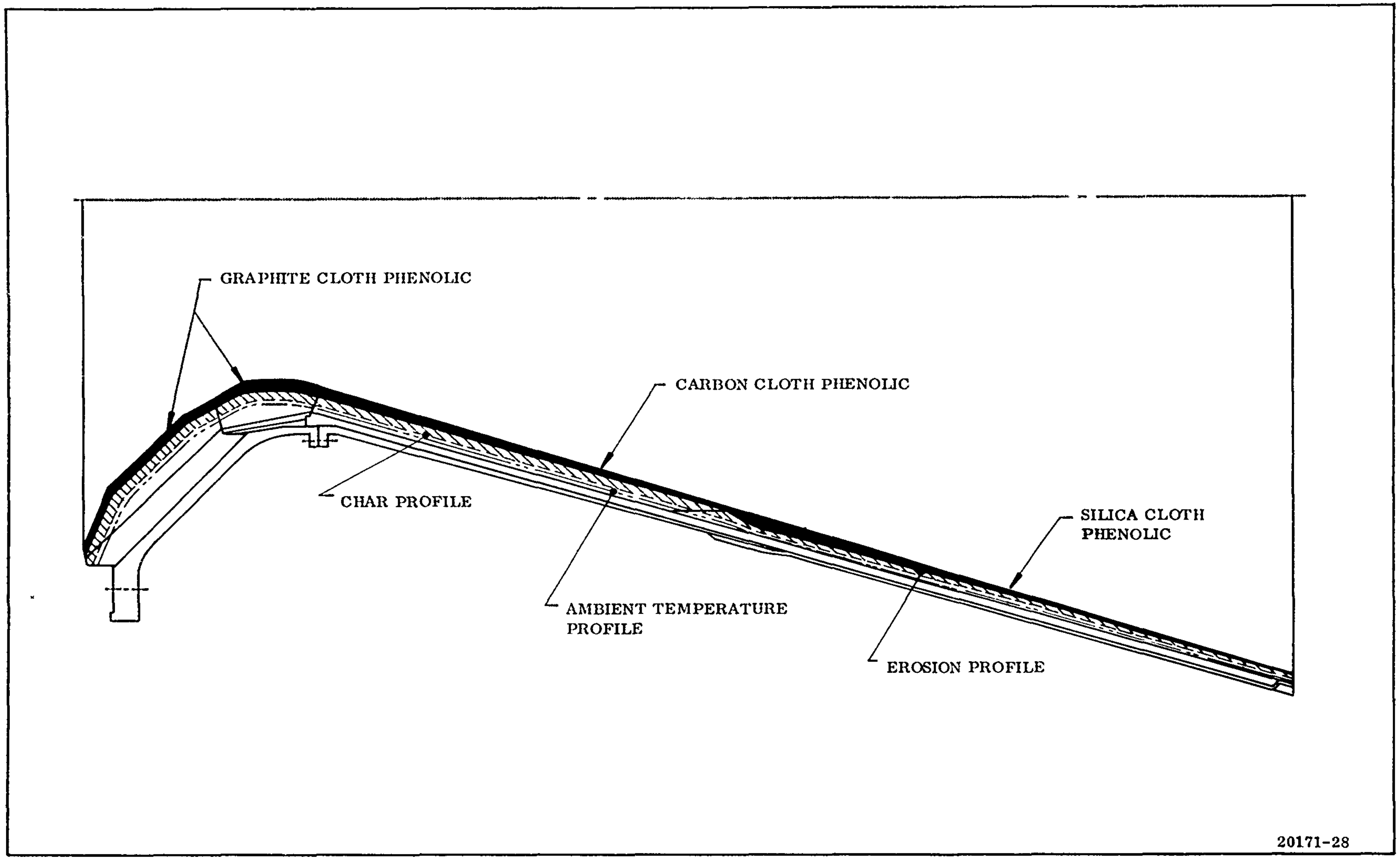

(U) Figure 138. Predicted Erosion, Char, and Ambient Temperature Profiles for 156-8 Nozzle

TABLE XLVI

PREDICTED EROSION COMPARISON

Thiokol Analysis			TRW Report		
Area Ratio	Depth (in.)	Rate (mil/sec)	Area Ratio	Depth (in.)	Rate (mil/sec)
-2.520	0.433	3.61	-1.800	0.665	5.54
-1.400	0.720	6.00	-1.130	0.809	6.74
1.000	0.910	7.57	1.000	0.998	8.42
1.260	0.734	6.12	1.059	0.746	6.22
2.030	0.432	3.60	1.200	0.606	5.05
3.000 (Carbon)	0.252	2.10	2.300	0.504	4.20
3.000 (Silica)	1.000	8.40	3.480	0.760	6.34
3.215	0.890	7.40	4.000	0.600	5.00
4.900	0.340	2.80	7.000	0.276	2.30
7.000	0.020	0.15			

(U) D. NOZZLE INSPECTION

(U) Upon receipt at Thiokol, the nozzle shipping container was opened and the nozzle exterior visually inspected. No discrepancies or damages were found.

(U) The nozzle was lifted and broken over with the handling fixture into a horizontal position and all interior surfaces given a thorough visual inspection. No cracks, delaminations, separations, or other discrepancies were noted other than some minor surface gouging on the exit cone inner surface. These indications were carefully checked and judged to be caused by either a dull tool or tool chatter during final true-up and clean-up machining of the cone inside surface. These gouges, although giving the cone surface a slightly rough appearance, were not of a magnitude sufficient to affect cone performance or integrity.

(U) Dimensional inspection was made of the nozzle inlet and motor interfacing area to verify compatibility with the motor case. In addition, the throat diameter and diameter 0.5 in. upstream of the exit cone end were checked. The dimensions inspected are shown in Figure 139 and results of the inspection are shown in Table XLVII. Because considerable time elapsed after nozzle arrival at Thiokol and test, inlet throat and exit cone diameters were measured just prior to testing (Table XLVIII). No significant differences can be seen between these values and those taken just after fabrication. No discrepancies were found and it appears that no physical change had taken place in the nozzle or its components after fabrication was completed.

(U) An evaluation was made to determine whether the nozzle had experienced any aging shrinkage or degradation. Visual inspection revealed no cracks or separations at any of the bondlines. Close attention was given to the bondlines between the plastic and steel. Any significant shrinkage would certainly be evident in these areas of a part of this size. A comparison of two diameters was made (Table XLVIII) with no indication of shrinkage. Only two dimensions were comparable between

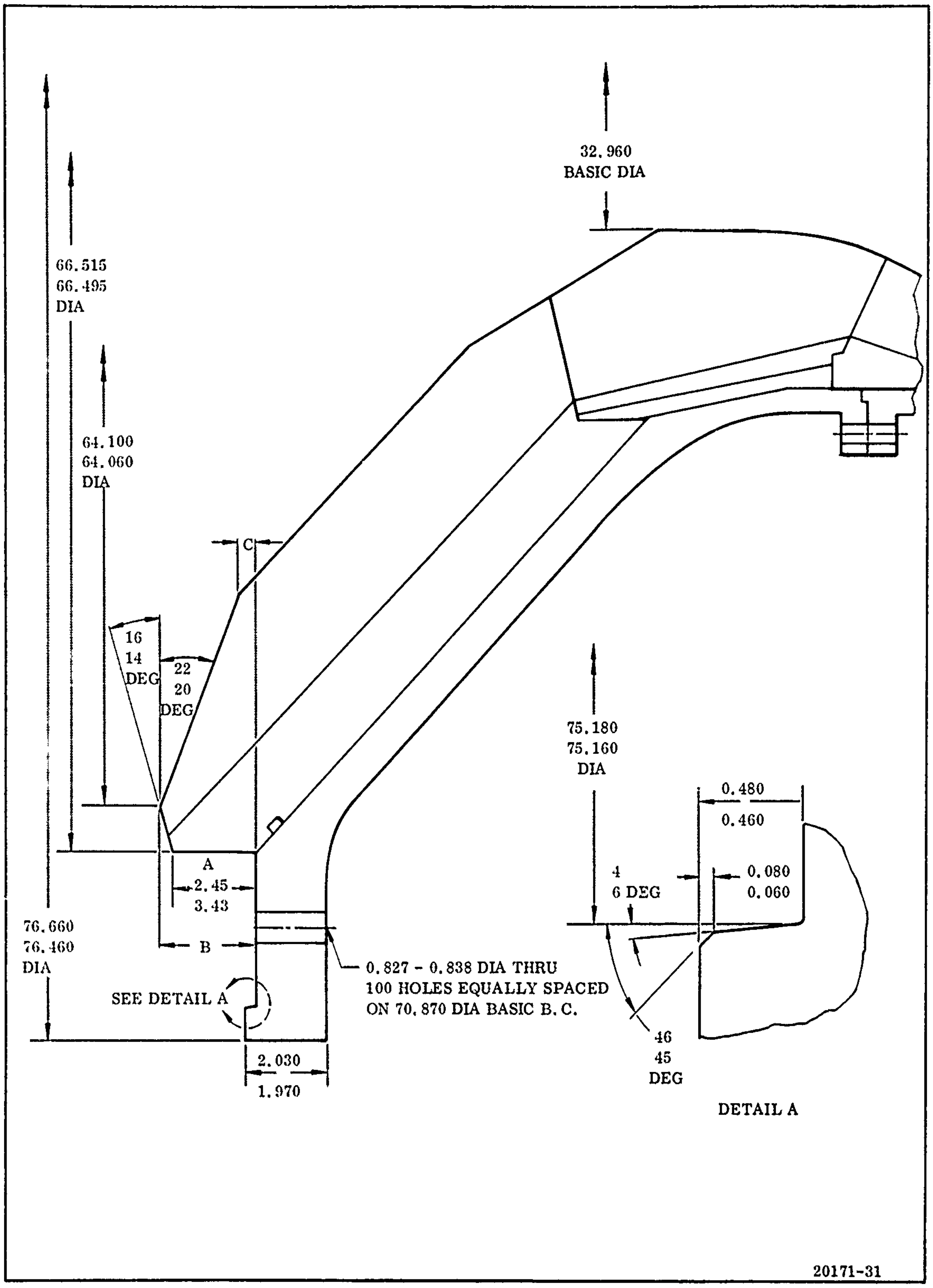

(U) Figure 139. Nozzle Inspection Points

TABLE XLVII

(U) NOZZLE INSPECTION RESULTS

Inspection Characteristic	Drawing Dimension	Tolerance	Actual at Delivery	
Diameter (in.)	76.660	Maximum		
	76.460	Minimum	76.52	
Diameter (in.)	75.180	Maximum		
	75.160	Minimum	75.178	
Angle (deg)	16	Maximum		
	14	Minimum	16	
Angle (deg)	22	Maximum		
	20	Minimum	20	
Angle (deg)	46	Maximum		
	44	Minimum	45	
Angle (deg)	6	Maximum		
	4	Minimum	4.5	
Dimension (in.)	2.45	Maximum	2.450	
	2.43	Minimum	2.448	
Dimension (in.)	2.030	Maximum	2.015	
	1.970	Minimum	2.012	
Dimension (in.)	0.080	Maximum		
	0.060	Minimum	0.073	
Dimension (in.)	0.480	Maximum	0.467	
	0.460	Minimum	0.467	
Hole Diameter, 100 holes (in.)	0.838	Maximum	0.830	
	0.827	Minimum	0.827	
			deg	in.
Dimension "C", four measurements	Record		0	0.478
			90	0.472
			180	0.477
			270	0.481

TABLE XLVII (Cont)

(U) NOZZLE INSPECTION RESULTS

Inspection Characteristics	Drawing Dimension	Tolerance	Actual At Delivery deg	Actual At Delivery in.	Actual Prior to Test deg	Actual Prior to Test in.
Dimension "A", four measurements*	Record		0	2.448		
			90	2.450		
			180	2.450		
			270	2.448		
Dimension "B", four measurements*	Record		0	2.763		
			90	2.760		
			180	2.758		
			270	2.766		
66.515 66.495 dia four measurements	Record		0	66.500	0	66.503
			45	66.498	45	66.491
			90	66.503	90	66.502
			135	66.499	135	66.496
64.10 64.06 dia four measurements	Record		0	64.060		
			45	64.060		
			90	64.080		
			135	64.080		
Throat Diameter	Record 32.96	± 0.010	0	32.956	0	32.954
			45	32.950	45	32.954
			90	32.954	90	32.954
			135	32.957	135	32.954
Inside diameter of exit cone 0.5 in. forward of exit edge	Record 86.87	nominal	0	86.910	0	86.849
			45	86.806	45	86.840
			90	86.880	90	86.857
			135	86.894	135	86.871

*Ref Figure 139.

TABLE XLVIII

(U) NOZZLE DIMENSIONAL COMPARISON

	Blueprint	Thiokol Inspection Deg	Thiokol Inspection In.	TRW Inspection
Throat	32.960 In. Diameter, Basic	0	32.956	32.959
		45	32.950	
		90	32.954	
		135	32.957	
	66.515 In. Diameter	0	66.500	66.507
	66.495 In. Diameter	45	66.498	
		90	66.503	
		135	66.499	

the Thiokol inspection and TRW. All others were made using datum type measurements during fabrication and were not obtainable at Thiokol, or were dimensions covered or destroyed during assembly of the nozzle. A close comparison is not practical since maximums and minimums were not given in the TRW log book, and the interior of the nozzle was painted subsequent to the TRW measurements.

(U) Continuity checks of the strain gage and thermocouple instrumentation were made by Thiokol Test Department personnel, and all instrumentation was considered to be in satisfactory condition. Additional checkout of the instrumentation was made prior to static test of the motor and nozzle.

SECTION XI

MOTOR TRANSPORTATION

A. METHODS OF TRANSPORTATION

Inplant transportation of case segments (empty and loaded) was accomplished using the 156 in. motor transporter. In conjunction with the transporter, a modular pallet was used to facilitate transport and handling. This pallet, made up of smaller modules, was used as an aid in lining, insulating, and transporting motor segments. Rollers were provided to facilitate case segment rotation for insulating and lining. Tiedown devices, capable of handling segments weighing 300, 000 lb, were incorporated and were compatible with the segment process harness. The modular pallet was secured to the transporter by four adjustable tiedown devices.

The transporter developed for the 156 in. dia motor program (Figure 140) was a modified standard flatbed trailer, fabricated from high strength steel to reduce the tare weight. Compared to Minuteman transporters, the only unique feature of this rig was size. (Temperature control equipment and air suspension were not deemed necessary for segment transportation because of average climatic conditions; special equipment, therefore, was not required.) Although this transporter is not suited for general highway transport because of high axle loading (50, 000 lb per axle), the rig is highly maneuverable, and is, therefore, well adapted for inplant handling. The prime mover is a commercially available, heavy duty tractor, powered by a 335 hp turbocharged diesel engine.

The motor segments were transported individually throughout the process until after static test of the assembled rocket motor. After static test, the fired motor case was handled and transported as a monolithic unit, on the 156 in. motor transporter described earlier.

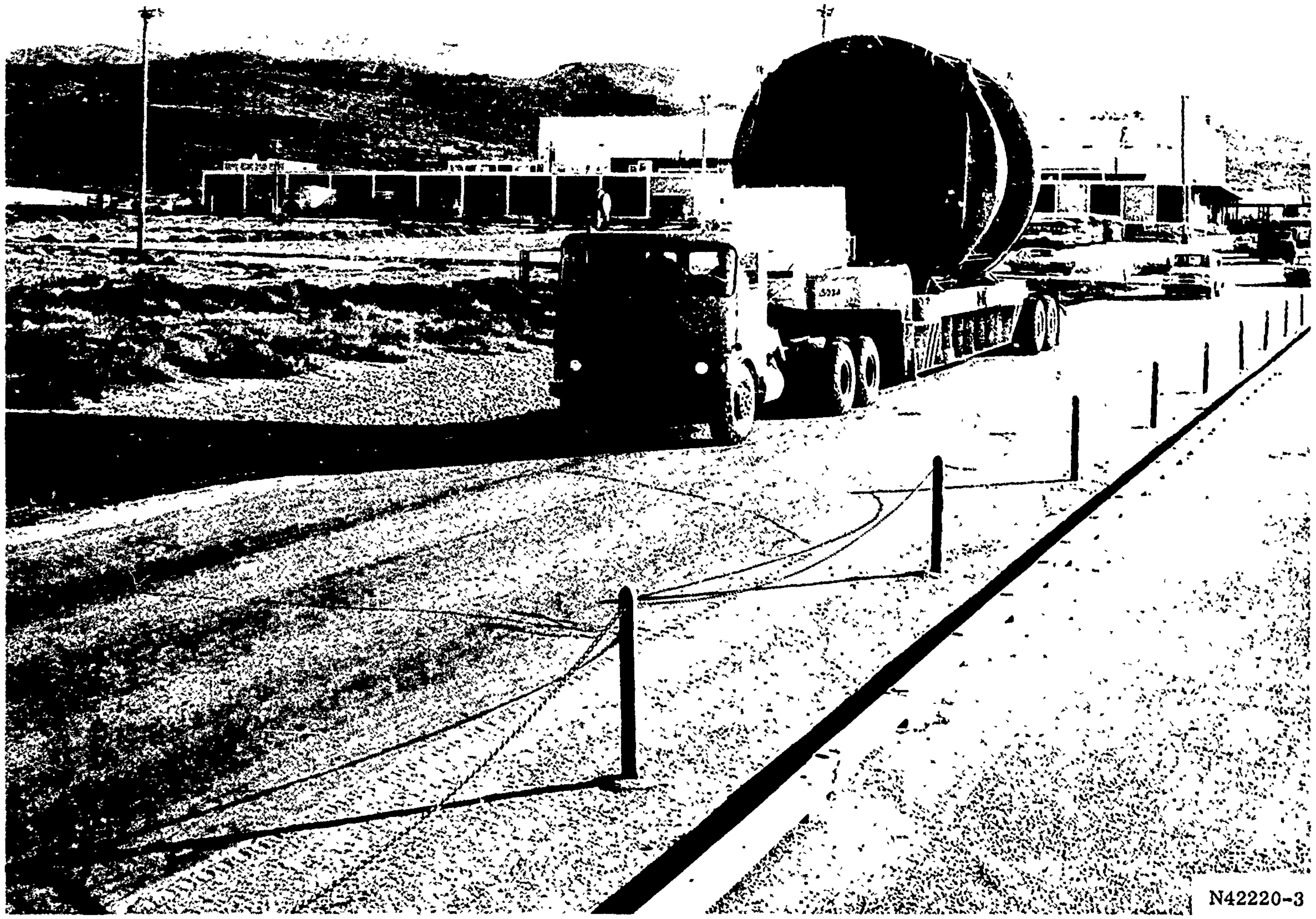

N42220-3

(U) Figure 140. 156 Inch Rocket Motor Transporter

B. ACCELERATION AND TEMPERATURE HISTORY DURING TRANSPORTATION

The loaded case segments were monitored for grain environmental temperature and g loads during transportation. The continuous recording hydrothermograph was placed in the grain. The high temperature recorded during transportation and storage was 98° F and the low was 24° F. These extreme temperatures were for only short periods of time and in no way reflected the actual grain temperature. These temperature extremes were not detrimental to the motor.

The g loads during transportation were monitored using accelerometers installed in accordance with Figure 141 on the forward and center segments. The maximum g loads were:

Segment	Accelerometer	Maximum g	Frequency (cps)
Forward	A 703	0.67	4.5
Center	A 702	0.35	4.0

These loads were not correlated to any specific road condition or speed. However, these data indicate normal transportation, using the Thiokol transporter, produces g loads far below any logical detrimental limits.

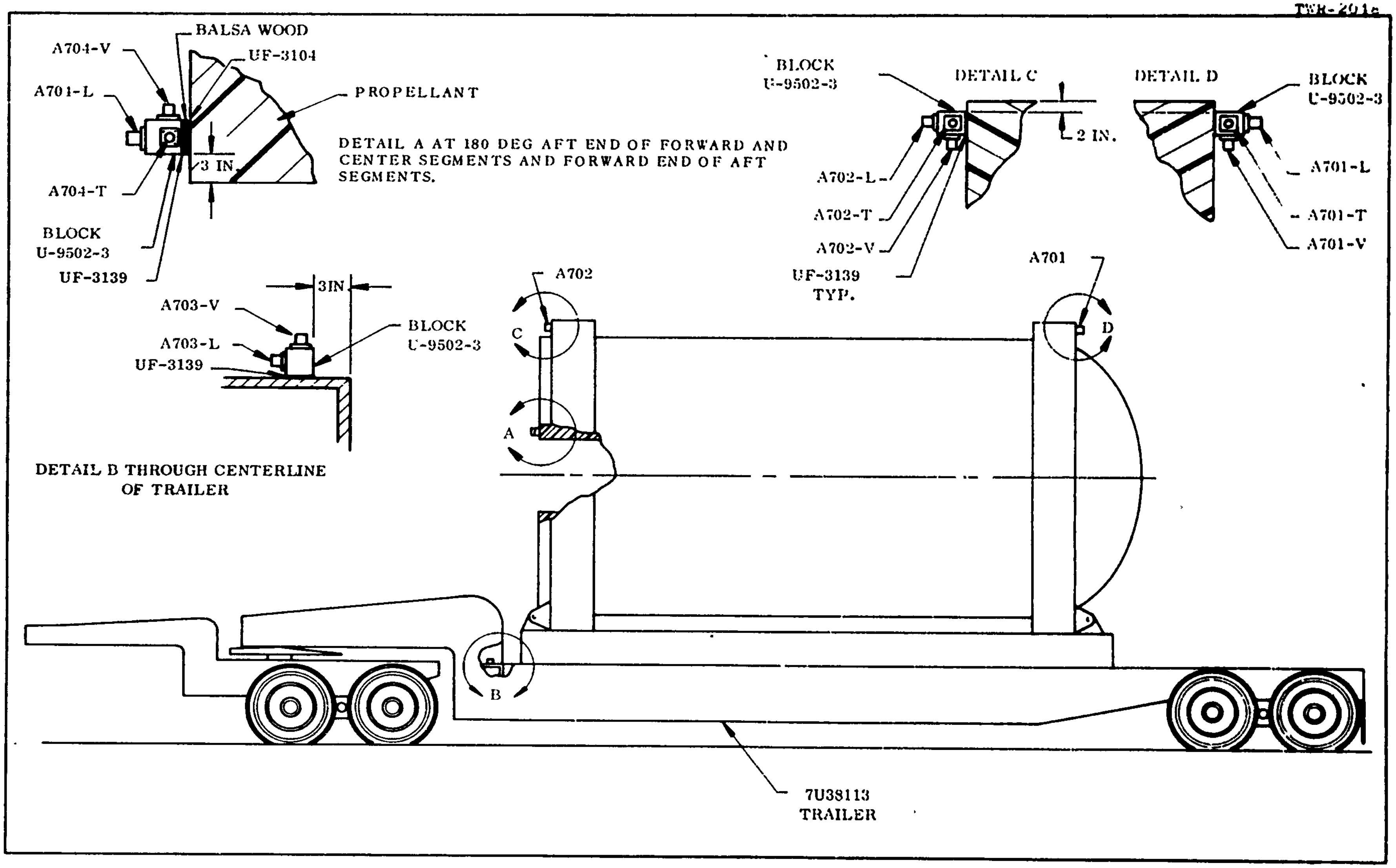

(U) Figure 141. Transportation Instrumentation Location

SECTION XII

(U) TOOLING

(U) A. MANUFACTURING TOOLING

(U) 1. HANDLING HARNESS

(U) The process harness (Dwg 2U25191) used to handle the 156-8 motor segments both in the empty and loaded configurations is shown in Figure 142. This harness evolved from the Minuteman Stage I Production Harness. The same case rounding features were incorporated in this harness as in the Minuteman harness. Clevis brackets (four per ring) used for lifting and breakover are attached to the face of each ring. Brackets in place of trunnions were used to reduce the required lifting beam span and to decrease the ring deflection and torsional shear. Each ring (box construction) was fabricated from 1 in. thick ASTM A-36 steel plate. Each harness ring weighed approximately 10 tons.

(U) Two rings were placed on the skirt of the forward and aft segments and were secured with bracketry. Each of the four joint adapter rings was machined for attachment to the tang or the clevis of the motor case segment joint. These rings rested against the ends of the segment joint to provide full bearing support. The rings were attached after insulation installation and were removed immediately prior to motor assembly. The harness rings were tied together with 16 preloaded tierods to transfer the segment weight to the lower joint during lifting.

(U) The motor segment process harness was installed with the case segments in the upright position and held the case round to within 0.030 in. of a true circle when shoes on the harness were adjusted. (The close tolerance was required for horizontal motor assembly.) Case roundness was maintained by filling any gap between the

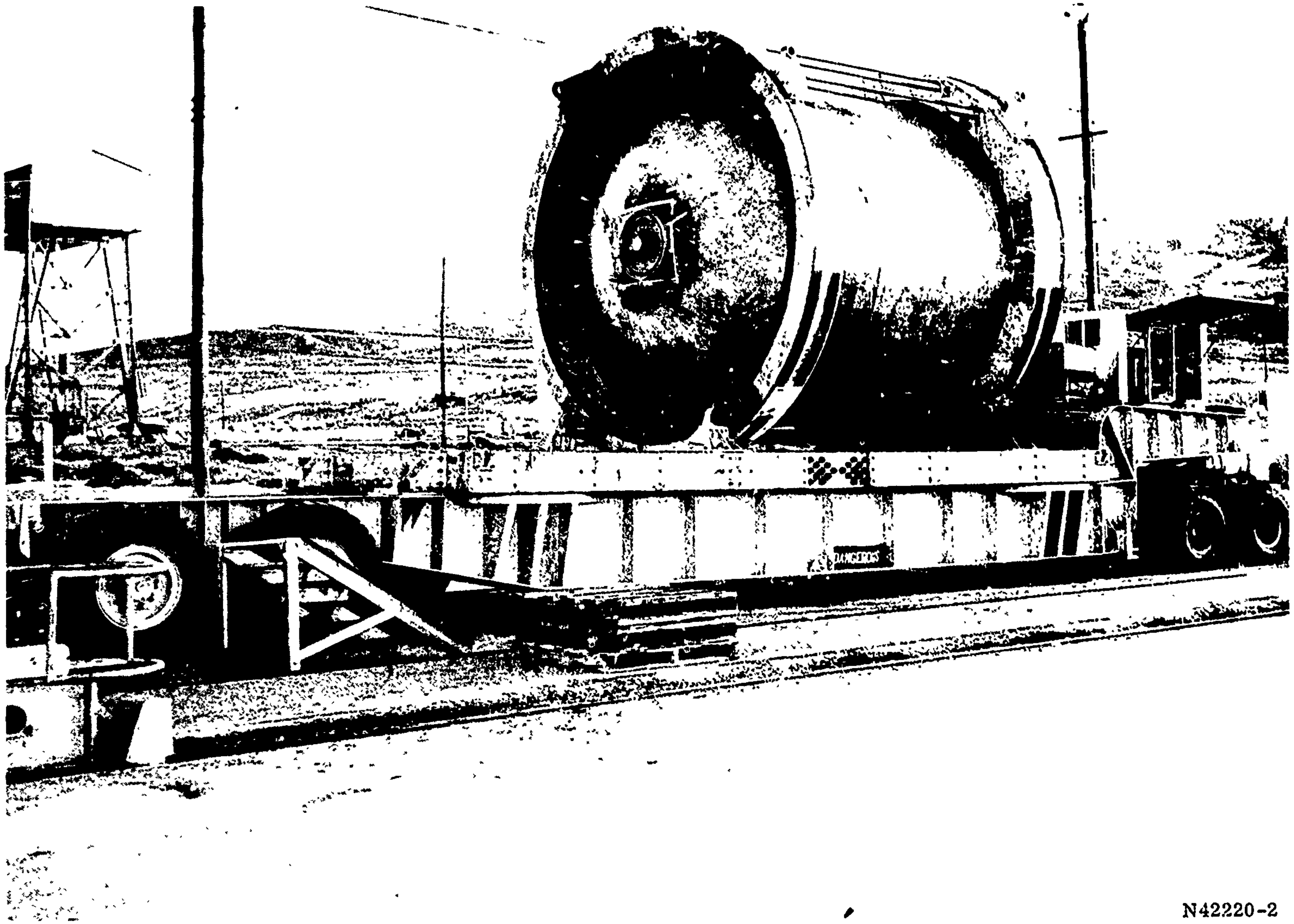

N42220-2

(U) Figure 142. 156-8 Handling Harness

harness and the case wall with an ambient-curing, epoxy compound (Epocast). The epoxy compound eliminated requirements for precise machining on the ID of the harness. Minor variations in tolerance from segment to segment were accommodated by varying the thickness of epoxy material. The harness OD had a machined surface so that the case could be rotated for cleaning and for installation of insulation material. This harness was compatible for use during all inplant motor processes and with all handling equipment.

(U) 2. INSULATION FABRICATION TOOLING

(U) Male molds for fabricating the case segment joint insulation were constructed in a 156 in. diameter autoclave. The autoclave was the center segment of the TU-412 (AF 156-1C) motor adapted with end closures and a heating element. The segment was positioned horizontally in the modular pallet (Figure 143) and fitted with a cable-winch assembly (Figure 144) to provide 360 deg rotation.

(U) A sweep template was fabricated in two configurations: (1) the contour of the ID of the clevis (female) joint area where insulation was required, and (2) the contour of the ID of the tongue (male) joint where insulation would be installed. The sweep template, mounted from the modular pallet, was positioned in the AF 156-1C center segment so the template was spring loaded against the end of the segment. Upon completion of layup, the end domes and heating unit were installed to complete the autoclave vessel.

(U) The AF 156-1 center segment was again used as a mold and autoclave combination for the forward and aft dome rubber insulation. The lower end dome was installed. Plaster was applied to this dome and screeded to the 156-8 dome contour using a template pivoted from the center. Steam heating coils were embedded in the plaster. After completion of insulation layup, the top dome and electrical heating unit were installed to complete the autoclave vessel.

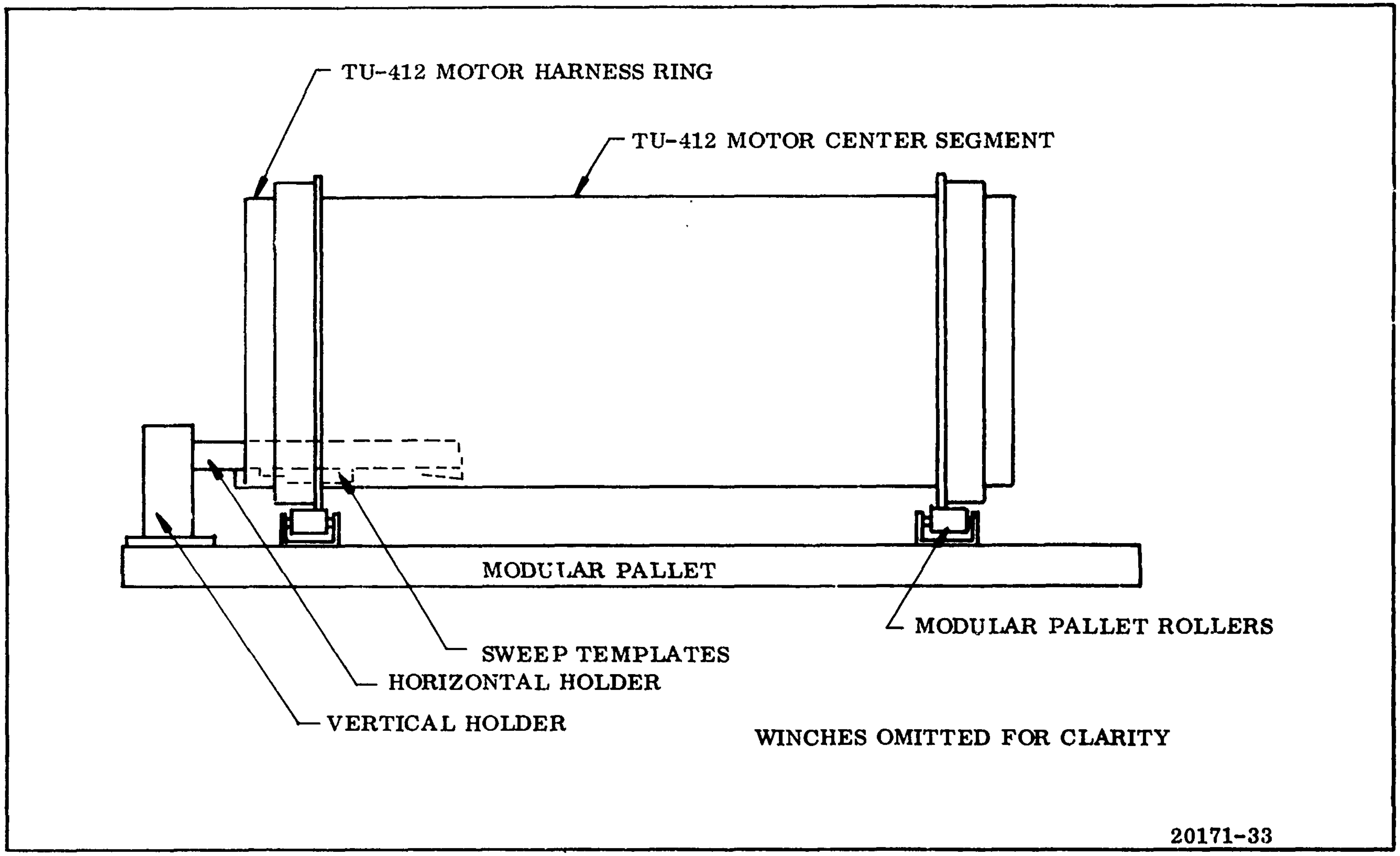

(U) Figure 143. 156-8 Center Segment on Modular Pallet

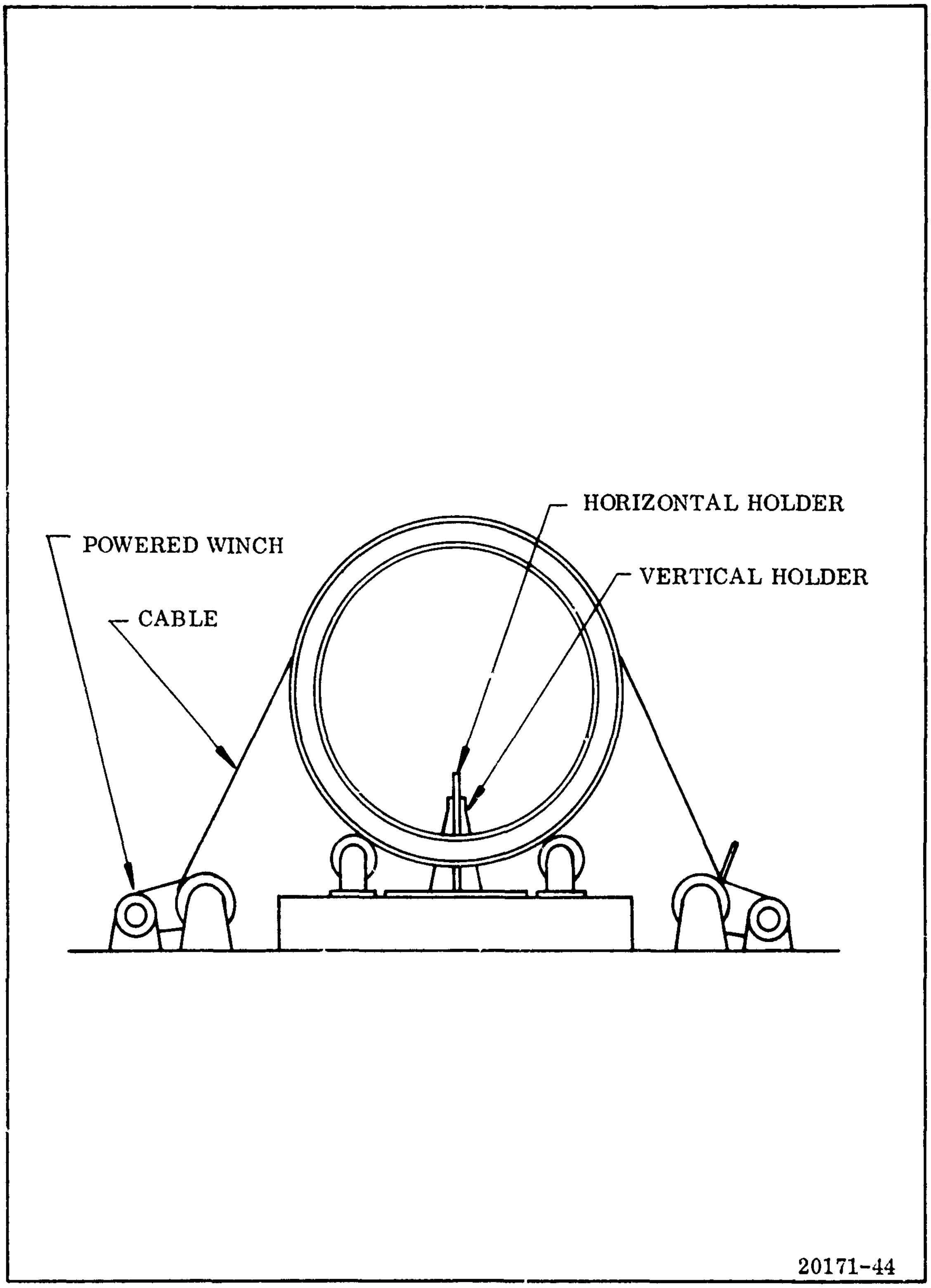

(U) Figure 144. Mold Rotation Apparatus

(U) After insulation layup and cure in the case segments, each unharnessed, unrounded segment was positioned vertically in a casting pit for joint insulation machining. A three legged, spider type frame was attached to the joint end and secured to the segment utilizing the joint pin holes. The center of the routing machine frame (Thiokol Dwg 2U25245-03) was attached to a pivot post in the center of the spider frame. The routing machine frame consisted of three legs, each 120 deg apart, with one leg carrying the router and router motor and the other legs providing support. Each supporting leg had a roller that rolled on the joint end while the leg carrying the router motor had a spring loaded roller arrangement that tracked the inside and end of the joint. This design allowed the router and router motor to duplicate the shape of the case segment as they tracked around the end of the segment. The router motor was powered by compressed air and the machine was pushed by hand around the segment end during machining operations.

(U) Depth of cut was controlled by adjusting the router motor up and down. The groove in the insulation for the joint seal was rough machined with a carbide burr cutter and finished with a diamond grit router operated at 8,000 rpm. The diamond grit routers for the angled and flat surfaces were designed to provide the required contours. These same routers had been used previously in machining the subscale case insulation.

(U) In general, machining of the installed joint insulation was accomplished without major incident and was satisfactory for a one time fabrication effort. Several areas were identified, however, where improvements in tooling for any future machining of joint insulation should be considered.

1. Because of problems encountered in the operation of the router due to the spring loading of the router head, vernier adjustments should be provided on the router head for more precise control of lateral and vertical movement of the cutting heads.

2. A positive means of rotating the router is required. Rotation could be accomplished by a friction wheel, riding against the outside of the case segment, attached to the router leg.

(U) 3. CASTING TOOLING

(U) The casting arrangement was per Dwg 2U27770. It consisted of two 8 in. dia flexible bayonets connected to a single line containing two hand operated Keystone valves, which in turn were connected to the 300 gal. casting can. The casting can was positioned on a dolly, which was driven by a rack and pinion powered by an air motor to retract the bayonets as required.

(U) The CP core (Dwg 2U25630) used to form the propellant core cavity was a one piece metal core previously used for loading the 156-1C (TU-412) motor. The core mold release utilized was polyethylene sheeting, which was secured around the assembled mandrel.

(U) The core was secured and sealed against the dome of the forward and aft segments. Vacuum putty was used to assure an adequate seal. The center segment was sealed off on one end using a large metal plate against which the core was secured and sealed. In each of the segments concentricity of the core was maintained by using a centering plate that was designed to index the core to the case wall.

(U) After propellant cure, core removal was accomplished by applying force on the lower end of the core using a hydraulic jack system to pop the core. The core was then lifted from the motor using the gantry crane.

(U) 4. IGNITER FABRICATION TOOLING

(U) The igniter for the 156-8 motor was fabricated from a standard TU-121 rocket motor case. The internal and external insulation consisted of NBR that was vulcanized in place using standard layup and autoclave cure techniques. No special tooling was designed for the insulation phase of the igniter fabrication. The casting fixtures for the igniter consisted of a one piece, 12 point star core casting sleeve, dispersion cone, and applicable fixtures to secure the case through the nozzle end of the igniter and to form the propellant configuration in the nozzle end.

(U) The propellant was vacuum cast into the igniter by adapting a deaeration assembly to the igniter case, creating a vacuum chamber. The deaeration assembly indexed on the casting sleeve and consisted of a Keystone valve with adapters to the casting sleeve and to the propellant funnel. A slit plate below the Keystone valve was used to form the propellant into thin ribbons, from which all air was flashed off in the vacuum chamber.

(U) After propellant cure, the core and other casting fixtures were removed from the igniter, and the forward propellant was cut to drawing requirements using a remotely operated cutting machine.

(U) 5. NOZZLE HANDLING TOOLING

(U) The nozzle was handled using a "clam shell" device, which braced the steel exit cone and forward flange to provide pivoting capability at the nozzle longitudinal CG (Figure 145).

(U) This arrangement was fitted with trunnions on the outboard ends which were lifted with cables from a large spreader beam. This tooling provided the capability of complete free rotation for breakover to any position.

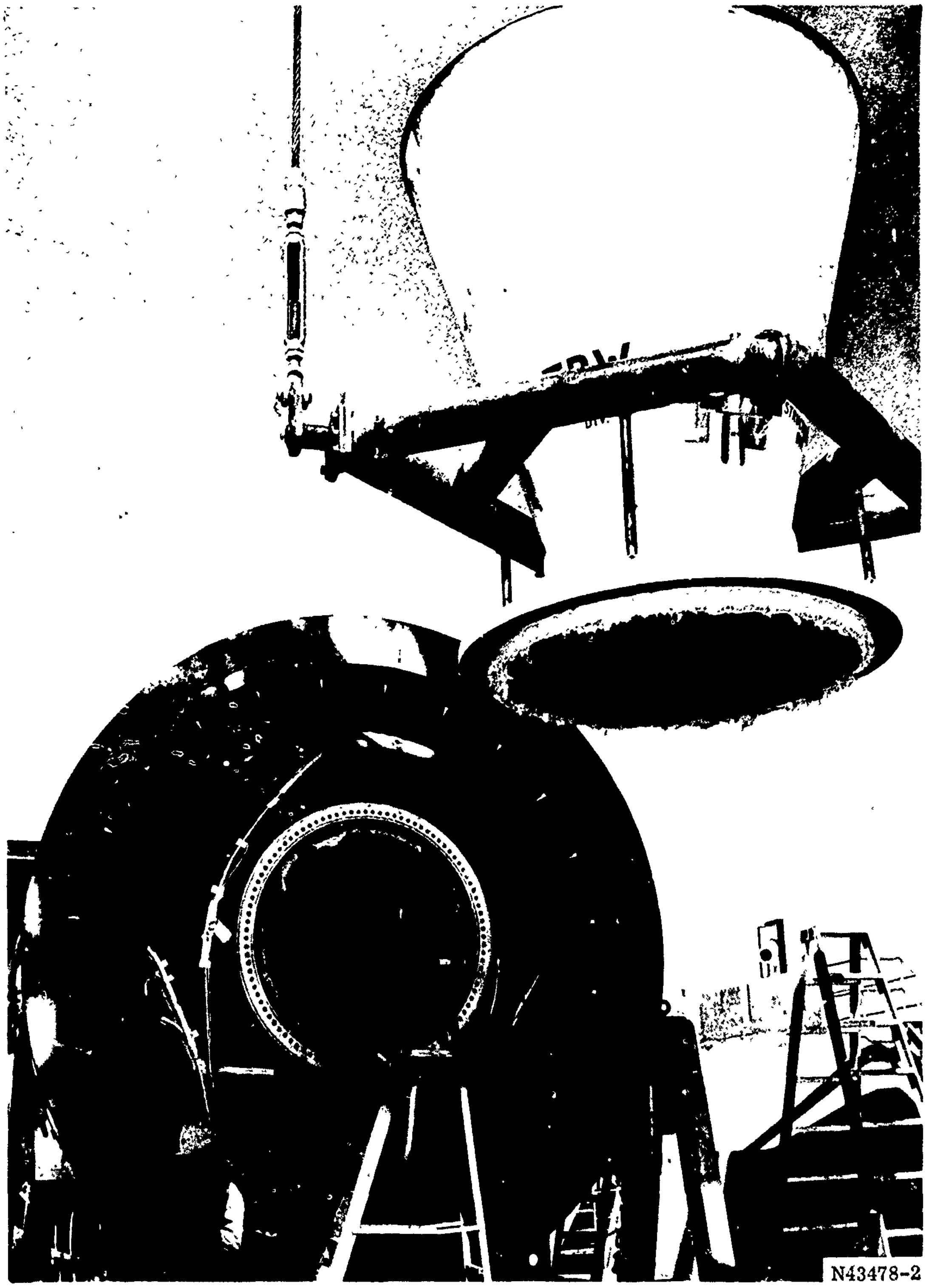

(U) Figure 145. Nozzle Handling Device

B. TEST TOOLING

(U) 1. STATIC TEST STAND

(U) The test stand (Dwg 2U25074) utilized for the 156-8 motor was initially designed and fabricated for the 156-1 motor; it required minor modification for this program. The motor (Figure 146) was supported by four straight-line supports. The design of these supports was such that over approximately 6 in. of travel, the supporting trunnion moved in a straight line. Side restraint was provided by tubular members; axial motion, due to thrust and growth, was accepted by flexures fabricated from I-beam sections.

(U) Due to the configuration of the test stand and motor, the axial thrust train and thrust adapter were initially installed and aligned on the test bay centerline. The motor forward segment was then installed and alignment checked; the remaining two segments were then installed. The straight-line supports and the nozzle were installed. Side supports were installed the day of the static test.

(U) 2. HYDROTEST FIXTURE

(U) The 156-8 hydrotest stand (Dwg 2U25060) was composed of a base structure, four segmented columns, an overhead structure and a piston-cylinder assembly (Figure 147).

(U) The base structure was constructed to support the forward skirt adapter-thrust ring and attach the vertical load columns. The full weight of the water-filled case was supported by this structure in addition to the reaction forces created by pressurizing the case to simulate motor firing conditions.

(U) Each column was fabricated in three main sections for a total length of 49 feet. The sections were made from 12 in. Sch 80 seamless steel tubing with bolting flanges welded on each end. Additional 8 ft long, 6 in. dia threaded solid columns

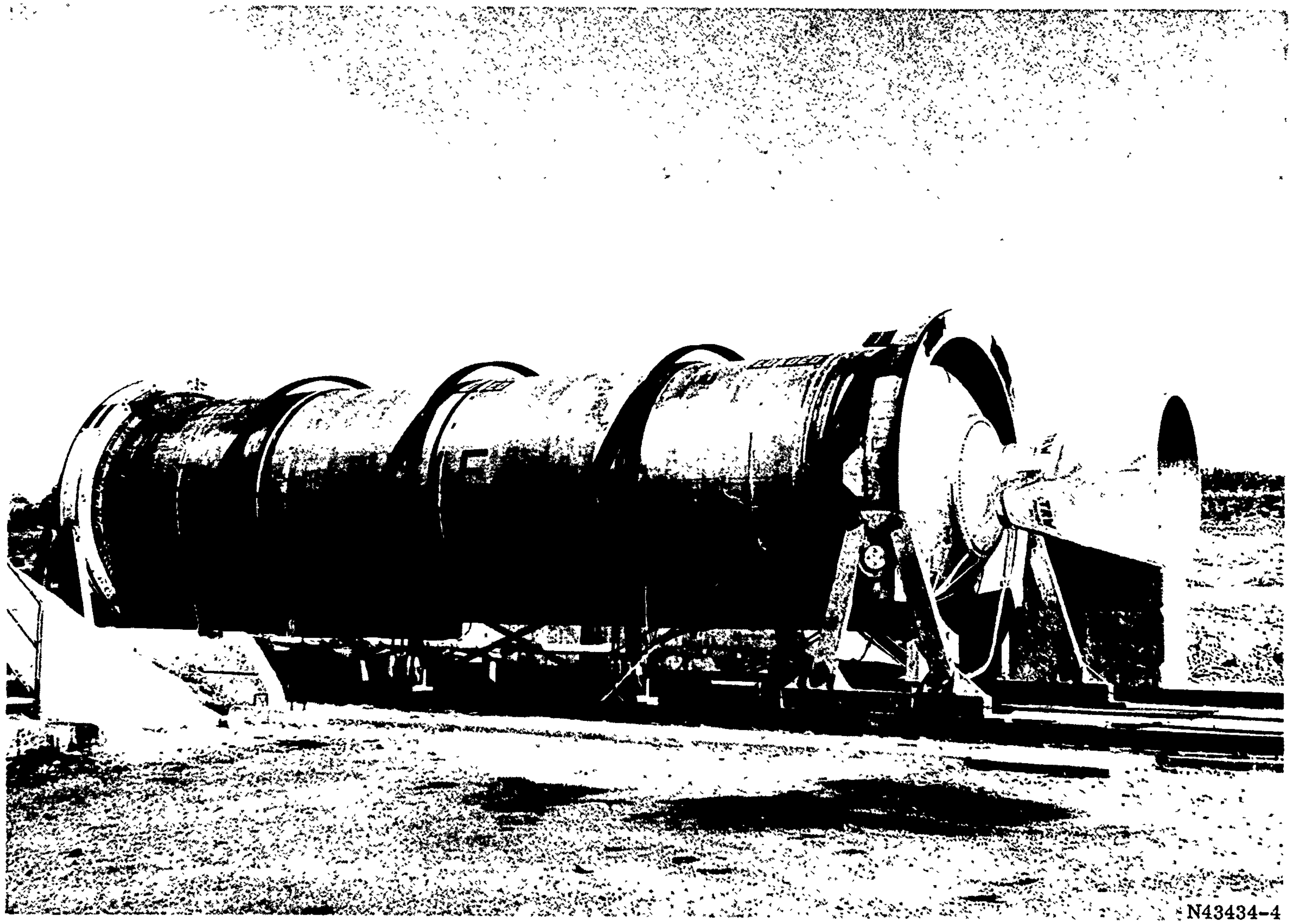

(U) Figure 146. 156-8 Motor in Static Test Stand

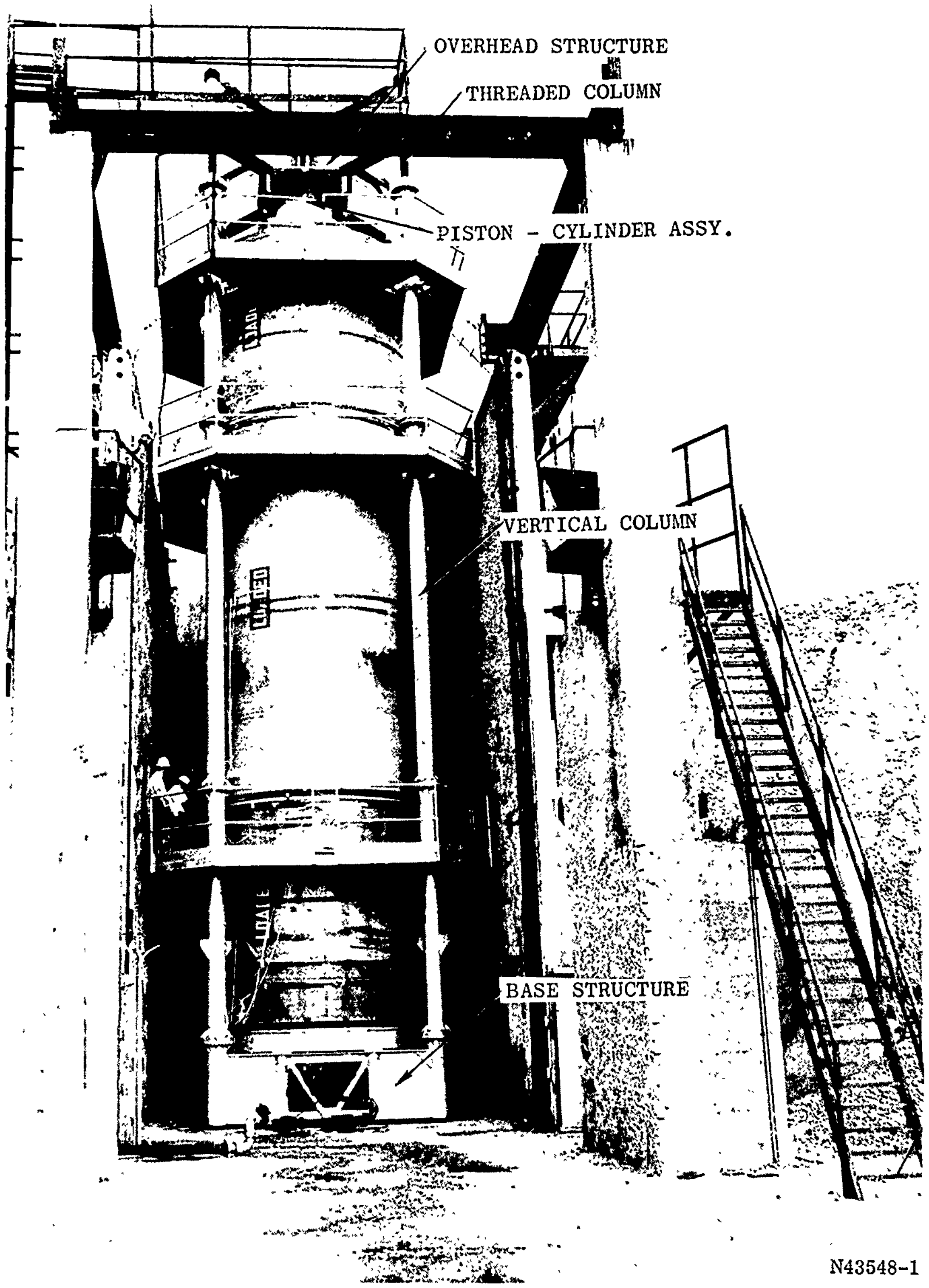

N43548-1

(U) Figure 147. 156-8 Motor in Hydrotest Stand were provided at the top to allow leveling and precise height adjustment of the overhead structure.

(U) The overhead structure attached to the vertical columns and was built to withstand the thrust force being reacted through the floating piston.

(U) The piston assembly was built with bearings to allow rotational motion in two directions from the horizontal plane and translation in two directions relative to the overhead structure. The cylinder was attached to the case at the aft boss. The floating piston within the cylinder allowed free expansion of the case while maintaining the pressure within the case and providing simulation of the thrust experienced during motor firing.

PRECEDING PAGE BLANK-NOT FILMED

Security Classification

DOCUMENT CONTROL DATA - R & D

(Security classification of title, body of abstract and indexing annotation must be entered when the overall report is classified)

1. ORIGINATING ACTIVITY (Corporate author) Thiokol Chemical Corporation Wasatch Division Brigham City, Utah	2a. REPORT SECURITY CLASSIFICATION Confidential 2b. GROUP 4

3. REPORT TITLE
Final Report, Demonstration of 156 Inch Motor with Segmented Fiberglass Case and Ablative Nozzle, Volume I.

4. DESCRIPTIVE NOTES (Type of report and inclusive dates)
Final Report (12 Apr 1966 thru 8 Aug 1968)

5. AUTHOR(S) (First name, middle initial, last name)
Walker, Thomas
Zeigler, Robert F.

6. REPORT DATE	7a. TOTAL NO. OF PAGES	7b. NO. OF REFS
December 1968	325	Four

8a. CONTRACT OR GRANT NO. AF 04(611)-11603 b. PROJECT NO. c. d.	9a. ORIGINATOR'S REPORT NUMBER(S) TC0-56-9-8 9b. OTHER REPORT NO(S) (Any other numbers that may be assigned this report) AFRPL-TR-68-159-Vol I

10. DISTRIBUTION STATEMENT
In addition to security requirements which must be met, this document is subject to special export controls and each transmittal to foreign nationals may be made only with prior approval of AFRPL (RPPR/STINFO) Edwards AFB, California.

11. SUPPLEMENTARY NOTES	12. SPONSORING MILITARY ACTIVITY
	SAMSO AND AFRPL

13. ABSTRACT

The primary objectives of the program were to successfully static test fire the rocket motor followed by a hydroburst test of the fiberglass case. These objectives were attained. The motor (156-8) was static test fired 25 Jun 1968 and all systems performed satisfactorily. This test successfully demonstrated the segmented fiberglass case design and the joint seal design. All motor and nozzle components were intact and in good condition at the completion of the test. The motor operated at close to predicted ballistic values. Post-test inspection of the motor and components disclosed that the internal insulation, nozzle design, and joint seal design were satisfactory and the nozzle performed as predicted. Inadequacies in the CO_2 quench system permitted some charring through of the insulation in the forward dome which necessitated repair prior to the hydroburst test on 8 Aug 1968. Burst occurred at 1,095 psi, starting in a heat affected area of the forward segment.

DD FORM 1 NOV 65 1473

Security Classification

THIS REPORT HAS BEEN DELIMITED
AND CLEARED FOR PUBLIC RELEASE
UNDER DOD DIRECTIVE 5200.20 AND
NO RESTRICTIONS ARE IMPOSED UPON
ITS USE AND DISCLOSURE.

DISTRIBUTION STATEMENT A

APPROVED FOR PUBLIC RELEASE;
DISTRIBUTION UNLIMITED.